



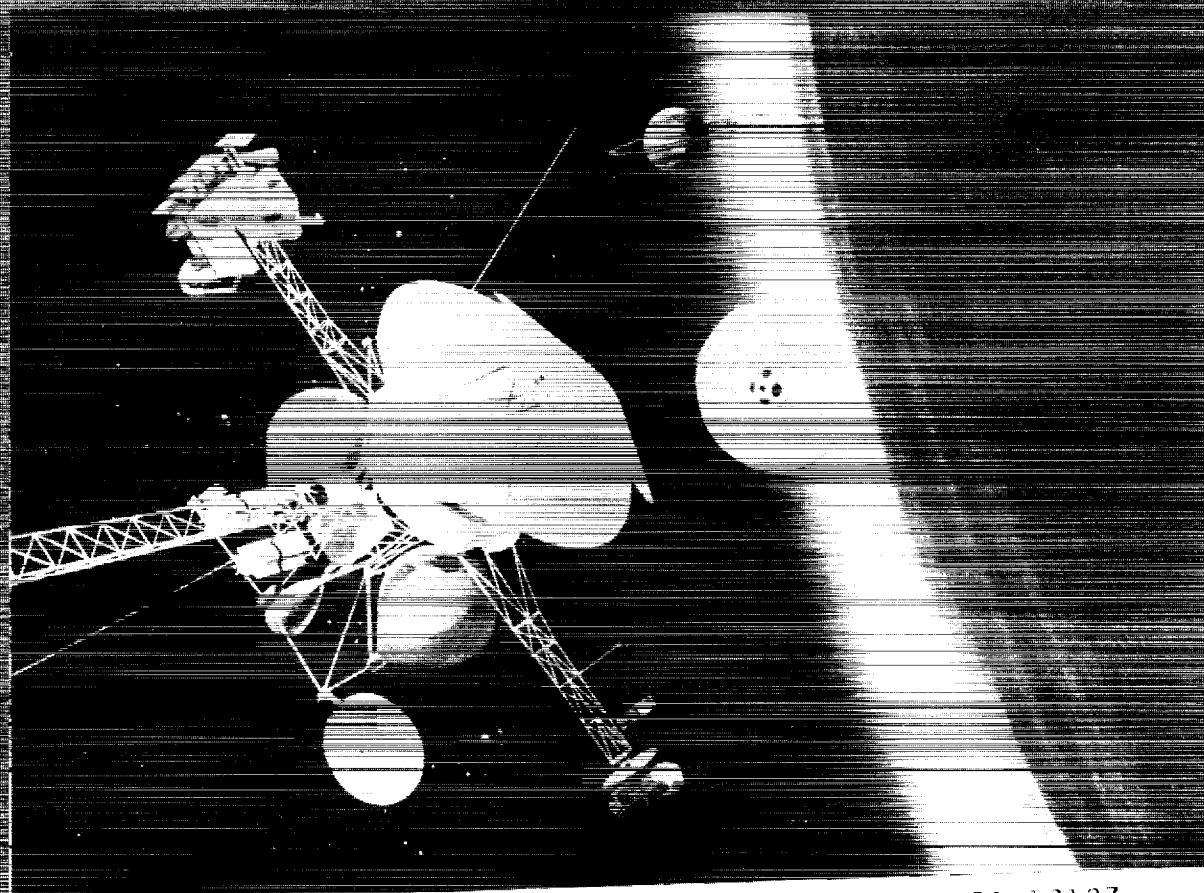
europaean space agency



National Aeronautics and  
Space Administration

# CASSINI

## REPORT ON THE PHASE A STUDY



(NASA-TM-103374) CASSINI. REPORT ON THE  
PHASE A STUDY: SATURN ORBITER AND TITAN  
PROBE (NASA) 46 p

CSCL 22B

N21-18187

Uncles

G3/18 0330111

### Cassini Phase A model payload (total mass 760 kg)

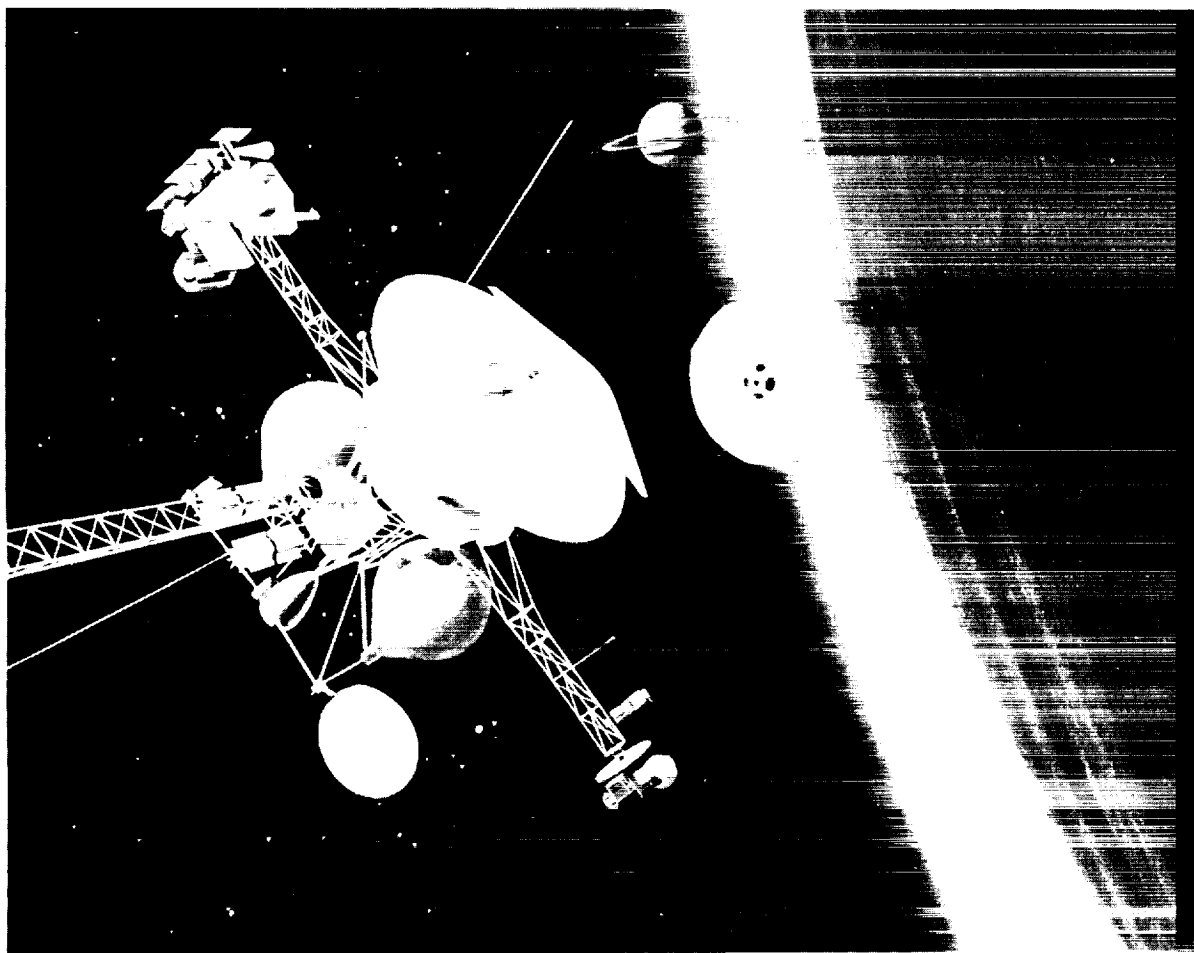
Instrument/investigation	Main scientific objective
Atmospheric Structure Instrument (ASI)	Atmosphere temperature and pressure profile, winds, etc.
Probe Infra-Red Laser Spectrometer (PIRLS)	Vertical profile of trace species, Nephelometry
Gas Chromatograph/Neutral Mass Spectrometer (GC/MS)	Atmosphere composition profile, Aerosol analysis
Aerosol Collector and Pyrolyser (ACP)	Aerosol composition profile, GC/MS is used as detector
Descent Imager/Spectral Radiometer (DISR)	Atmospheric composition and cloud structure, Surface imaging
Luminous and Radio-Emission Detector (LRD)	Titan lightning, Photochemistry
Surface Science Package (SSP)	Titan surface state and composition
Doppler Wind Experiment (DWE)	Probe Doppler tracking from the orbiter for zonal wind profile
Radar Altimeter Science (RAS)	Surface roughness and reflectivity, Subsurface sounding

### Titan Atmospheric Probe design and performance parameters

- Model Payload: Seven scientific instruments plus Radar Altimeter Science (RAS) and Doppler Science (DS) and Impact Surface Science (ISS)
- Launch of **Saturn Orbiter Titan Probe** composite on Titan 4/Centaur G' 1996/1997
- Mission: 8.8 yr interplanetary cruise, Probe post-Saturn orbit insertion, delivery, targeting and spin/separation at Titan encounter — 12 d. Entry and descent on day side. Entry latitude
- Autonomous operation during coast, entry and descent phases
- Entry velocity: 10.5 km/s
- Entry velocity: Nominally 7.2 km/s
- Entry angle: Engine 60°–90°; Nominally 65°
- Chemical separation (distance > 170 km)
- Impact velocity: 10 km/s
- Radio relay link: S-band; 1.4 m diameter antenna; two-axis antenna pointing mechanism and probe attitude subsystem on Orbiter
- Data rates: 512 bits/s to > 8 kbytes/s at impact
- Data transmission capability: 10–15 Mbit total
- Power: 1.4 kwn lithium sulphur dioxide (LiSO<sub>2</sub>) batteries
- Mass: 192.4 kg TPF

# CASSINI

## SATURN ORBITER AND TITAN PROBE



**REPORT ON THE PHASE A STUDY**



## FOREWORD

Cassini, a combined Saturn Orbiter and Titan Probe, mission was proposed to ESA by a consortium of scientists led by D. Gautier and W. Ip in November 1982 in response to a Call for Mission Proposals. The proposers suggested that the mission be carried out in collaboration with NASA. In 1983, the Solar System Exploration Committee (SSEC) of NASA's Advisory Council published their report recommending that NASA should include a Titan Probe/Radar Mapper in its core programme and should consider a Saturn Orbiter as a candidate for later implementation. The SSEC also recommended that international cooperation be sought for these missions. In June 1982, the Space Science Committee of the European Science Foundation and the Space Science Board of the National Academy of Sciences of the USA set up a Joint Working Group (JWG) to study possible cooperation between Europe and the USA in the area of planetary science. One of the potential cooperative missions recommended by the JWG was a Saturn Orbiter and Titan Probe mission.

A joint ESA/NASA assessment study of such a mission was conducted in mid-84/85. In February 86, the ESA's Science Programme Committee (SPC) approved Cassini for Phase-A with a conditional start in 1987. During the course of 1986, the outlook for a timely mission with NASA materialized and, upon recommendation by the ESA's Space Science Advisory Committee (SSAC), the SPC approved in November 1986 the ESA's executive proposal to proceed with a Phase-A study for the Cassini Titan Probe.

In 1987 - 1988, NASA carried out further the definition work on the Mariner Mark II spacecraft and on the two missions designed to use it, the Comet Rendezvous Asteroid Flyby mission (CRAF) and Cassini. In early 1988, NASA decided to combine CRAF and Cassini into a single Mariner Mark II programme and to submit this programme for a FY 1990 new start.

The Titan Probe phase-A was carried out by a European industrial consortium led by Marconi Space Systems from November 1987 to September 1988. In this report, the overall scientific objectives of the Cassini mission are described together with the mission and technical design studies of both spacecraft, with emphasis on the technical design studies of the Titan Probe System.

The membership of the Joint Science Working Group which supported the phase-A activities was as follows:

- M. Allison, Goddard Institute for Space Studies, New York, (USA) ✓
- S. Bauer, Karl Franzens Universität, Graz, (A)
- M. Blanc, Centre de Recherches en Physique de l'Environnement, St. Maur, (F)
- S. Calcutt, Dept. of Atmospheric Physics, Oxford, (UK)
- J. Cuzzi, NASA Ames Research Center, Moffett Field, (USA) ✓
- M. Fulchignoni, Universita "La Sapienza", Rome, (I)
- D. Gautier, Observatoire de Paris, Meudon, (F)
- D. Hunten, University of Arizona, Tucson, (USA)
- W. Ip, MPI für Aeronomie, Katlenburg-Lindau, (D)
- T. Johnson, Jet Propulsion Laboratory, Pasadena, (USA)
- H. Masursky, US Geological Survey, Flagstaff, (USA)
- P. Nicholson, Cornell University, Ithaca, (USA)
- T. Owen, State University of New York, Stony Brook, (USA)
- R. Samuelson, NASA Goddard Space Flight Center, Greenbelt, (USA) ✓
- F. Scarf, TRW, Redondo Beach, (USA), †
- E. Sittler, NASA Goddard Space Flight Center, Greenbelt, (USA), ✓
- B. Swenson, NASA Ames Research Center, Moffet Field, (USA). ✓

D. Gautier, W. Ip and T. Owen acted as "lead scientists".

Support to the study was also provided by: M. Bird, Univ. of Bonn,(D); R. Courtin, Obs. de Paris, Meudon,(F); E. Grün, MPI für Kernphysik, Heidelberg,(D); M. Flasar, NASA/GSFC,(USA); G. Israel, Service d'Aeronomie, Verrieres-le-Buisson,(F); V. Kunde, NASA/GSFC, (USA); E. Lellouch, obs. de Paris, Meudon,(F); S. Madsen, TU of Denmark, Lyngby,(DK); D. Muhleman, Caltech, Pasadena,(USA); H. Niemann, NASA/GSFC, (USA); F. Raulin, LPCE, Creteil, (F); M. Tomasko, Univ. of Arizona, Tucson,(USA).

The ESA members from the Scientific Directorate responsible for the phase-A study were:

- M. Coradini, Science Planning Office, ESA HQ, Paris.
- J.-P. Lebreton, Study Scientist, Space Science Department of ESA, ESTEC
- G.E.N. Scoon, Study Manager, Future Projects Study Office, ESTEC.

Support was provided by members from the Operations Directorate and by members from the specialist divisions of the Technical Directorate of ESA.

The NASA members responsible for the study were:

- J. Beckman, Study Manager (-6/88), JPL, Pasadena
- G. Briggs, NASA Headquarters, Washington ✓
- H. Brinton, NASA Headquarters, Washington ✓
- R. Draper, Mariner Mark II Project Manager, JPL, Pasadena
- L. Horn (6/88-), Assistant Study Scientist, JPL, Pasadena
- W. Huntress (-6/88), Study Scientist, JPL, Pasadena
- C. Kohlhase (6/88-), Science and Mission Design Manager, JPL, Pasadena

Support was also provided by D. Kindt, S. Kerridge, R. Stoller and other staff members of the Jet Propulsion Laboratory.

Additional copies of this report may be obtained from:

J.-P. LEBRETON  
Space Science Department  
ESTEC - Keplerlaan,1  
2201 AZ Noordwijk  
The Netherlands

G.E.N. SCOON  
Future Science Projects  
ESTEC - Keplerlaan,1  
2201 AZ Noordwijk  
The Netherlands

or to the Secretary of the Solar System Working Group:

M. CORADINI  
Directorate of Scientific Programmes  
ESA 8-10 Rue Mario Nikis  
75738 Paris Cedex  
France

†The members of the Science Team would like to take this opportunity to express their deep appreciation for the essential contributions to the Cassini Project made by Fred Scarf before his untimely death in July 1988. As a member of the JWG, Dr Scarf led the successful effort to include the Cassini mission as one of the options for a joint undertaking between the United States and Europe. His subsequent involvement in the activities of the Science Team and his unflagging support of Cassini in both the US and European scientific communities have been an important component in the successes this enterprise has enjoyed to date. He will be greatly missed.

# Contents

<b>1</b>	<b>Summary</b>	<b>1</b>
<b>2</b>	<b>Introduction</b>	<b>3</b>
<b>3</b>	<b>Scientific objectives</b>	<b>5</b>
3.1	Titan . . . . .	7
3.1.1	The Atmospheric Composition of Titan . . . . .	7
3.1.2	Thermal Structure and Meteorology of Titan's Atmosphere . . . . .	10
3.1.3	Titan Aeronomy and Interactions with Saturn's Magnetosphere . . . . .	11
3.1.4	Titan Surface and Internal Structure . . . . .	12
3.1.5	Origin and Evolution of Titan's Atmosphere . . . . .	13
3.2	Saturn . . . . .	14
3.2.1	The Interior . . . . .	14
3.2.2	Thermal Structure and Composition . . . . .	15
3.2.3	Atmospheric Dynamics and General Circulation . . . . .	16
3.2.4	Saturn's Ionosphere . . . . .	19
3.3	Saturn's Rings . . . . .	19
3.3.1	Structure of the main rings, and dynamical processes to be investigated . . . . .	22
3.3.2	Composition and size distribution of the ring material . . . . .	24
3.3.3	Dust and meteoroid distribution . . . . .	26
3.3.4	Interactions between the rings and the planet's magnetosphere, ionosphere, and atmosphere . . . . .	27
3.4	Icy Satellites . . . . .	29
3.4.1	The Satellite System . . . . .	29
3.4.2	Enceladus and Iapetus: Especially interesting bodies . . . . .	33
3.4.3	Other Problems . . . . .	34
3.5	Magnetosphere . . . . .	35
3.5.1	Magnetospheric Dynamics and Energetics . . . . .	36
3.5.2	Plasma Composition, Sources and Sinks . . . . .	38
3.5.3	Titan's Plasma Interactions . . . . .	39
3.5.4	Saturn's Plasma Wave and Radio Emissions . . . . .	40
3.5.5	Plasma-Solid Body Interactions . . . . .	41
3.6	Jupiter . . . . .	42
3.6.1	Atmospheric Science . . . . .	42
3.6.2	Magnetospheric Science . . . . .	44
3.6.3	Satellite Science . . . . .	46
3.7	Asteroid . . . . .	46
3.8	Cruise Science . . . . .	48

3.8.1	Thermal Structure and Thermodynamics of the Solar Wind . . . . .	49
3.8.2	Evolution of Turbulence and Mixing Processes . . . . .	49
3.8.3	Interstellar Ions . . . . .	50
3.8.4	Structure and Orbital Characteristics of the Interplanetary Dust Cloud . . . . .	50
3.8.5	Gravitational Waves . . . . .	51
3.8.6	Cruise Data Tracking . . . . .	51
<b>4</b>	<b>The model payloads</b>	<b>52</b>
4.1	The Orbiter Model payload . . . . .	52
4.1.1	The Orbiter Payload Composition . . . . .	52
4.1.2	Typical Orbiter Science Profile . . . . .	52
4.1.3	Instrument Description . . . . .	55
4.2	The Probe Model payload . . . . .	63
4.2.1	Probe Model Payload Composition . . . . .	63
4.2.2	Probe Science Profile . . . . .	63
4.2.3	Instrument Description . . . . .	64
<b>5</b>	<b>Project Requirements</b>	<b>69</b>
5.1	Mission . . . . .	69
5.2	Orbiter . . . . .	70
5.3	Probe System . . . . .	71
<b>6</b>	<b>Mission</b>	<b>72</b>
6.1	Mission Overview . . . . .	72
6.2	Interplanetary Trajectory . . . . .	73
6.3	Asteroid Flyby . . . . .	73
6.4	Jupiter Flyby . . . . .	73
6.5	Saturn Orbit Insertion and Probe Delivery . . . . .	75
6.6	Probe Mission . . . . .	76
6.7	Titan Physical Model . . . . .	76
6.8	Orbiter Mission . . . . .	80
<b>7</b>	<b>Launch Vehicle</b>	<b>84</b>
7.1	Launch Scenario . . . . .	84
7.2	Launch Vehicle Performance . . . . .	84
<b>8</b>	<b>The Orbiter System</b>	<b>86</b>
8.1	Orbiter . . . . .	86
8.2	Probe Support Subsystem . . . . .	90
8.3	Mass and Power Summary . . . . .	90
<b>9</b>	<b>The Titan Probe System</b>	<b>92</b>
9.1	General . . . . .	92
9.2	Probe Mission Phases . . . . .	92
9.3	System Budgets . . . . .	93
9.4	Probe Design . . . . .	93
9.5	Aerodynamics and Aerothermodynamics . . . . .	94
9.6	Payload Accommodation . . . . .	101
9.7	Structure and Mechanisms . . . . .	101

9.8 Thermal Protection Subsystem . . . . .	104
9.9 Thermal Control Subsystem . . . . .	105
9.10 Descent Control Subsystem . . . . .	105
9.11 RF Telecommunication Subsystem . . . . .	107
9.12 Command and Data Management Subsystem (CDMS) . . . . .	110
9.13 Power Subsystem . . . . .	112
9.14 Probe Sensors Subsystem . . . . .	112
<b>10 Mission Operations</b>	<b>116</b>
10.1 Mission Operations Concept . . . . .	116
10.2 The Mission Operations Process (Orbiter) . . . . .	117
10.3 Probe Operations . . . . .	117
<b>11 Management</b>	<b>120</b>
11.1 Management Provisions . . . . .	120
11.2 Proposed Cassini Science Plan . . . . .	120
11.3 Data Management . . . . .	121
<b>12 Development Plan</b>	<b>122</b>
12.1 Titan Probe model philosophy . . . . .	122
<b>A Titan's Organics: Molecules likely to be present in the Atmosphere (gas and aerosols) and the Ocean</b>	<b>b</b>
<b>B Engineering model of the atmosphere of Titan</b>	<b>f</b>
<b>C Bibliography</b>	<b>i</b>
<b>D List of Acronyms</b>	<b>l</b>

# List of Figures

3.1	<i>Model of ocean near surface and of thermal structure of the atmosphere of Titan. (From Lunine et al., Science, 222, 1230, (1989))</i>	8
3.2	<i>Schematic model of the Saturn interior. (Courtesy D.A. Stevenson)</i>	15
3.3	<i>Polar projection mosaic of Voyager images of Saturn's northern hemisphere. (Courtesy of D.A. Godfrey)</i>	18
3.4	<i>Schematic of Saturn's ring system showing the main (A, B, C) rings, the Cassini Division, and the tenuous D, E and G rings, along with the mysterious "kinky" F-ring and its associated shepherding satellites Pandora and Prometheus</i>	20
3.5	<i>Typical structure in each of the 3 classical ring regions: the A ring (top), the B ring (middle) and the C ring (bottom)</i>	23
3.6	<i>Narrow, kinky ringlets of similar type are seen both in the F Ring (left pair) and the Encke gap in the A ring (right pair)</i>	25
3.7	<i>Comparison of Saturn's satellites sizes. This figure illustrates the range of sizes among the satellites of Saturn. Titan, the largest, is approximately the size of planet Mercury</i>	29
3.8	<i>Enceladus</i>	31
3.9	<i>Dione</i>	32
3.10	<i>Meridional view of Saturn's inner magnetosphere</i>	35
3.11	<i>A schematic view of Saturn's magnetosphere as it will look during the tour phase of the Cassini mission</i>	37
3.12	<i>Nominal trajectory of Cassini through the magnetosphere of Jupiter for a launch in 1996</i>	45
4.1	<i>Data return profile during a typical 12-day high activity period</i>	54
6.1	<i>Launch period definition</i>	72
6.2	<i>Baseline interplanetary trajectory</i>	74
6.3	<i>Flyby of Asteroid 66 Maja</i>	74
6.4	<i>Jupiter flyby and location of galilean satellites</i>	74
6.5	<i>Initial Saturn Orbit and Titan Probe delivery sequence</i>	74
6.6	<i>Saturn arrival and Orbit Insertion geometry</i>	75
6.7	<i>Height of Spacecraft above ring plane during SOI</i>	75
6.8	<i>Probe separation and delivery scenario</i>	77
6.9	<i>Density profile as a function of altitude according to the Lellouch/Hunten model (see appendix 2). In addition to the nominal profile, the two extreme profiles are also shown</i>	77
6.10	<i>Profile of Titan's thermal wind</i>	78
6.11	<i>Probe targeting in Titan B-plane</i>	79
6.12	<i>The Probe's trajectory and operations in Titan's atmosphere</i>	79

6.13	<i>Probe descent profile</i>	80
6.14	<i>Landing site dispersion due to winds</i>	81
6.15	<i>Petal plot of representative Saturn system tour (88-01)</i>	82
6.16	<i>Ground tracks of Titan flybys (altitudes below 3000 km) during a representative Saturn system tour (88-01)</i>	83
7.1	<i>Titan IV/ Centaur configuration</i>	85
7.2	<i>Titan IV Centaur planetary performance (Current Best Estimate)</i>	85
8.1	<i>MM-II/ Cassini Spacecraft</i>	87
8.2	<i>MM-II simplified functionnal block diagram (CRAF and CASSINI)</i>	87
9.1	<i>Probe aerodynamic characteristics</i>	95
9.2	<i>Mach 1.5 altitude achievements vs. entry angle</i>	97
9.3	<i>Typical Probe trajectory parameters</i>	98
9.4	<i>Probe System configuration on the Orbiter</i>	99
9.5	<i>Probe configuration (dimensions in mm)</i>	100
9.6	<i>Probe top platform</i>	102
9.7	<i>Probe experiment platform:top view</i>	102
9.8	<i>Probe experiment platform:bottom view</i>	102
9.9	<i>Schematic of thermal control components</i>	104
9.10	<i>Titan Probe exploded view</i>	106
9.11	<i>Criteria and sequence for adaption of the descent profile</i>	107
9.12	<i>Probe telecommunication subsystem</i>	109
9.13	<i>PSS telecommunication subsystem</i>	110
9.14	<i>Command and Data management Subsystem (CDMS), before separation</i>	111
9.15	<i>Probe Power subsystem</i>	113
9.16	<i>Radar altimeter</i>	114
10.1	<i>MM-II mission operations organisation</i>	118
10.2	<i>Top level functional data flow</i>	118
12.1	<i>Probe development qualification/acceptance strategy</i>	123
12.2	<i>Cassini summary development schedule</i>	124
A.1	<i>Solubility of unsaturated hydrocarbons, inorganics and N-organics in Titan's model atmosphere ocean (94 °K, as a function of its CH<sub>4</sub> model fraction. Solubility of NH<sub>3</sub> at 112 °K is also indicated, for comparison.</i>	c
B.1	<i>Thermal and density profile of the atmosphere of Titan</i>	h

# List of Tables

3.1	<i>General characteristics of the Saturn's satellites</i> . . . . .	30
3.2	<i>Cassini asteroid candidates</i> . . . . .	48
4.1	<i>Cassini Orbiter model payload</i> . . . . .	53
4.2	<i>Cassini Probe model payload</i> . . . . .	63
5.1	<i>Cassini spacecraft mass allocation (kg)</i> . . . . .	70
5.2	<i>Manoeuvre budget <math>\Delta V</math> (m/s)</i> . . . . .	70
8.1	<i>Orbiter Mass summary</i> . . . . .	91
8.2	<i>Orbiter Power summary</i> . . . . .	91
9.1	<i>Titan Probe Mass Budget (kg)</i> . . . . .	95
9.2	<i>Probe Support Subsystems Mass Budget (kg)</i> . . . . .	96
9.3	<i>Probe System Energy and Power Budgets</i> . . . . .	96
9.4	<i>Probe-Orbiter Radio Relay Link budget</i> . . . . .	108
A.1	<i>Organic molecules likely to be present in Titan's atmosphere (in addition to the already detected compounds)</i> . . . . .	e
A.2	<i>Characteristics of the most intense IR bands of some organics in the 200-1200 <math>\text{cm}^{-1}</math> region and deduced upper limit of their mole fraction in Titan's atmosphere</i> . . . . .	e

# Chapter 1

## Summary

The new planetary mission presented in this phase A report proposes an in-depth, second phase exploration of giant Saturn, its richly complex magnetosphere and its elaborate retinue of rings and satellites. The mission gives special attention to Titan, Saturn's planet-sized moon, which is blanketed by an atmosphere thicker than our own and may be covered by a global hydrocarbon ocean. Chemical reactions presently taking place in Titan's continually evolving atmosphere provide possible analogs to some of the prebiotic organic chemistry on the primitive Earth. En route to the Saturn system, the spacecraft will take advantage of its Earth-Jupiter gravity-assist trajectory to make a close flyby of an asteroid and a Voyager-like encounter with Jupiter. In essence, Cassini thus represents a natural extension of the reconnaissance/first exploration of the Saturn system carried out so successfully by the Pioneer 11 (1979) and Voyager 1 and 2 (1980-81) flybys, while complementing the Galileo Jupiter mission (1995/97) and the proposed CRAF and Vesta missions to small bodies.

Appropriately named "Cassini" after the discoverer of several Saturn satellites and ring features, this advanced, joint ESA/NASA mission is carried out by an Orbiter and a Probe. The Orbiter carries the Probe and deploys it into the atmosphere of Titan where it makes detailed measurements during its 3-hour descent to the hidden surface of this strange satellite. The Orbiter performs a 4 year,  $\sim 36$  orbit tour of the Saturn system, changing its orbit continuously and ending in a highly inclined, nearly polar, orbit. Such a scheme provides a thorough investigation of the Saturn system, with special focus on Titan. It renews the assault on Saturn's complex and interacting system of satellites, rings and magnetosphere, with new and enhanced instrumentation, and will obtain the answers to many fundamental questions posed by the previous investigations.

At Saturn and Titan, Cassini will enable us to study thoroughly the interior, atmospheric structure and chemistry, dynamic meteorology, cloud physics and aerosols, ionosphere, and exosphere. The icy satellites will be studied in detail through close encounters, allowing observations of their diversified surfaces, including internal/surficial activities, their histories and relationships with the outside environment. The structure, composition, and physical processes of the complex ring system will be studied, focussing on the dynamics of the constituent particles and embedded moonlets (or mini-satellites), their evolution and interactions with the magnetosphere and the whole Saturnian system. The characteristics of the huge magnetosphere with its plasma and particles of dust and ice, will be studied intensively, exploring the generation and varying morphology of the electromagnetic fields and the interactions of this complex system with the solar wind, the rings and individual satellites.

Cassini also represents the state-of-the-art in deep space instrumentation. Among the new instruments proposed for the strawman payload, we can mention a neutral energetic particle imaging system to map the magnetosphere, a miniaturized GCMS on the Titan Probe, and a radar on the

Orbiter that will map the surface of Titan through the satellite's cloudy atmosphere.

On its way to Saturn, Cassini will traverse the asteroid belt twice, providing an excellent opportunity to fly by at least one asteroid just one year after launch. The selected asteroid will be a type not investigated by Galileo, thereby adding significant new information about the properties of these primitive objects. Cassini will obtain a good look at the object encountered, allowing a determination of its characteristics, shape and dimensions, mass, density, rotation and the temperature, chemical composition and morphology of the surface, as well as inferences on body structure, surface processes, history, and possibly internal structure.

Four years after launch, Cassini will fly by Jupiter at a distance of approximately 52 Jovian radii, thereby obtaining an additional boost to help it on its way to Saturn. During the course of this flyby Cassini will take advantage of its complementary instrumentation and trajectory to add to the findings of the Galileo spacecraft, scheduled to finish its nominal mission about two years earlier. In particular, studies of the magnetosphere, atmospheric structure, dynamics and composition will extend the reach of the Galileo mission in several significant ways.

The Cassini spacecraft - Orbiter plus Probe - can be developed in time for the favourable launch opportunity from Cape Kennedy in April, 1996 using a Titan IV/Centaur. The trajectory begins with a two year trip out to the asteroid belt and back to Earth for a flyby in June 1998 to pick up additional energy. Encounter with the C-type asteroid 66 Maja would take place in March 1997. From the Earth encounter, the spacecraft heads off to Jupiter for an additional gravity assist, obtaining new science during its pass at about 52  $R_J$  in February of the year 2000. Saturn arrival occurs in October, 2002, some 6.5 years after launch. The present baseline calls for a first orbit period of 100 days, providing favourable geometry for day-side observations of Saturn and leading to release of the Titan Probe on 31 December 2002. The Probe enters Titan's atmosphere at a velocity of about 6 km/sec. A large decelerator reduces the entry velocity of the Probe, protected by a nose cap/heat shield, to near-sonic speed, reached at some 170 km altitude (entry phase). Then, after jettisoning the decelerator system, a parachute system is deployed allowing a slower descent and atmospheric data gathering and sampling. The surface is reached in about 3 hours after entry (descent phase). If the Probe survives the landing, it will transmit data about the nature of the surface until the radio relay link with the Orbiter is lost. Throughout this period, the Orbiter relays all the data gathered by the Probe back to earth. For redundancy reasons, it also records the data on board for later playback.

After the Probe mission phase, the Orbiter begins an extensive 4-year Orbital tour of the Saturnian satellite system, using a Titan gravity assist for each of the ~36 orbits planned and ending with a nearly polar orbit. By varying the orientation of the line of apsides and inclination of the orbits, all the satellites can be encountered, remotely sensed and imaged to resolutions of a kilometer or less for most of them. With such an orbital tour, the Orbiter repeatedly passes over both Saturn and Titan allowing detailed observations of both bodies, and, of course, of the intricate rings of Saturn. The multiple passes through the magnetosphere at different inclinations (up to nearly 80°) and sun angles (afternoon to early morning petals) will allow continued and detailed study of the dynamics and composition of the magnetospheric plasma and its many faceted interactions with the ring particles, the extended neutral clouds from Titan and Saturn, the icy satellites and Titan itself.

The launch vehicle and the Orbiter are to be the responsibility of NASA, while the Titan Probe System is to be furnished by ESA. The two agencies will share project management and mission operations. Experiments for the payload of the Probe and the Orbiter are to be supplied by both US and European investigators.

# Chapter 2

## Introduction

The trail blazing observations by the Pioneer and Voyager spacecraft have yielded a wealth of information which has fundamentally changed our concepts of the Jovian and Saturnian systems and of the solar system as a whole. After Jupiter has been investigated in further detail by the Galileo mission, the Cassini mission proposed in this report is the next logical step in the understanding of the outer solar system. The scientific and technological complexities of such an ambitious mission and its cost, point towards the need for a joint effort by the scientific and technological communities of Europe and the USA. As described in this proposal, the Cassini mission consists of a Saturn Orbiter to be built by NASA and a Titan Probe to be built by ESA.

The Orbiter is instrumented for studies of Saturn, its rings, magnetosphere, and satellites. The nominal Orbiter mission lifetime is 4 years, during which encounters with Titan on every orbit are used for gravity assists to manage the orbital evolution. At the time the mission is terminated, the spacecraft will be in an orbit with an inclination of  $\sim 80^\circ$ , as close to polar as possible. Approaches to within 2 Saturn radii and orbits giving good views of the lighted face of the planet and rings are additional terminal configurations that can be considered. The large number ( $\sim 30$ ) of Titan encounters will permit an extensive remote sensing study of the atmosphere and of the surface. In-situ observations of the satellite's upper atmosphere will be made by the spacecraft down to an altitude possibly as low as 800 km.

Prior to the first Orbiter encounter with Titan, after orbit insertion around Saturn, the Probe is released to make a low velocity entry into Titan's atmosphere. It carries a full complement of instruments to study atmospheric composition and structure, including properties of clouds and aerosols. The descent to the surface takes approximately three hours. If the Probe survives the landing, additional experiments to characterize the surface can be carried out.

The Voyager flybys have not only laid the groundwork for Cassini, but they have also raised many specific questions that this mission is designed to address. Titan is one of the most fascinating bodies in the outer solar system; it has the size of a terrestrial planet with a reducing atmosphere that is thicker than that of the Earth. The preservation of reducing conditions on this relatively small body results from the fact that Titan is much colder than the terrestrial planets. It is therefore rich in ices and other volatile materials. Chemical reactions taking place in Titan's atmosphere today may resemble, in several important respects, the pre-biological chemical evolution on the primitive Earth. The Titan atmospheric circulation may be the only comparative analog in the Solar System to the Venus super-rotational cloud deck. Study of Saturn's rings has become almost a field of science in itself. It is providing insights into dynamical processes that may also have played a role in the formation of planets from rings of protoplanetary material. Saturn's magnetic field is unique in its axial symmetry. The magnetosphere is additionally noteworthy for the high degree of interaction among the charged particles it contains and the rings, icy satellites, and ionospheres

of Titan and Saturn. The Saturn atmospheric dynamics, with winds in excess of 400 m/s, provide an essential challenge to comparative theories of planetary meterology. The icy satellites include Iapetus, whose leading hemisphere is about ten times darker than its trailing side, for reasons we do not understand. In contrast, tiny Enceladus appears to have the brightest surface of any satellite, and large areas of it are geologically extremely young and perhaps still active. This moon also appears to be the source of the particles in the E ring, but the process(es) responsible for the production of these particles and the reworking of the surface are not yet established.

Finally, it should be remembered that despite the extraordinary achievements of the Voyager missions and the specific questions they have raised, Cassini is itself in large part a voyage of exploration. The Voyager spacecraft spent only a few days in a highly complex and variegated planetary system; it is highly unlikely that they discovered and recorded all of the unusual phenomena to be found there. We thus expect many surprises from Cassini, in addition to a thorough study of the many issues raised by our current knowledge.

The planet itself (atmosphere and interior), its magnetosphere, and its satellites are all well suited for detailed comparison with the corresponding components of the Jupiter system. Such comparisons are essential if the fundamental questions concerning the origin and evolution of these immense and complex planetary systems are to be properly addressed. In both systems, it is necessary to gain an understanding of the system as a whole while studying the important interactions among the various parts. This requires an ambitious, multi-pronged effort. For Jupiter, the Galileo Mission scheduled for launch in 1989 will meet this requirement. Cassini is the Saturn equivalent.

It is important to emphasize that the current mission scenario for Cassini includes remote sensing of an asteroid one year after launch and a Jupiter encounter just three years later. The Jupiter flyby will occur shortly after the nominal lifetime of the Galileo mission. It will therefore provide important complementary information, particularly for the planet and its magnetosphere, owing to the different trajectory and payload.

An Orbiter-Probe mission is perfectly suited to a division of effort between two partners, and offers high benefits to both the European and American scientific communities.

In the next section, we present a discussion of the scientific objectives of the mission and a description of the capabilities of the instrument payloads for achieving these objectives. This is followed by a description of the payloads for the Orbiter and the Probe and an outline of the mission design. The concluding sections of the report describe the launch vehicle, the spacecraft, and the management structure proposed to handle this cooperative enterprise.

# Chapter 3

## Scientific objectives

The following list summarizes the Cassini science objectives to be followed by a detailed description below.

### The Saturnian system: the primary target of Cassini

#### TITAN

- Determine abundances of atmospheric constituents (including any noble gases); Establish isotope ratios for abundant elements; constrain scenarios of formation and evolution of Titan and its atmosphere.
- Observe vertical and horizontal distributions of trace gases; search for more complex organic molecules; investigate energy sources for atmospheric chemistry, model the photochemistry of the stratosphere; study formation and composition of aerosols.
- Measure winds and global temperatures; investigate cloud physics, general circulation and seasonal effects in Titan's atmosphere; search for lightning discharges.
- Determine the physical state, topography and the composition of the surface; infer the internal structure of the satellite.
- Investigate the upper atmosphere, its ionization, and its role as a source of neutral and ionized material for the magnetosphere of Saturn.

#### SATURN

- Determine temperature field, cloud properties and composition of the atmosphere of Saturn.
- Measure the global wind field, including wave and Eddy components; Observe synoptic cloud features and processes.
- Infer the internal structure and rotation of the deep atmosphere.
- Study the diurnal variations and magnetic control of the ionosphere of Saturn.
- Provide observational constraints (gas composition, isotope ratios, heat flux,...) on scenarios for the formation and the evolution of Saturn.
- Investigate the sources and the morphology of Saturn lightning (Saturn Electrostatic Discharges (SED), lightning whistlers).

## RINGS

- Study configuration of rings and dynamical processes (gravitational, viscous, erosional, and electromagnetic) responsible for ring structure.
- Map composition and size distribution of ring material.
- Investigate interrelation of rings and satellites, including embedded satellites.
- Determine dust and meteoroid distribution both in the vicinity of the rings and in interplanetary space.
- Study interactions between rings and Saturn's magnetosphere, ionosphere, and atmosphere.

## ICY SATELLITES

- Determine the general characteristics and geological histories of the satellites.
- Define the mechanisms of crustal and surface modifications both external and internal.
- Investigate the compositions and distributions of surface materials, particularly dark, organic rich materials and low melting point condensed volatiles.
- Constrain the satellites' bulk compositions and internal structures.
- Investigate interactions with the magnetosphere and ring systems and possible gas injections into the magnetosphere.

## MAGNETOSPHERE OF SATURN

- Determine the configuration of the nearly axially symmetric magnetic field and its relation to the modulation of Saturn Kilometric radiation (SKR).
- Determine current systems, composition, sources and sinks of magnetosphere charged particles.
- Investigate wave-particle intercations and dynamics of the dayside magnetosphere and the magnetotail of Saturn and its interaction with the solar wind, the satellites and the rings.
- Study the effect of Titan's interaction with the solar wind and magnetospheric plasma.
- Investigate interactions of Titan atmosphere and exosphere with the surrounding plasma.

### Targets of opportunity

## ASTEROID FLY BY

- Investigate an asteroid not seen by previous missions, possibly a new class of asteroid, thereby adding important new information to the study of asteroids.
- Characterize global properties; determine composition and morphology of the surface; investigate properties of the regolith.

## JUPITER

- Extend the time for studies of atmospheric dynamics and variable satellite phenomena – specifically Io volcanism –, beyond the period accessible to the Galileo nominal mission.
- Infer global atmospheric thermal structure and composition with instrumentation not carried by the Galileo Orbiter, complementing the local in situ measurements of the Galileo Probe.

- Explore the dusk side of the magnetosphere and intermediate regions of the magnetotail unvisited by previous spacecraft.
- Obtain the first high-resolution images of the Io torus.

## CRUISE SCIENCE

- Extend the sensitivity of composition measurements of interstellar ions by approximately three orders of magnitude.
- Investigate the behaviour of the solar wind during solar minimum, for comparison with earlier Galileo and Ulysses measurements.
- Extend spacecraft searches for gravitational waves.
- Extend studies of interplanetary dust to the orbit of Saturn.

### 3.1 Titan

The encounters with Titan by Voyagers 1 and 2 have revealed the unique character of Titan in the Solar System. In many respects, however, including the nature of the surface of the satellite, the complex photochemistry occurring in its stratosphere, the origin and evolution of the atmosphere, Titan is still an enigma. The Cassini Mission to Titan will address the following major topics:

#### 3.1.1 The Atmospheric Composition of Titan

##### The Tropospheric Composition

SCIENTIFIC PROBLEM: DETERMINE THE TROPOSPHERIC COMPOSITION OF TITAN, SPECIFICALLY THE RELATIVE ABUNDANCES WITH ALTITUDE OF CO, Ar, N<sub>2</sub>, H<sub>2</sub>, and CH<sub>4</sub>.

In contrast to the oxidized atmospheres of terrestrial planets, Titan's predominantly nitrogen atmosphere is chemically reduced. The low tropopause temperature, around 70 °K (see figure 3.1) acts as a cold trap for most of the gases that could be present in the troposphere and limits their amount in the stratosphere unless they are formed there. Methane has been detected in the stratosphere in amounts that cannot exceed 3 or 4%, but it could have a mixing ratio as high as 10% at the 95 °K temperature of the surface. The presence of argon is suspected for cosmogonic reasons, but it has not been firmly identified. Its abundance can be anywhere between 0 and 20% given the present uncertainty in the mean molecular weight.

Accurate determinations of argon and other noble gases (and of their isotopes) are crucial to test theories of the origin of the atmosphere (section 3.1.5). On the basis of photochemical models, carbon monoxide should be uniformly mixed throughout the atmosphere, but a comparison of ground based infrared and millimeter observations suggests an unexplained depletion of CO in the stratosphere.

Molecular hydrogen was found by Voyager to have a mixing ratio of about 0.2-0.3%, which is expected to be a product of CH<sub>4</sub> dissociation. Methane must condense in the troposphere if its partial pressure reaches the limit defined by the saturation vapor pressure law. The methane in the upper troposphere and ethane descending from the stratosphere would be the principal constituents of the cloud cover (if any) below the tropopause. The determination of the abundances of hydrocarbons near the surface would help to determine the nature of the condensed materials that must exist there (see Section 3.1.4). Collision-induced absorption by nitrogen, methane and

hydrogen contributes to a greenhouse effect that warms the surface to 95°K. A determination of the exact composition of the troposphere remains a key problem.

### The Stratospheric Composition of Titan

SCIENTIFIC PROBLEM: DETERMINE THE VERTICAL AND HORIZONTAL ABUNDANCE DISTRIBUTIONS OF TRACE HYDROCARBONS, NITRILES AND OXYGEN BEARING COMPOUNDS IN THE STRATOSPHERE. SEARCH FOR MORE COMPLEX ORGANICS INCLUDING POLYMERS IN GASEOUS AND CONDENSED PHASES.

In addition to  $\text{CH}_4$ , six hydrocarbons ( $\text{C}_2\text{H}_2$ ,  $\text{C}_2\text{H}_4$ ,  $\text{C}_2\text{H}_6$ ,  $\text{C}_3\text{H}_4$ ,  $\text{C}_3\text{H}_8$ ,  $\text{C}_4\text{H}_2$ ) and three nitriles ( $\text{HCN}$ ,  $\text{HC}_3\text{N}$  and  $\text{C}_2\text{N}_2$ ) have been detected in Titan's stratosphere. Oxygen compounds are represented by  $\text{CO}$  and  $\text{CO}_2$ . Except for  $\text{CH}_4$ ,  $\text{CO}$  and possibly  $\text{C}_2\text{H}_4$ , the amounts of the detected species are much higher than would be permitted by the saturation law at the tropopause temperature (see figure 3.1). This implies that they are formed at stratospheric levels and above from a complex photochemistry initiated by dissociation of methane, nitrogen and water vapor by solar UV photolysis and bombardment by cosmic rays and high energy electrons trapped in Saturn's magnetic field.  $\text{H}_2\text{O}$  has not been detected, but its presence, presumably from a meteoritic source, may be required to explain the formation of both  $\text{CO}$  and  $\text{CO}_2$ . Photochemical models predict

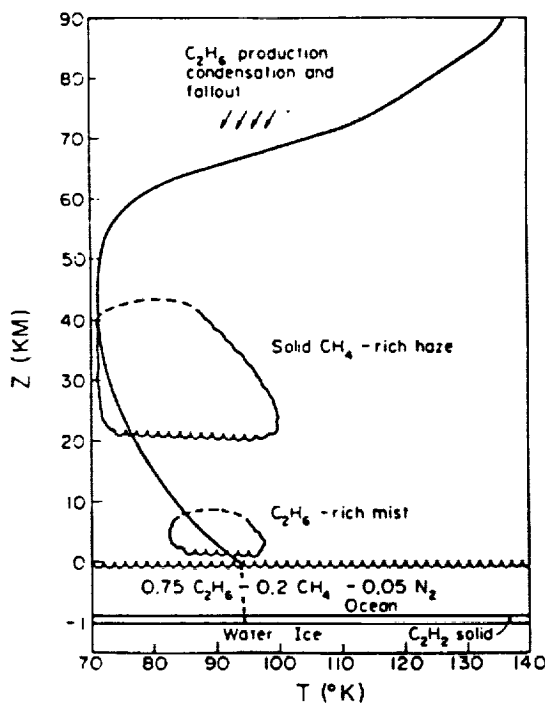


Figure 3.1: *Titan atmosphere thermal profile*

the formation of observed hydrocarbons from  $\text{CH}_4$  dissociation. Condensation of these products and other more complex compounds including polymers produce the aerosols which are responsible for the thick layer of smog surrounding the satellite. These aerosols absorb sunlight leading to a temperature inversion and an increase of the static stability of the stratosphere.

Because of the short radiative time constant at upper atmospheric levels, the latitudinal temperature field should be distributed symmetrically about the equator at the equinox. However,

an asymmetric temperature field was observed by Voyager at the 1 mbar level. Latitudinal distributions of aerosol albedos were also observed to be asymmetric by Voyager 1 suggesting that a complex interaction exists between thermal, chemical and dynamical systems. In particular, the remarkable change in the average albedo of the aerosols that occurs just at the satellite's equator is unique in the solar system and the distribution and composition of trace molecules and aerosols in Titan's stratosphere is thus a key problem. The acquisition of these data by Cassini at the local solstice compared with Voyager data acquired at equinox will permit a study of seasonal effects. Of particular interest is the distribution of the "parent" molecule  $\text{CH}_4$  which may not be uniformly mixed horizontally in the stratosphere.

One of the most important results of the Voyager encounter with Titan was the discovery of the three nitriles HCN,  $\text{HC}_3\text{N}$  and  $\text{C}_2\text{N}_2$ . The synthesis of complex organic compounds from mixtures of simple gases of reducing composition has been extensively studied in the laboratory since the famous experiments of Miller and Urey over 30 years ago. Indeed, laboratory experiments have demonstrated that HCN is a precursor of purines (in particular adenine) which are among the building blocks of the nucleic acids in living systems on the Earth. Similarly,  $\text{HC}_3\text{N}$  leads to pyrimidines which are also present in nucleic acids. Although the composition of Titan's atmosphere is certainly very different from that of the primitive Earth, (it is certainly much colder), abiotic organic synthesis in the atmosphere of Titan offers a test of how a Miller-Urey synthesis works on a planetary scale and what it produces over several billion years.

The key problem is thus to determine the abundances and distributions of organics in Titan's stratosphere, to establish the degree of complexity these compounds have achieved, and to determine the processes and pathways for producing them. A list of organic molecules likely to be present in Titan's atmosphere on the basis of laboratory experiments is given in Appendix 1.

Almost all expected organics condense at temperature conditions occurring in Titan's lower stratosphere. They must form droplets or solid particles that will precipitate with the larger aerosols to the surface where they will accumulate. Absorption of solar UV radiation by aerosols in Titan's upper stratosphere will lead to a temperature maximum somewhat similar to the terrestrial "stratopeak" caused by  $\text{O}_3$  absorption (Figure 3.1). At tropospheric temperatures the organics have very low abundances in the gas phase; they must pass through the troposphere as aerosols. The analysis of the composition of the aerosols in the lower stratosphere and/or the troposphere is thus of great importance.

## CAPABILITIES OF CASSINI

The Gas Chromatograph/Mass Spectrometer (GCMS) aboard the Titan Probe will measure the elemental and isotopic composition from about 170 kilometers altitude down to the surface. Through the use of a collector of aerosols, it will also be able to detect condensed organics. Search for organics in gaseous form and measurement of their vertical distributions can also be accomplished by this versatile instrument. However, fine-scale vertical distributions are much more in the purview of the Probe Infrared Laser Spectrometer (PIRLS), which can make continuous measurements. Its aerosol channel can measure the properties and distributions of smog particles, as well as snowflakes and raindrops. This instrument can also determine isotopic ratios and abundances of selected minor constituents. The far infrared-submillimeter spectrometer aboard the Orbiter will provide, at each encounter with Titan, the vertical distributions of HCN,  $\text{HC}_3\text{N}$ ,  $\text{C}_2\text{N}_2$  and of some hydrocarbons ( $\text{C}_4\text{H}_2$ ,  $\text{C}_3\text{H}_4$ ) at various locations on the satellite. It will also permit the detection of (or determination of upper limits for) new species such as other nitriles that are expected to be present in Titan's stratosphere (See Appendix 1). It will search for  $\text{H}_2\text{O}$  which should be present in the upper stratosphere as a result of meteoritic infall. The Orbiter microwave spectrometer will return

vertical distributions of HCN, HC<sub>3</sub>N, and CO over the 0-500 km altitude range. Various C, N, and O isotopes for these molecular species will also be determined. The UV solar flux penetration and the N<sub>2</sub> dissociation will be investigated with the UV spectrometer aboard the Orbiter. The thermal structure and the abundances of CH<sub>4</sub> and C<sub>2</sub>H<sub>2</sub> in the upper atmosphere will be obtained by observing the sun or a star occulted by the limb of Titan (as successfully done by Voyager). A combination of microwave and IR measurements may help to shed some light on the temperature structure in this altitude range.

### **3.1.2 Thermal Structure and Meteorology of Titan's Atmosphere**

#### **SCIENTIFIC PROBLEM: MEASURE WINDS AND TEMPERATURES; INVESTIGATE GENERAL CIRCULATION AND SEASONAL EFFECTS IN TITAN'S ATMOSPHERE**

Voyager infrared observations of Titan's stratospheric temperature field imply the presence of 100 m/s zonal winds, super-rotating some 5-6 times faster than the presumed 16-day rotation of the satellite body itself. If this inference is correct, then Titan's large-scale atmospheric motions may be in a class with those of Venus, which shows cloud-tracked wind speeds of comparable magnitude. Unlike Venus, however, Titan has a large (27°) obliquity more nearly comparable to that of the Earth and may, therefore, show substantial meteorological variations with changing seasons.

Progress in the study of these features requires direct measurements of the zonal winds, global mapping of temperature fields over a range of altitudes, and improved measurements of the vertical variation of clouds and aerosols. Zonal wind measurements will confirm the assumed balance between large-scale motions and north-south gradients in temperature previously applied to the analysis of Voyager infrared observations. Global maps of the temperature fields at an "instant" in time can then be used to extend the inference of thermal wind structure to other levels. The strength of seasonal fluctuations can be inferred by a comparison of Voyager and Cassini thermal measurements. Measured limits on the longitudinal variation of temperature will provide important information on the role of wave dynamics in the general circulation of Titan's atmosphere. Global mapping of the vertical and horizontal distribution of hydrocarbons and nitriles will provide important boundary conditions on dynamical models of the middle atmosphere. Measurements near the surface (see Section 3.1.4) will provide further important clues about the possible role of moist (hydrocarbon) convection in the Titan meteorology.

### **CAPABILITIES OF CASSINI**

The tropospheric thermal structure will be mapped at each encounter of the Orbiter with Titan by the far infrared submillimeter spectrometer and the microwave spectrometer. The stratospheric thermal structure will be studied by means of the microwave spectrometer and by a spectrometer operating in the middle infrared. A large number of tropospheric and lower stratospheric temperature profiles will be provided by radio-occultation experiments. The atmospheric Probe will measure the local temperature from 170 kilometers altitude down to the surface.

Doppler tracking of the Probe during its descent trajectory will provide a direct measure of the zonal winds at one location. Wind velocities will be determined to accuracies of 10 m/s or better at an altitude of 170 km and 5 m/s near the surface. Velocities in the upper stratosphere will be mapped using measurements of Doppler-shifted spectral lines by the microwave spectrometer. Measurements of latitudinal temperature gradients can then be used to extend the zonal wind mapping into the troposphere. The cloud structure along the descent trajectory will be observed by the descent imager and by the nephelometer aboard the Probe. These measurements, along with determinations of the vertical distribution of CH<sub>4</sub> by the Infrared Laser Spectrometer and the GCMS, will permit characterization of convective processes in the lower troposphere. Inference of

the net solar flux as a function of height by the descent imager will provide information on the vertical distribution of heat sources which drive the atmospheric circulation.

### 3.1.3 Titan Aeronomy and Interactions with Saturn's Magnetosphere

The ultraviolet spectrometers on Voyagers 1 and 2 have provided considerable information on Titan's upper atmosphere through a solar occultation and studies of the day-time airglow. The radio occultation experiment did not detect an ionosphere, giving an upper limit of 3000 electrons  $\text{cm}^{-3}$  a few degrees from the terminator. However, the nature of the interaction with the magnetosphere leaves no doubt that an ionosphere exists. The upper atmosphere is mostly  $\text{N}_2$ , with several percent of  $\text{CH}_4$  and a detectable amount of  $\text{C}_2\text{H}_2$ .  $\text{H}$  and  $\text{H}_2$  are probably present in the dayglow of Titan: although confined to the day side, it is 5-10 times brighter than what could be produced by the entire solar flux below 1000Å. Since the phenomenon is so mysterious, its investigation has a high priority. There is little doubt that the glow is excited by electrons with energies between 10 and a few hundred eV. Such electrons should be sought with in-situ instrumentation. These electrons are also the most likely source of Titan's ionosphere, rather than solar EUV radiation. Ionization produced by the interaction of these low energy electrons ( $\sim 100$  eV) will consist primarily of  $\text{N}_2^+$  and  $\text{N}^+$  as indicated from airglow observations. The principal ions in Titan's ionosphere, however, are expected to consist of nitrile (e.g.  $\text{H}_2\text{CN}^+$ ) and hydrocarbon (e.g.  $\text{CH}_3^+$ ) ions resulting from ion-molecule reactions between the originally formed  $\text{N}_2^+$  and  $\text{N}^+$  ions and  $\text{CH}_4$  present at ionospheric levels. Recombination of these ions will be a major source of HCN present in Titan's atmosphere. Jupiter's inner magnetospheric composition and energetics are known to be dominated by heavy ions of S and O ejected from Io. Ejecta from Titan (and other satellites) should similarly be important to Saturn's magnetosphere, though probably not dominant. A neutral torus of H atoms was detected by the Voyager Ultraviolet Spectrometer and  $\text{H}_2$  and N are expected as well, along with  $\text{H}_2\text{O}$  and O from the icy satellites.

## CAPABILITIES OF CASSINI

The Orbiter will carry a full complement of remote sensing and in situ aeronomy instruments. The UV spectrometer will examine the dayglow emissions, determine the global distribution of H around Titan, and map hydrocarbon distributions by observing stellar occultations. The ion and neutral mass spectrometer will determine the composition of the upper atmosphere, while the Retarding Potential Analyzer (RPA) and the Langmuir Probe (LP) will measure the density and temperature of electrons and ions. The latter investigation will include a study of the suprathermal electrons thought to be the source of the dayglow excitation/ionization in the upper atmosphere and the transport of momentum and energy in the ionosphere as function of height and local time. The Energetic Neutral Analyzer (ENA) will record energetic neutral ejecta from Titan populating the Saturn system. The plasma interaction between Titan and the Saturn magnetosphere is covered in section 3.5.3. Since most of the orbits pass through the upper atmosphere of Titan at an altitude down to 800 km, close to the ionization maximum, at least 30 separate sets of measurements will be accumulated over the four year lifetime of the mission. Repeated radio occultations and UV observations of occultations of the sun and stars by Titan's limb will add to this store of information. The mission design offers an opportunity to compare inferences from remote sensing observations with the "ground-truth" derived from periodic in situ measurements. From the Orbiter, these will reach as low as 800 km, and the Probe will carry a selected set to the surface. Thus the global coverage available from remote sensing can extend with confidence the localized but more detailed coverage provided by in situ experiments.

### 3.1.4 Titan Surface and Internal Structure

#### SCIENTIFIC PROBLEM: DETERMINE THE NATURE AND THE COMPOSITION OF THE SURFACE: INFER THE INTERNAL STRUCTURE OF THE SATELLITE.

The surface of Titan is masked by thick layers of aerosol. It is theoretically expected that Titan could carry large oceans of hydrocarbons, principally ethane and methane. The stratospheric production of hydrocarbons, nitriles and possibly other complex organics uses up methane, which is not recycled and therefore must be re-supplied, either by continuous outgassing from the interior, or by evaporation from a large liquid reservoir (an ocean), or both. A prime candidate for an ocean is liquid methane itself, but temperature gradients observed near the surface by Voyager do not correspond to theoretical wet adiabatic lapse rates implied by methane condensation. However, an ocean mainly composed of  $C_2H_6$  and containing large amounts of  $CH_4$  and dissolved  $N_2$  is consistent with observed temperature gradients and accounts for the persistence of  $CH_4$  in the stratosphere.

If any Argon is present in the atmosphere, it will easily dissolve in this ocean. On the other hand, it is possible that the topographic relief exposes solid crust that emerges from the ocean, covered in places by a thick layer of organics that continuously drop from the stratosphere and have accumulated since the formation of the satellite. Open questions include the existence, extent, depth and composition of the ocean. Titan's original surface may well have resembled those of Ganymede and Callisto - heavily modified by early, intense bombardment. How much of this cratering record remains and the extent of crustal tectonics and surface modification associated with the evolution of the atmosphere/ocean system is completely unknown at present.

The properties of Titan's interior are very poorly understood. Assuming that Titan consists of differentiated anhydrous chondritic rock and water ice, the density measured by Voyager ( $1.9\text{ g cm}^{-3}$ ) suggests that the satellite has a bulk composition of about 50% rock and 50% ices by mass, but the internal structure remains undefined. Even the rotational period of Titan has not been directly established.

### CAPABILITIES OF CASSINI

The radar aboard the Orbiter will disclose the nature of the surface (solid or liquid), the topography if any, and the rotational period of the satellite. The radar resolution should be sufficient to characterize the surface morphology and cratering record of any solid surfaces. The microwave spectrometer includes polarimetry observations of Titan for mapping of dielectric constant and surface roughness variations in order to distinguish ice/liquid regions and topographical variations. The imager aboard the Titan Probe will transmit pictures of the surface, and the near infrared spectrometer will analyze the composition of the surface. With additional data processing, as compared to what is required to fulfill its engineering function, i.e. altitude measurement, the radar altimeter on the Probe could complement the Orbiter radar by providing local measurements of surface roughness and reflectivity with high spatial resolution, ending at the landing site. Gravity measurements derived from trajectories of the spacecraft during the  $\sim 36$  scheduled encounters with Titan in the nominal four year duration of the mission will permit considerable improvements in constraints on interior models of Titan.

### Conditional Measurements if a Soft Landing Occurs

If the Probe survives its landing, further refinements are possible by conducting experiments on the surface. These experiments would be carried out on a best-effort basis; they are not mandatory within the mission guidelines. As examples, we point out the ability of an accelerometer readout just after impact to provide a measure of surface hardness; a picture by the Probe imaging system

that describes conditions in the immediate vicinity of the landing site, and measurements with the GCMS of surface composition afforded simply by heating one of this instrument's inlet systems. Dedicated surface science experiments -e.g. refractive index determination, X-ray Spectrometry, acoustic sounding- could make in situ measurements of the liquid or solid surface, given a soft landing and a sufficiently long radio relay link to the Orbiter.

### 3.1.5 Origin and Evolution of Titan's Atmosphere

#### SCIENTIFIC PROBLEM: DETERMINE THE ORIGIN OF N<sub>2</sub>, CH<sub>4</sub>, AND CO IN THE ATMOSPHERE

Voyager observations exclude the possibility that Titan's atmosphere was formed by direct retention of gases from the primitive solar nebula or from the Saturn sub-nebula (including an extended atmosphere of the forming planet). In these cases, the present Ne/N ratio in the atmosphere should be close to 1, leading to a mean molecular weight significantly less than the value of 28 inferred from observations. It is thus reasonable to think that Titan's atmosphere was formed by outgassing of volatiles from planetesimals that formed the satellite.

At the pressures and temperatures predicted for Saturn's subnebula, NH<sub>3</sub> and CH<sub>4</sub> were probably the dominant N- and C- containing gases close to the planet, with N<sub>2</sub> and CO more important at larger distances. The degree of radial mixing is difficult to model, in part because solid materials must have carried some of these gases. Both NH<sub>3</sub> and H<sub>2</sub>O would have condensed and solid H<sub>2</sub>O can trap large amounts of CH<sub>4</sub>, NH<sub>3</sub>, N<sub>2</sub>, CO and Ar, either as clathrates or simply through adsorption if the ice is in the amorphous form. The N<sub>2</sub> we now see in Titan's atmosphere may therefore have come either from N<sub>2</sub> or NH<sub>3</sub> liberated from the icy planetesimals that formed the satellite. In the second case, the surface temperature on Titan must have been about 150° K to allow a sufficient vapor pressure of NH<sub>3</sub> so that efficient photolysis and production of N<sub>2</sub> could occur.

On the other hand, the assumption that Titan's atmosphere was directly formed from outgassing of N<sub>2</sub> implies that the planetesimals that formed the satellite contained more N<sub>2</sub> than NH<sub>3</sub>, in disagreement with some models. Similarly, the tiny quantity of CO in Titan's atmosphere may come from the oxidation of CH<sub>4</sub> by oxygen derived from infalling ice particles or it may be primordial, released from the ices forming the satellite.

Measurements of noble gas abundances and isotopic ratios provide a means for discriminating between the primordial and photochemical models. The presence of a substantial amount of non-radiogenic argon (<sup>36</sup>Ar and <sup>38</sup>Ar) and other noble gases would support the idea that the N<sub>2</sub> and CO we find in Titan today were brought in by the ices, either as clathrates or as adsorbed monolayers.

The relatively high value of D/H determined by ground-based measurements already argues for this scenario, since the conversion of CO and N<sub>2</sub> to CH<sub>4</sub> and NH<sub>3</sub> should be accompanied by equilibration of D/H to the solar nebula value. On the other hand, a marked deficiency of primordial argon would support models suggesting that the nitrogen originated in the form of condensed NH<sub>3</sub>. In that case, the value of D/H would have to be explained in terms of chemical fractionation and/or escape processes operating in the upper atmosphere. The latter can also be studied through measurements of <sup>12</sup>C/<sup>13</sup>C and <sup>14</sup>N/<sup>15</sup>N.

## CAPABILITIES OF CASSINI

The GCMS aboard the Titan Probe will measure noble gas abundances and their isotopic ratios. It will also determine isotope ratios for the other abundant elements. The use of the gas chromatograph in combination with the mass spectrometer allows a clean discrimination between

molecules and their fragments that would otherwise have overlapping charge-to-mass ratios. Additional discrimination is provided for some species by using the Probe Infrared Laser Spectrometer (PIRLS).

## 3.2 Saturn

Despite the apparent similarities between the two largest planets in the Solar System, the Voyager encounters have revealed that Saturn is significantly different from Jupiter. The study of each planet will clearly benefit from comparative observations of the other. Following the Galileo mission to Jupiter, Cassini will allow us a much deeper level of comparison between the two largest planets in our solar System. The reasons for apparent differences in internal structure and general circulation for example, can be studied in ways beyond the reach of the Voyager spacecraft. The potential for advancing our knowledge is further enhanced by the fact that Cassini will arrive at Saturn during a different season from that of the Voyager encounters. Furthermore, the flyby of Jupiter, *en route* to Saturn, allows a direct comparison of observations of the two planets with the same suite of instruments, calibrated at Jupiter by the Galileo entry Probe.

### 3.2.1 The Interior

#### SCIENTIFIC PROBLEM: CONSTRAIN THE EXTENT OF INTERIOR STRUCTURE DIFFERENTIATION AND ITS COUPLING TO THE ATMOSPHERIC CIRCULATION.

Voyager observations of Saturn reveal an outer envelope depleted in helium with respect to a solar composition mixture and a strong internal heat source that is larger than can be accounted for by homogeneous cooling models. (These assume an evolution of internal structure essentially similar to a low mass submain sequence dwarf star, and are generally consistent with the observed heat balance of Jupiter and the estimated age of the solar system). The available Saturn data have been interpreted as indicative of a differentiated interior, with the excess heat supplied by the downward migration of helium into the metallic hydrogen interior. (See Figure 3.2). According to some model scenarios, the early bombardment of Saturn by small rock-ice bodies may have significantly affected its evolutionary history with an enrichment of heavy molecular species. Although inaccessible to direct observation, improved measurements of the shape of Saturn's figure, its gravitational moments, tropospheric composition, and latitudinal temperature and heat balance will all offer important constraints on the interior models. These in turn will contribute importantly to understanding Saturn's general atmospheric circulation as well as the peculiar symmetry of its dipolar magnetic field.

## CAPABILITIES OF CASSINI

Saturn's gravitational field will be measured throughout the Cassini mission by radio tracking of the Orbiter trajectory at a variety of inclinations. The radius of Saturn at low and high latitudes will be determined by a series of radio occultation measurements. The far infrared spectrometer and microwave instruments will retrieve temperatures and their variation with latitude at the top of Saturn's convection zone. Combined with radio-occultation retrievals, the infrared measurements will provide a more accurate determination of the helium abundance. Thermal emission measurements by the composite infrared spectrometer (CIRS) and observations of reflected solar energy by the near infrared spectrometer will be used to refine our knowledge of the global energy balance.

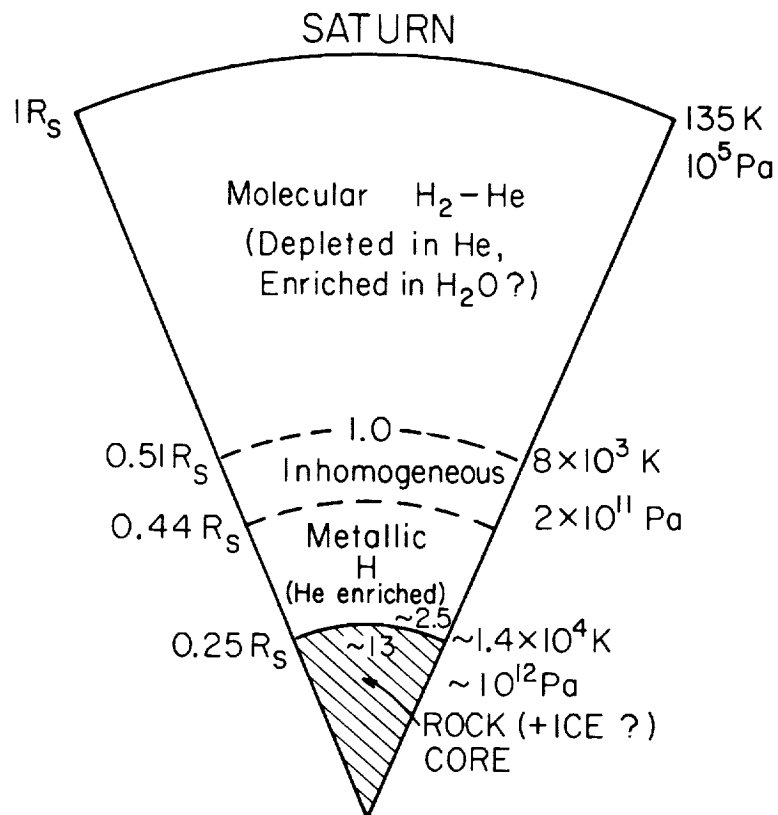


Figure 3.2: Schematic model of the Saturn interior. (Courtesy D.A. Stevenson).

### 3.2.2 Thermal Structure and Composition

SCIENTIFIC PROBLEM: DETERMINE TROPOSPHERIC AND STRATOSPHERIC TEMPERATURES AND THEIR VERTICAL VARIATION AT ALL LATITUDES. STUDY SEASONAL VARIATIONS OF TEMPERATURE. DETERMINE ORTHO-PARA RATIOS OF MOLECULAR HYDROGEN AT VARIOUS LOCATIONS ON THE PLANETARY DISK. INFER VERTICAL DISTRIBUTIONS OF CONVECTION TRACERS. INFER VERTICAL AND LATITUDINAL DISTRIBUTIONS OF HYDROCARBONS IN THE STRATOSPHERE. MEASURE THE HELIUM ABUNDANCE AND D/H RATIO. SEARCH FOR NEW ATMOSPHERIC CONSTITUENTS.

Voyager IRIS and Radio Science measurements have provided retrievals of vertical temperature structure at pressure levels between 1 and 1000 mbar. The Voyager IRIS data revealed latitudinal gradients in temperature in Saturn's upper troposphere which are strongly correlated with the cloud-tracked winds, but could not be measured at higher levels. A north-south hemispheric asymmetry of temperature was also observed, indicating a seasonal response (at a time near the equinox) with moderate thermal inertia. The altitude range of the retrieval of tropospheric profiles from Voyager IRIS data was limited by the lack of measurements below 200 wavenumbers ( $\lambda > 50\mu\text{m}$ ). Ground-based microwave observations also show strong latitudinal variations in tropospheric temperatures at pressure levels of a few bars, including a pronounced warm band at northern mid-latitude. These are difficult to interpret as kinetic temperatures owing to uncertainties in the  $\text{NH}_3$  abundance, but may be diagnostic of vertical motions.

IRIS determinations of the ortho-para ratio in Saturn's upper troposphere are uniformly near the equilibrium value, but may not have been sufficiently precise to detect small latitudinal variations. The measured value for the He mole fraction for Saturn is significantly less than that obtained

for Jupiter, but is still somewhat uncertain. An improved determination will be important for cosmogonical and interior structure studies of the planet (see 3.2.1).

IRIS determinations of the CH<sub>4</sub> abundance in the stratosphere indicate an enrichment of carbon amounting to approximately four-and-a-half times the solar abundance value. Limited information on the deep tropospheric abundance of NH<sub>3</sub> has been obtained from ground-based microwave measurements as well as from IRIS spectra. Indications of an NH<sub>3</sub> abundance near the saturation limiting value at 500-700 mbar were provided by Voyager radio occultation data. Conflicting results have been obtained for the stratospheric distribution of PH<sub>3</sub>. Various hydrocarbon constituents, such as C<sub>2</sub>H<sub>2</sub>, C<sub>2</sub>H<sub>6</sub>, C<sub>3</sub>H<sub>4</sub>, and C<sub>3</sub>H<sub>8</sub> have been detected in Saturn's stratosphere, but with only moderate spectral resolution and signal-to-noise ratio, which has prevented an accurate assessment of their abundances. Several other as yet undetected molecules are expected to be present in Saturn's atmosphere. If detected they would offer important clues to Saturn's atmospheric chemistry.

## CAPABILITIES OF CASSINI

Spectral measurements from 10 to 1400 cm<sup>-1</sup> (7 to 1000  $\mu$ m) will permit the determination of atmospheric composition and thermal structure between 100 and 1000 mbar as well as between 0.1 and 10 mbar. The planned 2002 arrival date will permit the measurement of atmospheric conditions near the solstice, providing an important comparison with Voyager observations. Good horizontal mapping and some vertical information on the ortho-para hydrogen ratio will be available from the Composite Infrared Spectrometer, partly by the assessment of the relative strength of the H<sub>2</sub> - H<sub>2</sub> and H<sub>2</sub>-He collision induced absorption lines. The hydrogen dimer (H<sub>2</sub>)<sub>2</sub>, detected by Voyager, will also be spectrally analyzed at 16 and 28  $\mu$ m, providing a very sensitive evaluation of its latitudinal variation. These determinations will importantly constrain the adiabatic lapse rate at deeper levels and also provide useful diagnostics of vertical motions. Latitudinal variations of methane emission will be measured in a limb-sensing mode at levels up to 1 microbar, which will yield the kinetic temperature with a vertical resolution of a scale height. Vertical and horizontal distributions of C<sub>2</sub>H<sub>2</sub>, C<sub>2</sub>H<sub>6</sub>, and other hydrocarbons can also be obtained by limb sounding in the middle infrared.

Radio occultation measurements will provide an independent retrieval of thermal profiles at selected locations, permitting a determination of the He/H<sub>2</sub> ratio in conjunction with the infrared measurements.

Ammonia (NH<sub>3</sub>) cloud optical depths will be mapped using spectral regions near 200 and 1000 wavenumbers and in the near infrared. Microwave radiometric observations at 3 cm will provide good horizontal mapping of the ammonia abundance. The near infrared spectrometer will yield further important constraints on cloud properties including particle sizes and relative heights of different cloud layers.

Information on the thermal structure and composition of the upper atmosphere will be acquired by observing the Sun or a star at the planetary limb with the ultraviolet spectrometer. The high speed photometer will measure high altitude atmospheric densities. Soundings of the deep atmosphere from 2-10 bar will be obtained by microwave radiometry. The opportunity for variable viewing geometry and, by use of the telecommunications dish, for high spatial resolution observations will aid in separating kinetic temperature and variable abundance effects.

### 3.2.3 Atmospheric Dynamics and General Circulation

SCIENTIFIC PROBLEM: PERFORM CLOUD-TRACKED WIND AND CORRELATED TEMPERATURE MEASUREMENTS AT ALL LATITUDES WITH SUFFICIENT TIME AND LONGITUDE COVERAGE TO ANALYZE EDDY-MEAN FLOW EXCHANGES. CONSTRAIN

## GLOBAL SCALE TEMPERATURE-DENSITY GRADIENTS AT SUB-CLOUD LEVELS. MEASURE VERTICAL WAVE PROPAGATION AT SELECTED LATITUDES.

Voyager imaging observations of large-scale motions on Saturn revealed a superrotating equatorial jet and at higher latitudes an axisymmetric and apparently long lived pattern of counter-flowing jet streams. Although these features of the atmospheric circulation are qualitatively similar to observed motions on Jupiter, the Saturn jet streams are a few times stronger, somewhat wider, and more dominantly prograde, measured with respect to the planet's rotation period. Two extreme model interpretations have been suggested for the general circulation of both giant planets. In one view the observed jet streams are the manifestation of counterrotating cylinders of convection, concentric with the planetary spin axis, and extending deep into the interior of the molecular hydrogen envelope. In the other view the observed motions are confined to a relatively shallow layer extending no more than a few scale heights below the cloud tops and supported by strong latitudinal gradients in temperature and composition. Further measurements will be required to distinguish between the two models. The Voyager observations of Saturn's high wind speeds and its enormous equatorial jet provide an even greater challenge to theoretical understanding than the observations for Jupiter and have served to emphasize the distinction between the two extreme models. The diagnostic assessment of wave-mean flow exchange and cloud-temperature correlations are also more problematic for Saturn. Present knowledge cannot provide definitive answers to the most fundamental questions about the nature of the Saturn meteorology. How deep do the jet streams extend into the interior? How does the deep internal convection couple to the motions at the cloud tops? Do small scale horizontal eddies feed the large scale jets or do the jets support the eddies? What is the role of moist latent heat release and ortho-para hydrogen conversion in the global circulation balance?

Progress in answering these questions will require more elaborate measurements extended to longer time frames and other vertical levels of the atmosphere than were available from the flyby Voyager encounter. Voyager infrared measurements of north-south gradients in temperature just above the cloud tops imply a reduction of the wind speeds with altitude toward a net west-to-east directed flow. The extension of these measurements to higher levels of the upper stratosphere will offer important clues to the circulation balance at deeper levels. Long wave microwave sounding combined with radio occultation measurements of vertical temperature profiles will place important constraints on the horizontal gradients in temperature and composition. Measurements of the ortho-para hydrogen ratio and its variation with latitude will provide important information on the thermodynamic state of the wind layer and diagnostics of the vertical motion field. Measurements of zonal mean and eddy scale cloud velocities over several months of observations will characterize the zonal momentum balances. Studies of the motion of small scale cloud features and waves will serve as an additional diagnostic of the wind structure at deeper levels.

## CAPABILITIES OF CASSINI

The Composite InfraRed Spectrometer (CIRS) will provide horizontal temperature gradients in the upper troposphere and stratosphere which can be used in thermal wind analyses of the Saturn jet streams. This will permit characterization of the zonal wind field in both the troposphere and stratosphere, including inference of the vertical jet decay at high levels. Microwave radiometry at 10 cm can provide a measure of horizontal gradients below the cloud deck, imposing constraints on shallow layer circulation models. Zonal thermal structure will be used to analyze tropospheric wave modes, while a combination of zonal structure and vertical structure with a resolution better than 1 scale height obtained from limb sounding and radio occultations will provide information on stratospheric wave propagation. These results, combined with determinations of the latitudinal

ORIGINAL PAGE  
BLACK AND WHITE PHOTOGRAPH

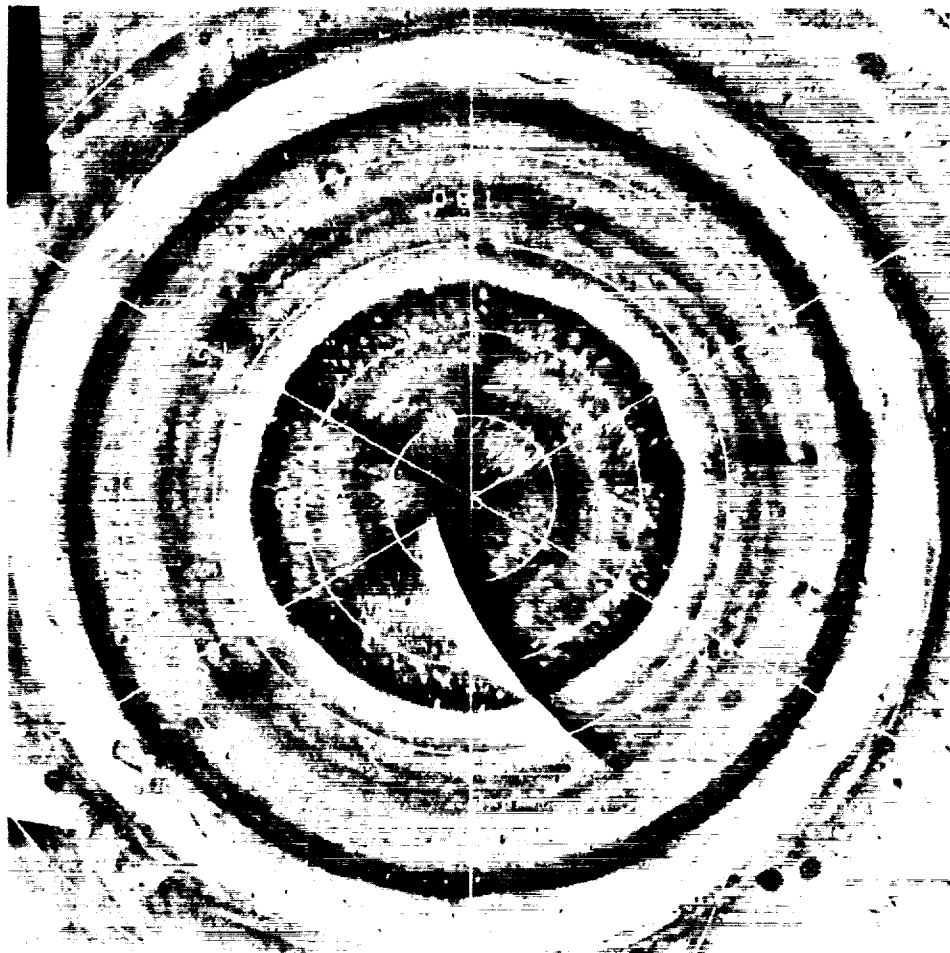


Figure 3.3: *Polar projection mosaic of Voyager images of Saturn's northern hemisphere. (Courtesy of D.A. Godfrey).*

variations of hydrocarbon abundances, can be used to define stratospheric circulation and transport. Extended visible imaging observations during day-side petal orbits of the Saturn disk will provide measurements of zonal winds in the upper troposphere and the localized motion of atmospheric waves and vortices (Figure 3.3). Radio occultation measurements will provide data on the figure of Saturn, which, combined with improved determinations of the gravitational moments, will place important constraints on the rotational state of Saturn's interior.

### 3.2.4 Saturn's Ionosphere

**SCIENTIFIC PROBLEM: DETERMINE FROM RADIO OCCULTATIONS THE DIURNAL VARIATION OF IONIZATION. ESTABLISH THE ROLE OF PLASMA TRANSPORT AS WELL AS CHEMICAL PROCESSES ASSOCIATED WITH H<sub>2</sub>O FROM THE ICY RINGS.**

Radio occultation observations from Pioneer 10 and Voyagers 1 and 2 have established the existence of an ionosphere with a peak density of  $\sim 2 \times 10^4 \text{ cm}^{-3}$ . In addition, the Voyager Planetary Radio Astronomy experiment (PRA) has provided an indirect measure of the diurnal variation of the peak ionospheric density through its observations of Saturn Electrostatic Discharges (SED), thought to originate from lightning in the lower atmosphere. The SED frequencies (which necessarily exceed the electron plasma frequency) also constrain the allowable diurnal variation to a maximum of greater than  $10^5 \text{ cm}^{-3}$  around local noon and a minimum of less than  $10^3 \text{ cm}^{-3}$  near dusk. Although these variations are suggestive of ion pair production by solar extreme ultraviolet radiation, there is an indication of rising electron densities during the night which is inconsistent with a simple photochemical explanation. It has been suggested that ion loss processes arising from conversion of H<sup>+</sup> to H<sub>2</sub>O<sup>+</sup> and H<sub>3</sub>O<sup>+</sup>, may be driven by an injection of H<sub>2</sub>O from the icy rings. The possible role of plasma transport processes in controlling the height of the ionospheric peak also remains an unsolved problem.

## CAPABILITIES OF CASSINI

Repeated radio occultations of Saturn by the Cassini Orbiter are expected to provide a wealth of new ionospheric data. Ion chemistry (possibly including H<sub>2</sub>O transport) can be studied by the UV spectrometer. SED's containing ionospheric information will be observed by the plasma/radio wave experiment. Measurements of the polar wind and possible field aligned flows from the ionosphere by the plasma instrument can provide direct information about the ion composition of Saturn's ionosphere at high latitudes. Altogether, these data will contribute substantially to understanding the origin and variability of Saturn's ionosphere.

## 3.3 Saturn's Rings

Saturn's rings are composed of countless orbiting particles with sizes primarily between a few centimeters and ten meters, along with a sprinkling of fine dust. The ring particles are mostly icy material, but contain impurities of an unknown nature, the abundance of which varies regionally and locally. These impurities are most abundant in the inner, or C ring and in the Cassini division between the dominant A (outer) and B (middle) rings (see Figure 3.4). The F ring is a little understood, clumpy strand or belt of objects at the outer edge of the main rings, where Saturn's disruptive tidal effects are beginning to weaken. The constant bumping and jostling by the ring particles, and the minute, but steady gravitational influences of their largest members, determine the structure of the main rings. Many of the interactions currently seen in Saturn's rings must have occurred in the particle disk which preceded the formation of the planets from the solar nebula.

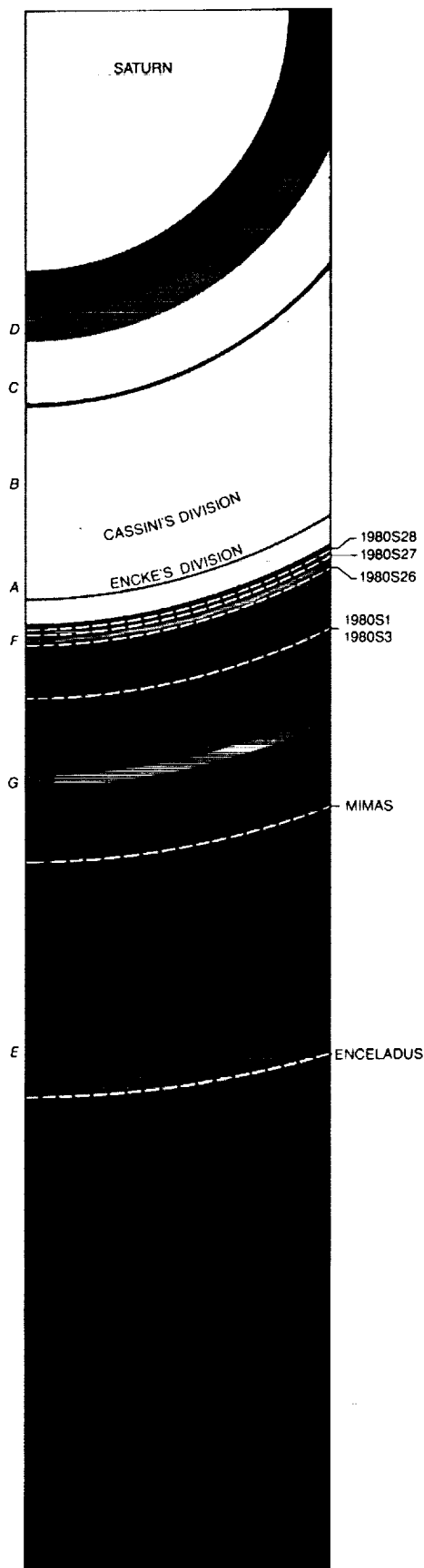


Figure 3.4: *Schematic of Saturn's ring system showing the main (A, B, C) rings, the Cassini Division, and the tenuous D, E and G rings, along with the mysterious "kinky" F-ring and its associated shepherding satellites Pandora and Prometheus.*

This makes the study of the forces at work within Saturn's rings today an especially appealing challenge.

The Voyager encounters with Saturn profoundly affected our outlook on this already archetypal system. The vast amount of unexpected and puzzling structure seen in the rings of Saturn has provided several important theoretical breakthroughs and still shows no sign of exhaustion. We now know that all four outer planets possess retinues of rings and ringmoons, which show a hauntingly similar trend from a few large moons far from the planet, through smaller and more numerous satellites closer to the planet, grading into and intermingling with a ring system. Saturn provides us with the ultimate prototype of a planetary ring-ringmoon system, containing elements which span the entire range of phenomena seen in the ring systems of Jupiter, Uranus, and Neptune, as well as its own wealth of unique structure. It is unlikely that we will understand the accretion of planets from the primordial planetary disk until we can answer the questions posed by the diversity of planetary ring structure. However, the answers to these key questions will not be found in the Voyager data set or by observations from Earth or Earth-orbiting telescopes.

The Cassini Mission will answer most of our outstanding questions and provide a vital data set for future study of particle disks. The makeup and spatial variation of the widespread, but unevenly distributed non-icy "impurities" will be determined. Also, the size distribution of ring particles ranging from microscopic grains to asteroid-sized moonlets will be measured throughout the ring system. These new discoveries will provide strong constraints on the formation of the ring system. It finally will be possible to probe the thickest and most complex ring regions, which were opaque to the Voyager experimenters due to the geometry and sensitivity of their observations. It will be possible to separate radial, azimuthal, and temporal variations in ring structure, providing crucial constraints on the nature of the dynamical processes involved. One of the most profound puzzles of the ring system is the short lifetime of the rings ( $10^7 - 10^8$  yr) inferred from different aspects of their observed properties. Are Saturn's rings (and other ring systems) really much younger than the Solar system? Cassini observations of satellite orbital evolution, meteoroid flux, ring composition, and other currently unknown elements will solve this puzzle. These and other fundamental advances are discussed in more detail below.

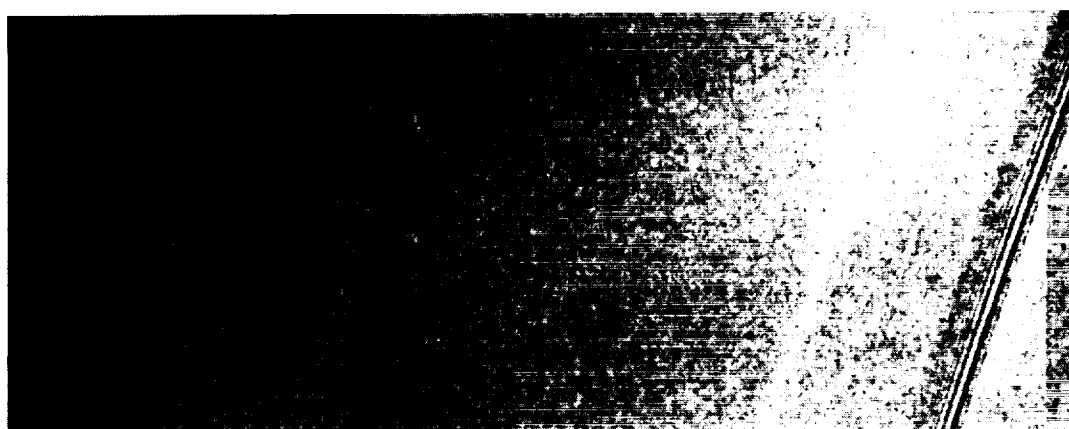
### 3.3.1 Structure of the main rings, and dynamical processes to be investigated

One of the most memorable aspects of the Voyager discoveries is the structural complexity and variety seen in the rings of Saturn (see Figure 3.5). Voyager images revealed structure everywhere on scales as fine as several kilometers, which differs from region to region and sometimes changes with viewing geometry. One full stellar occultation and one radio occultation, each with roughly 100 meter resolution, revealed abundant additional structure on even smaller scales. Study of much of this fine structure is only now beginning. It appears that the form of the structure seen in a region varies with the optical depth, or particle area fraction, in the region. The optically thinnest regions contain empty gaps with sharp edges, often at resonances, and isolated opaque ringlets similar in some ways to the rings of Uranus. Some narrow ringlets are incomplete strands which may be multiple, kinked or crossing, possibly similar to the "ring arcs" of Neptune. The optically thickest regions are characterized by an irregular fine structure which is manifested sometimes in optical depth fluctuations, sometimes in particle albedo variations, and possibly sometimes both. It is not yet clear whether this structural variability implies different processes, or merely the operation of similar processes under different conditions. In the discussion below, it will become clear that ring structure is strongly dependent on the distribution of "ringmoons": small, asteroid-sized satellites which lie both within and around Saturn's main rings, as well as sharing the orbits of Saturn's major satellites.

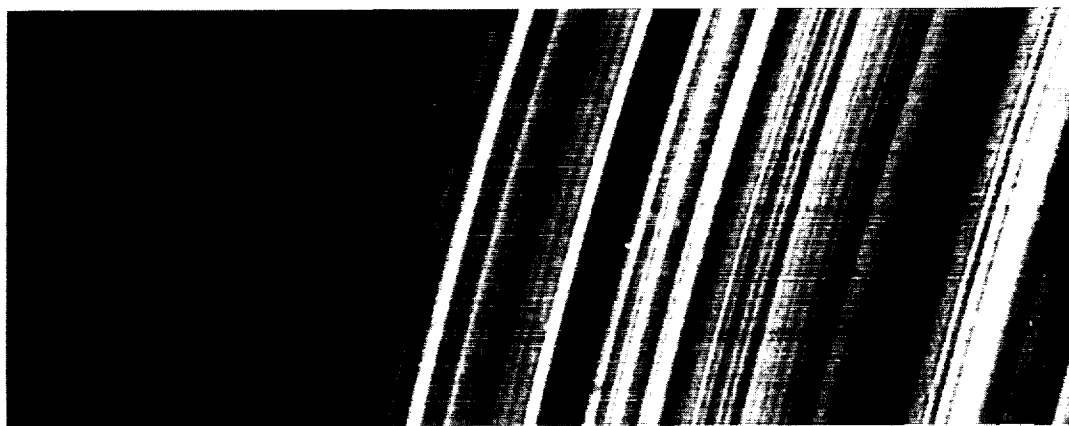
#### Spiral density waves

It is now well established that Saturn's rings contain many examples of spiral density waves and spiral bending waves driven at orbital resonances with Saturn's close-in satellites, or ring moons. Great progress has been made since the Voyager encounters in the understanding of these features. We now have good theoretical models for the formation by ringmoons and damping by viscosity of strongly forced spiral waves such as seen in Saturn's main (A, B, and C) rings. We know how to use observed wave profiles to measure the local surface mass density and viscosity. It may even be that traveling waves in the planet's atmosphere or envelope could drive waves seen in the C ring; confirmation and study of these relationships could provide unique insight into the interior structure of the planet itself. Theoretical advances resulting from studies of spiral waves are also directly applicable to several other astrophysical problems such as the arms of spiral galaxies and planetary accretion in the protoplanetary disk. Calculations of the angular momentum transported by observed spiral density waves imply timescales which are so short ( $10^7 - 10^8$  years) that we are puzzled as to the continued existence of the ring-ringmoon system. However, important uncertainties remain because of limitations in the data. For instance, a full understanding of the transport of material by waves requires a better measurement of the density in the very narrow and opaque crests of the waves than is attainable from Voyager data.

The expansion of the orbits of the ringmoons, caused by the torques exerted on them by density waves in the A ring, should occur at such a high rate that, in the time span between the Voyagers and Cassini, the mean motion of the F ring shepherding satellites, for instance, should be changed by an observable amount. Observations of the Voyager quality in conjunction with the earlier existing Voyager and planned Space Telescope observations, would be capable of detecting the predicted change. The added ability of Cassini to repeatedly image all orbital longitudes will greatly improve the accuracy of the measurements by eliminating eccentricity as an uncertain parameter, and will provide a definitive constraint on this intriguing hypothesis. If the ringmoons are found to be evolving outwards on such a timescale, it will imply that they and/or the rings must be much younger than the rest of the solar system, with deep implications for our understanding of the whole Saturnian system.



A



B



C

Figure 3.5: *Typical structure in each of the 3 classical ring regions. The A ring (top) is generally featureless except for regular trains of spiral density and bending waves at resonances with known moons. The B ring (middle) shows a bewildering confusion of irregular structure which seems to represent independent fluctuations of both optical depth and particle albedo. The C ring (bottom) contains broad plateaus and empty gaps which harbor narrow, Uranian-type eccentric ringlets; no shepherding moons have been found in these gaps, and the plateaus remain a mystery.*

## Moonlets and Shepherding

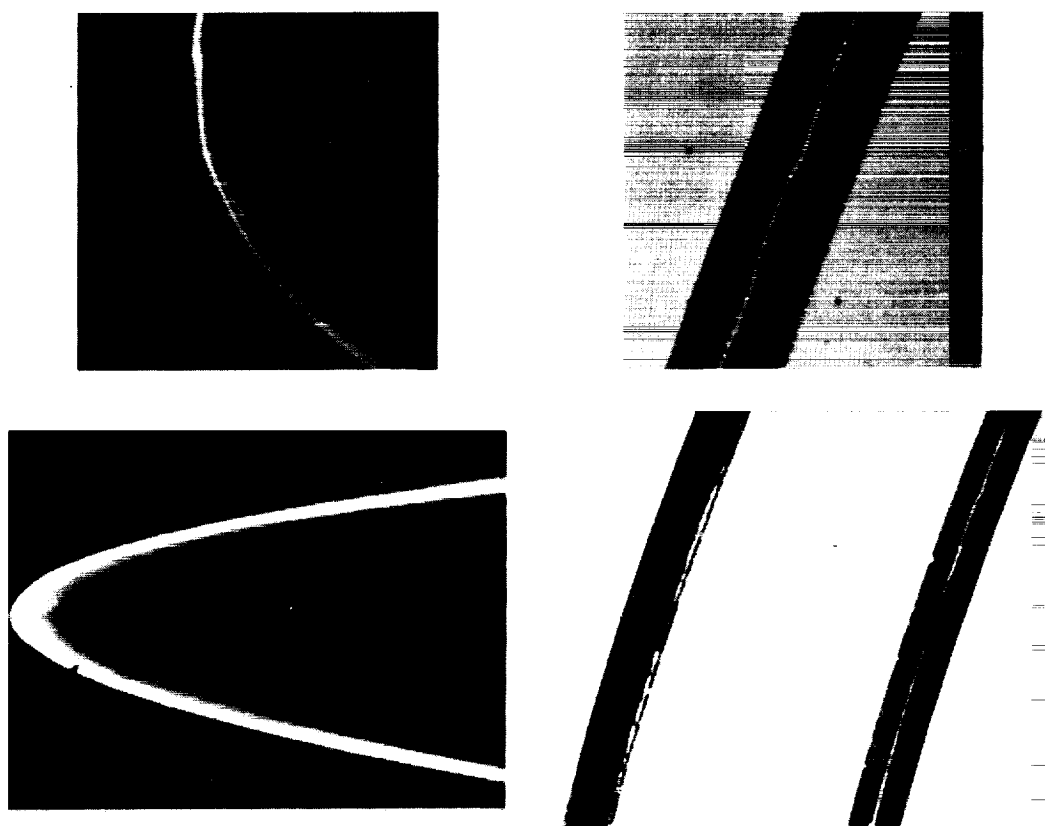
The physics of local ring-ringmoon gravitational interactions, or "shepherding", has also taken great steps since Voyager. However, many important problems remain. The F ring, for instance, usually described as a "bizarre anomaly of nature", is now believed to be strands of ring particles undergoing gravitational impulses from nearby moons in eccentric orbits. However, whether the nearby ringmoons Pandora and Prometheus are able to account for the observed structure is uncertain, and the multiplicity of strands is not understood. We now have strong indirect evidence that the same sort of process, involving at least one embedded moonlet, is active in the Encke Gap in the A ring (figure 3.6): perturbations, or "wakes", predicted along the edges of the gap due to such a moonlet have been observed in images and in the stellar and radio occultation data. However, the moonlet itself is not detectable in the Voyager images because of the limited high-resolution coverage. In fact, no moonlets have yet been directly observed within the F ring or main ring system, so this process remains an hypothesis, despite all the circumstantial evidence. Consequently, about a dozen clear gaps, good candidates for embedded moonlets, need to be explored in more detail both with direct imaging and multiple stellar and radio occultations. An adequate characterization of the azimuthal variation of the wakes caused by such moonlets requires many occultation traces over a range of longitudes and times. It is possible that the 2000 km wide zone between the F ring "shepherds" contains, in addition to the very narrow F ring itself, numerous km-sized fragments too small to be imaged by Voyager. Cassini would provide the necessary time and sensitivity needed to explore this region fully. It is near the edge of Saturn's "Roche Zone" and could be illustrating the transition between rings and moons. It may be that interactions between members of such a population replenish or confine the incomplete ring arcs known to orbit Neptune and possibly the rings of Uranus as well.

## Irregular Structure

One of the biggest outstanding problems is the irregular fine structure seen in the optically thickest parts of the A and B rings. This structure is manifested in fluctuations of optical depth and particle albedo, which may or may not be correlated, on all radial scales down to our resolution limits. This structure changes appearance with illumination and viewing geometry and also with azimuth around the ring. Although several hypotheses have been advanced to explain it, some involving small embedded moonlets, none is currently capable of explaining the vast complexity of this structure. For instance, it may be that the ring material undergoes an instability between "gas-kinetic" type viscosity and "liquid" type viscosity in these regions. In spite of the fact that it covers the majority of the area and mass of the rings, this is unfortunately the least well sampled of all structures because of its high optical depth. The Voyager radio occultation in particular was rendered almost useless in these regions because of the very small elevation angle of the Earth-spacecraft line at the time of the flyby and the long ensuing path length through the rings. Many occultations and extensive imaging over a wide range of observing geometries and time, and with much higher sensitivity than provided by Voyager, will be necessary to deconvolve radial, azimuthal, and possibly temporal variations of the irregular structure.

### 3.3.2 Composition and size distribution of the ring material

One of the most important constraints on the origin and evolution of the rings is the composition of the ring material. Voyager confirmed that the classical ring regions differ not only in their characteristic structure, but also in the brightness and color (and probably therefore composition) of their constituent particles. It is known from ground-based infrared, radio and radar observations



ORIGINAL PAGE  
BLACK AND WHITE PHOTOGRAPH

Figure 3.6: *Narrow, kinky ringlets of similar type are seen both in the F Ring (left pair) and the Encke gap in the A ring (right pair). These kinky ringlets are suggestive of nearby, asteroid-sized moonlets, but the details of their structure are not understood and no moonlets have been directly detected.*

that the A and B ring particles are primarily icy. However, their colours are more reddened than pure ice, and whole-ring reflection spectra display weak absorption features probably caused by silicate material. Voyager high-resolution color images reveal global color and brightness variations that are sometimes abrupt and sometimes gradual, as well as small-scale color and brightness variations. These differences probably imply variations in the (possibly quite small) local content of rocky or carbonaceous material; however, it is not known whether the impurities come from external bombardment by primitive carbonaceous objects, or contamination by internal fragments of differentiated and subsequently disrupted parent objects. It is of great scientific importance to map out the distribution of this non-icy material, and to distinguish between carbonaceous and silicateous impurities, in order to constrain hypotheses of ring, satellite, and even planetary origin.

The size distribution of the ring particles, as inferred primarily from Voyager radio and stellar occultation observations, is consistent with a broad power-law dependence between radii of several microns and a few meters; much of the surface area is contained in the centimeter to meter size range, and nearly all of the mass is in the form of the largest (meter-sized) particles. Direct determinations of the form of the particle size distribution, from Voyager observations of the radio signal scattered by the rings, have only been obtained as averages over spatial scales of thousands of kilometers, and only in regions of moderate-to-low optical depth (excluding, for example, the entire B ring). Nevertheless, these and complementary, but less direct, inferences from the Voyager stellar occultation data indicate significant variations of the maximum and minimum ring particle sizes on both global and local spatial scales. It has also been suggested that the sizes measured are merely those of transient and fragile groupings of smaller particles. The detailed shape of the ring particle size distribution could provide important constraints on the processes of accretion and destruction in the rings, as well as clues to similar processes which controlled the accretion of planetesimals in the protoplanetary nebula. An important objective of Cassini is thus to characterize, to the greatest extent feasible, the size distribution of ring particles and to correlate variations in the size distribution with location, optical depth, particle composition, and possibly even time.

The broad, diffuse E and G rings are apparently composed primarily of tiny particles, which are short-lived due to a combination of sputtering and plasma transport. The maximum density of the E-ring is essentially coincident with the orbit of the satellite Enceladus. These facts and the indications of its geologically recent surface activity suggest that Enceladus may be even today the source of the E ring material (see Section 3.4). Nevertheless, due to the lack of suitable observations of the size and composition of the E ring particles, there is as yet no theory that unequivocally connects Enceladus with the E ring or accounts for the energy required to produce and expel the ring material from the satellite.

Our understanding of the G ring, which also has a large fraction of short-lived dust particles, is even more primitive. No satellites have yet been identified as possible sources or shepherds for this ring. Hence, even its existence remains a puzzle. Other more distant rings have been suspected on the basis of fluctuations in magnetospheric density, but their reality is in some doubt.

### 3.3.3 Dust and meteoroid distribution

The current population of interplanetary debris is a remnant of the primordial planetesimals, most of which accreted to form the planets of our solar system. The final stages of this accretion are manifested in the many large impact craters that scar the faces of the airless planets and satellites, but even the currently diminished population may be having significant effects on the structure and composition of planetary rings. The reason why meteoroid bombardment is so influential for planetary ring structure and evolution is simply that the ratio of the ring surface area to mass is typically  $10^5$  to  $10^7$  times greater than a satellite of comparable mass. In fact, it is currently

believed that the rings are impacted by their own mass of meteoritic material over the age of the solar system, coming primarily in projectiles of 10 - 100 micron radius. In addition to providing an important compositional input, this bombardment and the associated ballistic and electromagnetic transport of the ensuing ejecta can redistribute angular momentum substantially within the rings, which may affect the ring structure on a timescale much less than the age of the solar system. Creation and destruction processes associated with this bombardment have also been invoked to explain the short-lived dust rings in the Jovian and Uranian systems as well as the incomplete "ring arcs" found in the Uranian and Neptunian systems. A great uncertainty in all of these inferences is the intensity and size distribution of the incident meteoroid flux. Given an accurate measurement of the impinging projectile flux, and a good bulk measurement of the composition and abundance of impurities, it may be possible to estimate the age of the rings using the brightness of the ring particles.

In addition, impact on the rings of some of the larger (10 - 100 cm size) members of the interplanetary projectile population may be the primary cause of the "spokes" which flicker sporadically across the face of the rings. Subsequent interactions of an electromagnetic nature between the rings and the planet are also apparent in this mysterious phenomenon, as discussed in section 3.3.4 below.

The number and velocity distribution of the interplanetary projectiles is an extremely important diagnostic of their orbital distribution. It is ultimately of great interest, for example, to know whether the population of interplanetary debris in the outer solar system is dominated by objects with "Oort cloud" type orbits or by a population with direct orbits more confined to the ecliptic.

### 3.3.4 Interactions between the rings and the planet's magnetosphere, ionosphere, and atmosphere

The rings lie within a region of the inner magnetosphere connected along magnetic field lines to planetary mid-latitudes. Due to the combination of meteoroid bombardment and solar photopumping, a partially ionized ring atmosphere results which allows currents, charged molecules, and tiny particles to flow in either direction between the rings and the planet. Several peculiar and unique phenomena have been observed in the rings and in the planetary ionosphere and atmosphere which may result from this unique coupling, and which need to be better understood.

As mentioned in section 3.3.3, meteoroid bombardment may trigger "spokes" in the rings; however, the subsequent evolution of spokes requires the interaction of ionized plasma with ring particles in regions far from the actual impact, and possibly an extended period of current flow between the planet and the rings as well. The creation rate of spokes is modulated by a peculiar high-latitude sector of Saturn's planetary magnetic field, which is also associated with bursts of kilometer-wavelength radiation (SKR) observed by Voyager. The process by which planetary magnetic and/or ionospheric activity is conveyed to the rings is not at all understood, however; for instance, the ring radial region showing spokes is connected along dipole field lines to low and mid-planetary latitudes, whereas the peculiar magnetic sector seen in SKR and auroral activity is really only evident at latitudes higher than 80°. Thus, a better understanding of "spokes" requires more numerous, more sensitive observations of both the rings and the planet.

Transfer of ring material from the rings to the planet in the form of charged molecules and tiny grains has been suggested as an explanation for Saturn's surprisingly low ionospheric electron density and for certain anomalously high molecular abundances in the atmosphere of the planet, and the associated loss of material from the rings is predicted to have a radial dependence in reasonable agreement with certain radial variations of ring optical depth and optical properties. If such mass transfer is the explanation for the observed behavior, the amount of mass transferred is quite large and provides another argument for a ring lifetime much shorter than the age of the solar

system. However, many uncertainties remain in the observations and parameters of the theories which need to be better understood before firm conclusions can be drawn.

## CAPABILITIES OF CASSINI FOR RING STUDIES

The Cassini Mission offers an outstanding opportunity to answer these fundamental questions, and to provide a data set of lasting, historical significance. First, Cassini will answer fundamental questions left unanswered by basic geometrical and sensitivity limits on the Voyager data set. The timing of the baseline mission is optimal: at arrival shortly after the year 2002 the rings will be well-opened as seen from the Earth and Sun. This, combined with improved instrumentation, will allow the optically thickest and most puzzling ring regions to be probed by imaging and multiple radio and stellar occultations with a quantum leap in effectiveness. This improved geometry and the multiple observations made possible by an extended Orbiter mission will allow us to disentangle radial, azimuthal, and temporal variations in ring structure.

Variations of ring brightness with illumination/viewing geometry will be more systematically and completely studied, leading to a better understanding of the variations of particle brightness, surface properties, ring volume density or porosity, and dust content which are important clues to local dynamics. Microscopic grains which are especially highlighted in forward scattering delineate the "spokes", which may contain information about unique ionospheric/magnetospheric instabilities. Extensive imaging coverage at low phase angles will permit the detection of moonlets embedded in the main rings and undetected moonlets in the F- and G-rings; Since these objects are too large to accrete within the Roche limit, their distribution will provide fundamental constraints on ring origin scenarios.

Also, Cassini will carry critical new remote and in situ experiments, and yield information which will never be obtained any other way. For instance, the near-infrared reflectance spectrometer and thermal emission radiometers sensitive from the mid-infrared out to the millimeter/centimeter-wavelength range can map out the local and regional variations in total mixing fraction, and composition, of the rocky and/or carbonaceous "impurities" in the rings, and allow us to look back in time to the probably heterogeneous origin of the ring material. Measurements of diurnal thermal variation along and across the rings, both on their lit and unlit faces, can provide unique information on the local vertical structure and dynamics. The Orbiter will be making several new in situ measurements of importance to ring studies. The dust detector will directly measure the flux, mass and velocity distributions of erosive meteoroids during cruise to Saturn and during an extended period while at Saturn, which will determine the importance of erosion as a structural or evolutionary process. The Orbiter will also be spending a great deal of time within Saturn's E ring, which is composed primarily of micron-sized and smaller particles. Determination of the size, velocity, and composition of these particles may cast light on their mode of origin - presumably from Enceladus.

Finally, the long time baseline between Voyager and Cassini will provide answers to important questions involving time-variable structure on timescales of weeks to decades. Problems with possible time-variable aspects include, for example, the orbital evolution of the ringmoons, possible changes in the F ring and B ring structure, and the nature of the "spokes". The transience of specific features in planetary rings on timescales of years, and the possible transience of ring systems in general on timescales much shorter than the age of the solar system, would necessarily impact our ideas about the origin and evolution of our solar system.

### 3.4 ICY SATELLITES

#### 3.4.1 The Satellite System

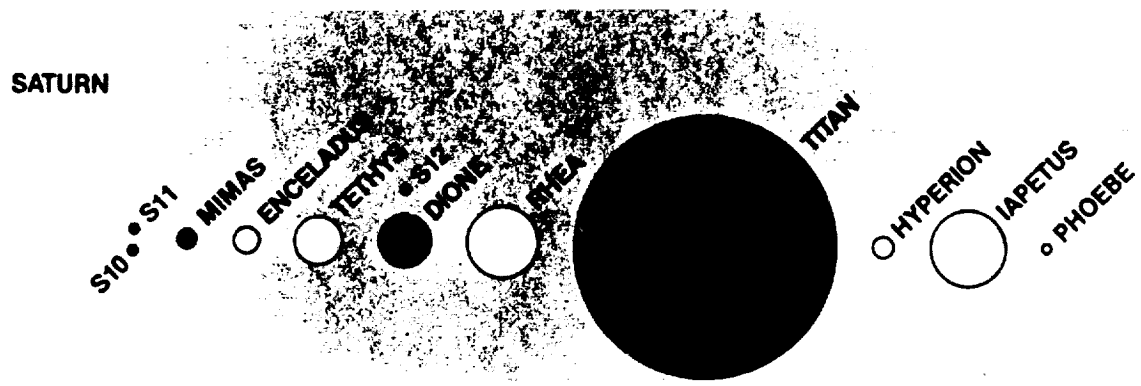


Figure 3.7: *Comparison of Saturn's satellites sizes. This figure illustrates the range of sizes among the satellites of Saturn. Titan, the largest, is approximately the size of planet Mercury.*

The satellites of Saturn form a collection of objects of great interest to solar system science. They range in size from small, icy fragments only a few tens of kilometers in diameter to giant Titan, which rivals Mercury and Ganymede in size and possesses a thick atmosphere (figure 3.7). Most of the Saturnian system is regarded as regular in the dynamical sense, with the satellites having nearly circular, coplanar orbits; distant Phoebe is in a retrograde orbit, suggesting an origin different from the others. Voyager radio team determinations of several of the satellites' densities show that these objects are all ice-rich bodies, with water ice the most likely dominant constituent. Telescopic infrared observations confirm the presence of water ice or frost on the surfaces of many of the major satellites. Table 3.1 gives the general characteristics of the satellites. In addition to water ice, the satellites contain varying amounts of dark, non-ice material. This is probably composed of a mixture of silicates and organic-rich compounds similar to those found in the most primitive meteorites. Major questions for Cassini to study are (1) the nature and composition of this dark material, (2) the origin of the dark material, whether derived from early accretion, internal geologic activity, or subsequent modification of the surface by in-falling matter and/or charged particle bombardment and (3) the relationship of the dark organic rich material in the Saturnian system to that observed on asteroids, comet surfaces and other outer planet satellites. Another major objective of satellite observations is to determine the relationship between the types of geologic activity seen on the different satellites and to search for evidence of non-water frozen volatiles, such as ammonia hydrates and methane clathrates that may help explain the degree of geologic activity seen on some of the satellites.

The Voyager results showed the Saturnian system to be remarkably diverse, and left planetary scientists with many new problems to solve with future observations. With such a large number of satellites as potential targets, Voyager was often able to provide only a global characterization. Resolution and coverage were particularly limited for two of the most interesting satellites, Iapetus

Satellite	Orbital semi major axis ( $R_S$ )	Radius (km)	mass ( $10^{21}$ kg)	Relative Mass	Density g/cm <sup>3</sup>	Geometric albedo	Surface composition
Titan	(20.25)	2575±2	1345.7±0.3	$2.36 \times 10^{-4}$	1.881	0.2	$N_2/CH_4$ atm.
Rhea	(8.736)	764±4	24.9±1.5	$4.4 \times 10^{-6}$	1.33	0.65	ice
Iapetus	(59.03)	718±8	18.8±1.2	$3.3 \times 10^{-6}$	1.21	0.4-0.04	ice carbonaceous?
Dione	(6.256)	559±5	10.5±0.3	$1.8 \times 10^{-6}$	1.44	0.55	ice
Tethys	(4.884)	524±5	7.6±0.9	$1.3 \times 10^{-6}$	1.26	0.80	ice
Enceladus	(3.945)	251±5	0.8±0.3	$1.5 \times 10^{-7}$	1.24	1.04	pure ice
Mimas	(3.075)	197±3	0.38±0.01	$6.6 \times 10^{-8}$	1.17	0.77	ice
Hyperion	(24.55)	(175±15) (120±10) (100±10)	-	-	-	0.25	dirty ice
Phoebe	(214.7)	(115±10) (110±10) (105±10)	-	-	-	0.06	carbonaceous?

$R_S = 60330$  km (Radius of Saturn)

Table 3.1 : *General characteristics of the Saturn's satellites. (Adapted from: Satellites, T. Gehrels and M.S. Matthews, eds., Univ. of Arizona Press, Tucson, Arizona, 1984.)*

(best resolution only 20 km) and Enceladus. Figure 3.8 illustrates this paucity of data with the best current map of Enceladus. Two general themes run through current ideas about the Saturn satellites: thermal evolution and collisional evolution. The existence of Saturn's extensive ring system, the heavily cratered regions of many satellites and the presence of numerous sets of Lagrange satellites (smaller satellites in essentially the same orbit as a larger one, librating about one or more of the Lagrange points), all suggest that the system has undergone extensive collisions and fragmentation. But the large smooth areas on the surface of Enceladus and the "wispy" terrains on Dione (See Figure 3.9) seem to require at least partial resurfacing due to some kind of internal heating and the consequent geological processes. Prior to the Voyager encounters, it was expected that the thermal and geological histories of all of the satellites except Titan would prove to be relatively straightforward, as the smaller satellites are incapable of retaining significant amounts of radioactively generated heat. The only major exception to this expectation was a suggestion that the presence of ammonia or methane along with water might allow melting and therefore, geological activity at much lower temperatures than required for silicate or pure water-ice volcanism.

Voyager imaging data suggest a wide variety of geological activity on the satellites, occurring over time spans ranging from 3 to 4 billion years ago to the geologically recent and possibly currently active. Dione, Rhea, and Tethys in particular show regions of markedly different crater populations, indicating that resurfacing must have occurred at least during the period when the impacting crater flux changed, probably three and a half billion years ago. Both Rhea and Dione also exhibit regions of "wispy" terrain dominated by long bright features of uncertain but possibly internal origin; these features all occur on the areas of these satellites which Voyager observed only at low resolution. These features may be indications of ancient geological activity or of more recent events. Another possible indication of recent activity is the observation by the Voyager Plasma Wave Spectrometer that Saturn Kilometric Radio emissions seem to be modulated with a period equal to Dione's revolution; the Pioneer 11 magnetometer also detected ion-cyclotron waves suggestive of plasma injection in the vicinity of the Dione L-shell, and Voyager 1 plasma observations indicate a large scale interaction between Dione and the magnetospheric plasma.

Major unanswered questions concerning the nature of the collisional histories of these objects

ORIGINAL PAGE  
BLACK AND WHITE PHOTOGRAPH

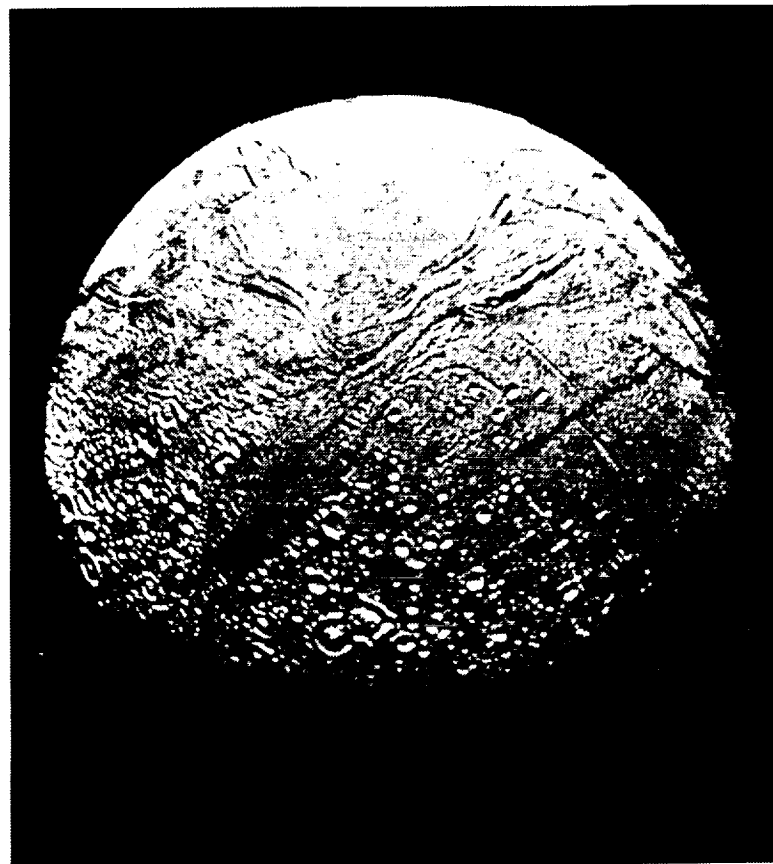


Figure 3.8: Although limited in extent and resolution, the Voyager images show evidence for a complex geological history involving cratering, crystal faulting, flooding and resurfacing and viscous relaxation of topography.

ORIGINAL PAGE  
BLACK AND WHITE PHOTOGRAPH

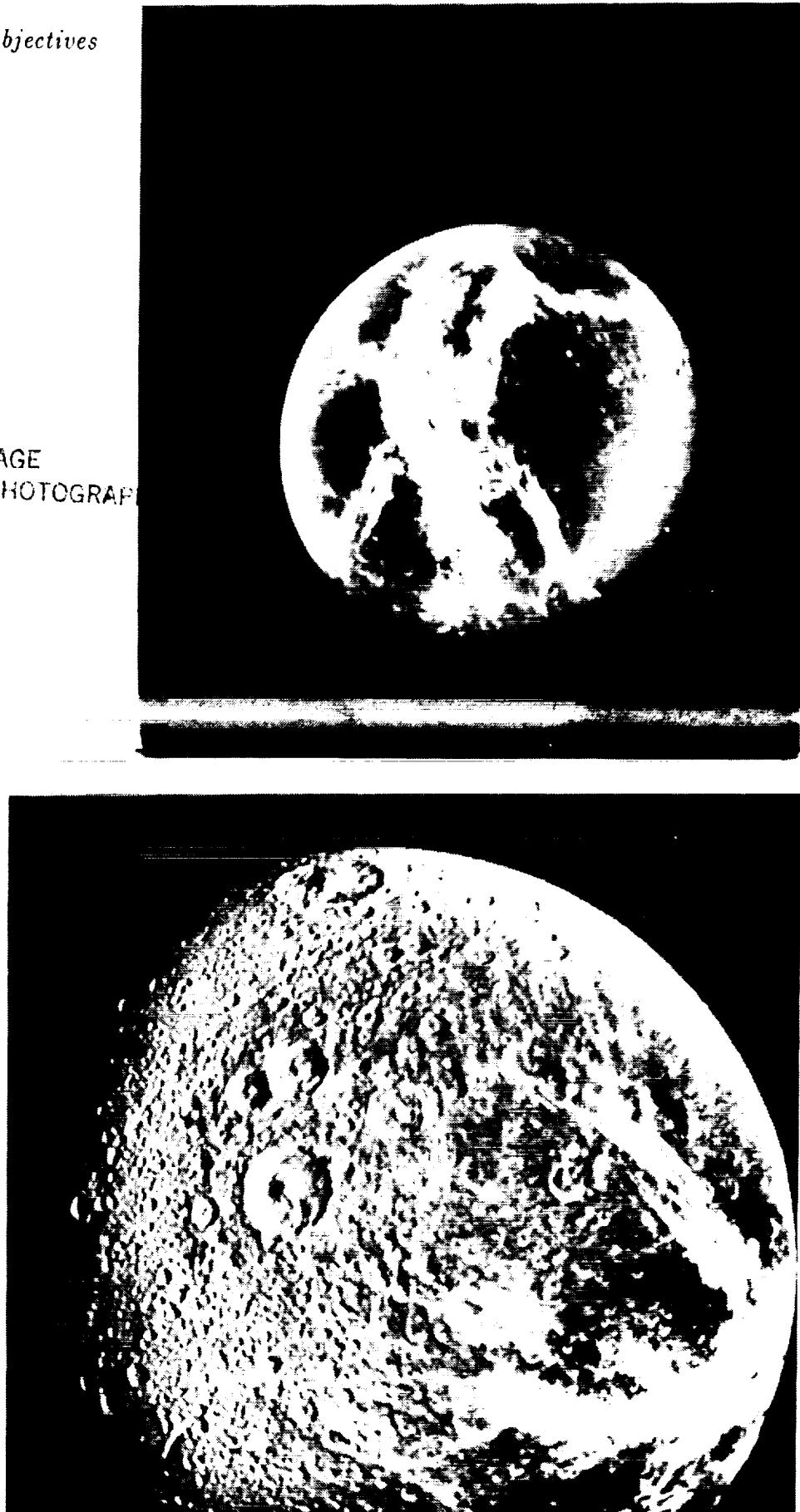


Figure 3.9: *Dione*: These two views of Dione illustrate the different types of surfaces typical of the "medium" sized icy moons. The "wispy" terrain in (a) is believed to result from internal activity at some time in the satellite's history, while the different crater population in (b) suggest early episodes of resurfacing.

include:

Have the smaller satellites undergone multiple disruptive collisions followed by reaccretion? Is the ring system related to such an event(s)? What populations of impacting bodies were involved in the early heavy bombardment of the satellites - what were the relative proportions of cometary objects from the outer portions of the solar system, asteroidal/cometary flux from the inner system, and material orbiting Saturn?

### 3.4.2 Enceladus and Iapetus: Especially interesting bodies

The most striking example of recent geologic activity is the small ( $D = 500$  km) moon Enceladus. Despite its small size Enceladus exhibits a remarkable variety of surface features, ranging from cratered regions similar to those seen on other satellites, through regions containing fewer, viscously relaxed craters, to extensive areas with long ridges or "wrinkles" and no craters of any size down to the resolution limit of the Voyager pictures (a few km). These characteristics suggest major geologic activity lasting much longer than for the other satellites; estimates of the age of the uncratered regions suggest that they are less than one billion years old and may be much younger, possibly still active. Another suggestion of recent activity is Enceladus' association with the E-ring. The E-ring appears to be most dense right in the vicinity of Enceladus' orbit, and estimates of the lifetime of E-ring particles suggest that they must be less than  $10^3$  to  $10^4$  years old. The strange appearance of Enceladus' surface and the location of the ephemeral E-ring may be a coincidence, but there is a strong probability that they are connected in some manner, possibly through current eruptive activity on Enceladus. This would be consistent with the uniformly high reflectivity ( $\sim 100\%$ ) of the entire visible surface; deposits of geologically young material are apparently thick enough in some areas to bury previously formed topography.

Although the eruptive plumes and high heat flow of Jupiter's moon Io are perhaps the most spectacular examples yet seen of planetary satellite thermal activity, in many ways Enceladus' geologic record is even more of a puzzle. With a thousandth the mass of Io and a mostly icy composition, initial heat and radionuclide decay must play a small role in its current heat budget. Although Enceladus does have a gravitationally forced orbital eccentricity, theoretical estimates of the amount of tidal energy which is currently available to heat this satellite fall short of melting ice by about a factor of ten. As with the evidence of resurfacing on some of the other satellites, the solution to this problem may lie in other volatiles being present in addition to water ice, thus allowing melting at lower temperatures.

The outermost of the bigger satellites, Iapetus presents an array of unusual problems. Since its discovery by Cassini in 1671, this moon has been known to have an unusual distribution of light and dark material on its surface; on average, the leading hemisphere is almost a factor of ten darker than the other! This phenomenon has been studied extensively using telescopic disk-integrated photometry and spectra. These studies have served to characterize the situation but not to explain it. Prior to the Voyager encounters in 1981 the major issue concerning Iapetus was the relative importance of exogenic versus endogenic processes in creating this unique surface. Exogenic modification by infalling debris, from the outer retrograde satellite Phoebe, was a popular pre-Voyager theory. Voyager results provided considerable fuel to heat the Iapetus controversy but not as much light. Limited to 20 km resolution at best, Voyager's cameras were able to define the boundaries of the dark leading side markings and to detect many densely packed craters on the icy trailing side of the moon. However, few distinct features are discernible in the dark areas and the images were not of sufficient resolution to determine the nature of the processes responsible for this satellite's strong hemispheric dichotomy. Without a near IR spectrometer, the Voyager spacecraft were unable to make any direct determinations of the composition of the dark material.

Even after Voyager's fascinating reconnaissance, the debate about Iapetus rages on. Current theories include both modifications of the Phoebe infall hypothesis and models involving almost complete internal genesis of the dark, presumably carbon-rich material on the leading hemisphere. Ideas for heating low mass, volatile-rich moons are applicable to Iapetus, but its extreme difference from the other icy satellites raises difficult questions concerning the self consistency of any of these models.

### 3.4.3 Other Problems

In addition to the problems raised by considering the satellites individually, there are a number of other important questions concerning the system as a whole and its interaction with its environment (see Section 3.5). One set of goals associated with the system as a whole concerns the smaller satellites and the dynamics of the system. Ground-based observations and Voyager data have added many satellites to the list of Saturn's retinue; presumably more satellites, some in dynamically unusual orbits, remain to be discovered. Searches for such satellites and the study of objects such as Hyperion, which is believed to be an example of a "chaotically rotating" body are important objectives for further study of the Saturn system.

## CAPABILITIES OF CASSINI FOR ICY SATELLITE STUDIES

The Cassini Mission is capable of addressing most of our current major questions about the Saturnian satellite system, and, of course, will undoubtedly make its own discoveries, raising newer and even more interesting issues in planetary science. One of the most basic measurements will be mass determinations with improved accuracies. Radio tracking will provide good mass values for satellites encountered during Cassini's orbital tour and may allow searching for evidence of internal structure in some cases.

Imaging of the satellites will be one of the most important tools for studying their geologic histories. While Voyager was only able to acquire a few images of each satellite, and from great distances, Cassini will provide a steady stream of high quality imaging data for four years, allowing tremendous improvements over Voyager in resolution, coverage and viewing conditions. Significant coverage of many satellites with resolutions better than 1 km should be possible, with highest resolutions of 100 m or better. Imaging studies of this sort should be able to: 1) determine the nature of the different crater populations on the satellites' surfaces, 2) study the nature of the wispy terrain on several of the satellites and determine its relative age, 3) study the nature of the tectonic processes which have disrupted the crusts of many of the satellites, 4) search for currently active geologic processes on the satellites, particularly Enceladus and Dione, 5) determine the nature and age of the dark markings on Iapetus and study the character of its boundaries with other icy units.

Multispectral observations with the imaging system, with multiple filters between 0.3 and 1.0  $\mu\text{m}$ , will provide key information on the nature and distribution of compositionally distinct units on the satellite surfaces. This is particularly important for determining the origin and modes of emplacement of dark material on some of the satellites. To identify the composition of surface units, the primary tool will be the Near Infrared Spectrometer (NIRS). Identification of absorptions from surface materials such as different types of ices, silicates, and organic-rich dark materials, spectral resolutions of 1% in the spectral range 0.7-5.2  $\mu\text{m}$  will be pursued (further information can be derived from data in the 0.3-0.7  $\mu\text{m}$  range as well; some combination of imaging and NIRS data may be necessary to achieve this). Spatial resolution and mapping coverage are essential to 1) determine the spectrally distinct units on the satellites, their locations and extent and determine their composition, (2) identify important materials (such as short-lived clathrates and hydrates) that may exist in significant abundance only in small regions and (3) relate the compositional

information to geological data from high resolution imaging. This is critical to understanding such issues as the origin of the dark, presumably organic rich material on Iapetus, wispy terrain on Dione and Rhea, and the nature of volcanic resurfacing activity (and possibly E-ring interactions) at Enceladus. Coverage of a complete satellite surface at 20-50 km resolution with smaller regions of high interest mapped at 1-10 km resolution is required for the satellites of highest priority. A spectral mapping instrument with an angular resolution of 0.5 mrad, capable of acquiring a spatial-spectral "cube" of data rapidly enough to prevent smearing due to spacecraft-target motion can provide the required data. Thermal properties of the upper few cm of these satellite surfaces will be inferred from infrared and microwave brightness temperature observations as a function of solar illumination.

The Plasma Spectrometer (PLS) and possibly the Ion/Neutral Mass Spectrometer (INMS) will provide in situ information about the compositional makeup of the satellite surfaces which emit gas due to sputtering from magnetospheric charged particle bombardment and subsequent ionization of this gas by the magnetospheric plasma. With sufficient mass resolution, ammonia and methane molecular ions will be discernable. If mass loading is minimal, the pick up energies for these molecular ions will exceed several hundred eV, and the PLS instrument will be the appropriate device to carry out these measurements.

### 3.5 MAGNETOSPHERE

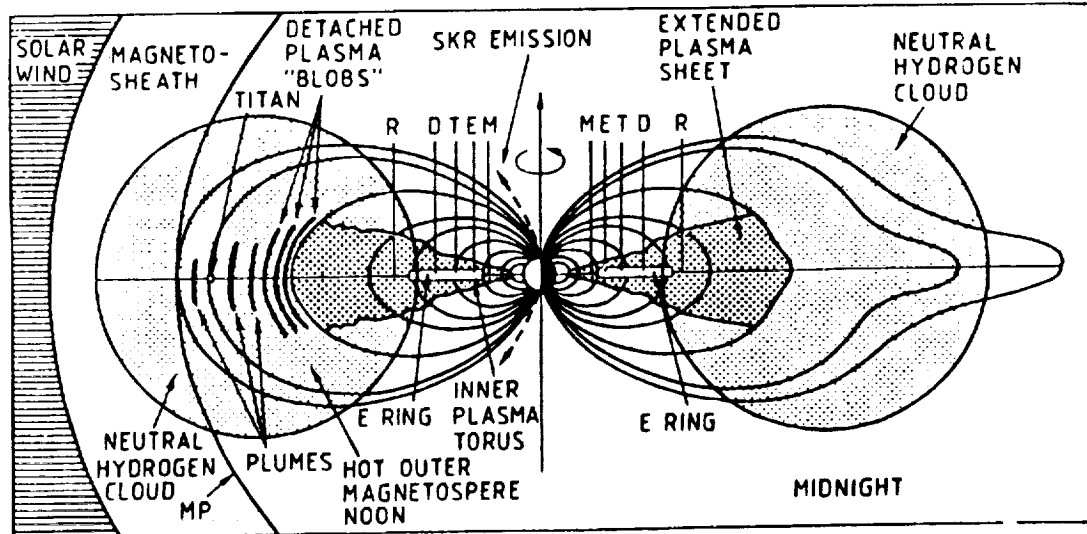


Figure 3.10: Meridional view of Saturn's inner magnetosphere showing the different plasma regimes, Titan hydrogen torus, satellite positions : (R=Rhea, D=Dione, T=Tethys, E=Enceladus, M=Mimas), and the E ring.

Figure 3.10 provides a summary of the Saturnian magnetosphere as derived from the Pioneer 11 and Voyager encounters. The internal magnetic field is primarily that of a dipole of moment 0.21

gauss- $R_s$ ,<sup>3</sup> (where Saturn's radius  $R_s = 60330$  km), but there are significant contributions from the quadrupole and octopole moments. The internal magnetic field is nearly axially symmetric about the planetary rotational axis and thus unique among all the planetary magnetic fields observed so far. However, the strong periodic modulations of Saturn's radio emission imply the existence of a departure of the near-surface fields from axial symmetry.

Though the plasma environment is poorly understood, it is known to be extremely complex and time-variable. For instance, while the average bow shock stand off distance is about  $22 R_s$ , there is large variation in its position as a function of solar wind condition, implying that Titan (at  $20 R_s$ ) could be in the solar wind at times. In the outer region, the hydrogen and nitrogen-gas torus emitted by Titan and the extended hydrogen exosphere of Saturn contribute to the spatial distribution, sources and sinks of the magnetospheric plasma. Overlapping the Titan torus between  $8$  and  $15 R_s$ , there is a significant ring current system stretching the magnetic field lines outward. This ring current, which occupies the same volume as an extended plasma sheet, is driven by centrifugal stresses and pressure gradients. Outside the outer edge of the extended plasma sheet, plasma irregularities were seen by Voyager which may be related to the ejection of ionospheric plasma from Titan, or could be the result of a centrifugally driven fluid instability. Other possibilities also exist. The termination of the extended plasma sheet at about  $8 R_s$  may be related to the sweeping effect of the icy satellites and E ring particles. In place of the energetic charged particle population, the inner magnetosphere is characterized by a thermal plasma population ( $< 10$  eV/charge) centrifugally confined close to the equatorial plane, which might be mainly water and oxygen ions of satellite and/or ring origin and neutral clouds of water molecules produced from sputtering due to the interaction of the thermal and hot plasmas with the satellites and rings. Interaction of the rings with cosmic ray particles generates a component of energetic protons  $> 50$  MeV distributed between  $4 R_s$  and the outer edge of the A ring. Satellite and ring absorption of energetic magnetospheric particles show up prominently in the Saturnian magnetosphere.

Since it is the strong interactions with icy satellites and the rings which are most characteristic of the Saturnian magnetosphere, several of the major issues to be resolved by the Cassini mission will be outlined here – with the understanding that the long-term observations and extensive three-dimensional coverage afforded by this mission will yield important insights into the many physical processes involved in solar wind interactions with magnetospheres.

The inclusion of a high inclination ( $i > 80^\circ$ ) polar orbit would provide in situ information about the SKR emission mechanism, solar wind entry into the magnetosphere within the polar cusp and would measure the precipitating charged particle fluxes into Saturn's upper ionosphere. The latter would yield a direct measurement of the energy deposition into the atmosphere that is responsible for auroral emissions. Furthermore, the inclusion of several advanced instruments in the comprehensive science payload will guarantee information far superior to that provided by the Pioneer 11 and Voyager 1/2 observations. These include the plasma instrument with high mass resolution, the energetic neutral analyzer with the type of magnetospheric imaging, the aeronomy package providing in-depth exploration of the upper atmosphere of Titan, and last but not the least, the Ultraviolet Spectrometer/Imager (UVSI) which permits first-rank narrowband EUV-FUV mapping of the atmospheric emissions connected with magnetosphere-atmosphere couplings at Saturn and at Titan.

### 3.5.1 Magnetospheric Dynamics and Energetics

Generally speaking, the magnetospheric system of Saturn is distinctly different from those of the Earth and Jupiter. While the large-scale configuration of the terrestrial magnetosphere is strongly affected by large-scale convection cells induced by the solar wind electric field, and the Jovian one

by the mass injection and transport of heavy ions from Io, the Saturnian magnetosphere, a large part of which probably follows the planetary rotation, can be characterized by the importance of its interactions with the rings, icy satellites, and Titan's gas torus. Since Saturn's spin axis will be inclined by about  $26^\circ$  relative to the Saturn-Sun line during the Cassini mission, as shown in Figure 3.11, a hinge in the plasma sheet is expected to form in the midnight hemisphere at a radial distance of about  $30 R_s$  from Saturn, where the tail current system begins to dominate over currents driven by Saturn's rotation. Satellite tour orbits with apoapsis  $60 R_s$  within the tail would be required to

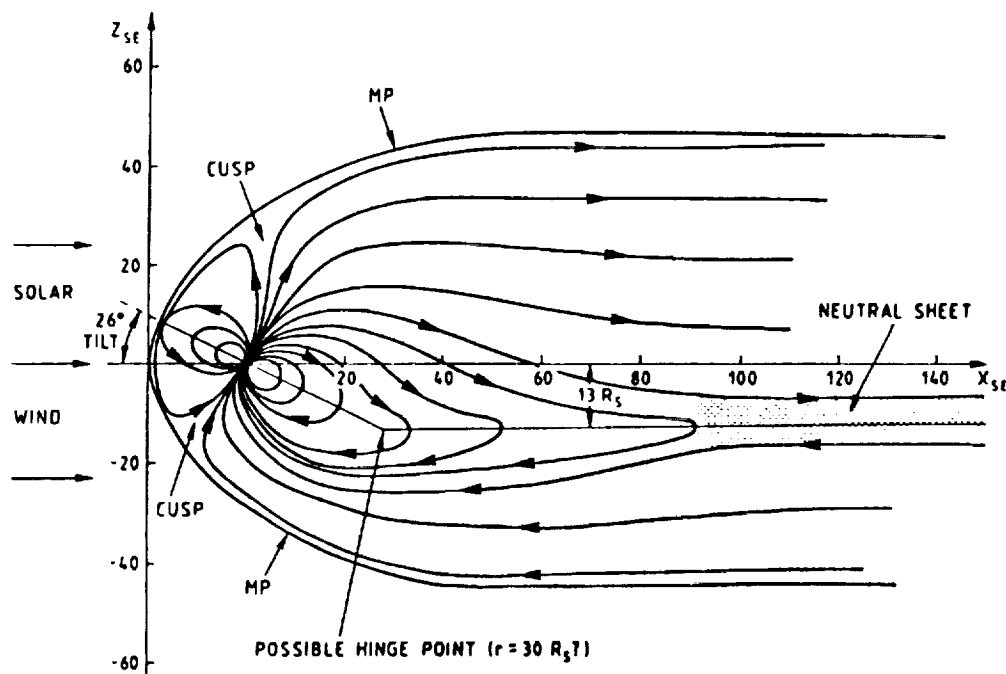


Figure 3.11: A schematic view of Saturn's magnetosphere as it will look during the tour phase of the Cassini mission. Because of the  $26^\circ$  tilt of the ring plane relative to the solar ecliptic plane, a hinge in the plasma sheet may form at about  $30 R_s$ .

confirm the presence of such a hinge point in the plasma sheet. Observations in the tail region will also allow detection of a planetary wind if present, with the formation and movement of plasmoids or magnetic bubbles down the tail when plasma detachment takes place. This latter phenomenon may be the dominant mechanism for loss of plasma from Saturn's magnetosphere.

Important for understanding the dynamics and energetics of the magnetosphere are measurements of the individual particle distributions of the thermal and suprathermal plasma. Because of the complex composition of Saturn's magnetospheric plasma, this can only be done if the plasma analyzer ( $E \sim 1 \text{ eV-30 keV}$ ) and hot plasma composition ( $E \sim 1 \text{ keV/nucl-3 MeV/nucl}$ ) experiments have adequate mass and charge resolution such that the major ions (i.e.,  $\text{C}^+$ ,  $\text{N}^+$ ,  $\text{O}^+$ , and  $\text{H}_2\text{O}^+$ ) can be separated in the measurement. Of equal importance is the requirement that 3-D measurements of the plasma be provided. With these capabilities it will be possible to make accurate estimates of plasma flow velocities and pressures from which centrifugal stresses and pressure gradient forces transverse to the magnetic field can be determined. These forces will produce the observed ring current which may be coupled through field-aligned Birkeland currents to Saturn's ionospheric current system, thus providing Ohmic heating of Saturn's upper atmosphere. In ad-

dition to the ability to compute plasma flow velocities and pressures, 3-D measurements of the plasma will yield information on pressure anisotropies, loss cones and field aligned particle beams. All of these can provide the free-energy sources in the particle distributions that are needed to produce plasma waves capable of energizing the plasma and causing precipitational losses into Saturn's atmosphere. This topic of an atmospheric sink is important to aeronomy studies for two reasons. First, the precipitation of magnetospheric charged particles at the auroral zones could be a significant energy source for heating and ionizing the upper atmosphere, at least in the polar region. In situ measurements in polar regions ( $i > 80^\circ$ ) will allow resolution of the loss cone and direct measurement of the precipitational charged particle fluxes depositing this energy into the atmosphere and producing the auroral emissions. Secondly, the very strong day-night asymmetry of the H<sub>2</sub>-emission over the planetary global disks of both Jupiter and Saturn has been suggested to be the result of electron impact, while the source mechanism of the suprathermal electrons is still unknown. Plasma measurements as well as UV emission mapping during the Cassini Mission should yield important information on the electron-energizing process and its relation to other magnetospheric processes as well as evaluating other alternative mechanisms. In a significant way, the measurements by the Energetic Neutral Analyzer/Imager (ENA or ENI) should provide unprecedented information on the spatial structure and temporal evolution of the ring current system during different phases of the magnetospheric dynamics. The Cassini mission would therefore be equipped with the most modern kind of magnetospheric research instruments to probe the very new frontier of planetary plasma physics.

### 3.5.2 Plasma Composition, Sources and Sinks

In the Saturnian magnetosphere, there are several plasma sources of significance. They include:

- the solar wind
- the atmosphere of Titan
- the atmosphere of Saturn
- the rings and icy satellites
- the Titan hydrogen (and nitrogen) torus.

Each of them could be important in different regions of the magnetosphere. For example, in the outer magnetosphere, the Titan torus is expected to be a major plasma source (H<sup>+</sup>, H<sub>2</sub><sup>+</sup> and N<sup>+</sup> ions) as a result of photoionization and electron impact ionization of the neutral gas cloud; in the inner region, the heavy ion plasma torus as observed by the Pioneer 11 and Voyager 1 and 2 spacecraft is likely to be supplied by the rings and icy satellites. Besides direct ion pickup in the near-vicinity of the satellites, the distributed neutral clouds in the Titan torus and in the inner region could be very important in defining the plasma composition and charge state of the magnetospheric charged particles via charge exchange, electron impact ionization, and photoionization. In the Cassini Mission, ion composition measurements by the plasma instruments should be able to separate the oxygen (from the icy satellites and rings) and nitrogen (from Titan) ions clearly and hence provide much needed information on how the ionized gas is injected into the magnetosphere from different sources. It is desirable that the plasma instrument provide sufficient mass resolution to resolve molecular ions such as H<sub>2</sub>O<sup>+</sup>, and ammonia molecules NH<sub>3</sub><sup>+</sup>, NH<sub>2</sub><sup>+</sup>, to provide information about the composition of the icy satellites. From examination of the charge state of the heavy ions, the entry and circulation of the solar wind plasma in the magnetosphere could be determined. Measurements by the energetic neutral analyzer should also provide essential information about the charge exchange process which is prevalent in the Saturnian magnetosphere and in the upper atmosphere of Titan.

The sink mechanisms for the magnetospheric plasma are no less intriguing. One can list at least 6 competing processes:

- satellite absorptions
- ring absorptions
- charge exchange loss in the Saturn/Titan torus and neutral clouds of the icy satellites
- precipitation to Saturn's upper atmosphere
- Titan's atmospheric absorption
- possible planetary wind outflow.

The first three act as sinks for the medium and high energy charged particles, but at the same time, they are sources for the thermal and low-energy plasma. The last three represent a net loss of the magnetospheric plasma, each with important consequences for the atmospheric environments of Saturn and of Titan, and for the global dynamics of the magnetosphere. So far, all of these items have only been partially characterized by very limited quantitative estimates by the Pioneer 11 and Voyager observations. One of the basic aims of the Cassini Mission therefore, is to clarify these many interwoven processes in such a manner that the diffusion, convection, storage, and loss of the trapped charged particles may be fully understood.

As noted before, a significant amount of mass is being contributed by escape from the upper atmosphere of Titan. From the dynamical point of view, the question of how this mass is stored, transported and energized constitutes the central theme in magnetospheric physics for the Cassini Mission. In this respect, the nitrogen ions from Titan may be used as compositional tracers to probe these different processes. By the same token, the water and oxygen ions would allow us to trace the dynamical process in the inner region, while the  $H_2^+$  plus  $H_3^+$  ions could be used to study the polar wind flow from Saturn's ionosphere. As a result of atmospheric escape from Titan and surface sputtering of the icy satellites and the E-ring particles, the Saturnian magnetosphere is filled with tenuous neutral gas. This implies that plasma-neutral gas interaction, via electron impact ionization or simply charge-exchange effects, will be very important. To examine this unique environment thoroughly requires measurements of high sensitivity and high mass resolution by the plasma and hot plasma analyzers and an energetic neutral analyzer/imager capable of making energy and composition analyses.

To accommodate the requirements of 3-D measurements by the plasma and aeronomy experiments on the Cassini Mission, the fields of view of these sensors will be carefully considered. The plasma instruments are accommodated on a turntable which is mounted at the end of a boom. As for measurements of thermal plasma, electrostatic and magnetic cleanliness, effects of the photo-electron sheath of the MMII spacecraft and provisions to avoid differential charging problems will be incorporated into the spacecraft design.

### 3.5.3 Titan's Plasma Interactions

The Titan flyby of Voyager 1 indicated the formation of a magnetic tail (the intrinsic magnetic field of Titan has been estimated to be < 4 gamma at the equatorial surface, from Voyager observations). Second, strong absorption signatures of magnetospheric charged particles were observed, indicating direct precipitation. Most interesting of all, an intense airglow of  $N_2$ -emission from electron impact excitation was discovered. No adequate interpretation has yet been given for this intriguing phenomenon, but, as in the case of Venus' neutral atmosphere-solar wind interaction, electrodynamic coupling between Titan's upper atmosphere and the external plasma environment might be important.

As shown by the Pioneer Venus observations of Venus, several effects such as mass-loading of the solar wind plasma via charge exchange, pile-up of the magnetic field, and formation of a magnetic tail in the wake of Venus, combine to make the plasma interaction of a non-magnetic planet a very interesting problem to study. Indeed, the ionospheric dynamics and chemistry of Venus have been found to be significantly affected by the solar wind interaction process. It is difficult to separate the aeronomical processes from the relevant plasma effects. At Titan, we could find close analogies in these many topics. In the Cassini Mission, the numerous encounters of the Orbiter spacecraft with Titan will permit probing of different regions of Titan's atmospheric and plasma environments. Answers would then be found as to whether the observed N<sub>2</sub>-dayglow is caused via impact excitation by direct atmospheric precipitation of magnetospheric electrons, by in-situ acceleration of electrons in the upper atmosphere, or by particle acceleration in the magnetic tail of Titan.

The issue of the N<sub>2</sub>-dayglow is interesting as it may be closely related to the formation of Titan's ionosphere and, hence, ion chemistry involved in the synthesis of complex molecules in the upper atmosphere. Since the N<sub>2</sub>-emission region and the ionization maximum of the ionosphere at 1000 km will be accessible to the Cassini spacecraft, instruments specific to aeronomical study (i.e., INMS and RPA/LP), plus other plasma instruments should provide a comprehensive picture of Titan's ionospheric interactions with the solar wind and the magnetosphere. These instruments will provide important information about energy deposition into the ionosphere and the transport of energy and momentum as functions of local time and height in Titan's ionosphere. The scientific requirements are that they should be able to measure electrons from temperatures  $\sim$ 200° K to at least several hundred eV energy; and the INMS should be sensitive to H<sub>2</sub> as well as to elements with heavier masses.

As Titan orbits through different plasma regimes of the Saturnian magnetosphere, the nature of the atmosphere-plasma interaction could vary greatly. This would allow the investigation of interesting MHD processes seldom encountered in other situations. Because of its rather extended atmosphere, Titan's solar wind interaction is believed to be intermediate between those of Venus and comets. The Cassini Mission would therefore constitute an important step in the exploration of solar wind and magnetospheric interactions with the neutral atmospheres of non-magnetized planetary bodies.

### 3.5.4 Saturn's Plasma Wave and Radio Emissions

Because of the absorption by the icy satellites and the rings, there is significant depletion of the energetic charged particles in the inner magnetosphere. For this reason, no synchrotron emission was detected from the ground or by the Voyager spacecraft. But one surprising result from the Voyager observations is that Saturn displays intense radio emission at kilometric wavelengths which has a very different emission pattern from the kilometric radiations at the Earth and Jupiter. The emission of the Saturn Kilometric Radiation (SKR), with spectral peak at about 200 kHz, was found to be confined to a small arc near local noon (1000 LST - local solar time) at high latitudes ( $\sim$  80°) in the vicinity of the polar cusp whereas the Earth's Auroral Kilometric Radiation (AKR) is mainly concentrated on the nightside between 18 hr and 22 hr local time. This signifies that the patterns of magnetospheric precipitation (and hence magnetospheric dynamics) at Saturn and the Earth must be very different.

Another surprising discovery by the Voyager spacecraft concerns the strong effect of magnetic longitude modulation of the SKR by an approximately axially symmetric magnetic field. From correlation of the SKR and the UV observations of hot spots in the north and south auroral zones, there seem to be magnetic anomalies near the magnetic footprints of the SKR emission regions.

A combination of the in situ measurements by the particles-and-fields instruments and remote sensing by the plasma/radio wave analyzer should bring new insight to this puzzling phenomenon. In the case of the Earth, the AKR is generally associated with the so-called 'inverted V' events from parallel-electric field acceleration of electrons. This means the plasma instruments should be tailored to measure the directional electron flux as well as the waves and fields signatures. To optimize this investigation, polar passages (with orbital inclination  $> 80^\circ$ ) with low-altitude coverage near local noon are essential at some phase of the mission. It is in fact very important to have the opportunity to investigate in detail the magnetic field anomaly at high latitudes at distances  $< 1 R_p$  to the planetary surface.

The much more complete global coverage in the Cassini Mission would also allow very detailed study of other aspects of the radio emission such as:

- the physics of generation, emission, and propagation;
- the modulation by planetary rotation and its influence on magnetic anomalies;
- solar wind control; and
- possible correlation with spoke activity in the rings

The magnetometer experiment on Pioneer 11 detected intense ion cyclotron activities near the L shell of Dione, which may be responsible for pitch-angle scattering and hence atmosphere precipitation of the energetic ions. The magnetometer experiment should have sufficient sensitivity to detect lower hybrid and ion cyclotron waves in the inner magnetosphere where the DC magnetic fields of the planet are large. Quantifying the plasma-wave interactions requires a detailed knowledge of the plasma wave spectrum below the radio bands. Measurement of the wave spectrum is important for other reasons, for such waves can provide information on anomalous diffusion, resistivity, and other transport effects, as well as provide a local diagnostic of electron density at times attainable in no other ways. The Cassini Mission would permit a much more thorough study of these plasma effects than was possible before.

The plasma and radio wave analyzer can also provide supplementary information on the atmospheres of Saturn, Titan, and other icy satellites. For example, some indication of modulation of the SKR by the satellite, Dione, has been found by the Voyager 1 wave experiments. It was speculated that perhaps such modulation was the result of an occultation by an ion cloud associated with Dione. While this issue is still to be clarified, it opens up the interesting possibility that plasma wave observations can be used for remote-sensing of the near environment of the icy satellites (i.e., Dione and Enceladus) to search for surface outgassing activities.

Next, the Saturn Electrostatic Discharge (SED) which is an impulsive (15-400 ms), broadband (20 kHz to 40 MHz) radio emission with a recurrent period of about 10 h 10 min is now thought to be related to extended thunderstorm systems in Saturn's atmosphere. One interesting result from the Voyager observations of the SED is that Saturn's equatorial ionosphere could have a very large diurnal variation in its electron content. In the Cassini Mission, we expect to determine the SED variations in activity and its possible correlation with atmospheric dynamics and features, to monitor the equatorial ionosphere, and to locate directly the SED emission region(s).

As far as detection of lightning in the mid-latitude atmosphere is concerned, observations of the whistler waves would be important; furthermore, as demonstrated by the Pioneer Venus plasma wave experiment, detection of lightning at Titan, in principle, could be feasible, provided wideband spectrograms during Titan encounters are made available.

### 3.5.5 Plasma-Solid Body Interactions

In addition to the search for outgassing and tenuous ionospheres, the Orbiter flybys of the icy satellites permit detailed investigation of absorption of magnetospheric plasma by the satellites and the

microscopic absorption and refilling processes. This information is essential to the understanding of the general loss of magnetospheric particles as well as the radial diffusion process. Observations of depletions of magnetospheric protons and electrons have proved to be extremely sensitive to the presence of tiny moons and/or very small quantities of microscopic particulates in and between the orbits of the known rings and satellites, some of which may be the result of accretion/destruction processes acting on timescales of hours to weeks. These observations will provide unique constraints on the nature and contents of the ring-moon system. Potential new topics to be explored in this respect include: local plasma effect associated with a satellite-magnetosphere interaction, and surface electrostatic charging and transport of fine dust. The latter effect — in combination with surface sputtering by energetic charged particles — could have strong influence on the surface morphologies of the icy satellites. Measurements by the PLS instrument and possibly INMS could provide information about the composition of these bodies by detection of the ions from the surface sputtering by interaction with the magnetospheric plasmas.

## CAPABILITIES OF CASSINI FOR MAGNETOSPHERIC STUDIES

Because of the close alignment of the magnetic axis with the rotational axis, information on the latitudinal variation of the Saturnian magnetosphere has been very scanty from previous flyby observations. The characteristics of the satellite/magnetosphere tour in the Cassini Mission, covering a wide range of orbital inclinations, are thus ideal. The night and dusk regions, crucial to an understanding of the magnetospheric convection system, have not yet been explored, and it is important that observation of these regions be incorporated into the mission design objectives. Furthermore, with the long-term coverage available, physical processes of different time-scales, such as solar wind modulation and substorm activities, could be investigated in detail.

Another important factor permitting major findings in the Cassini mission concerns the full set of magnetospheric physics and aeronomy instruments as defined in the model payload. The emphasis on the compositional analysis, for example, would mean that the plasma observations in the Cassini mission should bring much needed new insights to the whole issue of sources and sinks of the magnetospheric plasma and the compositional make-up of the icy satellites. The complement of aeronomy instruments carried on the Orbiter with the particles-and-fields experiments would also be ideal in clarifying the plasma processes in the vicinity of Titan.

## 3.6 Jupiter

### 3.6.1 Atmospheric Science

Cassini should fly by Jupiter in February 2000 when, if the current baseline is maintained, the Galileo Orbiter will have completed a detailed exploration of the system lasting twenty months. Much significant new information about the Jovian atmosphere will nevertheless be provided by Cassini, since the Orbiter payload includes several instruments specifically designed for remote sensing of the thermal structure and composition of planetary atmospheres, whereas the payload of the Galileo Orbiter was designed primarily for studies of the solid bodies in the Jovian system.

Investigations using instruments common to both spacecraft will benefit from the extended temporal coverage. Differences in the cloud morphology between the Pioneer and Voyager missions have shown that significant changes can occur on a timescale of a few years. Small differences in both cloud and thermal structure were even noticed between Voyagers 1 and 2.

The spectral coverage of Cassini is almost continuous between 0.3  $\mu\text{m}$  and centimeter wavelengths, whereas Voyager has serious gaps in the visible, near-IR, submillimeter and microwave

ranges. The spatial and spectral resolutions for the Cassini instruments tend to be comparable to or significantly better than those for Voyager. However, Cassini's spatial resolution is strongly dependent upon the distance of closest approach during flyby. The flyby distances are 50  $R_J$  and 168  $R_J$  for 1996 and 1997 launches respectively. If Cassini launch is delayed beyond the 1996 baseline the spatial resolution at Jupiter will be very seriously degraded.

Atmospheric thermal structure, composition, cloud morphology, and dynamics are interrelated in a complex manner. Spectral features of various trace gases can be used to infer large scale atmospheric motions. Clouds form where a particular combination of thermal structure and gas abundance leads to condensation. The colors of these clouds are produced by chromophores generated through atmospheric chemistry, and their motions trace out small- and intermediate-scale dynamical patterns. Meridional thermal gradients give rise to zonal winds which in turn contribute to Jupiter's banded appearance. Generally, information in latitude and longitude depends on instrument spatial resolution, whereas except for limb scanning close in, vertical information depends on spectral resolution. Cassini has the capability of addressing all these issues simultaneously in a more satisfactory manner than either Voyager or Galileo.

### Composition

The photodissociation of  $\text{CH}_4$  in the stratosphere leads to the creation of the hydrocarbons  $\text{C}_2\text{H}_2$ ,  $\text{C}_2\text{H}_4$ ,  $\text{C}_2\text{H}_6$ , and  $\text{C}_3\text{H}_8$ . The  $0.5 \text{ cm}^{-1}$  spectral resolution of CIRS will permit measurements of hydrocarbon vertical abundance profiles up to about the 0.1 mbar level and mapping of stratospheric hydrocarbon distributions.

The abundance and vertical distribution of  $\text{NH}_3$  and  $\text{PH}_3$  in the upper troposphere will be obtained by the CIRS. Because its spectral coverage extends to much longer wavelengths (up to  $1000 \mu\text{m}$ ) than any instrument previously flown to Jupiter, the possibility exists of detecting new species expected, from thermodynamic considerations, to be present in the Jovian atmosphere. These include  $\text{H}_2\text{S}$ , HCP, HF,  $\text{HB}_2$ , HI and  $\text{H}_2\text{Se}$ . The HCN tropospheric mixing ratio will also be obtained, as well as the D/H mixing ratio from the R(0) HD line at  $112 \mu\text{m}$  and the  $\text{CH}_3\text{D}$  band at  $8.6 \mu\text{m}$ . The latter mixing ratio has cosmological significance, and comparisons with values for the other Jovian planets are very important.

The global averaged  $\text{H}_2$  ortho-para ratio can be inferred in two ways. One way is to fit the far-IR spectrum between 50 and  $600 \text{ cm}^{-1}$ . This procedure was used with Voyager data, but Voyager was limited to wavenumbers above  $200 \text{ cm}^{-1}$ , and signal to noise was much inferior to that anticipated for Cassini. The other procedure is to spectrally analyze the hydrogen dimer  $(\text{H}_2)_2$  features at 16 and  $28 \mu\text{m}$ . The two methods can be used to cross-check each other as well as to provide a crude vertical distribution. Important information regarding the vertical motion field will result. An additional check on the  $\text{H}_2/\text{He}$  ratio will also be obtained.

Finally the  $5 \mu\text{m}$  "window" will be explored by NIRS. This spectral region is relatively transparent, enabling sounding to the 2-3 bar level in local "hot spots"

### Thermal Structure

Thermal maps in the upper troposphere will have spatial resolutions comparable to those of Voyager, though with considerably less noise. Vertical structure down to the 1 bar level will be obtained from CIRS spectra between  $10$  and  $600 \text{ cm}^{-1}$ . MSAR will extend this information to 2 bars. Stratospheric thermal maps will be of considerably higher quality than those from Voyager. Vertical resolution from nadir sounding of the  $\text{CH}_4 1304 \text{ cm}^{-1}$  band of CIRS will yield a vertical resolution of about two scale heights, or 50-60 km.

## Clouds and Dynamics

Images of Jupiter show motions on all scales, although velocities associated with these different scales tend to be comparable. This suggests that mass motions are responsible for much of the changing fine-scale structure, although some wave structure information also exists. Hence cloud motions can be used as tracers of wind velocity, primarily by ISS.

At the largest scale, cloud tracers can be used to measure the zonal wind profile as a function of latitude. It is important to compare with previous results from Galileo and Voyager to determine any time dependence. Thermal maps in the upper troposphere from CIRS will yield wind shears, and the ratio of these to the wind speed will give a measure of the decay scale of the zonal jets.

High resolution tracking by the narrow angle cameras on both Galileo and Cassini will permit the determination of eddy velocities. However, a wide angle camera is vital for establishing the relative displacement of features with time, and this is unavailable on Galileo. Also, Galileo does not have Cassini's ability to infer zonal mean winds from far infrared data. If both the zonal mean and eddy velocities are known, along with the relative altitudes to which they pertain, it can be determined whether the eddies feed energy and momentum to the zonal jets or vice versa. For clouds larger than 2000 km in size it should be possible to infer these altitudes from gaseous optical depths above the cloud layer at selected wavelengths between 0.4 and 14  $\mu\text{m}$  using spectra from NIRS and CIRS.

These same instruments provide the wide spectral base required to infer cloud particle sizes and mass loading from the variation of opacity with wavelength. Although it is generally assumed that most of the visible clouds are condensed  $\text{NH}_3$ , the colours that some clouds exhibit show that other substances are present. The wide spectral base, coupled with the adequate spectral resolution of NIRS and CIRS, make it feasible to search for spectral signatures identifying the composition and/or trace impurities of the different clouds. A combination of near infrared  $\text{CH}_4$  band strengths and measured vertical thermal structure will permit inferences to be drawn about the altitudes at which condensation occurs.

The unique capability of CIRS to provide high resolution thermal maps in the stratosphere allows the extension of wind shear calculations into this region, greatly improving our understanding of how the zonal jets behave with altitude.

Longitudinal thermal structure leads directly to a determination of the preferred zonal scale of wave propagation in the stratosphere. A much better defined structure for the stratospheric polar region "hot spots" discovered by Voyager and ground-based observations will also be determined.

### 3.6.2 Magnetospheric Science

The Cassini flyby of Jupiter will provide an opportunity to obtain unique and significant new information on the dynamics of the Jovian magnetosphere. The new science will be available because: a) Cassini will travel through regions unexplored by Pioneer 10, 11, Voyager 1, 2, Galileo and Ulysses, and b) the Cassini measurement capabilities in some vital areas will greatly exceed those achieved on the earlier Jupiter spacecraft. We consider these two points separately.

#### Exploration of New Regions in Jupiter's Magnetosphere

Figure 3.12 shows the nominal Cassini Trajectory through Jupiter's magnetosphere, and this illustrates that Cassini will move through regions previously unexplored by Pioneer 10, Voyager 1, 2 and even Galileo (Pioneer 11 and Ulysses are not shown, but basically these spacecraft traverse only the dayside of the magnetosphere). Figure 3.12 shows that only Cassini will be able to measure phenomena on the dusk side of the magnetosphere where co-rotating plasma is expected to collide

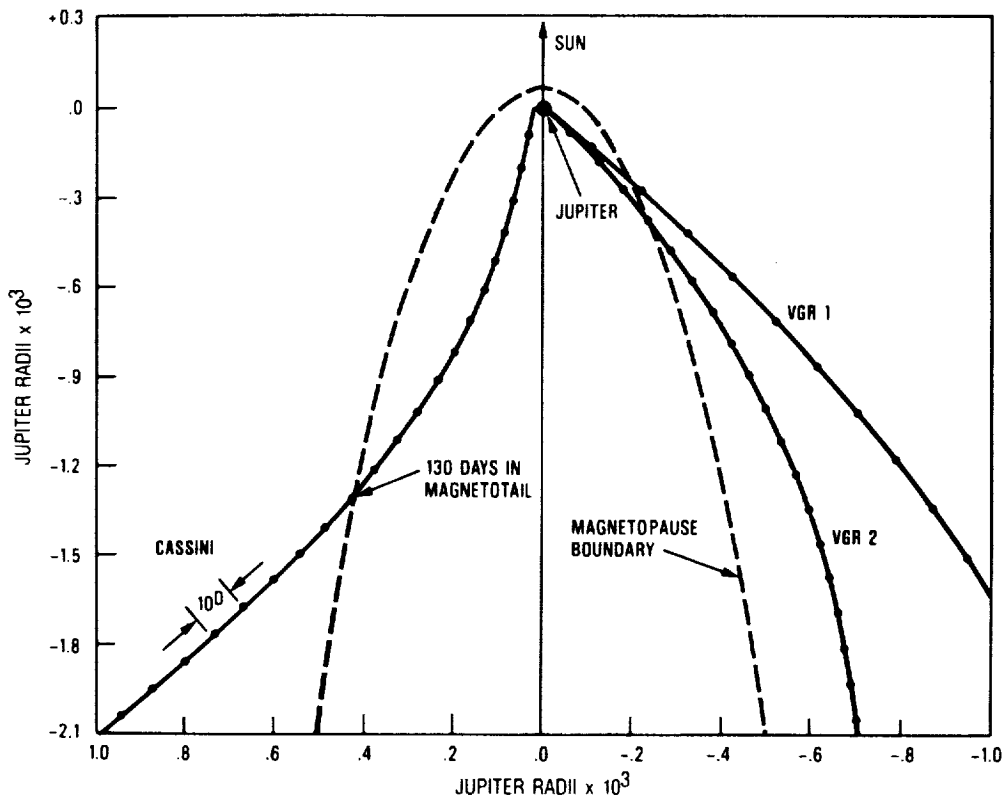


Figure 3.12: *Nominal trajectory of Cassini through the magnetosphere of Jupiter for a launch in 1996*

with plasma convecting in from the Jovian tail. Moreover, since the Galileo tail petal will only extend to  $150 R_J$ , and the Voyager 2 distant crossings of the Jovian tail involved encounters at several thousand  $R_J$ , only Cassini will provide in situ information on near-tail phenomena in the region beyond  $150 R_J$ .

#### New Cassini Measurement Capabilities

The Cassini model payload includes instrumentation with important new capabilities for magnetospheric science of Jupiter. We tabulate some of these and comment briefly on the new science below:

- 1) UVSI: The proposed ultraviolet investigation will have imaging capability, and this should provide the first high-resolution global images of the Jovian aurora and of the Io plasma torus.
- 2) MIMI: The imaging of hot plasma regions with the energetic neutral analyzer will provide the first images of the Io torus, images of the inner plasma sheet and perhaps discern the plasma current flow on a global scale.
- 3) PLS/MIMI: The plasma and energetic ion measurements will be able for the first time to measure uniquely the charge state of various ionic species with energy, mass, and charge state determined separately. Such separation is essential in determining the source of magnetospheric plasma, (i.e. whether it is of satellite, ionospheric or solar wind origin), and the physics of the Io torus ( $S^{2+}$  versus  $O^+$ ).
- 4) PRWS: The planned plasma radio/wave spectrometer will have several capabilities that are new for Jupiter. For instance, the Cassini instrument will measure E and B simultaneously (no wave experiment on Pioneer, no B on Voyager, E and B sampled sequentially on Galileo) and the

instrument will also provide the first triaxial B-field data.

### 3.6.3 Satellite Science

On the 1996 launch trajectory, Cassini will not pass within the boundaries of the Galilean satellite system on its flyby of Jupiter. Closest approach to any satellite will be about 3.5-4.0 million kilometers. At these ranges, Cassini will add little to high resolution imaging and multispectral coverage of the satellites obtained by Voyager and Galileo. However, studies of time variable phenomena, particularly associated with Io, may be very useful, either as extensions of Galileo's observations or possibly in conjunction with an extended Galileo mission (the Cassini flyby will be approximately 2 years after Galileo's nominal end of mission). For example, the larger eruptive plumes on Io should be detectable by Cassini cameras along with large-scale changes in surface markings. These observations, combined with remote measurements of the torus and in situ sampling of the magnetosphere will serve to characterize the state of Io's activity and its effect on the inner magnetosphere during the epoch of the Cassini flyby. There is also the possibility that Galileo will discover further (as yet unknown) satellite-related phenomena which may be usefully followed up with Cassini measurements.

The outer irregular satellites of Jupiter are interesting bodies in their own right. As the Cassini trajectory becomes better defined the possibility of fortuitous encounters with these objects will be investigated. Even distant observation may be valuable in defining the satellites' relationships to asteroids and other irregular outer planet satellites, such as Phoebe at Saturn. The multi-spectral capability afforded by the Cassini instruments is vital for this task.

## 3.7 Asteroid

Asteroids are an important and diverse group of planetary bodies which are scientifically interesting in their own right and have considerable significance for studies of the early history of the solar system. Because of the large number of interesting and compositionally different objects among the asteroids, reconnaissance flybys using spacecraft directed toward other targets have already been recognized as an important element in the planetary programs of both NASA and ESA.

The first such flyby should be an encounter with the asteroid Gaspra by the Galileo spacecraft. A second flyby of asteroid Ida may be possible if Galileo is launched during the early portion of its primary launch period in October 1989.

The information carried by asteroids on the early processes affecting the growth of planets is subdivided in the members of the population; the more objects of various types that are observed, the better the overall knowledge will be.

Future missions traversing the asteroid belt, including CRAF, Vesta and Cassini, will plan in advance for such encounters. Based on the preliminary studies of what can be achieved with the payload on Galileo and CRAF, we may expect the Cassini asteroid encounter to be quite similar in its observational characteristics to the one planned for the Galileo opportunity. In general, flyby distances of about one hundred asteroid radii are envisioned for these encounters.

The most interesting flyby opportunities found for the 1996 launch are listed in Table 3.2 (the candidate list is insensitive to flight time for a given launch year). The current mission planning baseline includes a flyby of 66 Maja, a large C-type asteroid. Other opportunities also exist and the final selection would be following the official selection trajectory toward Saturn. Asteroid 66 Maja might be a good choice in that sense, because several of the envisaged flybys for the other missions concern other types of asteroids. If Cassini flies by 66 Maja it would then perform one of the first explorations of a dark primitive C-type asteroid which is important for its cosmogonical

implications. Comparison with data collected by Giotto, Phobos, Vesta and CRAF will clarify the relationships among various asteroid types and between comet nuclei, the Mars Satellites and dark asteroids. Small asteroids ( $D < 10$  km) might be an interesting alternative, also in terms of the quantity of propellant needed to approach the object. The exploration of one of such bodies, which may be "fragments" produced by a catastrophic encounter of two asteroids, will give information on the possible collisional evolution of the population. The knowledge of a representative sample of the lower tail of the mass/size distribution of the asteroids will clarify the parental relationships between asteroids and meteorites.

Cassini Orbiter instruments offer exceptional capabilities for remotely sensing asteroids, i.e.:

- Camera and radar for shape surface morphology, evidence of differentiation and rotational properties
- Near IR spectrometer for surface chemistry, mineralogy
- Far IR and microwave observations for inference of surface thermal properties
- Plasma experiments and dust detector; for asteroid environment.

The general objectives of an asteroid encounter are summarized below:

- Characterization of Global Properties
  - Accurate Size/Shape
  - Mass Estimates
  - Rotation Period
  - Pole Orientation (precession?)
  - Cratering statistics and "age" of surface
  - Search for close satellites
- Characterization of Compositional Properties
  - Mass–Volume–Density estimates
  - Surface composition (minerals, metals, etc.)
    - \* Global properties
    - \* Heterogeneities
    - \* Stratigraphy in craters
- Characterization of Surface Morphology
  - Morphology of craters as function of diameter
  - Evidence of past internal activity (volcanism, tectonism, etc.)
  - Search for spallation features
  - Ejecta patterns
- Characterization of Regolith Properties
  - Stratigraphy
  - Ejecta dispersal
  - Photometric properties
  - Polarimetric properties
  - Radiometric/thermophysical properties
- Comparative Processes
  - Other asteroids
  - Phobos/Deimos
  - Small ice satellites
- Ground-truth for Assessing Interpretations of ground-based Observations.

ASTEROID	RADIUS (km)	TYPE	FLYBY SPEED (km/s)	DATE	FLIGHT TIME (YRS)	COMMENTS
574 REGINHILD	4	S	11	NOV.1996	6.3	
2096 VAINO	4	-	10	OCT.1996	6.3	
1966 TRISTAN	3	-	14	DEC.1998	6.4	
66 MAJA	46	C	7	MAR.1997	6.5	Fyby at solar conjunction
2824 FRANKE	5	-	11	NOV.1996	6.6	
1808 BELLEROPHON	6	-	6	APR.1997	6.7	
1218 ASTER	4	-	16	DEC.1998	6.8	
1190 PELAGIA	7	-	17	NOV.1998	7.0*	
238 HYPATIA	77	C	15	JAN.1999	7.1*	
2611 BOYCE	13	-	12	MAR.1999	7.3	
AA56 KIRA	5	-	6	JUL.1997	7.3	

\*Flight time must be raised to  $\sim 7.3$  YR to avoid conjunction constraint at Saturn.

Table 3.2: *Cassini asteroid candidates*

### 3.8 Cruise Science

The Cassini spacecraft with its complement of particle and fields instruments provides an excellent opportunity to provide unique and important measurements of the distant solar wind. Although the region between 1 AU and 10 AU has been surveyed by the Pioneer and Voyager spacecraft, and the region between 1 AU and 5 AU will be surveyed by Galileo, Ulysses and CRAF, Cassini will provide important new opportunities for discovery. Using advanced instrumentation on Cassini, such as time-of-flight mass analysis for the plasma/hot plasma instruments, Cassini will provide measurements of the ion distribution functions of all the major solar wind (thermal and suprathermal) ions and interstellar ions under all stream conditions. Assuming the launch of Ulysses at the end of 1990, and arrival over the solar pole in mid-1994, the Cassini instruments can provide in-ecliptic comparison with Ulysses. The latter is well equipped with instruments to study both composition and dynamics of the solar wind and Cassini should be similarly equipped. Cassini will extend composition measurements of the interstellar medium by  $\sim 3$  orders of magnitude (to  $< 1$  keV/nucl) which will allow one to study shocks at lowest energies with composition. Cassini will provide measurements of energetic neutral fluxes with high sensitivity in the interplanetary medium and composition studies of the anomalous component to very low energies ( $\sim 10$  keV/nucl).

The Voyager observations from 1 AU to 10 AU were made during the ascending phase and solar maximum when many transient streams were present. In contrast, Cassini will be launched during solar minimum when large coronal holes extending down from the polar regions of the Sun are expected to dominate the Sun's corona and subsequently, corotating high speed streams with flow speeds  $> 700$  km/s are expected to dominate the solar wind stream structure. At the time of orbit insertion with Saturn, Cassini will be located near the peak of the interstellar O<sup>+</sup> density distribution in the heliosphere. These measurements will provide important information about the composition of the interstellar medium. The dust analyzer should provide measurements of interplanetary dust within the asteroid belt. The UV spectrometer can provide important measurements of the UV background from the surrounding interstellar gas and the nature of the interface between the solar wind and interstellar medium.

More specifically, Cassini offers the opportunity to make significant advances in our understanding of the interplanetary plasma and magnetic field in the following ways:

1. Thermal structure and thermodynamics of the solar wind
2. Evolution of turbulence and mixing processes
3. Interstellar ions.
4. Radial structure and orbital characteristics of the Interplanetary dust cloud.

### 3.8.1 Thermal Structure and Thermodynamics of the Solar Wind

The large-scale dynamical processes in the solar wind are primarily controlled by the magnetic and thermal pressure forces. The electron pressure is presumably comparable to the ion pressure, but almost nothing is known about the electron temperature beyond  $\sim 5$  AU. Theoretical models of flows in the outer heliosphere must either neglect the electrons (which is unjustified) or incorporate assumptions about the electrons which have no theoretical or experimental justification. In order to fully understand and properly model the flows in the outer heliosphere, it is essential to measure the electron temperature there, and to determine the laws governing the transport of energy by electrons. It is also important to make good measurements of the strahl component of the electron distribution function, since these are believed to be the remnant of the field-aligned runaway electrons of the solar corona which set up the interplanetary potential and subsequent ion acceleration in the solar corona. The radial evolution of this component (energy spectrum and angular width) will provide important information about the thermal transport of energy by electrons and the magnetic topology (open vs. closed) in the interplanetary medium at different radial distances from the Sun. The instrumentation required on Cassini for the planetary objectives can make the needed measurements in the solar wind. Since electron measurements are not available from either Pioneer or Voyager beyond 5 AU, Cassini can provide new measurements of fundamental importance.

The ion portion of the Cassini plasma instrument should yield measurements of the ion distribution functions for all the major solar wind ions. These measurements will allow one to study the heating of ions under different stream conditions (Alfvén waves, wave turbulence, shocks, etc.) and the variation of ion temperature with radial distance for a wide range of ion mass and charge states. Since, for ions of greater  $M/Q$  the ion cyclotron frequency shifts to lower values where there is more wave power, one might expect more effective ion heating and acceleration for those ions of greater  $M/Q$ . Since these relatively rare heavier ions can be considered test particles, they should not influence the power spectrum of the wave turbulence which makes modeling of this phenomenon straightforward once the power spectrum of the waves is given.

### 3.8.2 Evolution of Turbulence and Mixing Processes

It has been established that the interplanetary medium contains a mixture of waves and turbulence. The turbulence appears to grow in relative importance with increasing distance from the Sun, and there is evidence that it extends to lower frequency with increasing distance from the Sun. The evolution of MHD turbulence is of fundamental physical significance, it has applications to a variety of astrophysical situations, such as the evolution of large-scale interplanetary flows.

In order to study the evolution of the turbulence in the frequency range of interest (periods between 2 days and the local characteristic plasma wave periods) it is necessary to have continuous plasma and magnetic field measurements. In the case of Pioneer and Voyager, real time tracking was used and the DSN could not provide continuous tracking with gaps of several hours or more each day. In the case of Cassini a store-and-dump strategy will be used and continuous measurements will be possible with only modest bit rates required. It would also be desirable occasionally to obtain continuous measurements at a high rate with continuous tracking in order to study the

dissipation range of the turbulence. If this tracking were done, for example, one solar rotation in a year, one would also be able to study shocks at these greater distances.

One might expect that mixing processes related to turbulence may occur in the interplanetary medium. Very little is known about such processes for a collisionless MHD flow such as the solar wind, and essentially nothing is known about the mixing process in the outer heliosphere. The availability of state of the art composition measurements on Cassini together with observations of the MHD turbulence provides unprecedented opportunity to study mixing in the solar wind. One expects that mixing will become increasingly important with increasing distance from the Sun.

### 3.8.3 Interstellar Ions

It is important to make measurements of the different kinds of interstellar ions such as  $H^+$ ,  $He^+$ ,  $N^+$  and  $O^+$  in order to make composition measurements of the interstellar medium. Theoretical modelling of the interstellar wind interaction with the heliospheric medium will have to be used to compute the composition of the interstellar medium from the interstellar ion observations by Cassini. Because of the lower ionization energy of hydrogen, nitrogen and oxygen relative to that for helium (interstellar  $He^+$  has peak density inside 1 AU) the interstellar  $H^+$ ,  $N^+$  and  $O^+$  density peak will occur at heliocentric radial distances  $\sim 10$  AU. In all cases the density maximum will be confined to the downstream side of the heliosphere relative to the interstellar wind, which fortuitously happens to occur along the Saturn-Sun line at the time of Saturn Orbit Insertion (SOI) for Cassini. The maximum pick up energy for  $O^+$  ions for solar wind speeds between 300 km/s and 1000 km/s is 30 keV and 336 keV, respectively; while for  $H^+$  the range of maximum pick up energies is 1.9 keV and 21 keV, respectively. Therefore, interstellar  $H^+$  and  $He^+$  can be monitored by the plasma experiment, while interstellar  $N^+$  and  $O^+$  will be monitored by the hot plasma experiment. The interstellar ions will be distributed in velocity space in the form of a pick up shell distribution in the solar wind frame of reference; the 1-2 meter boom and turntable on Cassini will provide the angular coverage required to measure these ions. These ions will be identified by their low ionization charge states and shell-like energy-angular distributions in the spacecraft frame.

### 3.8.4 Structure and Orbital Characteristics of the Interplanetary Dust Cloud

Recent observations by the IRAS satellite indicated that collisions among asteroids produce large amounts of dust particles giving rise to the thermally emitting "asteroidal bands". However, passages through the asteroidal belt of Pioneer 10, 11 and Voyager 1, 2 spaceprobes did not find signs of a significant enhancement of the spatial micrometeoroid density in the asteroid belt. This result may be partially due to the very limited capabilities of the dust detectors onboard Pioneer 10 and 11.

Comets are believed to be the major source of the interplanetary dust cloud, at least in the inner solar system. Very little is known in the outer solar system where ice grains could contribute a major share to the dust cloud. Information on the orbits of these dust particles will show their generic relation to comets, asteroids and outer planets.

The knowledge of flux, size and orbital distribution of interplanetary dust particles is needed to understand some dynamical processes in the outer planetary systems: e.g. the bombardment by micrometeoroids crushes the surface material on satellites and ring particles causing the formation of a regolith and the generation of small ejecta particles. Measurements of the interplanetary dust distribution by Cassini will complement similar measurements made by Galileo and Ulysses inside and at Jupiters orbit and will aid the better understanding of phenomena observed by Cassini in the Saturnian System.

### 3.8.5 Gravitational Waves

In the mHz range there are three possible sources of gravitational waves: bursts from violent events in galactic nuclei; cosmological background, and periodic waves. Cassini will provide an excellent platform to extend, after Galileo and Ulysses, the searches for low frequency gravitational waves. A Cassini gravitational wave experiment would offer the following advantages over Ulysses and Galileo: The Earth-spacecraft distance is greater, thus facilitating the detection of lower frequency (and more intense) sources; the mission has three oppositions, around which three measurement runs can be performed with more observing time; the three measurements would then be performed when the spacecraft is at different distances from the earth, thus allowing a better separation of continuous signals from the noise; the Deep Space Network capabilities will be improved at the time of Cassini.

### 3.8.6 Cruise Data Tracking

In order to accommodate the data receiving problem, a cruise science format could be designed using the 25 megabits solid state storage device that could be read out once per week. A complete set of instantaneous cruise measurements (plasma, fields, waves, energetic particles, dust) requires approximately 3 kilobits, and the concise format would thus permit a continuous sequence of snapshots at a rate of one every half hour.

During these weekly periods of tracking, it will be straightforward to use the telemetry link to extend current searches for gravitational waves. These could be detected through their signature in the Doppler tracking of the spacecraft, if sources with sufficient intensity and frequency exist.

# Chapter 4

## The model payloads

### 4.1 The Orbiter Model payload

#### 4.1.1 The Orbiter Payload Composition

The Orbiter payload contains 15 instruments designed to address in a very comprehensive way the science objectives stated in chapter 3. The instrument characteristics and their capabilities are summarized in table 4.1

#### 4.1.2 Typical Orbiter Science Profile

##### Introduction

A typical orbit period is  $\sim$ 32 days ( $\sim$  2 Titan revolutions) most of which is spent at large distances from the discrete targets, e.g. icy satellites, Titan, rings, and Saturn; thus, the spacecraft is operating at a low data rate. This period is referred to as the orbital cruise phase, during which time the particle and field experiments are collecting continuous data pertinent to the Saturnian magnetospheric system. The high activity period, nearly centered about Saturn's closest approach, typically lasts 8-12 days depending on the spacecraft orbit orientation. Thus the spacecraft spends only 25-35% of one orbit period in the high activity region during which time 82% of the total data collected on that orbit are taken. Thus, the design of the spacecraft data system must be adequate for the high-activity periods. During this typical orbital period, observations are made of Saturn, Titan, Enceladus, Dione, Rhea, Saturn's Rings, Titan's torus, and the inner magnetosphere.

##### Orbital Cruise Phase

Continuous data at a rate of  $\sim$ 2.8 kbps are collected by the DA, PLS, PRWS, MAG, MIMI, INMS, and RPA/LP instruments. Continuous data are required due to the highly complex and time-variable nature of the magnetosphere, the various current systems, and the existence of various sources and sinks of magnetospheric plasma.

##### High Activity Periods

Figure 4.1 shows a typical 12-day high activity period. Typical observations of Saturn are: global maps, North/South scans, East/West scans, high resolution cylindrical maps, and discrete feature tracking campaigns, carried out with the complete suite of remote sensing instruments. Near Saturn's closest approach remote sensing observations are made of three icy satellites, Dione, Enceladus, and Rhea. Two extended periods of dedicated ring observations are taken, one each at low

Instrument/investigation	Main scientific objectives	Mass (kg)	Power (W)	Data rate (kbps)
Imaging Science Subsystem (ISS)	Imaging atmospheres, satellites and rings	36.3	30.0	115.2
UV Spectrometer/Imager(UVSI)	Saturn and Titan atmospheric composition, ionosphere remote sensing	8.0	6.5	4.0
Near IR Spectrometer (NIRS)	Compositional identification and mapping of icy satellites, rings and cloud structure	18.5	14.3	11.5
Composite IR Spectrometer (CIRS)	Atmosphere composition and vertical, horizontal distribution of constituents. Deep sounding of Saturn and Titan	22.9	17.6	3.0
Microwave Spectrometer and Radiometer (MSAR)	Atmospheric abundance of CO, HCN, HC <sub>3</sub> N, and surface properties of Titan. NH <sub>3</sub> abundance in Saturn	17.0	10.0-24.0	1.0-5.0
High Speed Photometer (HSP)	Stellar occultation measurements for atmosphere and ring science	1.5	2.0	1.0
Titan Radar Mapper (RADAR)	Imaging/Mapping/Altimetry of Titan surface. Subsurface sounding of Titan and icy satellites	18.0	50.0	1.6-352.0
Radio Science (RS)	Titan and Saturn atmospheric structure profiles. Ring physical properties. Satellite masses and gravitational moments of solid bodies. Gravitational waves	6.3	-	-
Dust Analyser (DA)	Physical properties of dust particles	5.0	2.0	0.024
Plasma/Radio Wave Spectrometer (PRWS)	Spectral frequency characteristics of magnetospheric and ionospheric emissions	6.8	7.0	0.9
Plasma Spectrometer (PLS)	Composition, charge-state and energy distribution of magnetospheric plasma; 3-D measurements	12.5	14.5	1.6-16.0
Magnetospheric Imaging Instrument (MIMI) Hot Plasma Detector (HPD) Energetic Neutral Analyzer (ENA)	Composition, charge-state and energy distribution of energetic ions and electrons. Detection of fast neutral species. Remote imaging of magnetosphere	16.0	14.0	1.5-14.0
Magnetometer (MAG)	Magnetic field measurements	3.0	3.1	3.6
Ion/Neutral Mass Spectrometer (INMS)	Titan aeronomy and chemical composition of Saturn's magnetosphere	6.0	15.0	1.0
Retarding Potential Analyzer and Langmuir Probe (RPA/LP)	Cold plasma measurements	3.4	4.5	1.5

Table 4.1: *Cassini Orbiter* model payload

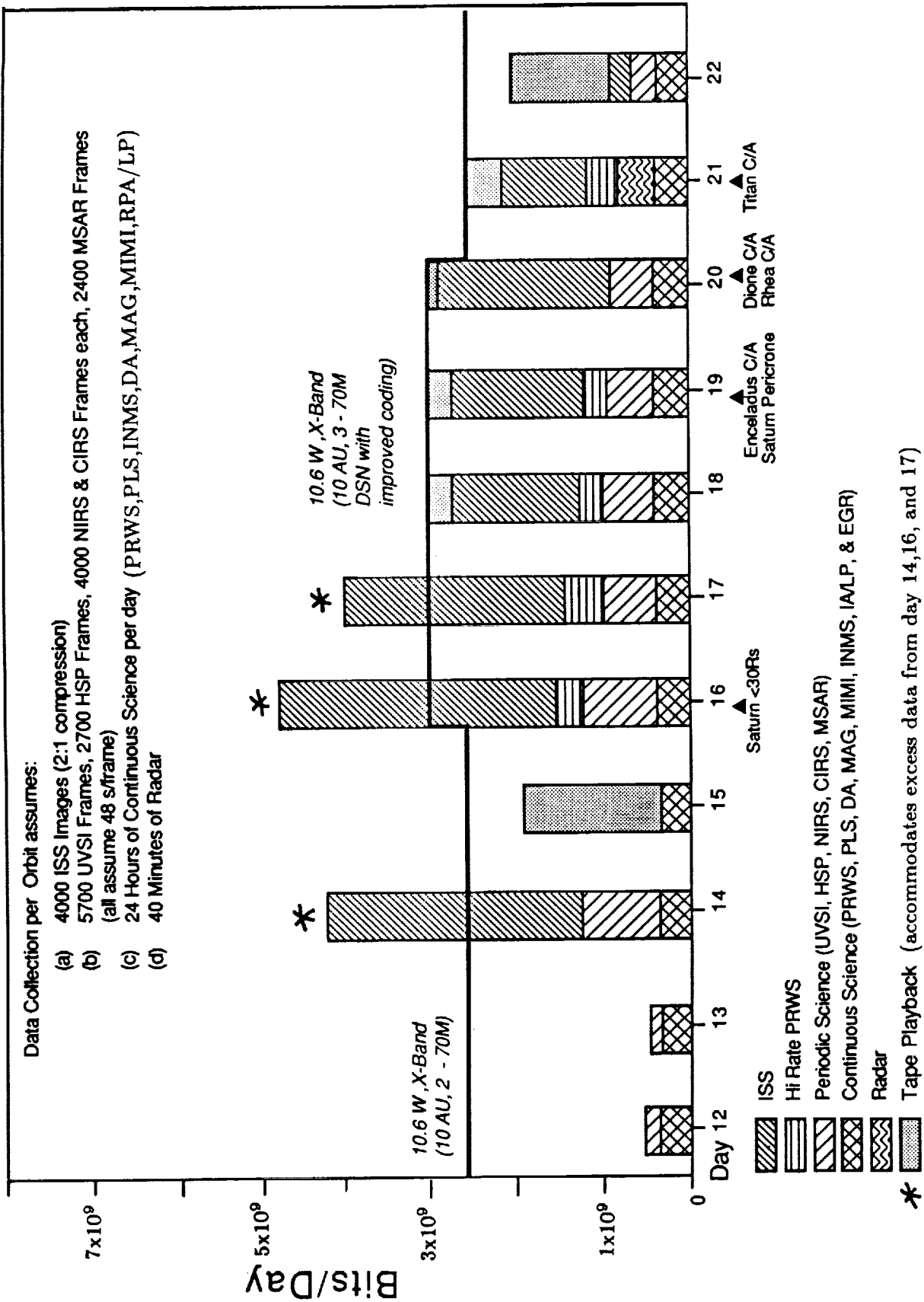


Figure 4.1: *Data return profile during a typical 12-day high activity period*

and high solar phase angles. These occur at E-9 hours and E+28 hours, respectively (E is the time of Saturn encounter). During the Titan flyby at E-42 hours, the complete suite of remote sensing instruments are used together with the radar, aeronomy instruments, and particle and field instruments, all in their high data rate modes.

#### 4.1.3 Instrument Description

##### Imaging Science Subsystem (ISS)

This facility instrument is a pair of framing cameras using separate, but identical two-dimensional (1024x1024) charge coupled device (CCD) arrays. The Narrow Angle Camera has a field of view of  $2.93^\circ \times 2.93^\circ$  (focal length 2m) and an angular resolution of 8mrad/pixel; the Wide Angle Camera has a field of view of  $6^\circ \times 6^\circ$  (focal length 200-300 mm) and an angular resolution of 50  $\mu$ rads/pixel. Spectral resolution is achieved by filters (22 in the Narrow Angle; 14 in the Wide Angle) covering the spectral range from 200 to 11000 nm. Expected dynamic range is about 4000; 12 bit encoding will be used. Maximum data rate will be about 400 kbits/sec. Data compression (at least 2x) will be available. Primary scientific objectives include: detailed morphology and spatial variation of albedo and color of satellite surfaces; photometric functions and figures of some satellites; search for additional small satellites; atmospheric vertical cloud structure on Titan and Saturn from photometric studies, mean vertical wind profiles at regional boundaries on Saturn, separation of atmospheric mass motions from wave motions on global scales; temporal variations in structure of Saturn's rings; color and photometric properties of rings to derive column densities and size distributions of particles; search for small embedded satellites; investigate correlations between the ambient electromagnetic field and ring morphology. The instrument will provide the primary visual reference for the spacecraft, furnishing optical navigation data and pointing support information for other instruments. Secondary scientific objectives include detailed imaging of Jupiter, its satellites and at least one asteroid during flybys.

##### UV Spectrometer/Imager (UVSI)

The Ultraviolet Spectrometer-Imager (UVSI) will provide spatially-resolved spectrography and low spatial resolution imaging of Saturn, Titan, Saturn's magnetosphere, and its rings at wavelengths from 500 to 3200 Å. Its spectral resolution will be better than 5 Å.

The UVSI will probe the atmospheres of Saturn and Titan, and the structure of the rings, by observing occultations of the sun and stars. Absolute column abundances are determined independently of instrument calibration. Characteristic absorption signatures identify species. Distributions of species in altitude, and hence the temperature structure of the atmosphere, follow directly. Within its wavelength range, the major constituents of the atmospheres are accessible, as well as hydrocarbons, which are important to our understanding of photochemistry. Good altitude resolution and wide coverage in latitude and local time are inherent in the mission design for Cassini.

Spectroscopy and imaging of Saturn will map and monitor dayglow and auroral emissions. The latter can be especially well studied from the higher-inclination orbits possible in the later portion of the mission. Mapping of hydrocarbon distributions through measurements of the solar reflection spectrum will complement the occultation observations. Aerosols will be studied using the same techniques.

At Titan, the UVSI will map emissions of H Ly<sub>α</sub> and from several N<sub>2</sub> band systems in the EUV and FUV. By this means it will identify the excitation mechanism and clarify our understanding of the interaction between Titan and the magnetosphere. Measurements of neutral H in the vicinity of Titan by observations of resonance scattering of the solar line, will help to understand the escape of H to the magnetosphere. The distribution of hydrogen, nitrogen, and oxygen within the

magnetosphere will be addressed by low-resolution imaging of resonantly scattered sunlight from the system.

The composition of the rings will be investigated by measurements of their albedo, and it may be possible to infer the distribution of water vapor in the ring atmosphere by observing OII emissions.

### **Near Infrared Spectrometer (NIRS)**

The Near Infrared Spectrometer (NIRS) on the model payload is based upon the VIMS facility instrument on the CRAF mission. It is a grating spectrometer with spatial mapping capability operating in the range 0.35 to 5.3  $\mu\text{m}$ , with an element field of view of 0.5 mrad. A similar instrument has already been built and tested for the Galileo mission, and another was selected for Mars observer. The instrument is designed to meet key science objectives relating to the composition of satellite surfaces, asteroids and rings. The near infrared reflectance spectrum is a particularly diagnostic region for composition of all of these bodies and the NIRS spatial scanning capability will allow compositional mapping of satellites surfaces and searches for rare, non-H<sub>2</sub>O volatiles.

The spectral region around 5 microns can be used to measure abundances of minor constituents (PH<sub>3</sub>, GeH<sub>4</sub>, CO, CH<sub>3</sub>D) in the deep atmosphere of Saturn. NIRS, with a spectral resolution of only around 0.025  $\mu\text{m}$ , is not well suited to this investigation. A conceptual design exists which improves the spectral resolution in this region to allow atmospheric studies, but the design is too immature to consider for the model payload.

Observations of the atmospheres of Saturn and Titan, over a range of phase angle geometries, will be diagnostic of the aerosol properties, including the distribution of aerosols within the atmospheres.

### **Composite Infrared Spectrometer (CIRS)**

The Composite Infrared Spectrometer (CIRS) will use a dual configuration following the MIRIS concept developed for Voyager; a polarization interferometer will operate in the far infrared (10-700  $\text{cm}^{-1}$ ) and a conventional Michelson interferometer will cover the middle infrared (700-1400  $\text{cm}^{-1}$ ). The spectral resolution will be 0.5  $\text{cm}^{-1}$  apodized. Integration time per spectrum will be 25 seconds. Both interferometers share a 50 cm diameter Cassegrain telescope. The far infrared focal plane will contain a 1x5 array of thermopile detectors, each with a 4.3x13 mrad field of view. Two 1x43 HgCdTe detector arrays will be used in the mid-infrared focal plane, with each detector covering a 0.1x0.3 mrad field of view. The mid-infrared focal plane will be radiatively cooled to 90 °K, while the instrument and far infrared focal plane will be maintained at 170 °K. The CIRS will be used in three observing modes. Mode 1 applies to limb sounding within 0.5 hours of Titan closest approach. Here the five far infrared fields of view will be observed simultaneously at 0.5  $\text{cm}^{-1}$  resolution, along with an average of the 43 mid-infrared fields of view. Mode 2 will be used within 20 hours of Titan and Saturn to perform limb sounding at 20  $\text{cm}^{-1}$  resolution. In this case 20 of the 43 mid-infrared fields of view will cover the limb and be observed simultaneously. Mode 3 will be for nadir viewing within 10 hours of Titan and 60 days of Saturn. One of the far infrared fields of view will be used here, along with an average of the 43 mid-infrared fields of view. Modes 1 and 2 will resolve 1 vertical scale height and Mode 3 will resolve 0.5 to 2.5 scale heights.

### **The Microwave Spectrometer and Radiometer (MSAR)**

A microwave instrument has multiple applications, from diagnosis of the surface state of Titan to measurements of important atmospheric species with excellent vertical resolution. The MSAR

instrument is a configuration of four radiometer channels with nominal bandwidths of 1 GHz centered at 230 GHz, 177 GHz and 2 channels at a frequency near 15 GHz. The 2 mm channels form independent spectrometers for remote sounding of molecular species in the atmosphere of Titan and Saturn, and will be used to observe planetary satellites and Saturn rings. The 2 cm channels will act as a polarimeter to study the surface of Titan, other satellites, asteroids and the rings of Saturn. The 4 receivers and the 30 cm telescope are mounted on the science instrument scan platform with a field of view from the nadir to both the in-track and cross-track horizons. The outputs of the 2 mm wavelength channels are sent to a spectrometer of total bandwidth of about 500 MHz with spectral channel resolution of 1 MHz. The center 40 MHz will be further analyzed in 200 KHz channels for the measurements of winds. The two 15 GHz channels will be fed by signals from the telescope in 2 orthogonal planes of polarization and each will be square-law detected. The brightness temperature in each of the 1 MHz spectral channels will be measured with a precision of +/- 0.25° K in a 10 second integration, which requires a single-sideband system temperature no greater than 1200°K. The brightness temperatures in the broadband polarimeter channels will be measured with a precision of +/- 0.1° K and all systems will be "absolutely" calibrated to about +/- 2°K.

To minimize power usage, the 2 spectrometer channels and the polarimeter will operate one at a time, either in a programmed sequential mode or by earth-based command.

### High Speed Photometer (HSP)

The High Speed Photometer is designed primarily to perform stellar occultation measurements of Saturn's rings and secondarily to perform occultation measurements of the Titanian and Saturnian atmospheres. During the Cassini mission the rings are quite "open" and largely solar illuminated. It is thus necessary to minimize contributions to the measurement signal due to sunlight scattered from the rings in order to achieve an adequate signal-to-noise ratio in the more opaque ring regions. The most suitable spectral region is the ultraviolet below 200 nm, where the contribution from solar reflection is small, the detectors can be strongly solar-blind, and detector cooling is unnecessary. The wavelength range is 117 to 180 nm and the telescope aperture is 11 cm. Accurate, stable pointing is essential, and the absolute timing of each sample must be known to an accuracy of 10 msec.

Instead of this dedicated occultation photometer, alternative implementations are possible. These could make use of the relatively large telescopes incorporated by other instruments, such as the near- or far- infrared spectrometers, in order to improve the signal-to-noise ratio of the occultation data. It may also be possible to design a successful near-infrared ring occultation photometer, operating at 3.0 microns with a cooled detector array, if the more severe problem of scattered sunlight at this wavelength can be dealt with. It would be necessary to provide on-board hardware and software to remove the scattered light contribution from the total measured flux, substantially increasing instrumental complexity.

### Radar Experiment (RADAR)

The primary purpose of the radar experiment is to unveil the characteristics of the Titan surface, which is covered by a dense opaque atmosphere. The radar should answer questions such as: How much of the Titan surface is covered by land and ocean respectively? What are the most important geographic features? What is the topography? What are the small scale surface properties (such as surface roughness and dielectric constant)? Besides these primary questions, the radar might also be used in an attempt to sound the Titan surface and, thereby, measure the depth of an ocean, if

one is present. Also the radar can be used for targets other than Titan, such as asteroids and icy satellites.

The different questions to be addressed by the radar require different functional modes. To achieve wide swath, moderate resolution images, a real aperture side-looking radar (RAR) mode is necessary, whereas a synthetic aperture radar (SAR) can provide high resolution images over limited areas. The RAR coverage is expected to be greater than 50% of the Titan surface. The altitude and roughness measurements are performed with a high frequency altimeter and sounding is performed by a low frequency altimeter.

Frequencies of 14 and 30 GHz have been considered for the RAR, SAR, and altimeter modes. The advantage of the higher frequency is significantly better resolution in the important RAR mode, however, the signal-to-noise ratio will be degraded.

Using the telecommunications antenna with additional feeds, the RAR can map 300 km on each side of the ground track with a resolution ranging from 4 to 50km depending on altitude (800 - 3000km) and frequency (14 or 30 GHz). The SAR can map 50 km on both sides of the ground track with a resolution of 200 m (4 looks). The maximum operation altitude for the SAR will be 1200 km. The nadir pointing altimeter can achieve a height resolution of 10 m and a surface roughness accuracy of 2 m. The sounder also uses the telecommunication dish. It operates at S-band (2.2GHz) and has a height resolution of 10 m (free space).

### **Radio Science (RS)**

Radio Science embraces a group of experiments that utilize dual-wavelength (3.6 and 13 cm) microwave signals to probe Titan, Saturn, Saturn's Rings, Saturn's gravity field, and possibly gravity fields of Titan and other satellites. Information is derived from amplitude, frequency, and spectral perturbations introduced by these targets on an incident coherent CW signal whose amplitude and frequency are precisely controlled.

Traditionally (e.g., Voyager) Radio Science experiments have been conducted in a "downlink" configuration. A ~10-20 W signal is transmitted from the spacecraft and the perturbed Earth received signal is recorded for later off-line bandwidth reduction and analysis. A viable new configuration is the "uplink" configuration, where an ~200,000 W signal is transmitted from the Earth and the perturbed signal is received on board the spacecraft. An onboard dedicated signal processor is utilized to "compress" pertinent spectral information, significantly reducing the data volume to be relayed back to the Earth. With Cassini, a potential increase (over Voyager) of 30-40 dB in signal-to-noise ratio can be achieved with the uplink configuration, allowing for fundamental improvements on Voyager results.

The Radio Science objectives require orbit control to achieve multiple occultations by Titan, Saturn, and the rings. Desirable orbits correspond to moderate occultation distance (~2- 6 body radii) and need to be spread in space and time for coverage. Radio Science objectives also require the capability to execute accurate, preprogrammed high-gain antenna-pointing maneuvers or, alternatively, the use of a steerable antenna.

A closely related group of experiments is based on the use of radio tracking to study the gravity field of Saturn and its satellites.

### **Dust Analyzer (DA)**

The objectives of the Dust Analyzer are: to analyze the dust particle population in the Saturnian system and in interplanetary space; to determine the mass, speed and electrical charge of individual dust particles to understand the size distribution, orbital distribution and magnetospheric interaction of the dust particles.

An impact plasma detector counts individual impacts; charged grains are detected prior to these impacts by the charge which they induce when flying through an entrance grid. Ions and electrons of the plasma are accumulated by charge-sensitive amplifiers, delivering coinciding pulses of opposite polarity whose heights and rise times depend on the mass and speed of the impacting particles. The rise time, height and any induced charge is measured for particles whose impact speed is equal to or greater than about 1 km/s and impact angle is less than or equal to 70° with respect to the detector normal. This instrument is mounted on the turntable to allow a large fraction of angular space to be sampled. These data will be analyzed to investigate the physical and dynamical properties of small dust particles (masses between  $10^{-16}$  and  $10^{-6}$ g) in the Saturnian environment. These properties include mass, speed, flight direction, charge, impact rate and size distribution.

### **The Plasma and Radio Wave System (PRWS)**

A unified system to measure plasma waves and radio emissions at Saturn is named the Plasma and Radio Wave System (PRWS). The PRWS will utilize a pair of orthogonal 10 meter antennas in a manner similar to that employed on Voyager. At low plasma wave frequencies these elements will be used as a balanced dipole (effective length 7 meters) and at high radio emission frequencies the elements will be used as a pair of orthogonal unbalanced dipoles capable of providing information on wave polarization and direction of arrival.

The PRWS will also use triaxial magnetic search coils covering the frequency range 5 Hz to about 1 kHz. The signal processing will involve several well-proven techniques to provide precise information on general spectral characteristics, wave amplitudes, and rapid variations in frequency-time characteristics. The PRWS electronics unit will include multi-channel analyzers, sweep frequency receivers and a wideband waveform link similar to those employed on Voyager. The changes from Voyager and Galileo include: 1) use of triaxial search coils, 2) simultaneous measurements of E and B-fields, and 3) simultaneous measurements of responses in the triaxial search coils.

### **The Plasma Spectrometer (PLS)**

The PLS instrument will study the solar wind plasma, including the minor ions, out to radial distances of  $\sim 10$  AU, and establish the sources of plasmas in the Saturnian system (e.g., ionosphere, solar wind, rings, and satellites). It will study plasma interactions with Titan and the other Saturnian satellites and rings, investigate the roles of plasmas as a source of energetic charged particles, and evaluate the roles of plasma waves (measure sources of free energy in particle distributions), magnetic merging, rotational forces, pressure gradients, and field aligned currents in the dynamics of the Saturnian magnetosphere. It will study the foreshock region of Saturn's bow shock where reflected ions and electrons of solar wind origin coming from the bow shock are expected to occur; this will include looking for the leakage of magnetospheric plasma into the solar wind. Within Saturn's magnetotail at distances exceeding 100 Rs from Saturn it will observe evidence of a planetary wind, solar wind entry into the magnetotail (boundary layer), and the existence of a tail current sheet. During passage through Saturn's polar region solar wind entry into the polar cusp, ionosphere-magnetosphere coupling (field aligned currents), polar wind, and in situ measurements of the SKR emission region, will be studied.

This instrument is a multi-sensor plasma analyzer using electrostatic deflection with time-of-flight analysis. It makes in situ measurements of the ion and electron velocity distribution functions over the energy range from 1 eV to 50 keV and mass range from 1 AMU to 50 AMU with mass resolution  $\Delta M/M \sim 20$ . It has the ability to resolve the solar wind plasma and magnetospheric particle beams and loss cones with angular resolution  $\sim 2^\circ$  in one plane: in the other orthogonal

plane the angular resolution is  $20^\circ$ . The energy resolution  $\Delta E/E \sim 4\%$  will allow the resolution in energy of supersonic flows. The sensor geometrical factor is  $10^{-4} \text{ cm}^2$  per steradian. For both the solar wind and magnetosphere pulse height analysis, data from the solid state detector in the time-of-flight unit will provide mass and charge separation. The time-of-flight technique using double and triple coincident detection provides measurements of very low background and eliminates the contaminating effects of penetrating radiation. The preferred mounting is on the turntable at the end of a boom.

### **Hot Plasma Detector (HPD)**

The objectives of the Hot Plasma Detector are : to determine the composition, dynamics, sources and sinks of magnetospheric charged particles; to investigate solar wind interaction of Saturn's magnetosphere; to study interactions of the Saturnian magnetosphere with the icy satellites and the rings; to investigate Titan's plasma interaction processes; to study energetic solar particle events in the heliosphere.

The measurement requirements are based on the results obtained by the Voyagers and the Pioneer 11 encounters with Saturn. The energy range of the measurements should extend from  $\sim 20 \text{ keV}$  for ions and electrons to over  $100 \text{ MeV}$  for protons and  $\sim 5 \text{ MeV}$  for electrons. The flux dynamic range should extend from  $\sim 10^{-4}$  to  $>\sim 10^5 \text{ (cm}^2 \text{ sec sr keV)}^{-1}$  for protons and from  $\sim 10^{-2}$  to  $\sim 10^{-6} \text{ (cm}^2 \text{ sec sr keV)}^{-1}$  for electrons; the range for ions heavier than protons is correspondingly lower. Good spectral, elemental, charge state, and pitch angle distributions are necessary to characterize the particle population throughout the magnetosphere, especially at the lower ( $<\sim$  a few MeV) energies. The highest energy measurements are desirable in the inner ( $L <\sim 5$ ) magnetosphere where penetrating radiation, most likely from the CRAND source, dominates. Good spectral resolution in the measurement of energetic electrons is required, especially in the range  $\sim 400$  to  $1000 \text{ keV}$ , in order to distinguish resonance interactions of diffusing electrons with planetary satellites and, possibly, partial rings. Time resolution of the measurements must be such that microsignatures of electrons and/or ions during crossings of satellite L-shells can be detected ( $<\sim$  a few seconds).

A version of the HPD configuration has two separate solid-state detector telescopes mounted on a stepping platform which rotates  $180^\circ$  in discrete steps. A pulse height analyzer is used to analyze data from either of the telescopes. The count rates and pulse heights from the low-energy magnetospheric measuring system and the composition measuring system detector telescopes analyze energetic electrons and protons (energies greater than  $15 \text{ keV}$ ) and heavier ions (energies greater than  $1 \text{ MeV}$  per nucleon) as a function of energy, angle and particle species. This enables the identification of the plasma physics processes operating within the Saturnian magnetosphere and the identification of the overall magnetospheric configuration.

### **Energetic Neutral Analyzer (ENA)**

The scientific objectives of this experiment are to investigate the charge exchange and plasma-neutral interaction process in the exosphere of Titan so that its magnetospheric and solar interaction can be better understood. In addition, important information can be obtained on the plasma-neutral interaction in the magnetosphere of Saturn so that the general energy budget, angular momentum transfer and composition of the energetic charged particles can be clarified. Measurements during Jupiter flyby will be important in clarifying the plasma-neutral interaction process in the Jovian magnetospheric environment. A configuration of this instrument consists of two time-of-flight sensors in series to detect and analyze neutral particles at low density with

energy threshold of 100 eV. Compositional analysis resolving H, He and the CNO group can be performed within certain energy ranges.

### Magnetospheric Imaging Instrument (MIMI)

A combination of the capabilities of the HPD and ENA instruments into one single experimental package could allow significant enhancement in the scientific measurements of the magnetospheric environment, in particular in the areas of magnetospheric imaging and ion composition analysis. The new aspects are:

- Global configuration and dynamics through imaging of ring current, radiation belt, and neutral clouds in Saturn's magnetosphere
- Search for and monitoring of substorm-like activity at Saturn
- Imaging and composition studies of magnetosphere-satellite interactions at Saturn and formation of neutral hydrogen, nitrogen, and water product clouds
- Modification of satellite surfaces and atmospheres through plasma and radiation bombardment.

### Magnetometer (MAG)

The magnetometer requirements to meet science objectives of the Cassini mission (Saturn Magnetosphere) are based on the following:

The planetary field is known to be axisymmetric to 1 or 2 nT in 1000 nT; yet planetary radio emissions, and possibly ring phenomena (e.g., spokes) are periodic, implying a departure from axial symmetry. A better understanding of the internal field is essential from the point of view of dynamo theory and the planet's interior, in addition to better understanding magnetospheric phenomena. This objective requires a vector magnetic field measurement with an accuracy of better than 0.1 %, with a goal of 0.01 % (but consistent with spacecraft capabilities).

The Ring-Magnetosphere interaction objective can be met with a spacecraft trajectory that crosses field lines threading the rings at radial distances of 1.5 - 2.2  $R_s$ . The unambiguous detection and measurement of field-aligned currents associated with the rings requires that the spacecraft pass through them ( in the same manner that polar orbiting satellites at earth map out the distribution of auroral currents). Given a favorable trajectory, the instrument requirements would be for high sample rate (32 samples/sec) vector magnetic field measurements with nT ( or sub-nT ) resolution in a high ambient field (several thousand nT). These requirements are identical to those required for measurement of Saturn auroral currents from a polar trajectory.

Measurement of magnetospheric fluctuations can be accomplished by meeting the requirements set forth above. Measurement of the interplanetary magnetic field requires a vector instrument with high accuracy, and high resolution ,with a noise figure of 0.01 nT RMS over a 0 to 10 Hz bandwidth , operating in a low field (e.g., 16 nT range) environment. A resolution of better than 0.01 nT and absolute accuracy of 0.1 nT is desirable in this range. A sample rate of 16 or 32 samples /sec is required . High-inclination orbits will be valuable for defining the structure of the field, and also for observing possible field-aligned currents associated with aurora.

The magnetic sensing elements must be boom mounted, sufficiently distant from appreciable spacecraft-generated magnetic fields that the ambient magnetic field can be accurately determined. ( Booms up to 13 meters in length have been utilized on previous missions;the Cassini baseline is an 8 meter boom ) .

Spacecraft pointing accuracy (knowledge) is a critical parameter for a vector magnetic measurement in a strong field environment. Previous missions achieved 0.1 degree accuracy in attitude reconstruction; the Cassini requirement is 1 mrad S/C pointing knowledge.

### **Ion/Neutral Mass Spectrometer (INMS)**

This instrument is used to measure the chemical composition, absolute number densities and height distribution of the neutral gas and the low energy ions in the upper atmosphere of Titan. Kinetic temperatures and velocities of neutral and ionic species of low energy can also be measured directly or can be inferred from the height dependence. At a minimum distance from the surface of Titan of 1000 km it will be possible to detect the most abundant hydrocarbons up to the C<sub>3</sub> level to help in understanding the photochemistry and to assess the role of vertical transport of chemical species. If the miss distance is greater, most of the same measurements remain feasible. It will further be possible to measure the concentration of the most abundant nitriles and their height dependence in the upper atmosphere of Titan which will aid in the determination of their formation processes. As a second objective, the instrument will be used to measure the number densities of the major neutral species and low energy ions in the Saturnian inner magnetosphere and exosphere.

The instrument is a mass spectrometer with a minimum mass range from 1 to 65 AMU. It separates species of single or half mass unit, differing by a factor of 10<sup>5</sup> in abundance. The measurable neutral gas densities range is, under optimal conditions, from 10 particle per cm<sup>3</sup> to 10<sup>12</sup> particle per cm<sup>3</sup>. The ion flux detector threshold will be 10<sup>-3</sup> ions per cm<sup>2</sup> per sec. The acceptable ion energy range will be approximately from 0 to 100 eV. The neutral gas and ion composition will be measured separately by electronic mode switching. The instrument should be pointed primarily into the ram direction. Provision should be made for occasional scans away from the ram direction toward the wake.

### **Retarding Potential Analyzer/Langmuir Probe (RPA/LP)**

To provide basic information on the temperature and flow velocity of the thermal plasma population of Titan's ionospheric and magnetospheric plasma under a broad range of external plasma conditions (solar wind, magnetosheath, magnetosphere), a Retarding Potential Analyzer (RPA) may be adopted. Another possibility is to use a modified version of the Faraday Cup Analyzer flown on Voyager. The RPA will provide measurements of the ion density N<sub>i</sub>, ion temperature T<sub>i</sub> and ion flow velocity V<sub>i</sub> of the major ionospheric ions. The Langmuir Probe will provide information about the electron density N<sub>e</sub> and electron temperature T<sub>e</sub>. These measurements provide information about ionization rates, energy deposition rates, energy transport and momentum transfer to the ionosphere during its interaction with the surrounding plasma and solar UV. The LP will also provide measurements of the thermal electrons within Saturn's inner magnetosphere.

The RPA is designed with a tri-collector and modulator/retarding grid configuration. To reduce perturbation of charged particle paths by charges elsewhere on the spacecraft, it will be mounted on the ram platform located near the end of the boom supporting the turntable. By looking along the ram direction and measuring the thermal ion energy distribution for each collector, the ion density, temperature and bulk flow velocity of Titan's ionospheric plasma can be derived. The ion measurements are confined below 100 volts. The parameter range covered is 1.0 cm<sup>-3</sup> < N<sub>i</sub> < 10<sup>5</sup> cm<sup>-3</sup>, 100°K < T<sub>i</sub> < 10<sup>4</sup> °K and 25 m/s < V<sub>i</sub> < 10 km/s (the latter is achieved if 1/4° pointing accuracy is provided).

The Langmuir Probe measures the electron density and electron temperature in the range 1 cm<sup>-3</sup> < N<sub>e</sub> < 10<sup>5</sup> cm<sup>-3</sup> and 100°K < T<sub>e</sub> < 10<sup>5</sup> °K, respectively. The probe is a small (1-2 cm long) cylindrical collector at the tip of a short (1 m) lightweight boom, mounted near the end of either the turntable boom or magnetometer boom. The electron measurements are confined below 20 volts.

## 4.2 The Probe Model payload

### 4.2.1 Probe Model Payload Composition

The Probe model payload is summarized in Table 4.2. The first six instruments, to be provided by PI's, make most of their measurements during the subsonic descent phase. One of them, the ASI, also characterizes the upper atmosphere during the supersonic entry phase. One PI-provided instrument is dedicated to simple characterization of the surface. A few additional investigations take advantage of data from several Probe subsystems, which might be slightly augmented to increase their science capability.

Instrument/investigation	Main scientific objectives	Mass (kg)	Power (W)	Data Rate (bps)
<b>PI PROVIDED INSTRUMENTS</b>				
Atmospheric Structure Instrument (ASI)	Atmosphere temperature and pressure profile, winds and turbulence	3.8	6.3-13	40
Probe IR Laser Spectrometer (PIRLS)	Vertical profile of trace species. Nephelometry	5.4	15	140
Gas Chromatograph/Neutral Mass Spectrometer (GCMS)	Atmosphere composition profile. Aerosol analysis	16	17-45	32-500
Aerosol Collector and Pyrolyser (ACP)	Aerosol composition profile. CGMS is used as detector	4.7	40-60	50
Descent Imager/Spectral Radiometer (DISR)	Atmosphere composition and cloud structure. Surface imaging	6.0	8-18	60-4000
Lightning and Radio emission Detector (LRD)	Titan lightning characteristics	2.15	2.3-3.3	8
Surface Science Package: Refraction Index of Titan Ocean (RITO) and possibly other investigations	Titan surface state and composition	1.2	10	200-500
<b>INVESTIGATIONS USING PROBE ENGINEERING INSTRUMENTS</b>				
Doppler Wind Experiment (DWE)	Probe Doppler tracking from the Orbiter for zonal wind profile measurement	0.7	3	10
Radar Altimeter Science (RAS)	Surface roughness and reflectivity. Subsurface sounding	-	-	50-1000

Table 4.2: *Cassini Probe model payload*

### 4.2.2 Probe Science Profile

On board the Probe, the first scientific measurement will be performed by the ASI during the entry phase. The remainder of the Probe payload instruments, except the surface science instrument, will be activated, as required, early in the parachute descent phase. It is desirable that the first chemical sample be taken at 170 km altitude or higher. Optimization of the sampling and the data acquisition in the lower half of the descent will be aided by real-time altitude information provided by the Probe system radar altimeter. For example, the Descent Imager and Spectral radiometer (DISR) instrument requires altitude information to switch in the imaging mode at about 10 km altitude. Moreover, because it will require about 3 min to transmit a high resolution frame, proper timing of the exposure sequence in the last km of the descent will allow acquisition of the highest possible resolution images of the landing site. Altitude information will also be essential

to condition the other instruments, in particular the surface science instrument prior to impact, in order to insure the highest probability of Probe data return during the impact and possibly during the post impact phase.

#### 4.2.3 Instrument Description

##### PI provided instruments

###### **Atmospheric Structure Instrument (ASI)**

This instrument is comprised of pressure, and temperature sensors, a three-axis accelerometer, and an electronics box. During the high speed entry phase and later during the descent phase, the accelerometers, located near the center of gravity of the Probe, will measure the atmospheric density as a function of altitude from vehicle deceleration data. With the equation of state and hydrostatic equilibrium, the temperature and pressure can be obtained, following techniques established with Viking and several Venus probes.

Pressure inlet pipes and temperature sensors must have access to the unperturbed flow field outside the Probe boundary layer. The ASI is augmented with a surface hardness (penetration index) measurement capability. This is achieved by including a high speed accelerometer designed to record the Probe impact response. Careful consideration will have to be given to accommodate this accelerometer unit in such a way that the deceleration response to surface deformation will not be masked by Probe deformation.

###### **Probe InfraRed Laser Spectrometer (PIRLS)**

The Probe InfraRed Laser Spectrometer (PIRLS) instrument is a tunable diode laser infrared absorption spectrometer and nephelometer designed for the in-situ sensing of Titan's atmosphere.

The PIRLS instrument uses ten or more narrow bandwidth ( $0.0001\text{ cm}^{-1}$ ) tunable diode lasers operating near  $80\text{ }^{\circ}\text{K}$  at selected, mid-infrared wavelengths ( $3\text{-}30\text{ }\mu\text{m}$ ). For the absorption measurements, these sources would be directed over an open pathlength defined by a small reflector located about  $20\text{ cm}$  away. Because of the high sensitivity of diode laser harmonic (derivative) detection methods which allow peak absorptances of less than 0.01% to be measured for atmospheric pressures expected on Titan (up to 1.5 bar), volume mixing ratios of  $10^{-9}$  should be measurable for several species of interest: vertical profiles of the concentrations of molecules such as  $\text{CH}_4$ ,  $\text{CO}$ ,  $\text{CO}_2$ ,  $\text{HCN}$ ,  $\text{C}_2\text{H}_2$ ,  $\text{C}_2\text{N}_2$ ,  $\text{C}_3\text{H}_4$ ,  $\text{C}_3\text{H}_8$ ,  $\text{C}_3\text{HN}$ ,  $\text{C}_2\text{H}_2$ , etc. can therefore be determined simultaneously with a vertical resolution of less than a scale height from 200 km down to the surface, as well as certain isotopic ratios.

The nephelometer channel takes advantage of scattering in the same optical path to measure the vertical extent of the cloud structure, its physical properties such as the particle size distribution and number density, using shorter wavelength diode laser sources at  $0.78\text{ }\mu\text{m}$  or  $0.83\text{ }\mu\text{m}$ . Particle size measurements over a  $0.1\text{-}30\text{ }\mu\text{m}$  size range can be made using a combination of shadowgraph imaging and light scattering techniques. The method of measurement is direct, non-invasive, and, as an all solid-state light source plus detector combination, simple in concept.

###### **Gas Chromatograph / Mass Spectrometer (GCMS)**

The main objective of the GCMS instrument is to determine the chemical composition of the atmosphere of Titan, as a function of altitude. It will provide the vertical concentration profiles

of noble gases, of already detected organic and inorganic compounds and of other organics not yet detected. It will also give information on isotopic abundances.

This instrument must be able to analyze quantitatively the main constituents of the gas haze, its minor traces with mole fraction down to  $10^{-8}$ , and the samples obtained by vaporization or pyrolysis of the collected aerosols provided by the Aerosol Collector and Pyrolyser experiment (ACP), described below.

The GCMS instrument is a combination of a Gas Chromatograph and a Mass Spectrometer. The GC part allows the separation of the constituents of the samples, with the help of selected chromatographic columns, adapted to the separation of C<sub>1</sub>-C<sub>8</sub> hydrocarbons and N-containing organics. The MS part allows their detection and identification by giving mass fragmentation within the 1-250 AMU mass range. The GCMS will alternatively sample atmospheric gases directly with the MS and indirectly through the GC. The 2 parts could operate either independently or in a coupled mode. This would allow the operation of GC during direct MS analysis, increasing the capabilities of both parts of the instrument, and decreasing the risk of losing data.

The GCMS consists of two units: 1) the sensor unit which contains the atmospheric inlet, all the vacuum pumps and valves, and the MS; and for the GC: gas sampling valve, carrier gas cylinder and regulator, GC columns and detectors, 2) an electronics box.

The inlet pipe could be extended if needed and its opening needs to be as close as possible to the Probe stagnation point outside the boundary layer. Activation of the instrument will occur after inlet port cover ejection and inlet extension. The mechanical system to be used to extend the inlet tube will depend upon the configuration. The GCMS instrument is provided with a heated inlet which will allow injection of a vaporized surface sample for fast analysis by the MS. Such a sampling device should operate immediately following the impact of the Probe.

The ACP will be interfaced to the GCMS. The quality of the measurements to be achieved by these instruments depends strongly upon the performance of the ACP-GCMS interface.

### **Aerosol Collector and Pyrolyser (ACP)**

The objectives of the ACP instrument are to sample atmospheric particles during the descent phase of the Probe and by using pyrolysis techniques to get information on their chemical composition. In the stratosphere the aerosols to be collected include polymers formed in the upper atmosphere by photodissociation of methane, acetylene and HCN. These polymers act as nucleation centers for the condensation of organics with lower molecular weight which are synthesized in the lower atmosphere (mainly hydrocarbons and nitriles), and of the much more abundant methane.

Sampling will begin as soon as the instrumentation of the Probe can be operated (around 170 km). Two distinct sampling devices allow measurement in two different regions around 60 km (lower stratosphere) and around 45 km (troposphere).

The method is to use a two-step pyrolysis technique within a sealed chamber. The aerosol sample is first "heated" at the ambient temperature of the furnace chamber. The products of pyrolysis or evaporation are stored in the gas phase in the enclosed chamber. When the Probe reaches an altitude lower than 30 km, the chamber is opened and pyrolysis gas samples are injected for analysis. Next, the furnace is activated to bring the residual deposit of aerosols to the highest temperature allowed by power requirements - 600°C to 700°C. The produced pyrolysates are injected into the GCMS. At such a high temperature, it is assumed that a large part of the polymers, if they contribute enough to the bulk composition, will be pyrolysed.

The two sampling devices will be mechanically extended underneath the Probe, outside the boundary layer for access to the unperturbed gas/aerosol flow.

### Descent Imager/Spectral Radiometer (DISR)

The objective of the DISR is to measure the solar heating rate of the Titan atmosphere and the aerosol properties as a function of altitude. The DISR will also aim at studying the morphology of the clouds and at taking surface images. The principle of the instrument is to determine the upward and downward solar flux and to take downward and upward images.

The instrument comprises a sensor head and an electronics box. One sensor should have an unobstructed upward FOV from (zenith  $+5^\circ$ ) to near horizontal. The  $5^\circ$  offset from the zenith is to take care of the parachute clearance. In view of possible pendulum oscillations of the Probe suspended on the parachute this requirement may need to be relaxed to  $10^\circ$  or more. The second sensor head should have an unobstructed downward FOV from nadir to ( $>$  nadir  $+60^\circ$ ). The azimuthal FOV of the instrument is  $40^\circ$  required ( $60^\circ$  desired).

It is highly desirable that the sensor heads be protected by an optical window which should be heated slightly above the ambient temperature in order to avoid condensation. It is not required that the electronics box be located close to the sensor head.

In case the Probe would land and survive on a liquid surface, high resolution images of the ocean would be taken from the downward looking sensor head. Hence, it is desirable that the sensor head be located above the flotation level of the Probe.

### Lightning and Radio emission Detector (LRD)

The following short description is based on the LRD instrument designed and built for the Galileo Probe Mission. Details of an instrument for Titan will be subject to redesign.

The instrument consists of an RF sensor and two optical detectors connected to an electronics box. The RF sensor is a ferrite-core antenna sensitive to the magnetic field component of lightning-generated RF signals in the frequency range below  $\sim 200$  kHz. The antenna with preamplifier is mounted in a plane perpendicular to the Probe spin axis.

The antenna output is fed in parallel into a time-domain analyzer and into a frequency-domain analyzer. The time-domain analyzer uses the full antenna bandwidth with a sensitivity limited by the broadband noise. The time-derivative antenna output is integrated to retrieve the field versus time signature. During a measuring cycle, the mean noise level, the statistical distribution of pulse durations, pulse gaptimes and amplitudes are derived.

For the frequency-domain measurements the antenna output is fed in parallel to three narrow-band channels centered at 3 kHz and  $\sim 100$  kHz. In each of these narrowband channels the mean noise level and the amplitude distribution is measured. The voltage induced by the Probe rotation in the ambient magnetic field is used to determine the magnetic field component perpendicular to the Probe spin axis and for sectorization of the measurements with respect to the azimuth.

Two optical sensors which are sensitive photodiodes behind fisheye lenses are mounted  $180^\circ$  apart to cover a large fraction of a  $4\pi$  field of view. The AC optical signals are used in coincidence with the RF signals. The DC optical signals provide information on the brightness and opacity of the cloud system. This instrument requires the Probe to spin; a rate between 4 and 10 RPM is suitable.

### Surface Science Package (SSP)

The model payload is provided with the capability to investigate Titan surface state and composition. The need to include the relevant instrumentation to achieve this goal was only recognized after the end of the assessment phase. The appropriate instruments were only given due consideration if surface science would not become a Probe design driver, in particular if it would not impose

any new constraints regarding the survivability of the Probe up to and after impact.

Although several instruments were suggested, it was only truly possible to accommodate one of these, the Refraction Index of Titan Ocean instrument (RITO) in the model payload. However for completeness and to illustrate the ideas put forward during the study, a short description is provided for each of the proposed instruments.

Careful consideration was also given to evaluating the possibilities of doing measurements with the atmospheric payload. The capability of doing accelerometry measurements during impact was included in the ASI instrument and provision for vaporizing a surface sample in the GCMS was also incorporated. The need to manage the Probe resources efficiently at and after the impact in order to get the most science out of this critical phase is recognized.

The RITO is intended to obtain information on the composition of the liquid ocean, if one exists. A linear relationship is assumed between N and the indices of the compounds,  $f_i$  being their molar fraction.  $N = f_1 N_{C_2H_6} + f_2 N_{CH_4} + f_3 N_{Ar} + f_4 N_{N_2}$ . Measuring N will thus provide a constraint on the possible ocean composition. This assumption is supported by the low molecular association in these liquefied gases. For the measurement, a standard method is proposed, i.e. measuring the total reflection angle of a light beam at the interface between the ocean and a dielectric plane surface (a prism).

Other instruments include an X-ray fluorescence spectrometer (XFS) to obtain elemental composition, especially of silicates, and an Acoustic Sounder (AS) to measure the acoustic impedance of the surface material and characterize the planetary boundary layer.

In case of Probe survival to and after the low speed impact shock, investigations aiming at studying the state and the composition of the surface will be performed on a best effort basis.

The investigations may include:

- Study of the surface response to the Probe's impact by high speed acquisition and transmission of the Probe's accelerometers signals;
- Study of the Performance of the Radio relay Link;
- Surface sample intaking into the GCMS for fast analysis;
- Subsurface Sounding using the radar altimeter.

The above investigations will involve the coordinated and optimized utilization of Probe subsystems and Payload instruments.

## Science investigations using Probe Subsystems

### Doppler Wind Experiment (DWE)

The Doppler Wind Experiment will measure one component of the wind in the Titan atmosphere as a function of altitude by Doppler tracking of the descent Probe. With Ultrastable Oscillators (USO) on both the Probe and the Orbiter, their relative velocity can be obtained with useful accuracy, from which the projection of the horizontal wind along the Probe-Orbiter line of sight can be determined. Since the general circulation in the atmosphere of Titan is believed to be essentially zonal, the East-West component is of greatest interest. The optimization of this experiment requires that the Probe-Orbiter geometry be optimized for the best determination of this particular wind component.

Over a time interval  $\Delta t$  the Probe oscillator stability will place limits on the relative wind recovery accuracy. If the Probe USO frequency drifts by  $\delta\nu$  in  $\Delta t$ , then the apparent change in range rate is  $c\delta\nu/\nu_0$ . The corresponding error in wind velocities is larger in magnitude and can be determined from knowledge of the Probe-Orbiter geometry. The relative error due to the oscillator

drift can be reduced if the projection of the Probe horizontal wind velocity onto the line of sight is large. For a maximum projection the angle between the Probe local vertical and Orbiter direction ( $\alpha$ ) should be kept as large as possible for a significant portion of the Probe mission. Likewise, the line of sight azimuth should be minimized (close to 0 or 180 degrees) throughout the Probe mission. This latter requirement is most easily satisfied when Probe and Orbiter trajectories are nearly coincident in latitude. In view of the large range in possible trajectories, it is essential that the Probe oscillator be highly stable. A stability of 5 parts in  $10^{10}$  over 180 minutes will allow a relative wind measurement over the same time interval accurate to 2 m/sec for  $\alpha$  angles down to 4 degrees. Under ideal conditions, the Doppler Wind Experiment can measure winds to within a few percent.

### **Radar Altimeter Science (RAS)**

The Radar Altimeter is a Probe subsystem. Its main engineering function is to provide, in real-time, the altitude of the Probe above the surface.

Possible scientific investigations include the study of the surface morphology and roughness, surface reflectivity, and subsurface sounding. The radar would be switched on in surface altimetry science mode at about 10 km altitude. At about 1 km altitude, it would be switched into the subsurface sounding mode and to its highest bit rate.

Requirements for scientific use of the Radar Altimeter will mostly be met by an additional software module in the signal processor and by telemetry allocation. The science requirements will not drive either the mechanical or the electrical characteristics of the instrument.

# Chapter 5

## Project Requirements

The requirements/constraints on the design, development, and implementation of the mission are listed non-exclusively below:

### 5.1 Mission

- The launch shall occur during the Saturn opportunity of April 1996 and will be conducted from Kennedy Space Center as a single Titan IV/Centaur launch. All systems shall be compatible with a backup launch in July 1996. The launch period shall be a minimum of 10 days with a nominal one hour launch window per day.
- There shall be limited science data acquisition during the interplanetary cruise phase and the mission shall include at least one targeted asteroid flyby.
- The Orbiter shall carry into Saturn Orbit and target the Probe to Titan for entry and provide data relay and storage capabilities for the Probe during its entry and descent.
- All Orbiter subsystems shall be designed to operate for 12 years and Probe subsystems for 8 years from launch.
- The Saturn tour shall be 4 years in duration following Saturn Orbit Insertion (SOI).
- The mission design shall not require more than 3450 kg of bipropellant.
- The time of Saturn arrival shall be such that no solar conjunction occurs between SOI-45 days and SOI+112 days. This period is consistent with an initial Saturn orbit period of 100 days.
- The NASA Planetary Protection Requirement, which satisfies the COSPAR Requirements shall be met by all injected elements for all encountered bodies per the Planetary Protection Plan Document.

### Science Requirements on the Mission

The trajectory design will be responsive to the science requirements and will be developed to maximize the extent to which the science goals can be achieved.

- The Orbiter shall deliver the Titan Probe to an entry latitude between 60 N and 60 S.
- The Probe shall enter and descend through Titan's atmosphere on the dayside.
- The Probe shall be designed to start chemical sampling at a minimum altitude of 170 km above Titan's surface.
- The tour shall be designed to target the Probe and to satisfy multiple science objectives related to Titan, Saturn, the rings, the icy satellites, and the magnetosphere of Saturn.

- There shall be at least one close flyby (less than 1000 km) of Dione, Enceladus and two of Iapetus covering the two hemispheres with widely varying albedo.
- The mission shall provide adequate science pointing accuracy and knowledge, operational sequencing, power, and data return.
- The Orbiter shall fly by at least one asteroid at a range of 110 radii.
- The mission design shall support science acquisition during the asteroid and Jupiter flybys.

## 5.2 Orbiter

- The Orbiter shall accommodate the Probe Support Subsystem and the science instruments, including FOVs, power, data rate, pointing, and operational sequencing requirements.
- The Orbiter shall be designed to operate at distances ranging from 0.86 AU to 9.2 AU from the Sun and up to 10.2 AU from Earth.
- The mass allocations are summarised in Table 5.1.

Orbiter dry mass	1550.0
Probe Support Subsystem	61.3
Probe	192.3
Bipropellant	3133.0
Attitude Control Propellant	15.8
Total wet S/C	4952.4
Launch vehicle adapter	175.0
<b>Total injected mass</b>	<b>5127.4</b>

Table 5.1: *Cassini spacecraft mass allocation (kg)*

- The Orbiter shall perform the attitude control function, perform the required burns for navigation and science, and supply the required velocity increment ( $\Delta V$ ). The preliminary  $\Delta V$  allocations for the mission are given in Table 5.2.

Deep space manoeuvres (2)	1185
Interplanetary navigation	75
Saturn Orbit Insertion (SOI)	984
Initial Saturn orbit:	
Navigation	70
Pericrone Raise Manoeuvre	424
Orbit Deflection Manoeuvre	63
Tour	270
Reserve	30
<b>Total</b>	<b>3101</b>

Table 5.2: *Manoeuvre budget  $\Delta V$  (m/s)*

- The Orbiter shall target and deliver the Probe such that its asymptotic velocity with respect to Titan will be below 6.8 km/s.

- The Orbiter shall provide telecommunications to and from 34 m and 70 m DSN stations at multiple data rates up to 115.2 kbps at the asteroid and 67.9 kbps at Saturn, and shall provide on-board storage for at least  $3.6 \times 10^9$  bits of data for use during cruise, Probe mission and the tour.
- The Orbiter shall provide adequate pointing accuracy at Probe-Orbiter separation to establish the proper link geometry and the capability to receive Probe data for the full range of relay link geometries.
- The Orbiter shall be designed to withstand 52 R<sub>J</sub> Jupiter flyby, Saturnian and ring plane crossing environments in the clear zones, sparsely populated regions and upper fringes of Titan's atmosphere.

### 5.3 Probe System

- The Probe shall provide accommodation and resources for the science instruments and a means to enter the Titan atmosphere and implement the Titan Probe mission profile.
- The Probe Support subsystem shall provide the Probe's Spin Eject Device, the relay antenna and antenna pointing equipment, as well as the Probe Interface to the Orbiter for power, command and telemetry.
- The Probe mass allocation is 192.3 kg and the Probe Support Subsystem mass allocation is 61.3 kg.
- The outer envelope of the Probe system shall be compatible with the allowable envelope constraints of the Orbiter under the launch vehicle fairing.
- Telemetry and telecommand communication with the Probe shall be available through the Orbiter until separation of the Probe from the Orbiter. After Probe release, the only Probe communication will be the telemetry data relay via the relay link to the Orbiter and DSN.
- The Probe system shall be designed to withstand 52 R<sub>J</sub> Jupiter flyby, Saturnian and ring plane crossing environments, in the clear zones and sparsely populated regions.
- The Probe system shall be capable of activation for calibration once or twice per year.
- The Probe system shall be capable of activation to full operational status after an interplanetary cruise time of 6.5 years.
- The Probe will be targeted for Titan and be separated from the Orbiter during the first Saturn centered orbit. The second orbit is the back-up opportunity.

# Chapter 6

## Mission

### 6.1 Mission Overview

The primary objectives of the Cassini mission to Saturn consist of the delivery of the spacecraft into orbit about Saturn and a Probe into the atmosphere of Titan. The interplanetary trajectory design must be consistent with the expected launch capability of the Titan IV/Centaur Expendable Launch Vehicle (ELV) (see Chapter 7). This ELV will utilize Upgraded Solid Rocket Motors (SRMUs). While maintaining adequate margins, this launch vehicle can deliver the Cassini required injected payload mass of 5127 kg at the required  $C_3 = 30 \text{ km}^3/\text{s}^2$ . The breakdown of this mass is given in Table 5.1. The bipropellant tanks are not full, but contain sufficient propellant to carry out all required manoeuvres and still maintain an adequate injected mass margin over a 10-day launch period. This is illustrated in Figure 6.1. The first day available to launch is April 8, 1996.

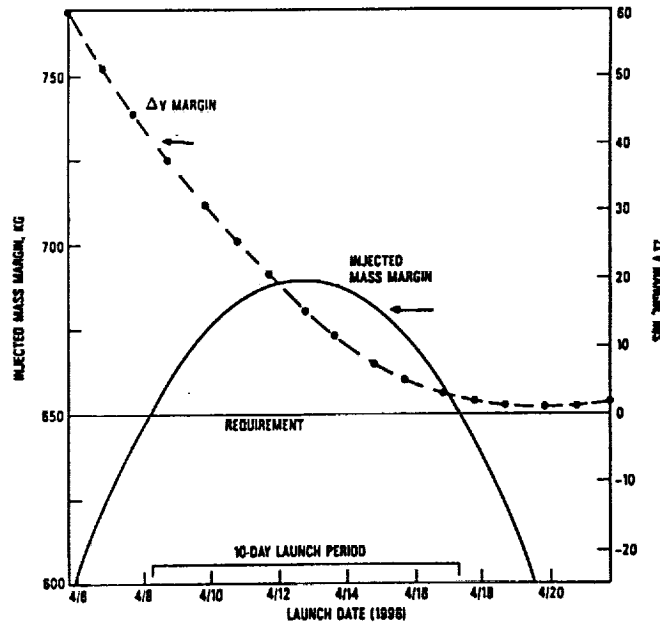


Figure 6.1: *Launch period definition*

## 6.2 Interplanetary Trajectory

The baseline interplanetary trajectory is illustrated in Figure 6-2. The designation of this trajectory type is:  $2^+ \Delta V$ -EJGA. This indicates that the launch is initially into an Earth return trajectory of duration slightly greater than 2 years (hence  $2^+$ ) with two intermediate manoeuvres. The Earth flyby boosts the heliocentric energy of the orbit such that the spacecraft can reach Jupiter. Jupiter's location, for launches in 1996 (as well as in 1995 and 1997), is suitable for enabling the spacecraft to travel on to Saturn via another gravity assist. It is only through the benefits of the flybys of Earth and Jupiter, as well as the expenditure of some bipropellant en route to modify the trajectory, that the Titan IV/Centaur can deliver sufficient mass to Saturn to accomplish the full science mission. 1996 has been selected as the launch year because the performance is the best of all possible opportunities in the next 20 years. The 1997 opportunity can accomplish the nominal mission, but there is a flight time penalty that must be incurred of about one year.

There is another factor involved in determining the flight time, and hence the arrival date at Saturn. This is the conjunction constraint imposed by telecommunications requirements. Communication and tracking quality is degraded when the Sun interposes between Earth and the spacecraft, a condition called conjunction. Thus, critical events, including asteroid flyby and Saturn arrival, are specifically designed to avoid the periods near conjunction. The arrival date of October 2, 2002 (6.5 year flight time) is consistent with both the performance issue and the conjunction constraint.

## 6.3 Asteroid Flyby

This trajectory type encounters the asteroid belt twice. The first occurs on the Launch-Earth return leg and the second on the leg from Earth to Jupiter. A survey was made of the asteroids that lie fairly close to the trajectory in order to assess if flybys of specific asteroids could be incorporated into the baseline mission design. The result of this study has been to include a flyby of the C-type asteroid 66 Maja, (radius = 39 km), on March 14, 1997, (see Figure 6-3), about one year after launch. This flyby occurs very close to conjunction which, if allowed to occur, would not provide the Doppler data required to determine the mass of the asteroid to sufficient accuracy. This is a prime scientific objective of an asteroid flyby. Consequently, the flyby date has been selected to ensure at least 20 days between the flyby and conjunction, thus enabling a mass determination to about 20% accuracy (assuming a closest approach at 100 asteroid radii, or 3900 km). The flyby of 66 Maja is particularly attractive because of its relatively low flyby speed of 7 km/sec. It should be noted that a significant performance penalty is incurred in order to incorporate 66 Maja into the trajectory. Conversely, for a small performance penalty, a second asteroid could also be incorporated into the mission. These considerations obviously imply future tradeoff possibilities with other mission elements.

Following the 66 Maja flyby, the spacecraft returns to Earth for a flyby at 300 km altitude on 13 June 1998, enroute to Jupiter.

## 6.4 Jupiter Flyby

Jupiter closest approach occurs on February 1, 2000 at a distance of  $52.1 R_J$ . This flyby distance imposes no significant radiation concerns. Figure 6-4 shows the flyby relative to the positions of the Galilean satellites at the time of closest approach. The orbit is inclined about  $7^\circ$  with respect to the Jupiter equatorial plane. The trajectory of the spacecraft through the huge magnetotail of Jupiter was shown in Figure 3.12. It spends nearly 130 days in this largely unexplored region.

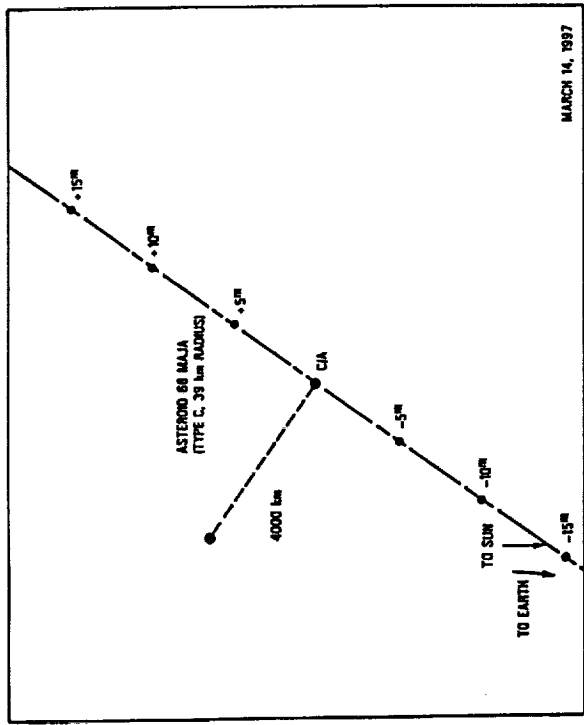


Figure 6.2: Baseline interplanetary trajectory

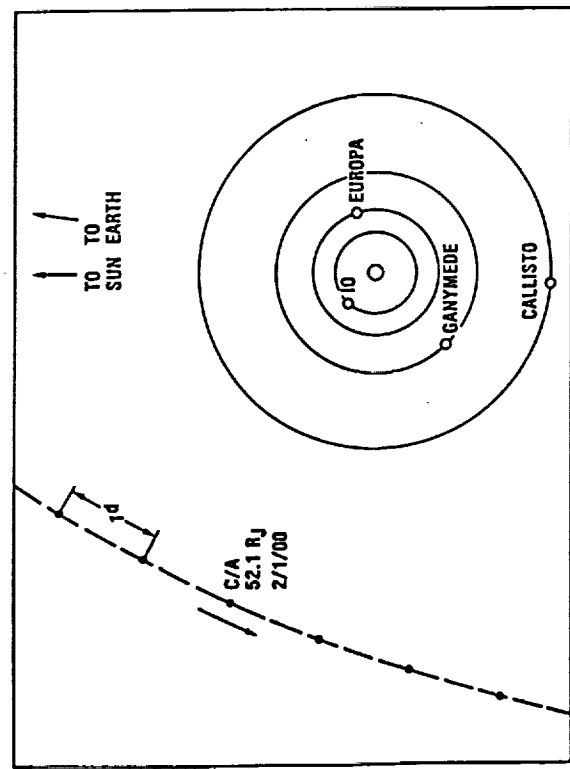


Figure 6.4: Jupiter flyby and location of galilean satellites

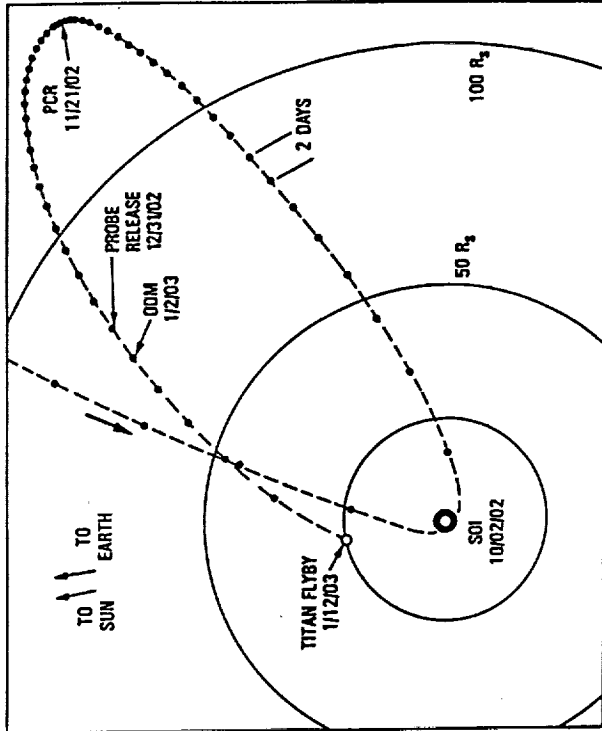


Figure 6.5: Initial Saturn Orbit and Titan Probe delivery sequence

Figure 6.3: Flyby of Asteroid 66 Maja

## 6.5 Saturn Orbit Insertion and Probe Delivery

Upon arrival at Saturn, the spacecraft is inserted into an initial highly eccentric Saturn-centered orbit with a period of 100 days and a periapsis radius of 1.8 Saturn Radii ( $R_S$ ) (see Figure 6-5). The incoming trajectory is inclined at about  $20^\circ$  with respect to the Saturn equator.

The ascending and descending nodes have been placed in potentially clear zones in the ring plane. The geometry of this SOI strategy is further illustrated in Figures 6-6, and 6-7.

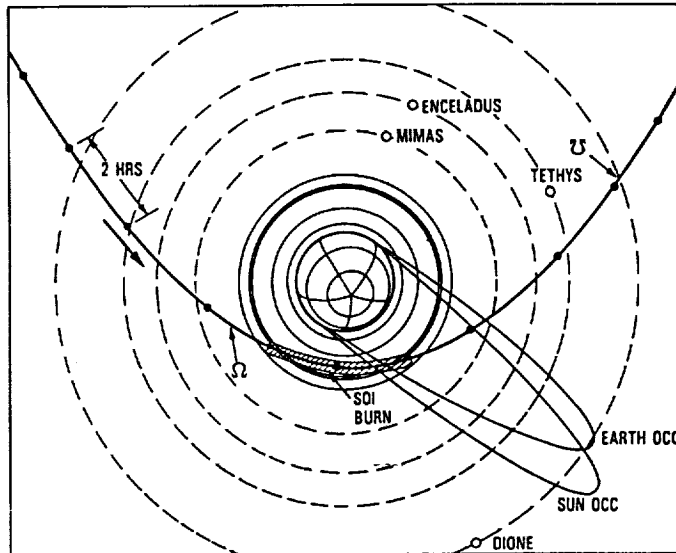


Figure 6.6: *Saturn arrival and Orbit Insertion geometry*

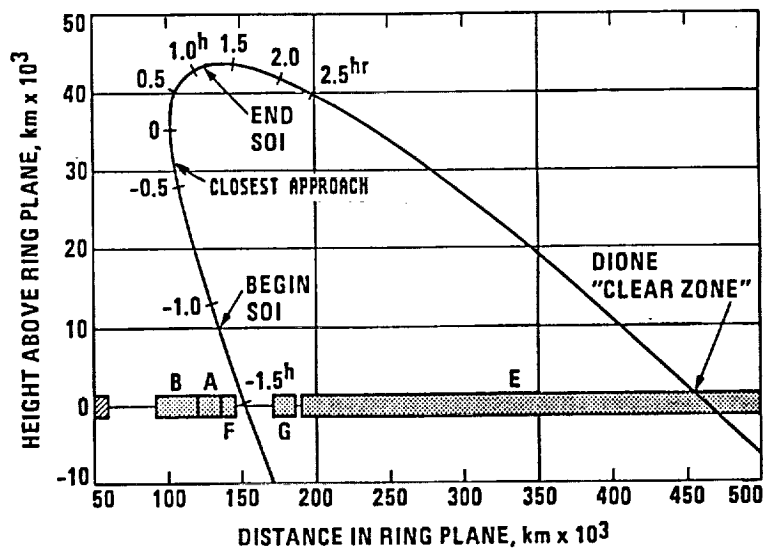


Figure 6.7: *Height of Spacecraft above ring plane during SOI*

Following SOI, the spacecraft travels out to an apocrone radius of about  $133 R_S$  where a PeriCrone Raise manoeuvre (PCR), is performed. This manoeuvre targets the spacecraft to Titan

in readiness for the separation and entry of the Probe into the Titan atmosphere. The size and orientation of the PCR manoeuvre determines the geometry of the spacecraft trajectory with respect to that of Titan, and, consequently, the relative entry speed of the Probe into the Titan atmosphere.

The asymptotic velocity ( $V_{\infty}$ ) of the Probe at Titan is restricted to the range 5.5-6.8 km/sec. Probe radio relay link and tour design studies in this velocity range have demonstrated adequate performance and fulfillment of the primary science objectives. For the baseline 1996 mission, the  $V_{\infty}$  of 5.5 km/sec with a Titan entry speed of 5.8 km/s is achieved by increasing the periapsis radius to  $9 R_S$  at the expense of a larger PCR velocity increment of 424 m/s.

The Probe is targeted for Titan atmospheric entry and separated from the Orbiter about 12 days before entry. Two days after separation, the Orbiter performs the Orbit Deflection Manoeuvre (ODM). This manoeuvre targets the Orbiter to the required overflight conditions at Titan, in order to establish and maintain the Probe relay link during the descent of the Probe through the Titan atmosphere. The duration of the descent is expected to be of the order of 2 - 3 hours.

The overflight conditions for the Orbiter must also satisfy the requirements of the subsequent tour of the Saturnian system, of which this Titan encounter is the initial event. Since Titan is the only Saturnian satellite that provides sufficient gravity assist to modify the Saturn-centered trajectory, all passes of Titan (while on inclined orbits, such as this initial one) must have post-flyby orbits that return to Titan. Titan has a period of almost exactly 16 days, which requires that the initial post-flyby orbit have a period that is a multiple of 16 days. For the current tour, 88-01, this period is 48 days and corresponds to a Titan pass in mid-northern latitudes at an altitude of 800 km. (This altitude will be raised in future mission studies). With the completion of the Titan Probe mission, the Orbiter begins its extensive investigation of the Saturnian system.

## 6.6 Probe Mission

The first phase of the Probe mission is illustrated in Figure 6.8.

## 6.7 Titan Physical Model

For the Mission Analysis studies the following Titan model was assumed:

- Titan is in a circular orbit at  $20.4 R_S$  in Saturn's ring plane. Titan's rotation and orbital period are 1:1 correlated.
- Titan is of spherical shape with mean radius  $R_T = 2575 \text{ km} \pm 0.5 \text{ km}$ . The GM of Titan is  $8978.1 \text{ km}^3/\text{s}^2$ .
- The atmospheric density is given by the Lellouch-Hunten model, Figure 6.9. The model provides a nominal density profile and lower and upper limits. (See Appendix 2).
- Zonal winds may exist in Titan's atmosphere, as inferred from Voyager measurements. The winds may blow either in W-E or E-W direction. The nominal wind profile is displayed in Figure 6.10. For the mission design, it is assumed that the wind profile may be in error by a factor of 2.
- The uncertainty in the topography of the surface of Titan is assumed to be  $\pm 2 \text{ km}$ .

### Probe Targeting

The targeting of the Probe at Titan is conveniently described in the plane perpendicular to the Probe's approach velocity (B-plane).

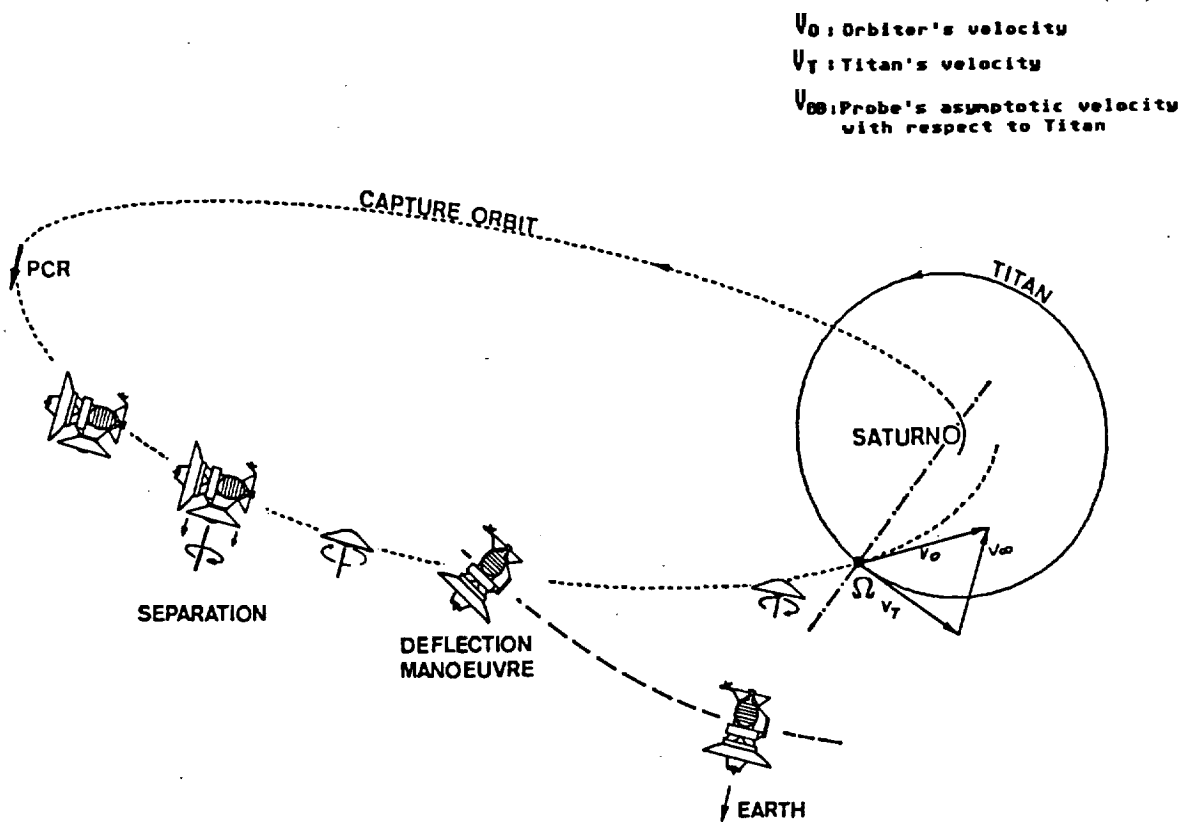


Figure 6.8: Probe separation and delivery scenario

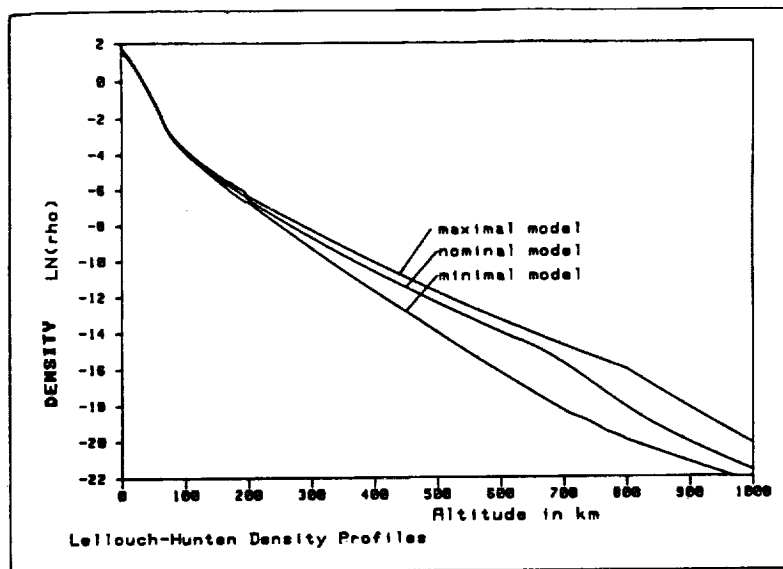


Figure 6.9: Density profile as a function of altitude according to the Lellouch/Hunten model (see appendix 2). In addition to the nominal profile, the two extreme profiles are also shown

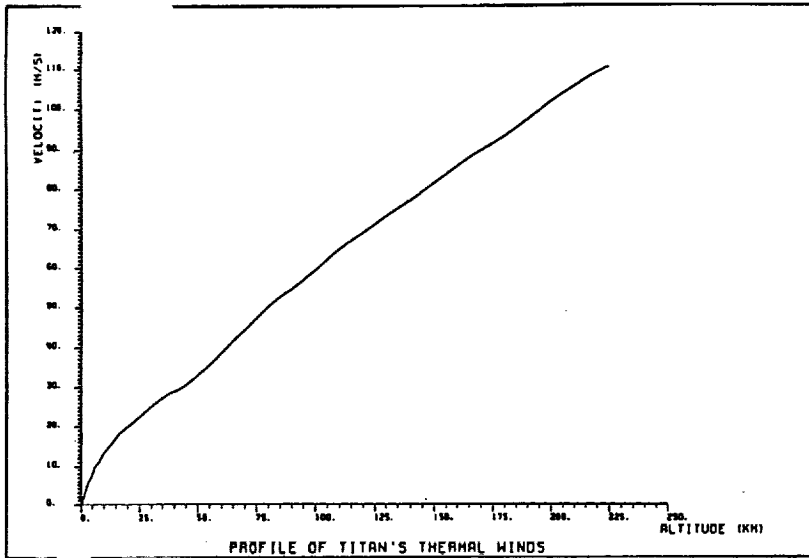


Figure 6.10: *Profile of Titan's thermal wind*

Figure 6.11 displays the projection into the B-plane of selected latitude circles and the loci of constant flight path angle at the reference altitude of 1000 km, for a Probe arrival on January 2003.

The targeting requirements are:

- Atmospheric entry and descent on the dayside of Titan.
- Atmospheric descent to be restricted to latitude between 60°N to 60°S.
- The flight path angle at  $H = 1000$  km must remain within  $-90^\circ < \gamma_{1000} < -60^\circ$ , including dispersions.

### Atmospheric Entry

The Probe's trajectory and operations during atmospheric entry and descent are illustrated in Figure 6.12. The maximum entry velocity at  $H = 1000$  km is 7.120 km/s, corresponding to an assumed worst case asymptotic velocity of 6.8 km/s.

Through aerodynamic braking by the Probe's decelerator, the entry speed will be reduced to Mach 1.5 (about 400 m/s) where the decelerator will be jettisoned, which marks the end of the entry phase.

Peak decelerations of up to  $\sim 240$  m/s<sup>2</sup> occur at about 260-290 km altitude. The only active science instrument during this atmospheric entry phase is the Atmospheric Structure Instrument. Science and engineering data gathered during the entry phase will be stored for later transmission during the subsequent atmospheric descent after the establishment of the relay link.

### Atmospheric Descent

The atmospheric descent phase begins with the deployment of the parachute, which will occur in the supersonic regime. This event will be completed at the latest at 170 km altitude, in order to satisfy the requirement to begin the chemical sampling. At this stage all experiments can be activated. About 1.2 hours after decelerator jettison, a second smaller parachute is deployed by

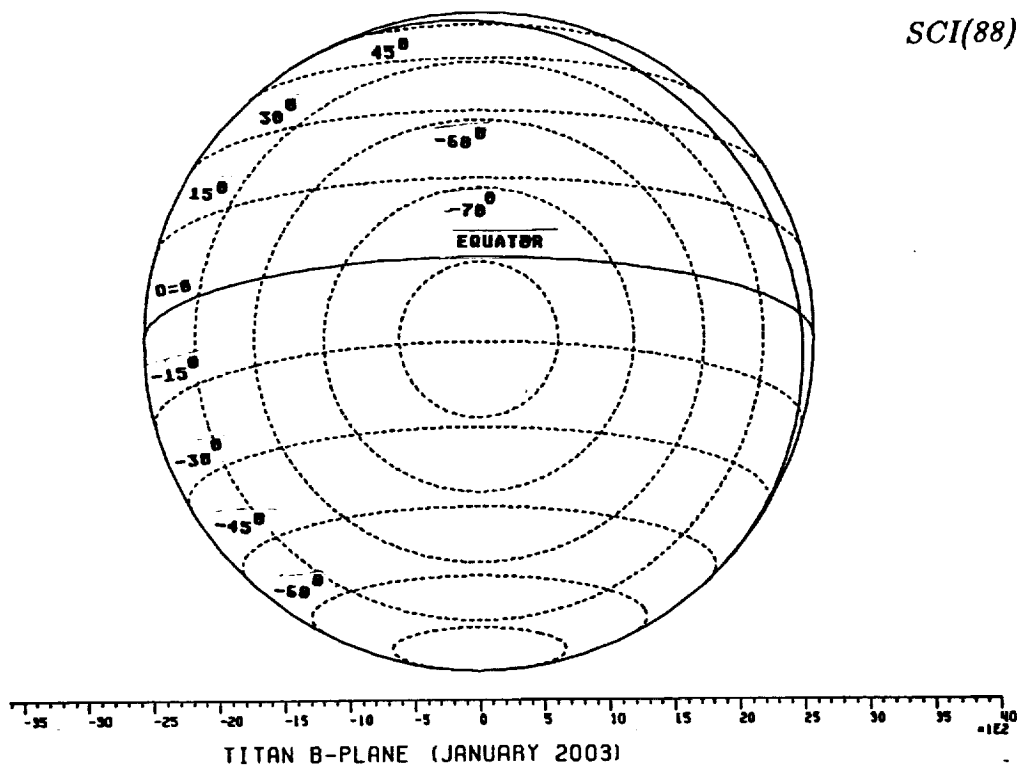


Figure 6.11: *Probe targeting in Titan B-plane*

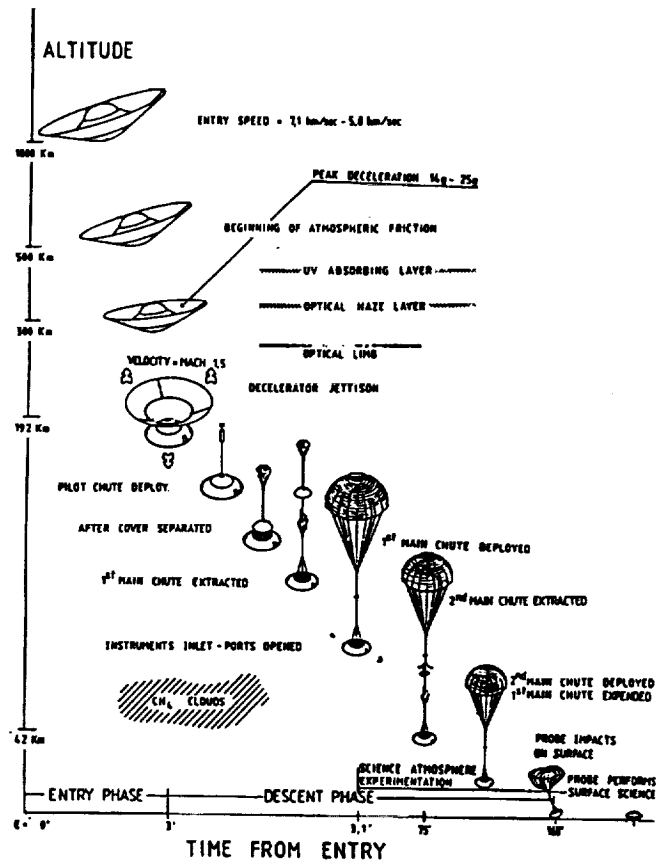


Figure 6.12: *The Probe's trajectory and operations in Titan's atmosphere*

use of the first chute which is subsequently released (see Figure 6.12). The science and engineering data are transmitted to the Orbiter via the radio relay link. The total descent time may vary from 120 min to 180 min. The terminal velocity at the surface can range from  $\sim 4.0$  to  $7.0$  m/s.

A typical nominal descent profile with a two parachute system is shown in Figure 6.13.

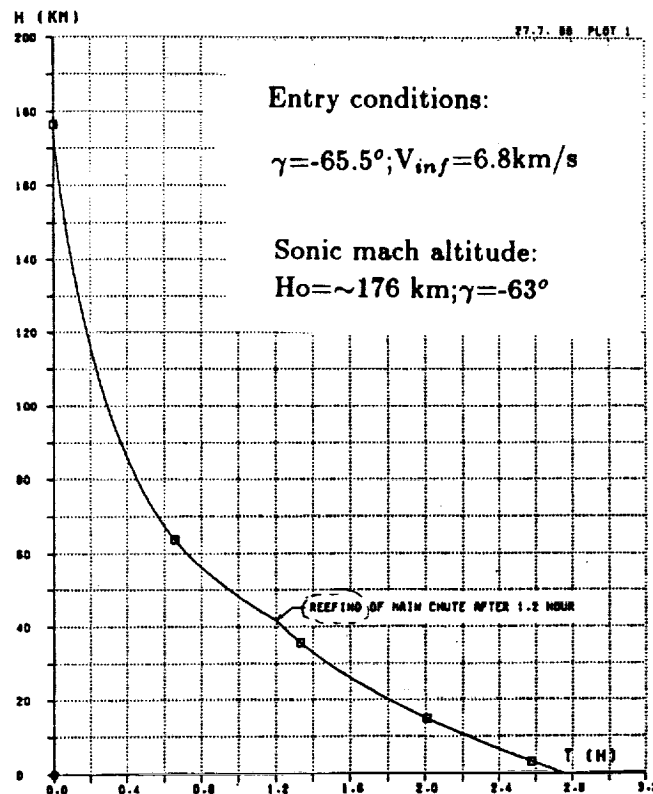


Figure 6.13: *Probe descent profile*

The effects of winds on the descent trajectory are displayed in Figure 6.14. The descent time is practically not affected by winds, however, the touch-down point may be displaced by about 300 km, assuming a nominal wind profile.

## 6.8 Orbiter Mission

The baseline Cassini tour begins with the initial Titan flyby, immediately upon completion of the Probe mission and lasts until 4 years after the date of SOI. It consists of about 36 Saturn-centered orbits connected by Titan gravity-assist flybys or small propulsive manoeuvres; the size and orientation of these orbits is dictated by the various science requirements. The first Titan flyby is used to reduce the period and inclination of the Orbiter trajectory, from the long-period insertion orbit to a low-inclination orbit with a 48-day period. The reliance on Titan flybys for gravity assist means that the Cassini mission has two separate targets, Saturn and Titan. During

ORIGINAL PAGE IS  
OF POOR QUALITY

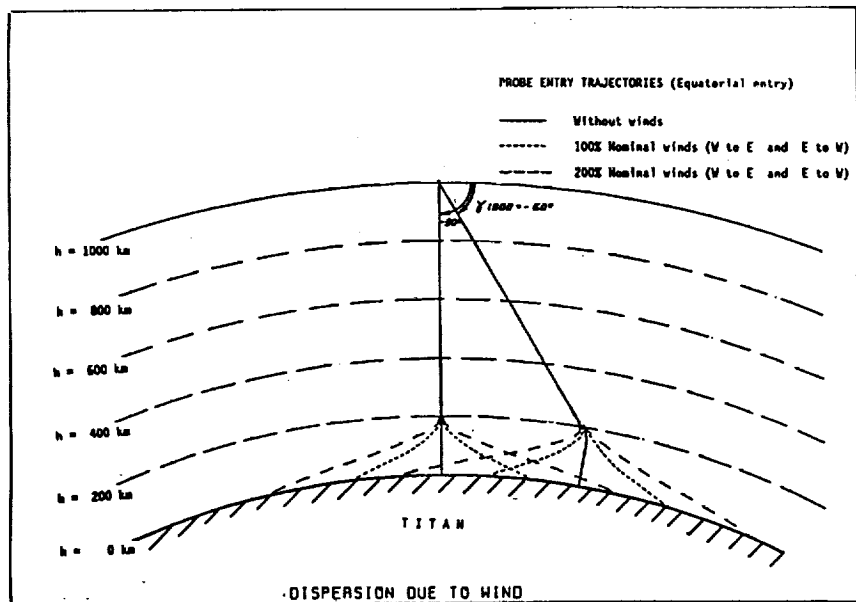


Figure 6.14: *Landing site dispersion due to winds*

the course of the 4-year tour of the Saturnian system, there will be many opportunities for study of these two bodies, the "icy" satellites, the rings, the magnetosphere and their mutual interactions.

The tour ends with the spacecraft in an orbit of period 7.1 days. From a trajectory design standpoint, there could be many opportunities for additional Titan flybys after the end of the nominal tour.

Figure 6.15 shows selected (for clarity purposes) orbits from the current Cassini tour, designated 88-01. While not every orbit is shown, enough have been included to depict the amount of orbit rotation that takes place during the tour.

### Initial Titan Flyby

The baseline strategy calls for an initial Titan flyby which is optimized from the point of view of the orbital tour, in that it occurs at a low altitude below 2500 km, and simultaneously reduces the Orbiter period and inclination. The initial Titan flyby must satisfy the requirements of the Probe's Radio relay link geometry, while efficiently initiating the Orbiter's tour.

### Subsequent Titan Flybys

There are 36 Titan flybys during the baseline orbital tour, all of which occur with a V-infinity of 5.2 to 5.5 km/s. At least eight of these flybys pass behind Titan as seen from Earth, resulting in Titan occultations of about 10-18 minutes duration. In the present tour design, these occultations occur fortuitously; no attempt has been made to optimize the flyby geometry to increase the number of occultations. Of the 36 Titan flybys, 30 occur at altitudes of 3000 km or less, and thus are useful for the radar instrument. The Titan flyby geometry must be chosen primarily to produce the desired effect on the Saturn-centered orbit, but it is likely that future tour iterations will focus more closely on optimizing Titan surface coverage. There will be some trade-off as a Titan flyby is perturbed away from the optimum gravity-assist parameters to a geometry that maximizes Titan flyby science, subject to safety considerations related to the upper atmosphere.

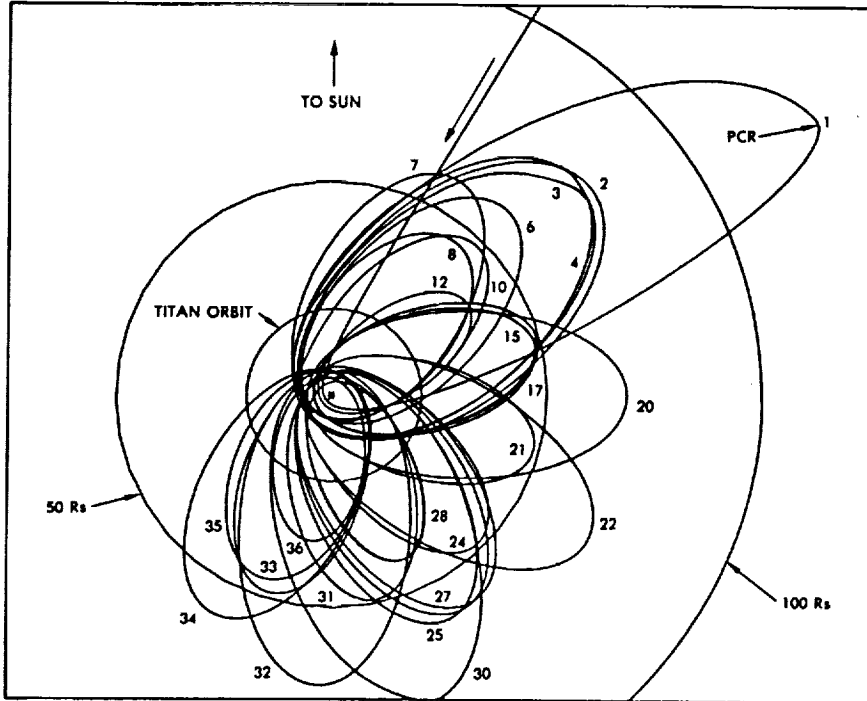


Figure 6.15: *Petal plot of representative Saturn system tour (88-01)*

Figure 6.16 shows a trace of the spacecraft ground tracks on a map of Titan, for those flybys with periapsis altitude less than 3000 km. These ground tracks do not show the actual width or location of the radar swaths, but indicate the approximate amount of surface coverage that will be obtained.

### Icy Satellite Flybys

The baseline tour includes two targeted flybys of Iapetus and one each of Enceladus and Dione, and a total of 26 other non-targeted encounters. The maximum altitude of a non-targeted flyby is currently set at 100000 km. The velocities of the icy satellite flybys range from about 3 km/s for the targeted Iapetus flybys to over 20 km/s for flybys of Mimas and Enceladus near the end of the tour. There are no close flybys of either Hyperion or Phoebe in the baseline tour. No restriction has been placed on the number of non-targeted encounters which can take place on a single Saturn orbit, since the gravitational effect of these encounters is negligible.

### Saturn Occultations

There are 4 equatorial and at least 5 high-inclination passes behind the disk of Saturn, and 9 additional passes behind the rings, during the baseline tour. These result in both Sun and Earth occultations. No attempt has yet been made to find useful stellar occultations during the tour, though they undoubtedly exist. The Saturn occultations will not generally occur "accidentally" during the tour as do the Titan occultations, so the requirement for Saturn occultations has a significant effect on tour design.

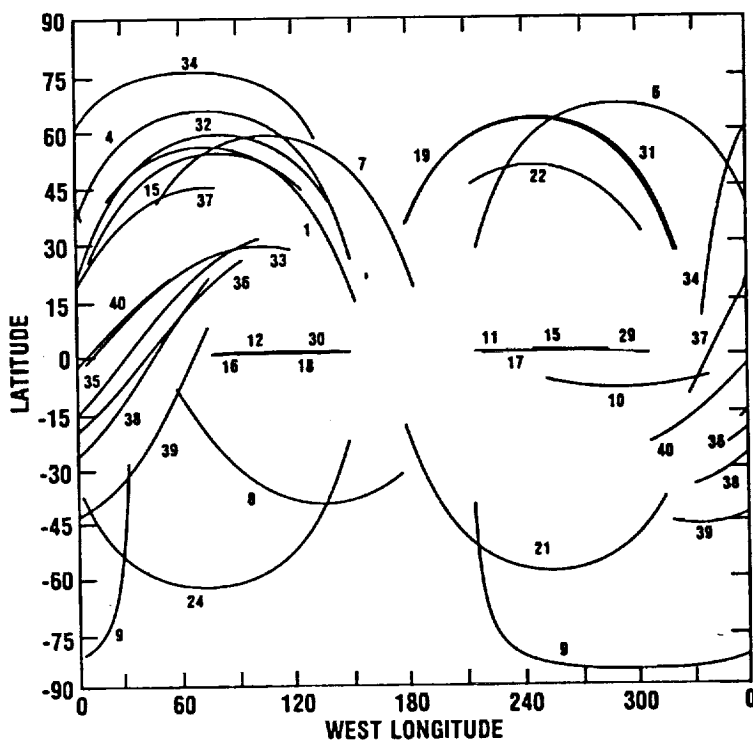


Figure 6.16: *Ground tracks of Titan flybys (altitudes below 9000 km) during a representative Saturn system tour (88-01)*

### High-Inclination Orbits and Ring Plane Crossings

The science requirements for investigation of the Saturn polar and SKR regions mean that the spacecraft must achieve an inclination (with respect to the Saturn equator) of about  $80^\circ$  during the tour. This can only be achieved by using “resonance hopping” and proceeds as follows. With the spacecraft in a Saturn orbit of a given period, there is a maximum inclination which can be reached using Titan flybys. As the inclination is increased, the periapse radius also increases, and each Titan flyby is successively less efficient at increasing inclination. In order to continue increasing inclination, then, it is necessary to reduce the orbit period and periapse radius. This can be done with a Titan flyby; however, it must be done in discrete steps, since the orbit must always be in some resonance with Titan’s orbital period. For example, the baseline tour uses 24-day orbits which are in 3:2 resonance with Titan to increase inclination up to about  $25^\circ$ . At this point, it is most efficient to jump to 16-day orbits which are in 1:1 resonance with Titan, and continue increasing inclination up to about  $45^\circ$  when a jump is made to 12-day orbits and a 3:4 resonance. This process continues until an inclination of  $77^\circ$  is reached, with an orbit period of 7.1 days in a 4:9 resonance. Thus, the requirement for high-inclination orbits means that low-period orbits are also required.

# Chapter 7

## Launch Vehicle

The following is a general description of the launch phase of this planetary mission using a Titan IV/Centaur. Figure 7.1 shows the typical Titan IV/Centaur configuration.

### 7.1 Launch Scenario

A typical Titan IV/Centaur mission begins with the ignition of the upgraded solid rocket motors (SRMUs). The vehicle ascends through maximum dynamic pressure at approximately 57 seconds from liftoff.

The Titan IV stage I ignites at approximately 116 seconds from liftoff and the payload fairing jettison occurs when free-molecular heating rate is sufficiently low. This event nominally occurs between 220 and 245 seconds from liftoff at an altitude of 116 km. Payload fairing jettison constraints are mission peculiar and can be adjusted to satisfy individual mission needs.

After Titan IV depletion and separation, the Centaur injects the spacecraft into a parking orbit, typically 148 by 176 km. The planetary transfer injection from this parking orbit is achieved by a second burn of the Centaur, followed by the spacecraft separation.

### 7.2 Launch Vehicle Performance

An estimate of planetary performance available with the Titan IV/Centaur using the SRMUs is given in Figure 7.2.

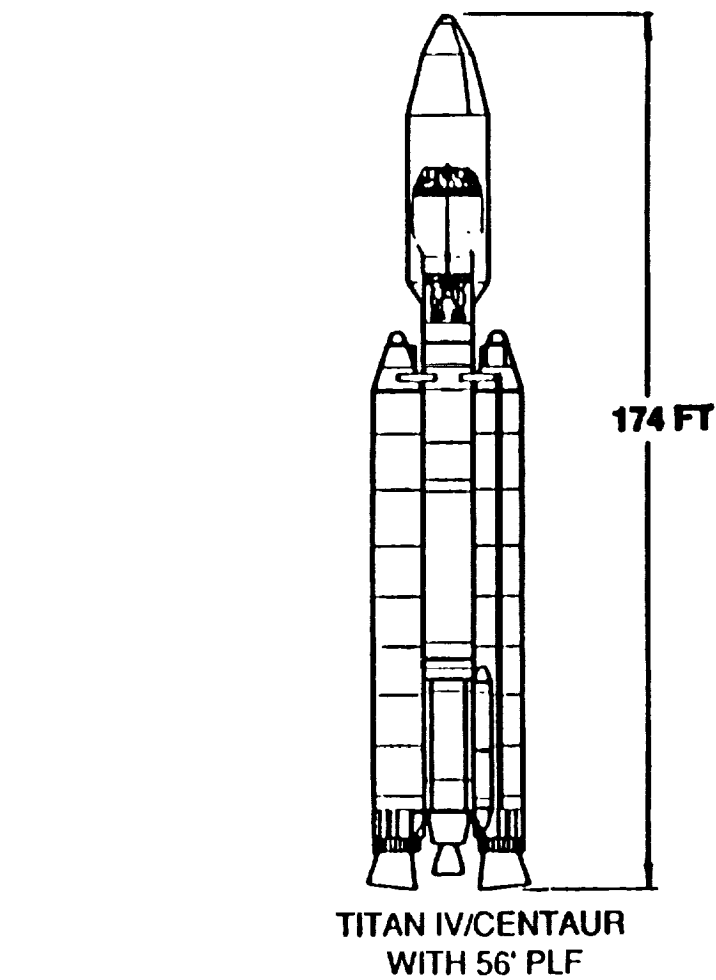


Figure 7.1: *Titan IV/ Centaur configuration*

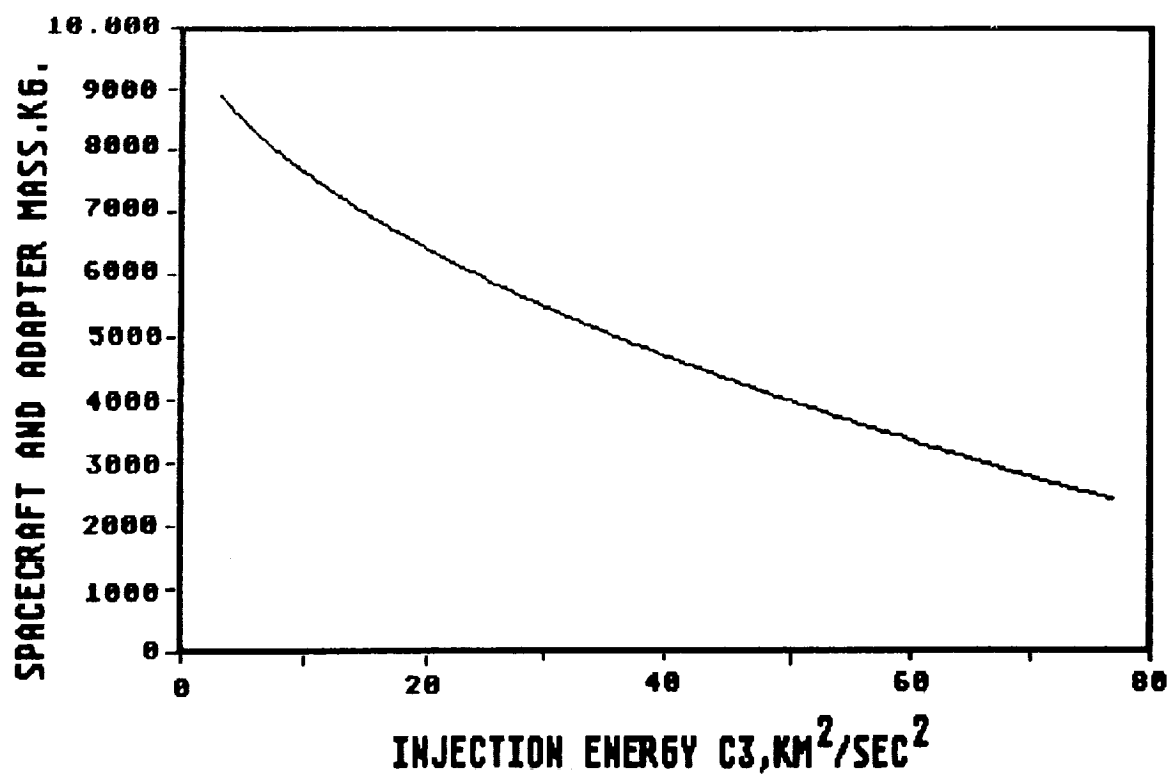


Figure 7.2: *Titan IV Centaur planetary performance (Current Best Estimate)*

## Chapter 8

# The Orbiter System

The spacecraft is comprised of a Saturn Orbiter and a Titan Probe. In addition, a launch vehicle adapter integrates the spacecraft to the Centaur during launch and interplanetary injection.

### 8.1 Orbiter

The Mariner Mark II (MM-II) family of NASA low-cost spacecraft are designed for high quality science return from cometary, asteroid, and deep space planetary science exploration. The combination of inheritance, common spacecraft modular components, and new technologies applied to the set of spacecraft reduce overall mission costs.

As part of the broad range of spacecraft performance capabilities, the Orbiter fulfils the requirements for electromagnetic and electrostatic cleanliness, equipotential external surfaces, Electromagnetic Interference (EMI) minimal generation and sensitivity, micrometeoroid protection, and immunity to a single event upset (SEU) to a linear energy transfer (LET) of 37, and completely immune to latchup. Radiation hardness of all bus-mounted (which provides 0.060 inches of aluminium equivalent) MM-II components is required to be at least 15 kilorads (Silicon) with tests run to 75 kilorads to determine margin. Non bus-mounted components must have equivalent radiation margins. The spacecraft (Orbiter) is designed to operate from 0.86 AU to 9.2 AU solar range, and at an Earth range greater than 10.2 AU. The Orbiter design lifetime is 12 years.

### Engineering Design

The MM-II engineering subsystems consist of all hardware and software required to mount, point, power, command, thermally control, and receive data from the science instrument subsystems. Engineering subsystems consist of structure, radio frequency, power and pyro, command data, attitude articulation control, cabling, propulsion module, thermal control, mechanical devices, digital tape recorder, antenna, and purge. The current spacecraft configuration is shown in Figure 8.1, and Figure 8.2 is a simplified block diagram of the MM-II Orbiter. Appendix 4 defines the acronyms used in Figure 8.2.

### Mechanical

The structure subsystem provides the core structure for the Orbiter which is a slightly modified Voyager-type 10 bay toroidal bus and the Propulsion module truss structure. The toroidal bus supplies a large volume for most of the electrical/electronics equipment. The 3.67 m high gain antenna (HGA) reflector (with low gain antenna at the top center) is supported from the top of

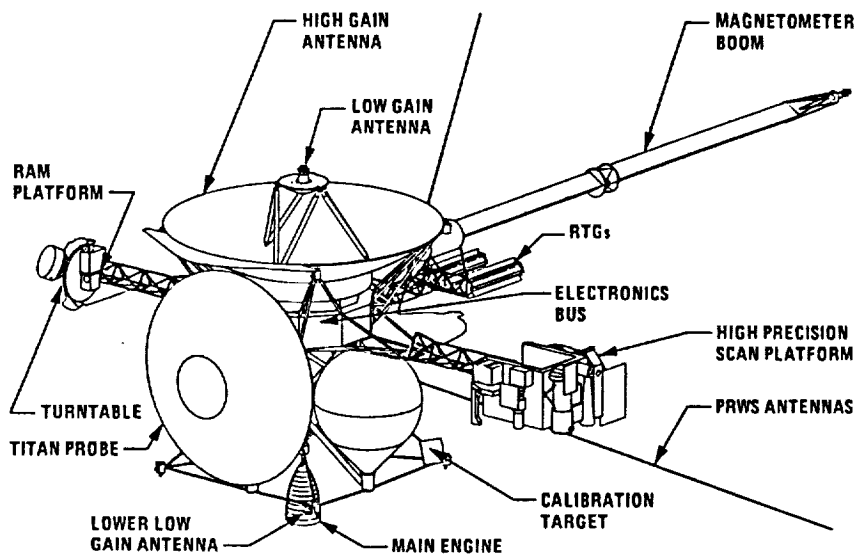


Figure 8.1: *MM-II/ Cassini Spacecraft*

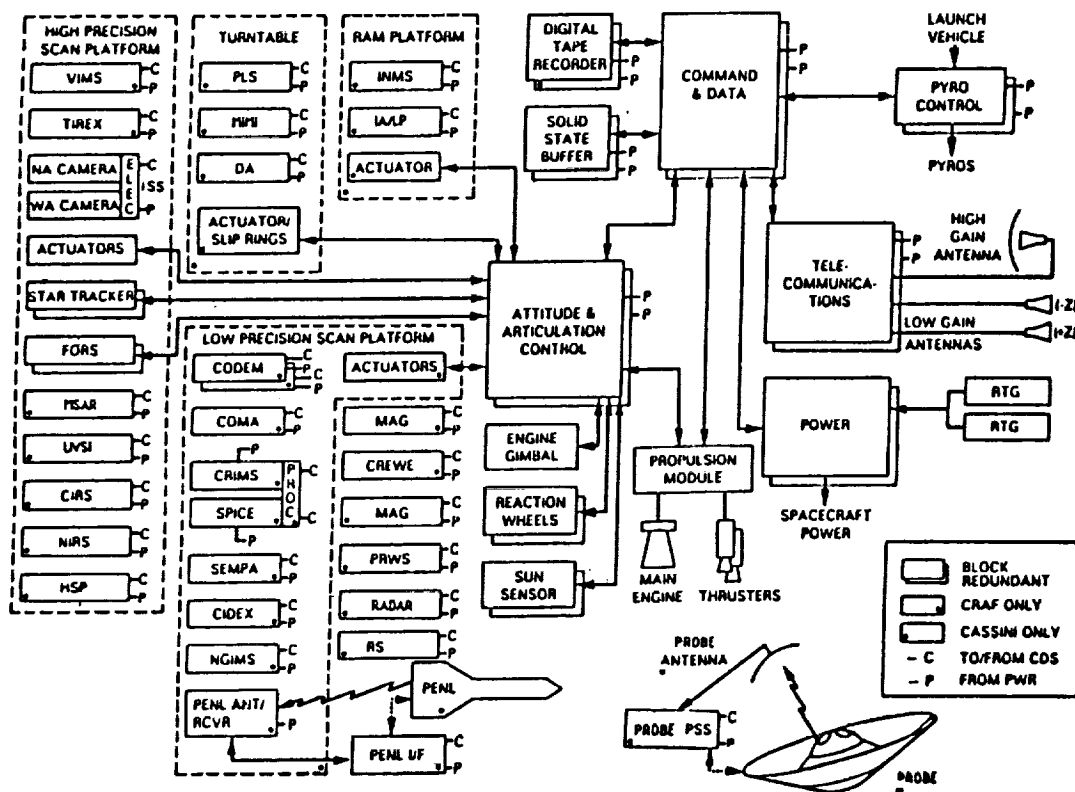


Figure 8.2: *MM-II simplified functionnal block diagram (CRAF and CASSINI)*

the bus. The bottom of the bus attaches to the propulsion module subsystem truss structure which forms the main load path through the launch vehicle adapter to the launch vehicle.

The Orbiter structure has three deployable booms: one for the science high precision platform (HPSP), one for the science turntable and RAM platform, and one for the RTGs and the magnetometer boom canister. The Purge Subsystem provides a nitrogen purge where required prior to launch.

## Telecommunications

The Antenna Subsystem (ANT) features an X-band feed for the 3.67 m diameter rebuild of the Voyager-designed HGA, and two X-band low gain antennas (LGA). The Orbiter has X-band uplink and downlink on both the HGA and the LGAs. A LGA is used for extended periods during the first two years of flight when the HGA cannot point at Earth (due to solar constraints and during main engine burns), and in the event of an emergency if HGA pointing is lost.

The Radio Frequency Subsystem (RFS) features redundant 10.6 Watt X-band solid state amplifiers, and a new NASA X-band transponder (NXT). The telemetry modulation function is included.

A clean telemetry channel is accomplished through use of a Reed-Solomon encoder in the command and Data Subsystem (CDS) and, a RFS supplied convolutional encoder. Using the HGA, this gives an overall bit error rate (BER) of  $10^{-6}$  using the NASA Deep Space Network (DSN). The X-band HGA downlink data rate while at Saturn varies from 27.6 kbps at maximum range with one amplifier operating to 67.9 kbps at minimum range with both transmitters operating simultaneously using a 70 m DSN ground station receiving antenna.

In addition, note that the ANT and RFS subsystems will be augmented, as part of radio science, to provide an S-band downlink beacon (carrier only) on the HGA.

## Power and Pyro

Two General Purpose Heat Source (GPHS) RTGs provide a total of 600 W at the beginning of the mission, decreasing to 462 W at the end of the mission. Two 135 Wh Nickel-Cadmium (Ni-Cd) batteries provide energy storage for short science sequences and engineering power peaks which exceed the RTG output power. DC power is supplied at  $30 \text{ V} \pm 0.75 \text{ V}$  ( $\pm 15 \text{ V}$  with respect to chassis with no chassis current) conditioned and distributed by the Power and Pyro Subsystem to users.

Solid State Relays (SSR) are used in the power distribution unit, replacing traditional electromechanical relays, thus eliminating fuses and providing programmable current limiting and enhancing fault protection.

The Power/Pyro subsystem also supplies energy and switching for all on-board pyrotechnic events. Pyro events are used to deploy booms, release the Probe, release the Probe relay antenna and actuate valves in the Propulsion Module Subsystem.

## On-Board Processors

A single, standard microprocessor design is used for all Orbiter flight subsystems. The amount of memory is variable. The baseline microprocessor is designed using the Sandia SA3300 chip family, which is radiation and single event upset (SEU) hard. The advantages of common, industry supported hardware are the shared development costs, common interfaces and the shared expertise. All flight software is programmed in the C language.

C-2

## Command and Data

The Command and Data Subsystem (CDS) controls the uplink, downlink, subsystem intercommunications, and sequence execution functions and provides command and telemetry functions to all Orbiter subsystems. The CDS also distributes engineering data of the spacecraft inertial attitude and rate, time, and each scan platform position and rate. All science instruments and engineering subsystems use a project-supplied standard MIL-STD-1553 B bus interface unit (BIU). All science telemetry is packetized, as is all engineering telemetry from subsystems with processors. The CDS creates packets for subsystems which have no processors.

The CDS design consists of redundant half subsystems. To minimise the bus rate and complexity requirements, multi-bus architecture is used, and consists of separate data buses for engineering (command and telemetry), low data rate instruments and high data rate instruments.

Collection, routing, and interpretation of all real-time, delayed, and programmed commands sent from Earth are the CDS's uplink tasks. All commands are verified by the use of parity bits and are then either executed, sent to the proper subsystem, or stored for execution at the designated time specified in the uplink message. Any subsystem or instrument with Random Access Memory (RAM) is able to have new memory loads sent from Earth to it via the CDS.

The CDS includes a non-mission critical redundant solid state buffer (25 Mbit capacity) using RAMs to match data rates between the science instruments and the Digital Tape Recorder (DTR), as well as between the DTR and the downlink.

The Digital Tape Recorder Subsystem (DTR) consists of two digital tape recorders with a capacity of  $10^9$  bits each and a BER of  $5.0 \cdot 10^{-6}$ .

Ground station track periods are approximately one pass per week during cruise and one or two passes per day during encounters. Stored sequences enable the Orbiter to operate autonomously, collecting scientific data and running fault protection programs for seven days before another uplink sequence is transmitted from Earth. Stored sequences are used primarily. Limited real-time commanding is available for backup to critical sequences such as orbit injection. Other limited real time commands may be used to modify science instruments modes, where they have no effect on any other Orbiter subsystem.

On-board fault protection is incorporated to correct critical Orbiter anomalies that cannot be corrected by ground controllers, due to the very long one-way light times  $\sim 80$  min and the lack of continuous ground monitoring.

## Pointing

The Orbiter Attitude and Articulation Control Subsystem (AACS) points the three-axis stabilized Orbiter (including the body-fixed HGA), articulates the HPSP and controls the science turntable and the RAM science platform, and controls the main engine and reaction thrusters burns and the main engine pointing.

The AACS sensors include a fiber optics rotation sensor (FORS), a star tracker (ASTROS II); and sun sensor (Adcole), all of which are fully redundant. The FORS (which provides inertial referencing with no moving parts) and the star tracker are mounted on the HPSP so that the pointing errors of the HPSP are minimized. The AACS compensates for Orbiter motion, as well as controls the HGA pointing, using a redundant reaction wheel assembly (RWA). The reaction wheels are unloaded by AACS using the reaction thrusters. The main engine is pointed by AACS using a (Viking Orbiter) residual gimbal.

All AACS processes are controlled by software residing in the redundant Attitude Control Electronics (ACE). Each ACE has a microprocessor (SA3300) with 256 kbytes of memory, and interfaces with the CDS.

The two-axis pointing for the remote sensing instruments on the HPSP is provided to an accuracy in inertial space of 2 mrad control, 1 mrad knowledge ( $3\sigma$ ). Maximum slewing rate is 17.5 mrad/s, which meets all science requirements and minimizes scan actuator mass and power.

A turntable, located on a boom opposite the HPSP, provides a field of view greater than  $2\pi$  steradian for the fields and particles instruments mounted on it. The turntable rotates at 1 rev/min (105 mrad/s) and is further than 2 m from the Orbiter bus.

Also mounted on the turntable boom is a RAM platform for the Titan aeronomy instruments. This small platform provides the capability for  $60^\circ$  scanning at a maximum rate of 17.5 mrad/s. It will typically be pointed by Modular Attitude Control System (MACS) in the direction of the velocity vector (RAM direction).

## Propulsion

The Propulsion Module Subsystem (PMS) includes two large conispherical bipropellant tanks (total capacity of 3450 kg), a small monopropellant tank, a helium pressurant tank, the main engine, reaction thrusters, and associated plumbing and structure. The bipropellant – monomethylhydrazine ( $N_2H_2$ ) and nitrogen tetroxide ( $N_2O_4$ ) – is used for the trajectory and orbit changes using the main (400-N) engine. The monopropellant – hydrazine – is used for the reaction control system located in eight identical clusters: four are symmetrically located at the periphery of the HGA, and four are at the bottom of the PMS. The pressurant tank is located in the center of the PMS.

The PMS provides structural support for the other Orbiter assemblies/subsystems: the bus, the RWA, the Titan Probe attachment structure, the LGA, and the Probe Antenna Assembly.

## Thermal Control

The allowable temperature limits of the Orbiter are maintained by passive techniques, such as sunshades, heat shields, surface property control, louvers, Radioisotope Heater Units (RHUs), multi-layer blankets (MLI), and radiators; and active techniques, such as electrical heaters.

The electronics bus temperature is regulated by standard size louvers mounted on each electronics bay face, and MLI blankets covering the remainder of the exposed bays. The PMS maintains its temperature limits and reduces temperature gradients between propulsion tanks through selection of proper emittance for surfaces on the structure and tanks. RHUs on the structure, main engine thrust plate and the RCS thrusters; and MLI blanketing wrapped around the entire PMS. The HPSP, turntable, and RAM platform temperature control use MLI, electrical heaters, radiators, and appropriate mounting of equipment to the platform.

## 8.2 Probe Support Subsystem

The Probe Support Subsystem (PSS) is the ESA-supplied portion of the Orbiter and consists of Probe Antenna Assembly (consisting of a relay antenna, antenna pointing mechanism, and signal preamplifiers); PSS electronics (consisting of the radio receiver, data handling/ processing electronics), which are mounted in one bay of the Orbiter bus; and the Probe attachment structure and Spin Eject Device.

## 8.3 Mass and Power Summary

Table 8.1 summarizes the subsystem masses and the total Orbiter mass. The values shown are the current best estimates. Contingencies are added in anticipation of growth that typically oc-

cers during the development phase. Reserves reflect the mass margin between the Orbiter's mass allocation and its current mass status.

Table 8.2 summarizes the power status of the Orbiter. A maximum of 252 Watts at Saturn arrival (205 Watts at end of mission) has been allocated for science electrical power. Peak power loads for some science instruments or engineering loads can be handled by the battery.

Subsystem	Mass (kg)
Orbiter without PSS (Current Best Estimate)	222.9
Structure Subsystem	24.4
Radio Frequency Subsystem	161.3
Power and Pyro Subsystem	24.0
Command and Data Subsystem	134.3
Attitude and Articulation Control Subsystem	78.0
Cabling Subsystem	373.6
Propulsion Module Subsystem (dry)	32.8
Thermal Control Subsystem	31.0
Digital Tape Recorder Subsystem	18.9
Antenna Subsystem	6.8
Strawman Science Instrument Subsystems (incl. cal targets, mag. cal.coil)	186.6
Ballast	2.7
Spacecraft Purge Equipment	
Dry Orbiter without PSS (Current Best Estimate)	1297.3
Orbiter without PSS (Contingency Reserve)	252.7
Dry Orbiter without PSS (Allocation)	1550.0
Probe Support Subsystem (Current Best Estimate)	53.0
Probe Support Subsystem (Contingency and Reserve)	8.3
Probe Support Subsystem (Allocation)	61.3
TOTAL Dry Orbiter (Allocation)	1611.3
Probe (Current Best Estimate)	178.3
Probe (Contingency and Reserve)	14.0
Probe (Allocation)	192.3
Launch Adapter (Current Best Estimate)	132.7
Launch Adapter (Contingency and Reserve)	42.3
Launch Adapter (Allocation)	175.0
TOTAL DRY Launch Mass (Current Best Estimate)	1649.0
TOTAL Dry Launch Mass (Allocation)	1978.6

Time from Launch (Days)	Arrival at Saturn (watts)	End/Mission (watts)
	2373	3760
Minimum RTG Power	513	462
System Contingency	- 41	- 37
Minimum engineering	- 138	- 138
Available for Science Optional engineering Support	334	287
Minimum Science	- 82	- 82
Optional for Science and Science Support	252	205

Table 8.2: *Orbiter Power summary*

# Chapter 9

## The Titan Probe System

### 9.1 General

The Probe system is designed to meet the Probe's scientific and mission objectives, with a cost-effective design whose performance meets the requirements with adequate system design margins.

Some of the main factors influencing the design are:

- scientific objectives
- mission scenario, duration and profile
- required performance
- availability of relevant European expertise and technology
- inheritance from other planetary missions
- a cost effective, reliable and flexible design approach

Technology studies performed during the 1984-1988 period, have provided a sound technological basis for the design trade-offs during both the Assessment and Phase A studies. The areas of technology studied were:

- aerodynamic concepts
- aerothermodynamic concepts
- aerodynamic deceleration systems
- parachute module concepts and characteristics
- planetary descent and thermal protection systems
- on-board autonomy
- autonomous modular power subsystems
- lithium power sources
- radio relay link
- spin eject devices
- microwave radar instrumentation

### 9.2 Probe Mission Phases

launch

Titan IV/Centaur launches Saturn Orbiter/Titan Probe composite spacecraft

### **cruise**

Nominal duration 6.5 years. The Probe is periodically checked out using Orbiter power via the umbilical.

### **Separation**

After targeting, the Probe will be simultaneously spun up to a nominal 10 rpm and separated at a velocity of 0.3 m/s by a spin eject device.

### **Coast**

After separation, the spin-stabilised Probe continues on a ballistic trajectory to encounter Titan. The nominal duration of the coast phase is 12 days. The Probe's on-board timer will be synchronised to the Orbiter's clock immediately prior to separation.

### **Entry**

The Probe approaches Titan at an asymptotic velocity (V-infinity) in the range 5.5 - 6.8 km/s (5.5 km/s baseline) and enters Titan's atmosphere at a speed in the range of 5.8 - 7.1 km/s. This phase lasts approximately 3 minutes culminating with the jettison of the Probe decelerator at a velocity of ~Mach 1.5 (~400m/s) and altitude of ~190 km. During this phase, the ASI is activated and the data stored for later transmission.

### **Descent**

After the Probe has deployed its first parachute, it also uncovers the experiment ports and initiates the acquisition of science data during the approximately 2 - 3 hr descent phase. During the period between the start of chemical sampling and up to approximately 1.2 hours afterwards the Probe's CDMS will determine the optimum moment to jettison the Probe's main parachute and deploy a second smaller parachute. This decision will be based on altitude data from the Radar Altimeter and data from accelerometers and pressure sensors. This procedure is designed to adapt the Probe descent profile to the scientific instruments operations profile, and to minimise the timing uncertainty in impact at Titan's surface for maximising the potential Science return.

### **Post-Impact**

After impact with the surface the Probe may continue operating and transmitting data which the Orbiter will receive, store and relay to Earth until loss of radio link with the Probe.

## **9.3 System Budgets**

The mass budget for Probe and PSS are given in Tables 9.1 and 9.2. Energy and Power Budgets are given in Table 9.3.

## **9.4 Probe Design**

The Titan Probe System is split into several subsystems:

- The Descent Module is comprised of Scientific Instrument Subsystems, Structure and Mechanisms, Thermal Control, Thermal Protection, Descent Control, RF Telecommunications, Command and Data Management, Sensors, and Power/Pyro subsystems.
- The Probe Support Subsystem comprises Spin Eject Device, Probe Attachment Structure, electrical equipment, the radio relay antenna and antenna pointing mechanism.
- The system design requirements calls for a system design which has a high degree of fault tolerance, good reliability and the ability to function autonomously after Orbiter/Probe separation. Redundant features are incorporated to maximise confidence in the reliable operation of the Probe for its mission lifetime, and to meet the requirement that no potential single point failure in the Probe's scientific payload or engineering subsystems will result in a catastrophic failure except for approved cases. Additionally, the system shall be designed to avoid failure propagation and subsequent degradation of system or payload performance.

The main system design drivers are:

- Spacecraft Post-Saturn Orbit Insertion (SOI) for Titan Probe release
- Delivery, targeting and spin separation at Titan Encounter - 12 d.
- Entry, descent and impact on day-lit side. Entry latitudes +60°N and 60°S.
- V-infinity: Range 6.8 - 5.5 km/s
- Entry velocity (1000 km): Range 7.1 - 5.8 km/s
- Entry angle (1000 km): Range -60° to -90° including uncertainties
- Orbiter flyby altitude: Range 800 - 2500 km
- Orbiter/Probe delay: Range 2.0 - 3.5 hours (nom.)
- Chemical sampling initiation > 170 km
- Descent time: Range 120 - 180 min
- Impact on Titan's surface before loss of signal
- Data rates: 512 bit/s at the beginning of the descent to >8 kbit/s near the surface
- Total data transmission capability: 10 - 17 Mbit
- Probe energy: 1.37 kWh
- Probe mass allocation: 192.3 kg.
- PSS mass allocation: 61.3 kg
- Design lifetime: 10 years including ground life
- Material selection: compatible with Science requirements

## 9.5 Aerodynamics and Aerothermodynamics

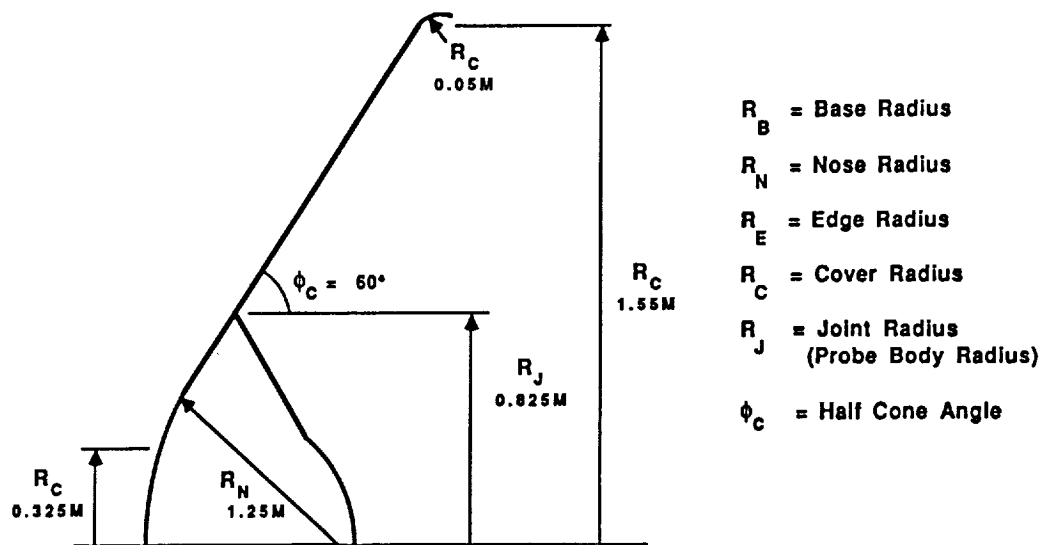
The Probe's aerodynamic shape, as shown in Figure 9.1, has been optimised as far as possible to match all the system and atmospheric science requirements. The aeroshell configuration and size is driven primarily by the mission requirement to start atmospheric experiments at or above 170 km. The need to minimise costs, and the existence of the relatively large scale height atmosphere, led to the adoption of an unguided ballistic aerobraking concept.

A sphere-cone configuration was chosen as giving the maximum drag and providing suitable stability for a given ballistic coefficient. This is required as the tip-off errors incurred at Probe/Orbiter separation may lead to large angle of attack at entry. The effects of atmospheric winds and unknown wind shears also influenced the need for a conservative aerodynamically stable design. A half cone angle of 60 ° was chosen as having good stability characteristics and near maximum drag coefficient.

<b>Payload Instruments</b>	39.9
Sensors (incl. Altimeter)	4.2
CDMS	8.9
Communications	6.6
Power and Distribution	25.2
Structure	16.9
Parachutes	7.6
Decelerator	23.8
TPS Forecone and Nose cap	23.0
TPS Aft Cone	5.7
TPS After Cover	3.0
Thermal Control	12.5
Balance Mass	1.0
<b>TOTAL</b>	<b>178.3</b>
Contingency and Reserve	14.0
<b>TOTAL Probe Mass (allocated)</b>	<b>192.3</b>

Table 9.1: *Titan Probe Mass Budget (kg)*

<b>PSS Support:</b>	
Structure	6
S.E.D.	9.4
Attachment	3.0
Connectors	1.6
<b>TOTAL</b>	<b>20.0</b>
<b>PSS Antenna Assembly:</b>	
Deploy and steering	4.5
Release	1.6
Antenna	4.8
Electronics	3.6
Thermal	2.2
Harness and Cabling	1.6
<b>TOTAL</b>	<b>18.3</b>
<b>PSS Electronics:</b>	
Telecommunications	6.8
CDMS	6.3
Power I/F	0.6
Harness, switches	1.0
<b>TOTAL</b>	<b>14.7</b>
<b>TOTAL PSS Mass</b>	<b>53.0</b>
Contingency and Reserve	8.3
<b>TOTAL PSS Mass (allocated)</b>	<b>61.3</b>

Table 9.2: *Probe Support Subsystems Mass Budget (kg)*Figure 9.1: *Probe aerodynamic characteristics*

System/Equipment	Switch on Time	End	Energy Required
RF System	*to	to +182 mins	97 Watthours
XTal Oscillations	to -20 mins	to +182 mins	3.5 " "
CDMS System	to -30 mins	to +182 mins	109 " "
Radar Altimeter	to	to +182 mins	45 " "
Power and Pyrotechnic	to	to +182 mins	45 " "
Sensors and Housekeeping	to -15 mins	to +182 mins	72 " "
Timer and Keep Alive	to -12 days	to +182 mins	172 " "
ASI Instrument	to -30 mins	to +182 mins	37 " "
PIRLS Instrument	to -30 mins	to +182 mins	55 " "
GC/MS Instrument	to -30 mins	to +182 mins	91 " "
ACP Instrument	to -20 mins	to +155 mins	54 " "
DISR Instrument	to -20 mins	to +182 mins	52 " "
LRD Instrument	to -10 mins	to +182 mins	8 " "
RITO Instrument	to +150 mins	to +182 mins	5 " "
DWE Instrument	to -30 mins	to +182 mins	10.5 " "
			856 Watthours
Pre-Separation Checks	to -(12days 15 mins)	to -12days	50 " "
Contingency 10%			91 " "
Growth 10%			100 " "
Distribution Losses 2%			22 " "
Battery Discharge Regulator Losses 8%			90 " "
Interface with Battery Loss 3%			36 " "
Probe Mission Energy Requirement			1245 " "
Battery Capacity Energy Loss ( 7.5 yrs Storage) 10%			125 " "
Battery Capacity Energy Requirement			1370 " "

\* to = start time of Probe descent phase

Note: Energy requirements are given for a maximum descent time of 3 hours

Table 9.3: *Probe System Energy and Power Budgets*

The large atmospheric density uncertainty and the adoption of the full range of entry angles resulted in the choice of a base diameter of 3.1 m, which can be accommodated in the space envelope of the Mariner Mark II spacecraft with an adequate margin.

The nose radius has been chosen primarily to reduce the total heat load to the vehicle surface, permitting the minimum mass for the radiative/heat soak forward Beryllium heatshield. The final feature of the geometry is a 5 cm radius at the expansion from the cone to the base region. This reduces hypersonic heat transfer and is designed to keep edge heating below nose stagnation point levels at zero incidence. A useful outcome is the stiffening of the aeroshell in this region.

### Aerodynamics

Aerodynamic data have been derived primarily from existing experimental data, using flowfield codes to interpolate between the experimental results. This approach gives maximum confidence in the aerodynamic configuration. Thus wind tunnel testing costs during the development phase will be minimised.

The entry configuration of the Probe is statically stable and full six degrees-of-freedom entry simulations have shown no dynamic instabilities or resonances. The Probe configuration must be stable after decelerator release and prior to parachute deployment.

The computed altitude achieved at Mach 1.5 over the full range of entry angles (-60° to -90°) is illustrated in Figure 9.2.

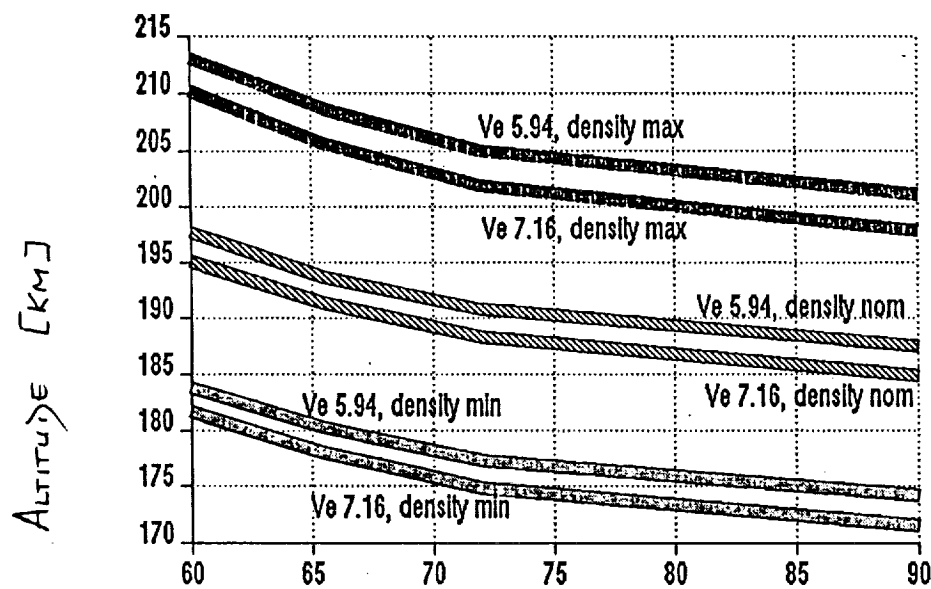


Figure 9.2: *Mach 1.5 altitude achievements vs. entry angle*

### Aerothermodynamics

The aerothermodynamic characteristics have featured heavily in the design of the Probe configuration. Convective heat transfer has been assessed using pressure coefficients from Eulerian flowfield

codes as the input to an energy and momentum integral boundary layer solution. These boundary layer solutions have been checked against existing heat transfer data for the configuration, adjusting the gas properties then being changed for the Titan atmosphere.

Chemical equilibrium analysis of the gases in the shock layer has been used to define gas properties for both flowfield and heat transfer calculations. Radiative transfer from the high temperature shock layer produces a small contribution to the total heat transfer to the vehicle. Reradiation from the decelerator interior walls to the Probe rear surface is the largest heating contribution and has been accounted for in the thermal design of the rear cover.

### Trajectory Analysis

Coupled 3-degree-of-freedom trajectory and heat transfer calculations have been made to assess entry heat transfer, deceleration loads and the achievement of the required atmospheric sampling altitude. Typical trajectory parameters are shown in Figure 9.3.

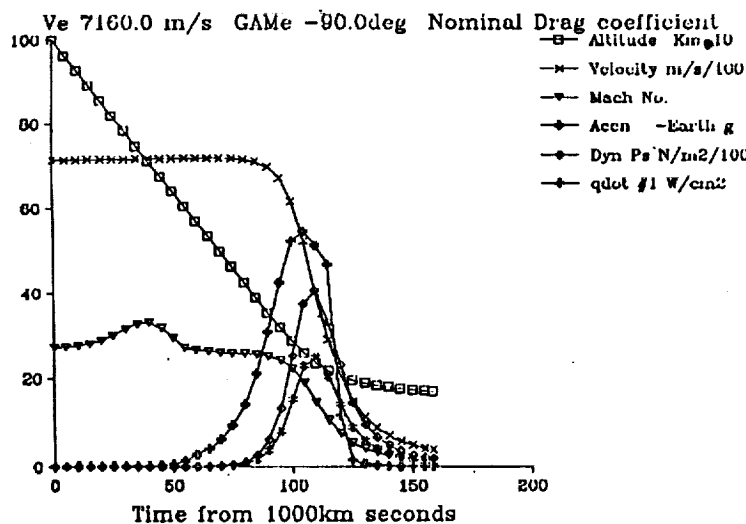


Figure 9.3: *Typical Probe trajectory parameters*

6-degree-of-freedom trajectory analysis has been used to quantify dispersions and loading extremes, and to develop tolerances for decelerator deformation and Probe mass properties for the entry phase. It was also used to determine separation timing sequences during and after the decelerator release. The angle of attack at the beginning of the entry phase has also been assessed to be an allowable maximum of  $15^\circ$ .

### Probe Configuration

The Probe system configuration is constrained by the requirements of the Cassini Orbiter Interface Requirements document (IRD). These requirements prescribe the accommodation volumes for the Probe and PSS items. The PSS interfaces with the Probe's power and CDMS interfaces via an umbilical throughout the cruise phase to provide periodic checkout and housekeeping functions, as well as monitoring and Probe functional status checks. Probe envelope and PSS envelope requirements are indicated in Figure 9.4.

The Probe consists of a blunt-nose, sphere-cone shaped central descent module with a half cone angle of  $60^\circ$  and a nose radius of 1250 mm, and an attached decelerator. The jettisonable deceleration concial frustum forms part of the entry thermal protection system and has a maximum

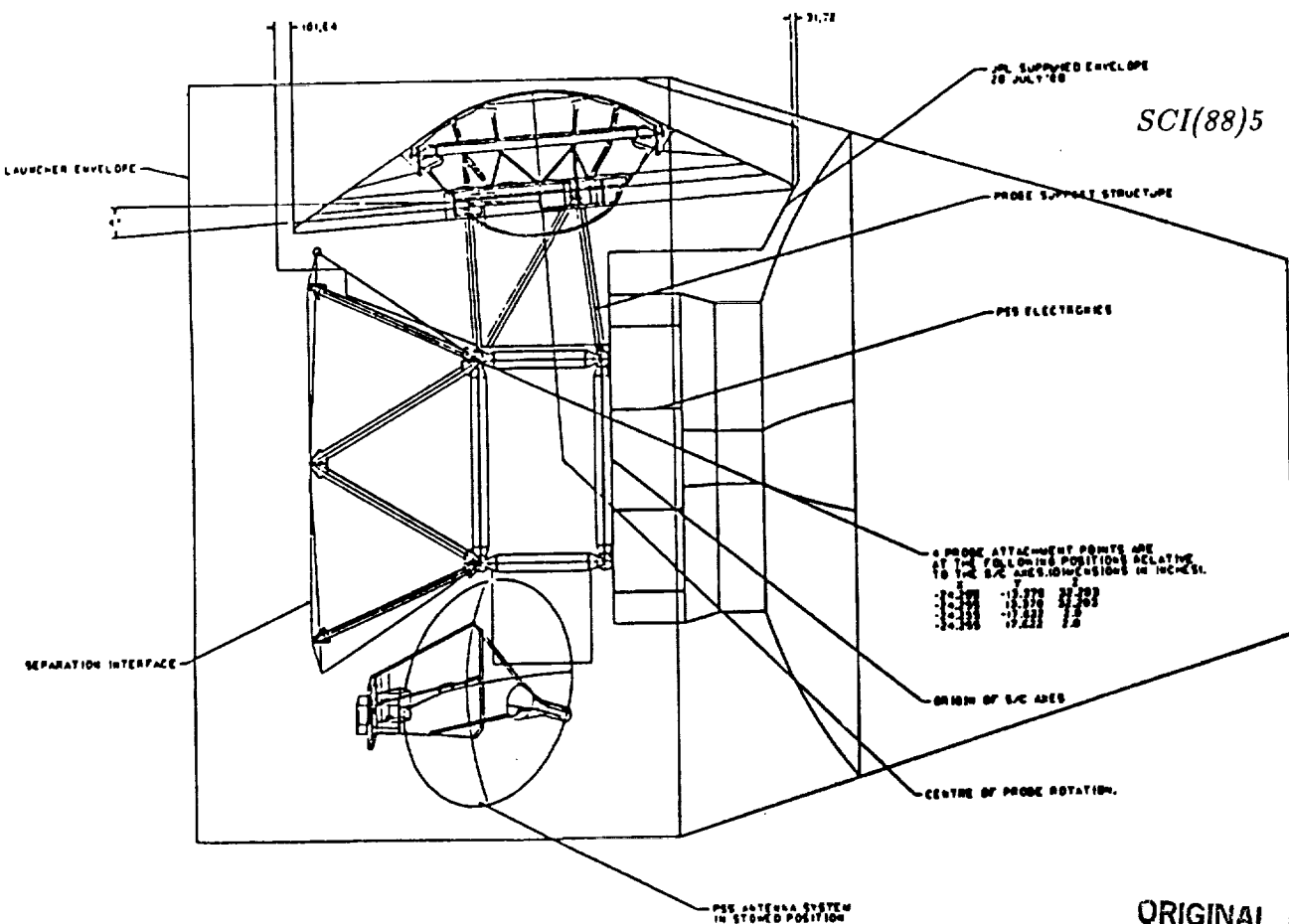


Figure 9.4: *Probe System configuration on the Orbiter*

ORIGINAL PAGE IS  
OF POOR QUALITY

diameter of 3.1 m. The descent module foreward heatshield has a central jettisonable nosecap with a diameter of 650 mm. A jettisonable after cover with a base diameter of 1.07 m, protects the equipment on the upper platform from aerodynamic heating and radiative heat transfer from the decelerator during the Entry phase and is also an element in the thermal control.

In order to ensure high stability during the spin stabilised coast and aerodynamic entry phase the major part of the instruments and the spacecraft equipment are mounted on one platform, which results in a high inertia around the spin axis and a low center of mass position.

The Probe is mounted in a "nose-out" configuration on the Orbiter, tilted at 4 degrees to the Orbiter "-x" axis, such that its spin axis will coincide with the Orbiter Centre of Gravity position at separation as shown in Figure 9.4. The Probe will be attached at three points of its aft interface and Spin Eject Device (SED) with six CFRP struts linked at four points to the Orbiter propulsion module structure.

The PSS Electronics will be accommodated in one bay of the Orbiter 10-bay spacecraft bus. The PSS Antenna Assembly will be accommodated at the location indicated in Figure 9.4. The PSS Antenna Assembly will be a self-contained item including RF feed and reflector, stowage mechanism, pointing mechanism, mechanism drive circuitry and low-noise amplifier electronics and is surrounded by its own thermal control elements.

The overall configuration of the Probe is indicated in Figure 9.5, the PSS configuration is indicated in Figure 9.4

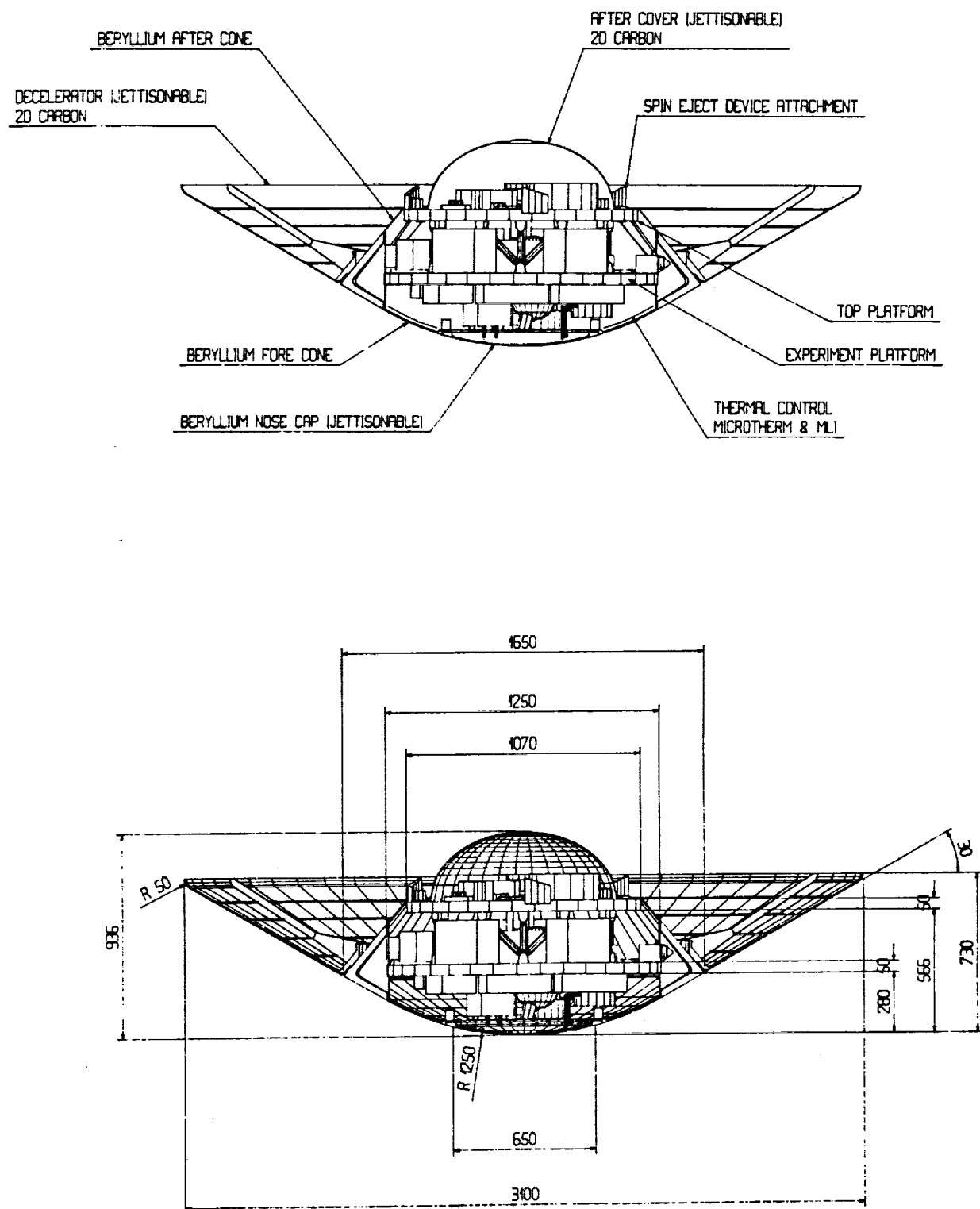


Figure 9.5: *Probe configuration (dimensions in mm).*

## 9.6 Payload Accommodation

### Experiments

There are 9 experiments in the model payload. 7 are scientific instruments and two experiments use engineering data from Probe Subsystems.

The instruments are listed in Table 4.2. The instrument accommodation on the platforms are given in Figures 9.6 ,9.7 and 9.8.

### Accommodation

The LRD antenna and sensors are located on the upper face of the top platform. The two LRD optical sensors are mounted 180° apart in order to provide a 360° coverage. The ASI triaxial accelerometer package is mounted on the lower face of the platform along the Probe's spin axis.

The engineering sensors and related electronics are also located on the top platform.

The remaining experiments are located on both upper and lower faces of the experiment platform.

The largest instrument in the model payload is the GCMS. Its accommodation requires a large, circular protrusion in the experiment platform. At the beginning of chemical sampling, the inlet tube on the front shield will be deployed out to the stagnation point. This tube is assumed to be the first item in the Probe to strike the surface on impact. In order to measure the impact acceleration as close as possible to the impact point, the sensitive linear accelerometer of the ASI instrument is mounted on the outer structure of this inlet tube.

The ACP has major interfaces with the GCMS and is mounted close to it on the bottom side of the platform. It has two inlet tubes which will be deployed outside the boundary layer of the Probe's flow field.

The sensors for the PIRLS and DISR instruments are mounted as shown in Figure 9.6. The sensors of both instruments are protected during entry by jettisonable protective covers. At the start of chemical sampling the PIRLS instrument will deploy a mirror out 200 mm from the side of the Probe. An aluminium membrane will be placed around the viewing port of PIRLS both to impede ingress of the atmosphere into or leakage of exhaust gas from the Probe interior. The ASI temperature sensor and pressure inlet are located outside the front shield and will be deployed into the free stream after nosecap jettison.

The surface science instrument, RITO, is mounted as shown in Figure 9.8. Its sensor is protruding through the front shield to ensure that immersion of the prism in a potential liquid medium after impact, will enable refractive index measurements to be performed.

For simplicity and reliability of port opening, group of four downward pointing instruments and the radar altimeter antenna are placed behind a single 650 mm diameter internally insulated nosecap jettisonable.

For instruments where the electronics can be separate from the sensors (PIRLS, DISR, LRD, Radar altimeter), the electronics boxes will be placed on the upper side of the main platform where the temperature environment is benign.

## 9.7 Structure and Mechanisms

### Structure

The Probe structure has been designed to meet all the Probe System requirements and to accommodate the payload and subsystems through all mission phases and ground activities.

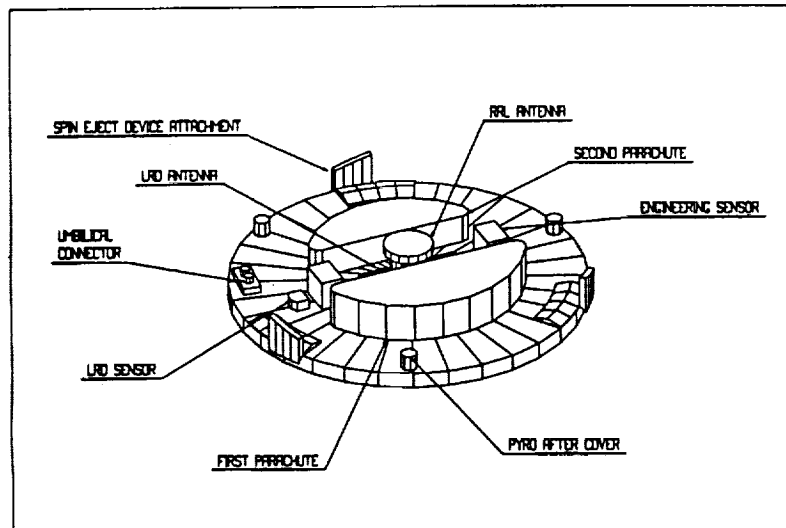


Figure 9.6: *Probe top platform*

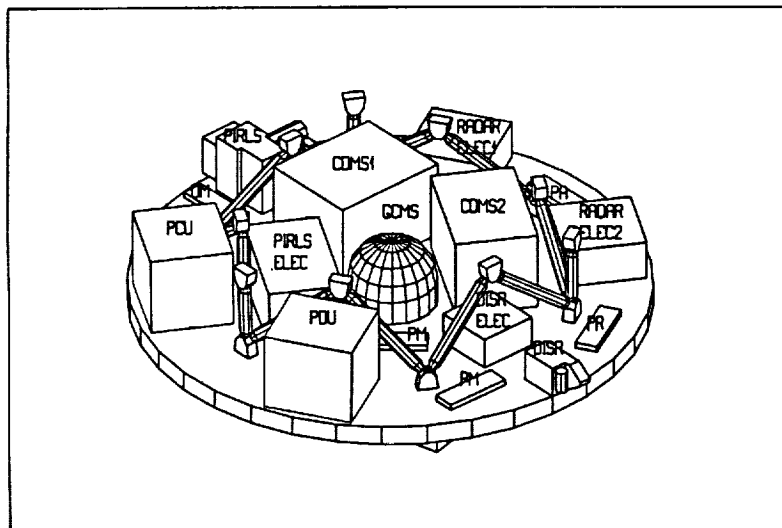


Figure 9.7: *Probe experiment platform: top view*

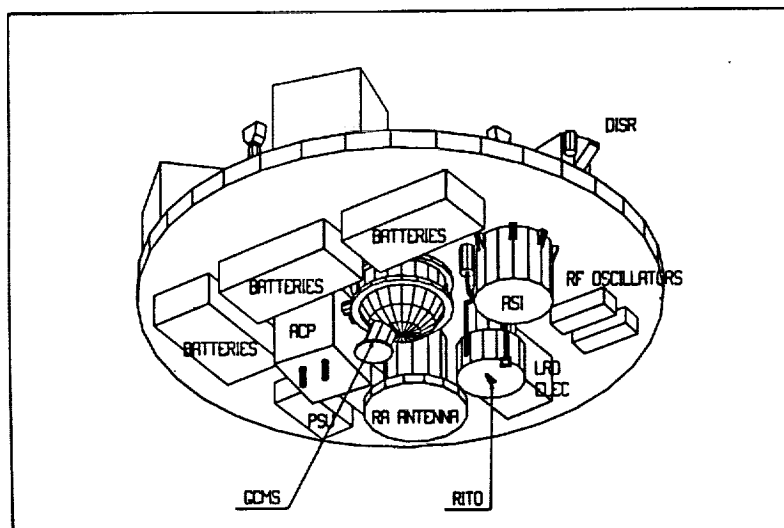


Figure 9.8: *Probe experiment platform: bottom view*

The descent module primary structure consists of two 50 mm thick aluminium honeycomb platforms which provide the required accommodation for the scientific instruments and engineering subsystems. They are supported by interconnecting struts which form the primary load path as indicated in Figure 9.7. The structural layout has been based on providing simple loads paths which optimise the strength and stiffness requirements in relation to minimum mass objectives. The experiment platform accommodates the major part of the science instrumentation on its upper and lower faces.

The top platform accommodates the Probe antenna, parachutes, engineering sensors and LRD sensors. The top platform is connected to the Orbiter-mounted Probe Attachment Structure and Spin Eject Device. The entry aerodynamic loads are transferred to the top platform through the stiffened after cone from the aeroshell. During entry the top platform is protected by the after cover.

Secondary structural items also attach and reinforce the thermal control blankets and experiment cover aperture closures. These items are indicated in Figure 9.9.

### Spin and Eject Device

A Spin and Eject Device is used to spin up the Probe to 10 rpm and separate it from the Orbiter at 0.3 m/sec after pyrotechnic release of the three attachment bolts, which connect the Probe top platform to the ends of the six-strut support tubes of the Probe attachment structure which is mounted on the Orbiter Propulsion Module truss structure.

### Mechanisms

Pyrotechnically operated mechanisms are required for the following items:

- Release of Probe from Orbiter - 3 double pyros used to detach Probe/PSS strut connections and enable the SED to operate (uses Orbiter power for operation)
- Release of umbilical connections between Probe and Orbiter - 1 double pyro (uses Orbiter power)
- Release of PSS antenna hold down - 3 redundant pyros operated sequentially (uses Orbiter Power)
- Probe decelerator release - 6 redundant pyros operated simultaneously to cause balanced release and jettison of the decelerator while travelling at Mach 1.5 in Titan's atmosphere at 190 km altitude.
- Parachute mortar - 1 redundant pyro to initiate gas generator and cause pilot chute deployment.
- Aft cover release - 3 redundant pyro devices to release cover and enable it to be pulled from the Probe by pilot chute line.
- Experiment cover release - 3 redundant pyros to cause release of two separate covers
- Nose cap release - 3 redundant pyros to release and enable cover rotation to cause gravitational pull.
- First parachute release - 3 redundant pyros to release parachute attachment eyes to separate it from the descent module, and deploy the second parachute.
- Experiment pyros - as required.

## 9.8 Thermal Protection Subsystem

This subsystem protects the Descent Module from the aerothermodynamic heating experienced during the entry into Titan's atmosphere.

Maximum temperatures in excess of 800°C are achieved by the TPS nose and fore cone and a maximum deceleration of approximately 240 m/s<sup>2</sup> (25 g) can occur with spin and aerodynamically induced vibration. It is therefore essential to provide the TPS with appropriate materials, attachments and insulation items while linking it to the primary structure and equipments of the Probe.

- The TPS will comprise a decelerator assembly of 3.1 m maximum outer diameter down to 1.65 m inner diameter and a forecone with nose sphere of 1.25 m.
- The TPS decelerator will be manufactured in 2D carbon and will be jettisonable as a single unit by the simultaneous firing of pyro release bolts at the end of the Atmosphere Entry Phase.

The forward TPS concept utilises a spherical beryllium nose, fore-cone and jettisonable 6 mm thick beryllium nose cap as a ballistically separated instrument cover.

- The insulated TPS aft cover supports the parachute mortar and covers the upper platform on which the parachutes and RRL antenna are located. Figure 9.10 indicates the position of all TPS items.

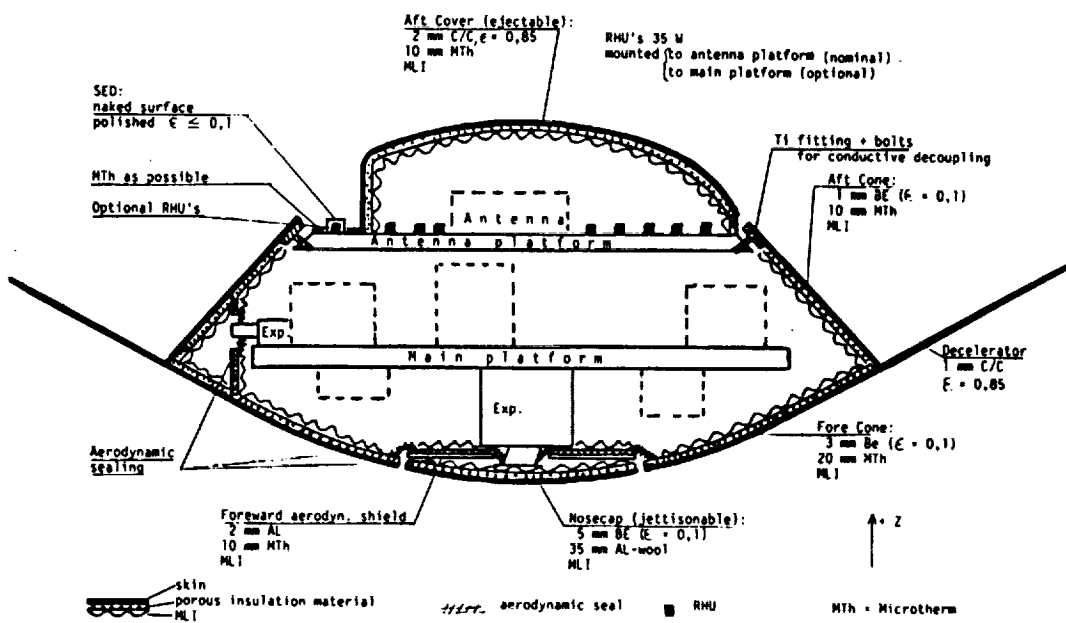


Figure 9.9: *Schematic of thermal control components*

## 9.9 Thermal Control Subsystem

The Probe utilises 35 x 1 W Radioisotope Heater units (RHUs) during all phases of the mission. A small number of RHUs are used to maintain the temperatures of the PSS Antenna Assembly.

The PSS Electronics will be accommodated within the environment provided by the Orbiter Temperature Control Subsystem.

Kapton Multilayer Insulation with performance  $0.03\text{-}0.06 \text{ W/m}^2/\text{°K}$  will form the basis for all high insulation elements, while insulating seals will minimise the ingress of the atmosphere and any resultant convective cooling of the Probe's equipment. Microtherm will be used to insulate the Descent Module.

The major thermal control components are indicated in Figure 9.10.

- Mathematical modelling of the Probe internal temperatures resulted in temperatures ranging between  $-20\text{°C}$  and  $+25\text{°C}$  for all mission phases.

The main features of the Probe's thermal design are:

- Instrumentation protected against environmental influence by a three layer system
- outside high temperature skin: front side and rear cone Beryllium
- porous insulation to withstand elevated temperatures and to keep a certain performance under atmosphere: Al-wool resp. Microtherm
- inside MultiLayer Insulation (MLI) of Kapton foils for high performance under vacuum conditions
- 35 x 1 W Radioisotope Heater Units (RHUs)
- Conductive path insulation between Be-skin and carrying structure (platform)
- Minimisation of forced convection flow inside the Probe during descent (sealing of experiment ports).

## 9.10 Descent Control Subsystem

The system requirement for aerodynamic deceleration of the Probe from atmospheric entry speeds in the range 5.8 km/s to 7.1 km/s to subsonic speeds above 170 km, defines the deceleration approach. The decelerator aerobrakes the Probe from its actual entry speed down to Mach 1.5, at which time the decelerator is jettisoned and a parachute descent system sequence is initiated.

The sequence is as follows:

- Deployment of pilot chute, separation of after cover and extraction of main chute
- Descent on 1st main chute for approx. 1 hr
- Release of 1st main chute and simultaneous extraction of 2nd main chute.
- Descent on 2nd main chute to the surface.

The criteria used for initiation of the decelerator jettison/parachute deployment sequence will be derived from acceleration measurements using the direct relationship between acceleration and velocity profiles.

The design of the Descent subsystem provides the required stability in terms of descent rate and rotation, in response to requirements on the descent trajectory imposed by the scientific payload. A nominal descent trajectory of 2.75 hr depicting altitude/time characteristics consistent with the payload operations profile was given in Figure 6.13. The subsystem consists of:

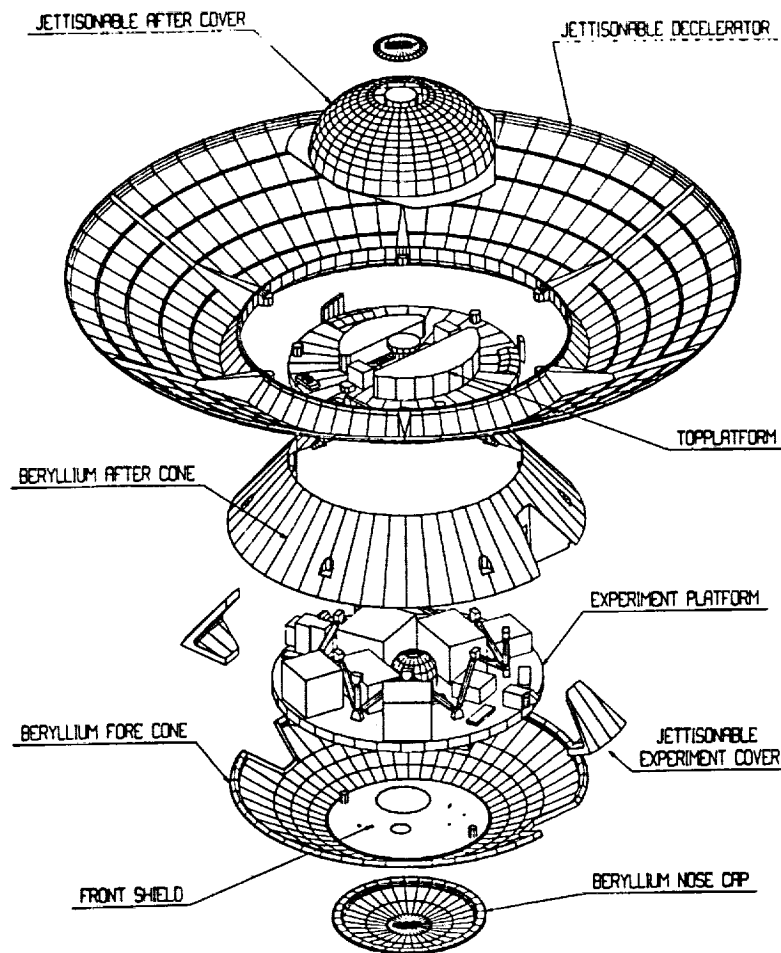
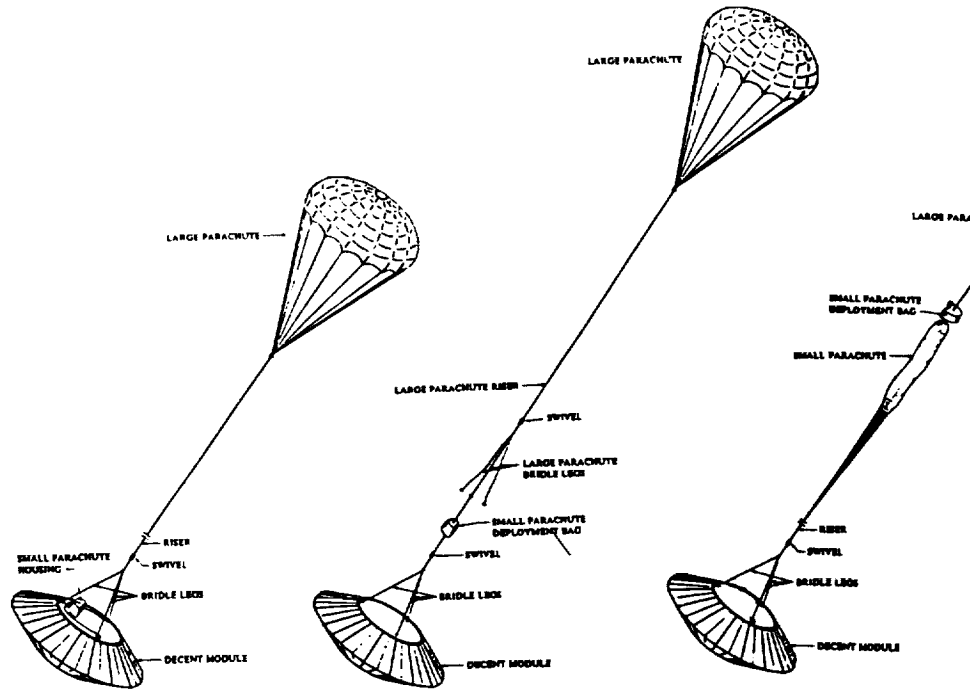


Figure 9.10: *Titan Probe exploded view*

- a  $20^{\circ}$  conical ribbon Kevlar pilot chute, diameter 1.84 m and a mortar for deployment at Mach 1.5
- a  $20^{\circ}$  conical ribbon Kevlar 1st main parachute, diameter 4.98 m, giving ballistic coefficient for the overall configuration of  $15.5 \text{ kg/m}^2$ . The maximum opening force is 2450 N.
- a  $20^{\circ}$  conical ribbon Kevlar 2nd main parachute, diameter 2.31 m, giving a ballistic coefficient for the overall configuration of  $46.4 \text{ kg/m}^2$ .



### Exchange of Main Parachutes

- Parameter identification (atmospheric density profile, drag coefficient)
- Trajectory prediction
- (Prediction of budgets for radio relay link and energy)
- Optimisation

Figure 9.11: *Criteria and sequence for adaption of the descent profile*

- swivel mechanisms for each main parachute to decouple the spinning descent module from its parachute systems.
- spin slots or vanes to induce asymmetries which will maintain spin rates varying from 20 rpm at higher altitudes decreasing to rates of 4-1 rpm near the surface.

The subsystem sequences are graphically illustrated in Figure 9.11.

The terminal velocity at impact is assessed to be ~5 m/s.

## 9.11 RF Telecommunication Subsystem

### Probe Telecommunications Subsystem

A one-way Radio Relay Link (RRL) will operate between the Probe and the PSS during descent for the transmission of science and housekeeping data to the Orbiter.

Initial acquisition of the RRL by the PSS will occur following parachute deployment. The nominal descent is approximately 165 minutes.

The RRL has been designed to work with the different slant ranges and link geometries resulting from entry angles between  $-90^\circ$  to  $-60^\circ$ . The Probe is required to transmit all buffered/stored science

data prior to impact, and thus to be in real time mode at least few minutes before the impact. This leads to a requirement to be able to switch to a bit rate of 8960 bps prior to touchdown, resulting in an estimated return capacity of 16.8 Mbits of data, based on impact time prediction accuracies of  $\pm 15$  min.

The RF subsystem utilises a single 60° Half Power Beam Width (HPBW) planar array antenna giving 4.4 dBW Effective Isotropic Radiated Power (EIRP), and hot redundant chains for Oscillator, Phase Modulator, Telemetry Modulator, Power Amplifier, Control Unit and RF power supply unit.

The Probe will radiate a wide-beam (120° beamwidth) circularly polarised signal at 2.1 GHz to the Orbiter. The Orbiter PSS will be equipped with a narrow beam 1.4 m diameter antenna capable of being pointed in closed loop by sensing the signal strength using the "hill-climbing technique".

Five switchable data transmission rates are provided to accommodate the different operational ranges of the RRL. One-third rate convolutional coding is used. As the Orbiter/Probe range decreases from approximately 80000 km to 20000 km, the bit rates increase from 560 bps through, 1120, 2240, 4480 bps to a maximum of 8960 bps few minutes prior to touchdown. Bit streams of convolutionally encoded data will first be BPSK/PM modulated onto the main carrier. Control of modulation index setting will allow optimised distribution of transmission power between the carrier and side bands. The link budgets are given in Table 9.4.

Probe Ant. HPBW	Deg	120	120	120	120	120
Bit Rate	bps	560	1120	2240	4480	8960
Slant Range	km	96,663	64,540	45,750	32,180	23,440
Orbiter Antenna Dia	m	1.4	1.4	1.4	1.4	1.4
Orbiter HPBW	Deg	7.15	7.15	7.15	7.15	7.15
Titan Angle Sight	Deg	3.04	4.58	6.42	9.17	12.55
Probe EIRP	dBW	4.99	4.99	4.99	4.99	4.99
Tx. Antenna Gain						
at Edge	dB	-1.5	-1.5	-1.5	-1.5	-1.5
Circuit Loss	dB	0.50	0.50	0.50	0.50	0.50
Pointing Loss	dB	0.00	0.00	0.00	0.00	0.00
Tx Power	W	5.0	5.0	5.0	5.0	5.0
Tx Power	dBW	6.99	6.99	6.99	6.99	6.99
Frequency	MHz	2100	2100	2100	2100	2100
Path Loss	dB	198.60	195.09	192.10	189.05	186.29
Polarisation Loss	dB	0.20	0.20	0.20	0.20	0.20
Atmospheric Loss	dB	0.10	0.10	0.10	0.10	0.10
Parachute Loss	dB	0.10	0.10	0.10	0.10	0.10
Orbiter Antenna Gain	dBi	26.75	26.75	26.75	26.75	26.75
Orbiter Pointing	dB	0.50	0.50	0.50	0.50	0.50
System Noise	dBK	23.51	24.01	24.44	24.49	24.49
Rx G/T on bore site	dB/K	3.24	2.74	2.31	2.26	2.26
Rx C/No	dB/Hz	37.33	40.34	42.90	45.90	48.66
Carrier Recovery						
TM Mod Index	Rad	1.175	1.175	1.294	1.294	1.36
Carrier Loss	dB	8.28	8.28	11.27	11.27	13.59
PLL Bandwidth	Hz	20.00	20.00	20.00	20.00	20.00
PLL Bandwidth	dBHz	13.01	13.01	13.01	13.01	13.01
Required S/N in Pull	dB	10.00	10.00	10.00	10.00	10.00
MARGIN	dB	6.04	9.05	8.62	11.62	12.06
TM Recovery						
Modulation Loss	dB	0.70	0.70	0.34	0.34	0.19
Implementation Loss	dB	1.50	1.50	1.50	1.50	1.50
Bit Rate	dBHz	27.48	30.49	33.50	36.51	39.52
Coding Gain	dB	5.5	5.5	5.5	5.5	5.5
Required Eb/No	dB	4.1	4.1	4.1	4.1	4.1
MARGIN	dB	3.55	3.55	3.46	3.45	3.35

Table 9.4: *Probe-Orbiter Radio Relay Link budget*

The block diagram for the Probe telecommunication subsystem is given in Figure 9.12. The subsystem consists of a prime and redundant chain without any hybrid cross-strapping. For sub-

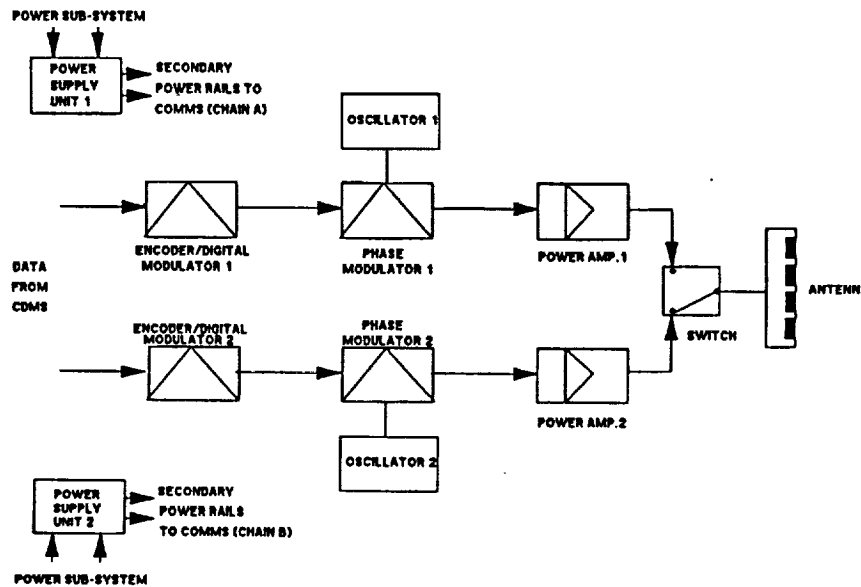


Figure 9.12: Probe telecommunication subsystem

system operation, redundant chain of equipment will be operated in hot-redundancy. Transmission of the signal will be provided by a 5W solid state amplifier. The antenna is a Micro-strip patch antenna with a gain of -1.5 dBi, mounted on the Probe's upper platform. Command and monitoring interfaces to the CDMS will be via CDMS mini Remote Terminal Unit (mRTU).

### PSS Telecommunications Subsystem

The block diagram for the PSS telecommunication subsystem is given in figure 9.13. The subsystem functions are:

- telemetry reception and demodulation
- closed-loop-antenna tracking

The subsystem will consist of two parts:

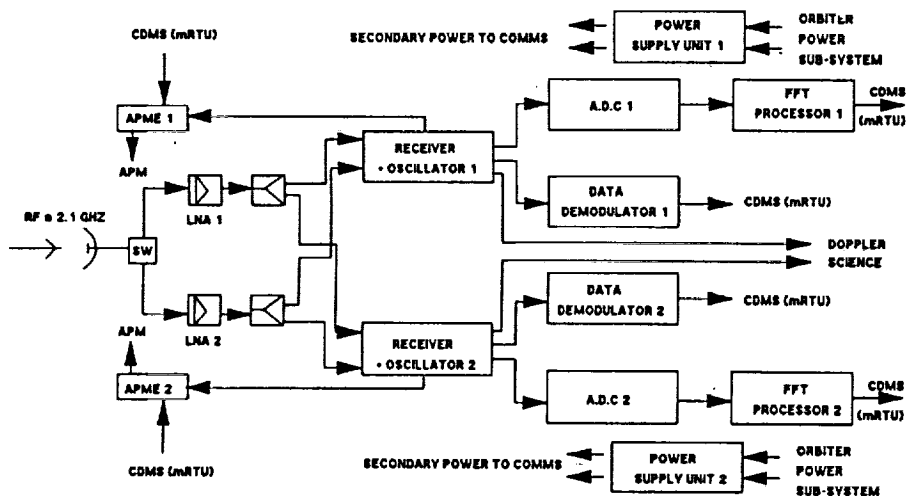
- antenna assembly
- electronics bay assembly

The antenna assembly will consist of a 1.4 metre diameter front-fed reflector, support structures and deployment mechanisms. The PSS antenna has a gain of 26.75 dBi. In addition, the antenna assembly will support the Antenna Pointing Mechanism Electronics (APME) and the redundant Low-Noise Amplifier (LNA) and switching stage mounted behind the antenna backing structure in a thermally conditioned box. The equipment bay assembly contains the remainder of the equipments mounted on subchassis within the bay.

ORIGINAL PAGE IS  
OF POOR QUALITY

### Doppler Wind Experiment Interfaces

An interface to the Probe RF telecommunications subsystem will be provided in order to allow potential implementation of an Ultrastable Oscillator for the Doppler Wind experiment.

Figure 9.13: *PSS telecommunication subsystem*

## 9.12 Command and Data Management Subsystem (CDMS)

The CDMS provides monitoring and control for all Probe and PSS units, interfaces experiments and units with the Orbiter data handling for all Telemetry (TM) and Telecommand (TC) requirements, and implements autonomous control and management of the Probe after separation.

The CDMS is divided in two parts, one located in the PSS and one in the Probe; the ESA standard OBDH bus provides connection among all units and between the two parts. The Probe is controlled by the PSS/CDMS prior to Orbiter/Probe separation and by the Probe's CDMS after separation.

### Functions

The following functions shall be provided by the CDMS:

- Cruise Phase
  - Interface with Orbiter data bus
  - Reception and distribution of commands
  - Periodic check of Probe and PSS, final checkout before release
  - Collection of housekeeping and calibration data
  - Reprogramming of PSS and Probe

- Pre-Entry

The Probe CDMS is activated by the timers, and performs warm up and calibration as required by Probe units in preparation for entry. The PSS CDMS is prepared for the entry phase by telecommand.

- Entry phase

#### Probe CDMS

- Collection and formatting of housekeeping and scientific data
- Buffering of TM data to comply with link budget profile

- Probe health monitoring
- Autonomous control of Probe descent (including redundancy management, experiment activation and control, timing and parachute staging).

### PSS CDMS

- Collection of PSS housekeeping
- Formatting of RRL data and merging with housekeeping data for transmission to Orbiter CDS
- PSS health monitoring, command distribution and redundancy management.

### System Design

A block diagram of the CDMS is shown in Figure 9.14. The control units (PSS and Probe) are

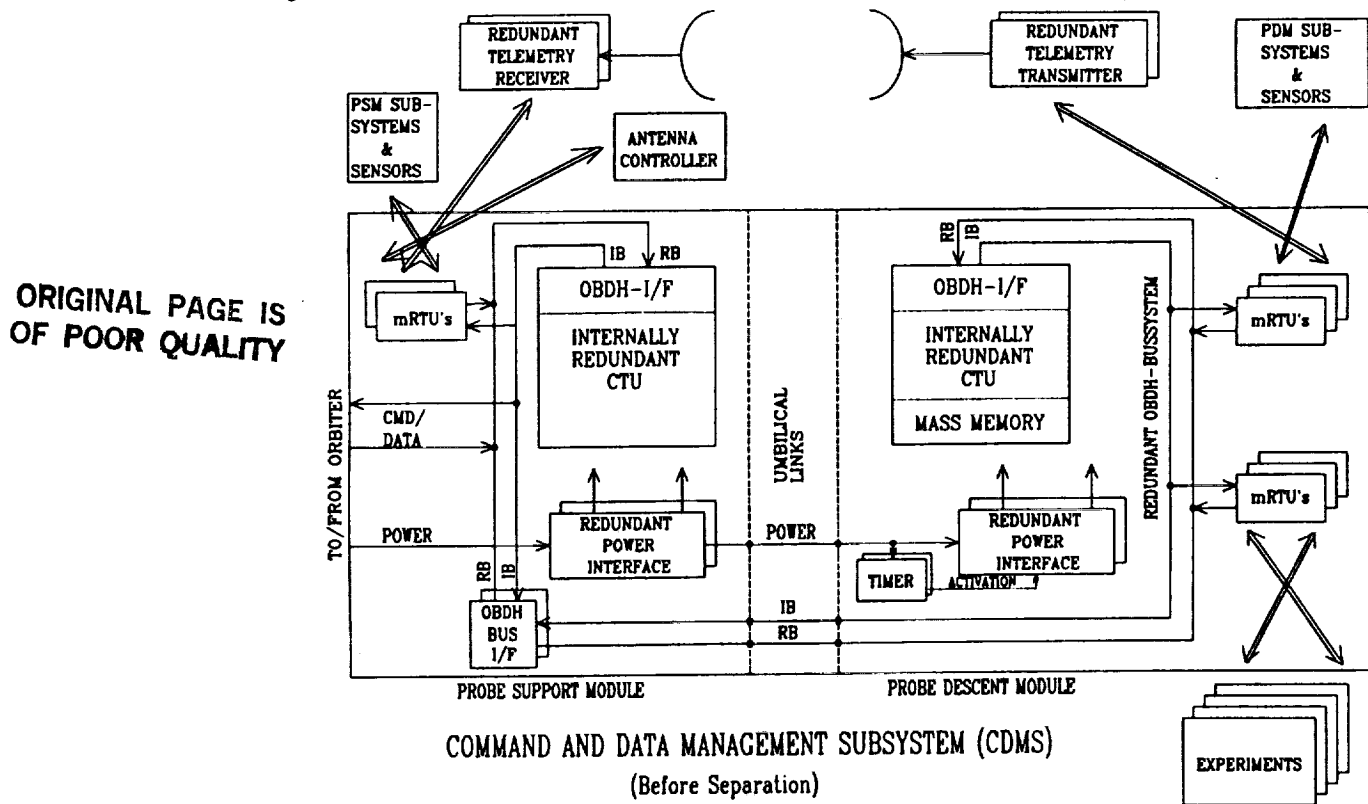


Figure 9.14: *Command and Data management Subsystem (CDMS), before separation*

micro processor based units, while the mini Remote Terminal Unit (mRTU) are hybrids that can be installed in experiments and subsystems. They provide an interface between the ESA OBDH bus and the parallel bus. The OBDH bus is a redundant full duplex serial bus, consisting of an interruption bus (IB) on which the CTU transmits and the other receive and a response bus (RB), where the CTU receives and the RTU transmits in C'TU-controlled time slots. A 6 Mbit mass memory is required for storage of application software and buffering scientific and housekeeping data when the data generated exceeds the RRL capability easily in the Descent phase RRL transmission. Preferred choice for the processor is a 16-bit CMOS processor.

### 9.13 Power Subsystem

The Orbiter Power and Pyrotechic subsystem provides the power and energy requirements of the Probe and PSS during all mission phases prior to operation of the Probe from the Orbiter. Power and energy requirements during these phases are necessary to allow periodic check-outs and calibrations (approximately every 6 months) of the Probe systems and experiments during the Cruise mission phase and prior to separation of the Probe from the Orbiter. After separation, the Orbiter continues to supply the PSS power and energy requirements for the Coast and Descent phases of the mission.

The energy requirements of the Probe for the Coast and Descent mission phases are provided by Lithium Sulphur Dioxide (Li-SO<sub>2</sub>) primary batteries which are located on the lower platform of the Probe. The batteries were sized to ensure that the worst case load energy requirements of the probe mission were satisfied with a 10margin. Due to mass constraints, no battery redundancy is incorporated however the design of the power system includes protections to ensure that single failures at cell or component level do not constrain or reduce the mission.

Figure 9.15 shows the baseline schematic design for the power system. Three batteries, each of 26 cells, are connected in parallel to three Battery Discharge Regulators (BDRs) which are housed in the Power Control Unit (PCU). Each BDR is sized to supply half of the mission power requirements thus failure of a BDR is not mission critical. The output of the BDRs is a regulated bus supply voltage mission of 28 volts D.C. This voltage is distributed to all experiments and systems by current limited switches in the Power Distribution Unit (PDU). Each load is supplied by a redundant switch thus failure at switch level is not critical. Failure at load level will be isolated from the power system by the fast current limiting characteristics of the switches. These switches protect the power system in the event of any load failure and ensure that failures do not propagate to other loads or result in interruption of mission operations. The CDMS system is supplied by two redundant DC/DC Converters to reduce the energy drained from the batteries during the 12 days coast phase of the mission.

Galvanic isolation of the Orbiter power bus from the Probe system is achieved by DC/DC Converters. Pyrotechnic power is supplied from battery tap voltages via arming and firing switches thus providing two levels of inhibit for safety purposes. Depassivation of the Li-SO<sub>2</sub> batteries prior to use is achieved by depassivation circuits in the PCU.

### 9.14 Probe Sensors Subsystem

The following parameters will be measured during the descent

- Altitude
- Pressure
- Acceleration (also measured during entry)
- Temperature

#### Radar Altimeter

The function of the radar altimeter is primarily to measure altitude starting from 170 km to surface impact. By processing the received signal, the rate of descent can be derived. Altitude will be determined using pulsed FM radar techniques to an accuracy of 1 km at start of measurement to better than 100 m at the limit of pulse operations (a height of 5 km). Below 5 km, the altimeter will use CW-FM radar techniques giving accuracies of  $5 \times 10^{-3}$  down to the surface. The altitude data will be used by the Probe system to initiate deployment of the 2nd parachute in conjunction

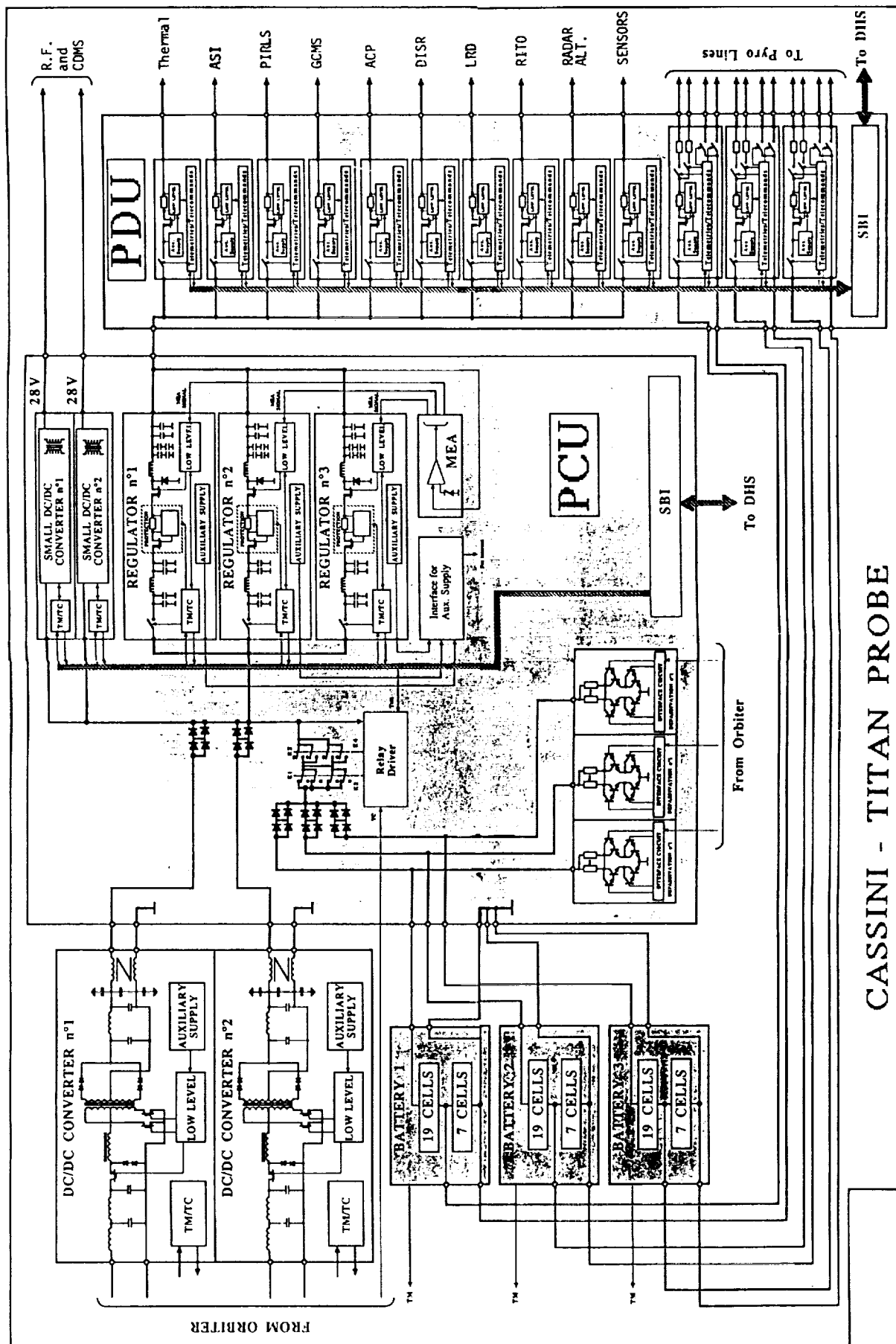


Figure 9.15: *Probe Power subsystem*

ORIGINAL PAGE IS  
OF POOR QUALITY

with the rate of descent data. It will also be used to optimise the instruments mode switching during the last kilometers of the descent and close to the surface.

### System Description

The functional block diagram depicted in Figure 9.16 shows the six constituent units.

- a) The Waveform Generation and Timing (WGT)
- b) The Frequency Generation Equipment (FGE)
- c) The Power Amplifiers
- d) The Antenna Unit
- e) The Radio Frequency Equipment (RFE)
- f) The Analogue-to Digital Processor (ADP).

The Power Amplifiers accept signals at 115 MHz and up convert them to 5.3 GHz. The solid state amplifier then produces 0.5W pulse power or 15 mW CW power. The Antenna Unit consists of 19 patch radiators placed on a plane circle with a diameter 250 mm in a hexagonal pattern. Spacing between radiators will be 0.88. The beamwidth will be  $12^\circ$

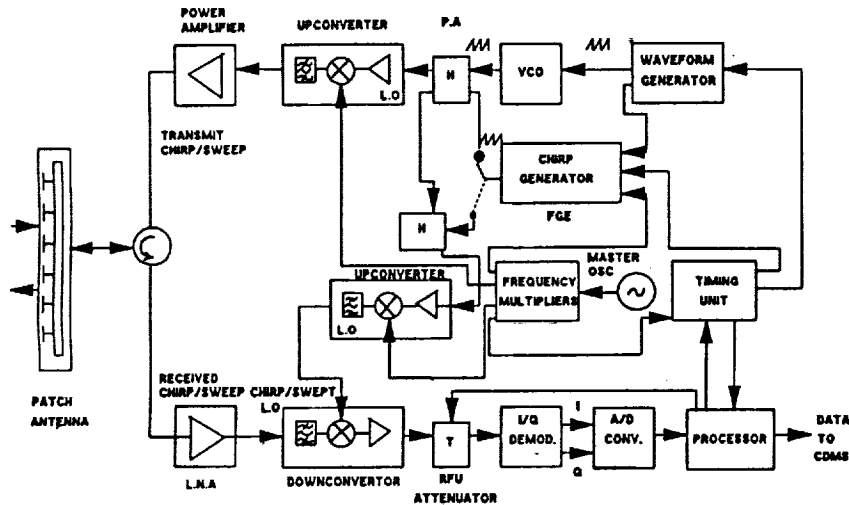


Figure 9.16: *Radar altimeter*

### Performance

Above 5 km:

- Use pulsed FM radar technique
- Resolution 150 m
- Accuracy: at 170 km:  $\pm 500$  m  
at 5 km :  $\pm 150$  m

Below 5 km:

- Use CW-FM radar technique
- Resolution 50 m
- Accuracy :  $\pm 1\%$

The rate of descent is determined by the split gate circuitry in the pulse radar mode. The accuracy of this measurement is better than  $10^{-2}$ .

The surface transmissibility is 98% for an ethane-methane ocean and 92% for water-ice. In order to optimise the performance of the size-restricted antenna, a carrier frequency of 5.3 GHz is proposed. This leads to attenuation of 0.03 dB/m for ethane-methane ocean and 0.04 dB/m for water-ice. This allows depths of up to 400 meters to be probed and may provide significant surface science return.

## Pressure

A pressure sensor will be mounted within the Probe. It will consist of an evacuated capsule with built-in strain gauge. The conditioning amplifier will contain its own voltage regulator, temperature compensation and bridge measuring circuit.

## Acceleration and Spin

Three acceleration measurements are required: a) That due to deceleration entry into the atmosphere b) That due to Probe spin variation c) that due to impact.

### Entry Deceleration

This acceleration is principally along the Probe axis. The predicted maximum deceleration is 25g. Two redundant piezoelectric accelerometers will measure over a range of 0.5g to 30g. They will be switched on before the start of the entry phase. The peak deceleration will be detected using an active filter which will remove high frequency (vibration) effects.

### Spin Variation

The accelerometers will be mounted at the edge of the lower platform, thus allowing them to measure the acceleration/deceleration caused as the Probe spin velocity changes.

### Impact

The accelerometer will be mounted such that the measurement of the deceleration peak caused by the impact will provide a marker for post-impact activities.

### Temperature

Temperature measurement will use platinum resistance sensors. Measurement bridges, amplifiers, power conditioning and multiplexers will be housed in a common unit with capacity of up to 10 temperature channels.

These channels will include:

- Three batteries
- Equipment Panel
- Antenna Panel
- 5 spares - to be allocated as required.

# Chapter 10

## Mission Operations

The Mariner Mark II (MM-II) Mission Operations System (MOS) is developed by the Jet propulsion Laboratory (JPL) and will conduct mission operations for the Cassini spacecraft and mission. The MM-II Mission Operations system jointly supports Cassini and the Comet Rendezvous Asteroid Flyby (CRAF) mission which is launched 8 months prior to Cassini. Both the Cassini Spacecraft and the CRAF Spacecraft share a high degree of commonality which allows a joint CRAF/Cassini mission operations approach. The joint CRAF/Cassini MOS will be called the MM-II MOS.

### 10.1 Mission Operations Concept

The MM-II MOS integrates Project unique elements provided by the MM-II Flight Project Organization (see MM-II MOS Organization in figure 10.1) with elements from the JPL Spaceflight Operations Center (SFOC), the JPL Network Operations Control Center (NOCC), the JPL Ground Communications Facility (GCF) and the Deep Space Network (DSN). The SFOC is a multimission facility which is managed by the JPL Flight Projects Support Office (FPSO) and the NOCC, GCF, and DSN are multimission facilities which are managed by the JPL Office of Tracking and Data Acquisition (TDA).

The MM-II MOS is located at JPL in a dedicated Mission Support Area (MSA). The MOS consists of the personnel, equipment, and procedures necessary to conduct flight operations of the Cassini spacecraft including the instrument payload and Titan Probe. The MOS is developed prior to launch in order to support the development and validation of basic flight sequences and to support the spacecraft-to-MOS compatibility tests. The MOS will support the spacecraft system test and launch operations phases and will assume spacecraft control at spacecraft launch.

The MM-II MOS performs the primary functions of spacecraft command and control, spacecraft data acquisition, science and engineering information processing, and data archiving and data management. These functions are performed with the aid of a network of interconnected data processors that are connected as nodes on a local area network.

All mission data stored in the project data base will be accessible to all flight teams, including the investigation teams geographically located throughout the world. Each of the investigation teams will be responsible for command request generation, health evaluation and science analysis associated with its experiment. The investigation teams will participate in the identification and resolution of science sequence request conflicts. Planning tools and data will be provided by the project to assist them in this process.

The project will provide a workstation and a communication link for each of the Orbiter science investigation teams including the Probe Science Team. The workstations will be used to receive

MOS generated and investigator generated data and planning products, inform the project of instrument health and status, plan investigation activities and prepare corresponding products for input to the sequence generation process, and return selected investigation results to the project data base. Flight team members in the MSA will use similar type workstations to analyse and control the Cassini spacecraft. Each workstation will consist of commercially available equipment configured to support the MM-II project.

A Cassini Probe Engineering Team may have team members resident at JPL in the MM-II MSA receiving the same support as the other MM-II Flight Teams. In addition, Probe real time data will be routed directly from the receiving Deep Space Station to the Probe Operations Control Center which is assumed to be located in Europe. The Probe real time data is also routed to the MM-II MSA for storage in the Project data base and for analysis by the Probe Engineering Team.

## 10.2 The Mission Operations Process (Orbiter)

The MOS process is an end-to-end process whereby the scientist investigates his remote domain of interest by specifying science observations which are translated into spacecraft events (uplink process). The data collected from these observations are transported from the spacecraft to the scientist at his designated remote site for detailed analysis (downlink process). Scenarios for the uplink and downlink processes are described below.

### Uplink and Downlink Processes

The uplink process is supported by elements from the NOCC, SFOC, and MM-II project which pertain to mission planning and spacecraft command generation. The Downlink process is a co-ordinated effort by the NOCC, SFOC, and Flight Project elements which support the monitoring and analysis of mission data.

The MM-II Flight Teams are illustrated in the MOS organization, Figure 10.1. Figure 10.2, Top Level Data Flow Diagram, illustrates the uplink and the downlink processes. and

## 10.3 Probe Operations

### Probe Operations Concept

Probe operations responsibility resides with ESA/ESOC, as part of the Cassini mission operations. Probe control and science operations will be conducted from ESOC-OCC. During critical mission phases a limited number of ESA staff will support mission operations from JPL. A joint ESA-NASA mission planning group will address joint Orbiter-Probe mission aspects; The control centers for the Probe (ESOC) and the Orbiter (JPL) will be connected through voice and data links. The ground-station network will be the NASA Deep Space Network. All Probe mission data will be routed to ESOC via the Madrid gateway. All Orbiter data will be routed to JPL. As the Orbiter carries the Probe, all commands and data related to the Probe will pass via the Orbiter.

### Operations Tasks

The main operations tasks are:

- mission planning in all phases
- from launch to Probe separation: periodic checks of the Probe (payload and subsystems)
- prior to separation: configuration of the Probe for separation and subsequent mission phases

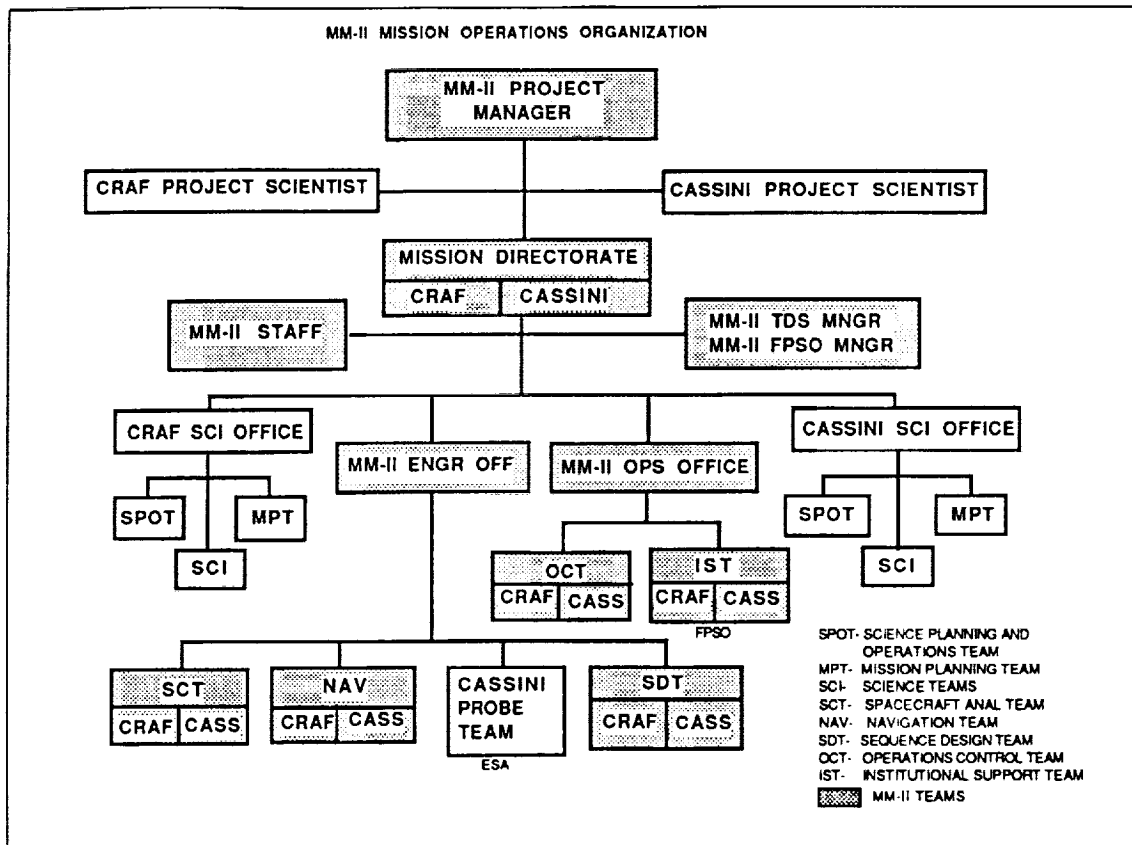


Figure 10.1: *MM-II mission operations organisation*

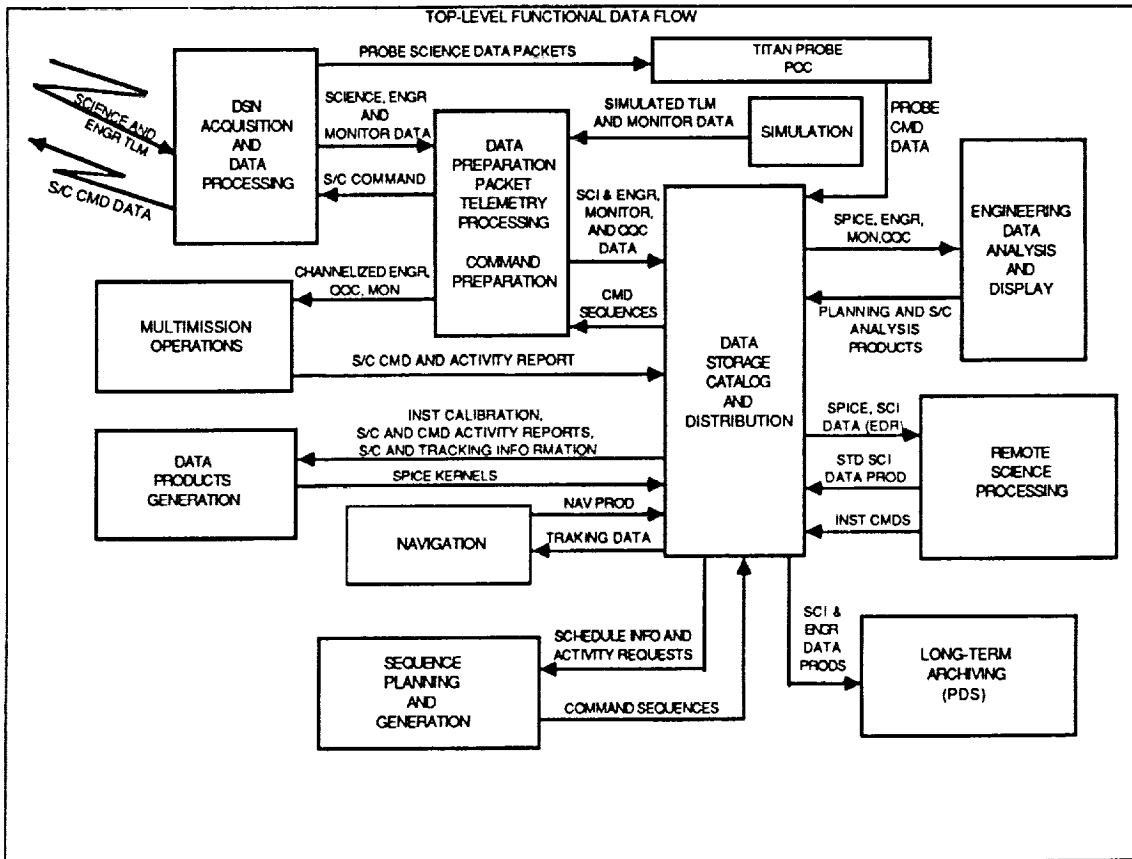


Figure 10.2: *Top level functional data flow*

- during atmospheric entry and descent: articulation of PSS relay antenna, Probe data reception
- post-mission data handling: merging of auxiliary data and distribution to PIs.

## Communication

The communication flow is as follows:

Data and telecommand: ESOC - NASA/JPL (via Madrid gateway)

Orbiter - Probe

Voice: ESOC - JPL (via Madrid gateway)

All Probe commands are generated at ESOC and transmitted to the Probe via JPL, DSN and the Orbiter interface.

## Tasks of the joint ESA-NASA Mission Planning Group

This joint Mission Planning Group will address all those mission phases which have a direct impact on both, Orbiter and Probe. Examples of such phases or events are

- selection of initial Saturn-centered orbit
- pericrone raise manoeuvre
- Probe separation
- Orbiter deflection
- navigation (prior to SOI until completion of Probe mission)

An outline of the Cassini Mission Operations Organisation is given in Figure 10.2.

# Chapter 11

# Management

The objective of the following paragraphs is to define the process and procedures through which the cooperation between ESA and NASA will be conducted within the framework of the Cassini mission, should this project eventually be approved by both ESA and NASA.

## 11.1 Management Provisions

- Within the context of the Cassini mission, the NASA Project Manager shall be responsible for overall Mariner Mark II Project, associated NASA resources and provision for major requirements, such as the launch vehicle, the Saturn Orbiter system, tracking and data acquisition, spacecraft integration, and flight operations.
- The ESA Project Manager shall be responsible for the overall technical and programmatic implementation of the Titan Probe system and shall be the formal contact for all matters concerning the Titan Probe implementation.
- Should ESA or NASA require review of these subjects, the interface shall be between the ESA Project Manager and the NASA Project Manager.
- The agreement between ESA and NASA to implement the cooperative project will be documented in the form of Memorandum of Understanding (MOU) between the two agencies.

The MOU will refer to a project Organization and Management (OM) plan to be agreed upon between the ESA and NASA project managers for the design, development and mission operations and data analysis phases of the project, which will specify:

- Project Organization - Structure and Interfaces
- Authority and Responsibilities
- Formal Interfaces - Technical and Management
- Schedule
- Reports, Meetings and Reviews
- Procedures, Applicable documents and Deliverables, Product Assurance and Configuration Control
- Provisions and Procurements by each participating agency (hardware, software, parts).

The Organization and Management (OM) Plan will provide the executive basis for joint management of the Project.

## 11.2 Proposed Cassini Science Plan

The proposed Cassini Science Plan envisages:

- Separate, coordinated AOs
- Separate, evaluation processes, with U.S. and European members on all panels. 2/3rd ESA and 1/3rd NASA for the Probe; 2/3rd NASA and 1/3rd ESA for the Orbiter
- Separate, coordinated selection, with exchange of observers
- No pre-arranged split of science payloads; selection based on science merit
- Joint U.S./European instrument encouraged
- The percentage of the ESA and NASA shares of the Orbiter and Probe payloads should be compatible with the ratio of the ESA investment to NASA investment.

Within the context of the AO activity, instrument proposals, proposers and participants of the following types are foreseen:

- Principal Investigator/Instrument (Orbiter and Probe)
- Facility Instrument (Team Leader or Team Member) (Orbiter)
- Interdisciplinary Scientist (IDS) (Orbiter and Probe)
- Participating Scientists (Orbiter) - to be solicited by later announcement

It is envisaged that minimum Cassini Orbiter facility instruments and Probe engineering data will be:

- Orbiter Instruments:
  - Imaging Science Subsystem
  - Titan Imaging Radar
  - Radio Science
- Probe engineering data from the Probe radio system, radar altimeter and other Probe's engineering sensors, will be made available for scientific evaluation.

### 11.3 Data Management

- First publication rights to data obtained from a Principal Investigator's or Facility Team Leader's instrument reside with the Principal Investigator or Facility Team Leader for six months from receipt of primary data and necessary spacecraft information.
- Investigators and Facility Team Leaders will be requested to share data with other Investigators or Facility Team Leaders, including Interdisciplinary Scientists and Participating Scientists to enhance the Scientific return from the mission under procedures to be decided by the Cassini Project Science Group (PSG).
- Following the period of first publication rights, records or copies of processed data will be deposited in the U.S. National Space Science Data Centre (NSSDC), in the Data Library of ESA, and will be listed with the World Data Centre for Rockets and Satellites. Such records will then be made available by the World Data Centre.
- Scientific results of the Cassini mission will be made available by the Principal Investigator or Facility Team Leader to the public through publication in appropriate scientific and technical journals and other established channels, and through publication of final engineering and scientific reports by ESA and NASA. Such publication shall include a suitable acknowledgement of the services afforded by the Agencies. The Principal Investigator or Facility Team Leader will provide ESA and NASA with appropriate copies of the publication. All publications will be located in the NSSDC and the Data Library of ESA.

# Chapter 12

## Development Plan

The proposed Development plan for the Cassini Titan Probe System and associated flight hardware within procured by the Agency will be based on the requirements specified the ESA Cassini System Requirements documents and Statement of Work.

Key requirements are summarised as follows:

- minimum number and maximum utilisation of these models with compatible phasing and resources allocation to ensure cost and schedule effectiveness
- verification by inspection and analytical methods
- maximum decoupling of new technology and software development
- comprehensive and timely feedback of design information from the development verification programme to the protoflight Qualification/Acceptance Programme
- availability of a functionally representative electrical model (EM), for timely resolution of potentially critical design aspects and system verification
- the verification programme shall be designed such that the required design margins, mission profile (long-life aspects) and inheritance from other missions (Voyager, Galileo and CRAF) may provide design information which supports qualification and minimises technical risks during flight model acceptance
- the verification programme shall be phased such that compatibility to external interfaces (launcher interfaces/Probe-Orbiter interfaces) can be verified early in the vehicle development programme
- ground support equipment hardware and software should support coherent testing and correlation at all levels (unit, subsystem, system) for a minimum of hardware/software development
- derived requirements for design feedback imply:
  - completion of subsystem development tests, before subsystem release for system integration
  - completion of the unit qualification programme before the start of unit acceptance and Protoflight Model Qualification Acceptance programme.
  - critical Design Review (CDR) prior to Flight Hardware fabrication.

### 12.1 Titan Probe model philosophy

A potential Development, Qualification and Acceptance flow chart based on this Protoflight model philosophy is given in Figure 12.1. Breadboard models of subsystems and experiments are expected to be available.

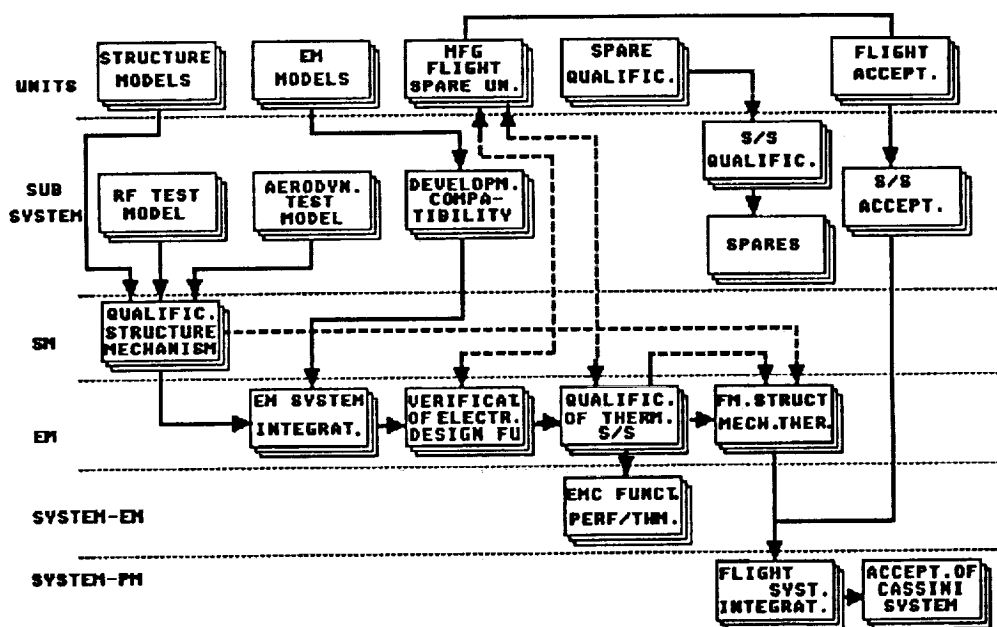


Figure 12.1: Probe development qualification/acceptance strategy

There are essentially 3 system models requiring:

- 2 structures + spares (SM/EM and FM)
- 2 thermal subsystems (SM/EM and FM) + spares
- 2 antenna subsystems (SM/EM and FM) + spares
- 5 sets primary sources (SM/EM and FM) + spares
- 2 mechanisms (SM/EM and FM) + spares
- 2 harness subsystems + SM Harness
- EM and FM subsystems with adequate flight spares
- EM and FM experiments

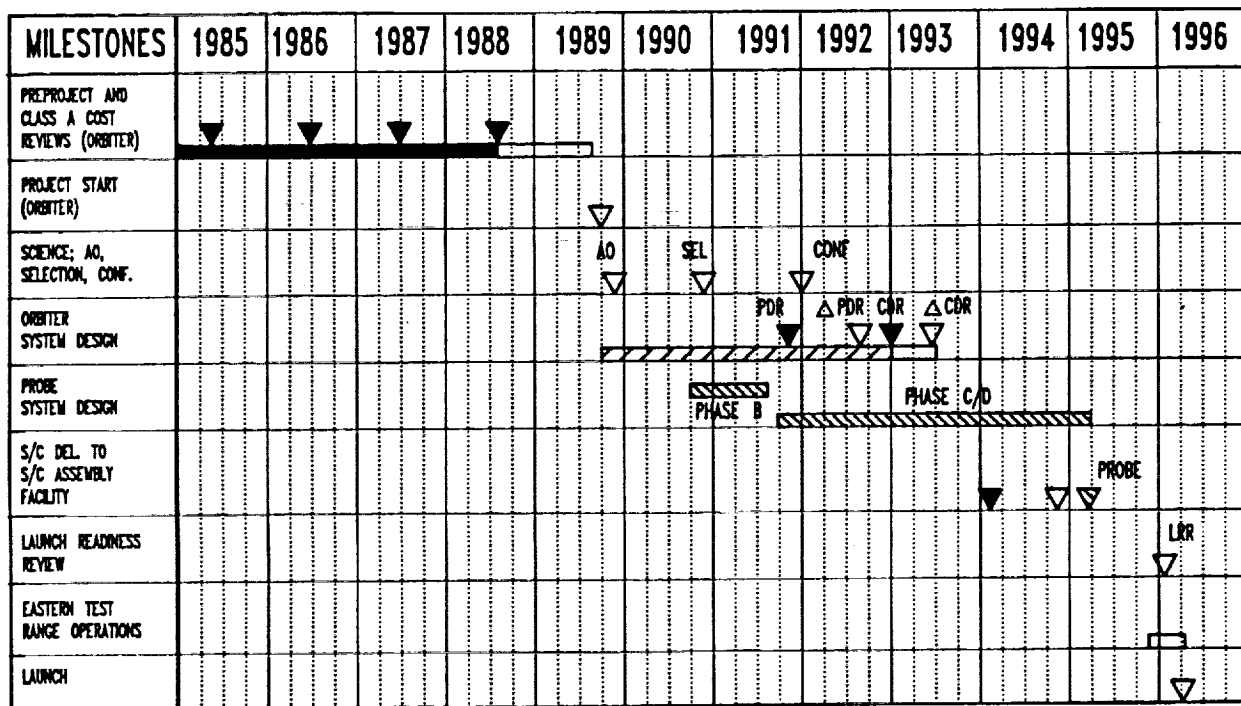
(SM = Structure Model, EM = Engineering Model, FM = Flight Model). There will be 2 subsidiary subsystem models :

- RF model
- Aerodynamic test model

The Development programme will be defined in a set of Plans listed non-exclusively below

- System Design and Development Plan
- Assembly, Integration and Verification Plan
- Software Development Plan
- Ground Support Equipment Development and Deployment Plan
- Quality Assurance Plan
- Safety Plan

A summarised Development Schedule is given in Figure 12.2.



▼ MARINER MARK II      ▽ CASSINI

Figure 12.2: *Cassini summary development schedule*

## Appendix A

# Titan's Organics: Molecules likely to be present in the Atmosphere (gas and aerosols) and the Ocean

### Gas phase

Experiments simulating the chemical evolution of  $N_2$ - $CH_4$  mixtures submitted to different energy sources show that such a medium is one of the most favourable for atmospheric organic syntheses, especially when hydrogen does not accumulate (Bossard et al., 1983). Three of the major N-containing organic compounds formed in these experiments: HCN,  $(CN)_2$  and CHCCN, have already been detected in Titan. This suggests that the results of these laboratory experiments can be extrapolated - at least qualitatively - to the case of Titan. This allows us to draw up a list of organics likely to be present in the atmosphere of Titan, as shown in table A.1. The gas phase infrared spectra of several of these still undetected compounds has been recently studied (Cerceau et al, 1985; Raulin et al. 1988). Upper limits of their mean abundance in Titan's atmosphere can be deduced from these spectroscopic data (table A.2). With the exception of benzene (about 5 ppbv), the obtained values are in the range of the mean abundance of the already detected nitriles. Thus, there is no contradiction between their non detection and the predictions from simulation experiments. Most of these compounds, because of the cold temperatures, must condense in the low stratosphere. In this region, and around the tropopause, the concentration of condensable trace constituents in gas phase must be very low. This is probably the best region to collect the aerosols.

### Aerosols

The condensation of low molecular weight organics would be induced by the sub-micron particles formed in the higher zones of the atmosphere by photopolymerization processes of  $C_2H_2$ ,  $C_2H_4$  and HCN, followed by in situ condensation. These sub-micron particles, after sedimentation down to the lower atmospheric layers, would act as nucleation centers, allowing the condensation of lower molecular mass compounds. The resulting aerosols cloud would be constituted of particles covered by an external layer of more volatile organics and having a mean radius increasing with decreasing altitude.

Modelling of those processes using microphysical approach (Frère et al., 1988) indicates that near the surface of Titan, the aerosol particles would consist of a core of several tens of microns mean diameter, mainly composed of nitriles with a small fraction of oligomers and covered by a thick envelope of  $C_1$ - $C_2$  hydrocarbons. In these droplets, most of the organics would be highly enriched relative to the atmosphere. For instance, the concentration  $C_2$  and  $C_3$  hydrocarbons and that of HCN and  $HC_3N$  would be 3 to 5 orders of magnitude higher in the aerosol than in the gas phase.

Consequently, the aerosol to be collected would be composed of two different classes of compounds:

- Low molecular weight organics:

- constituting the main part of the particles;
- mainly hydrocarbons and nitriles, with C+N smaller than about 10;
- with concentrations highly increased relatively to the gas phase;
- vaporizable at the temperature of the Probe.
- High molecular weight organics:
  - including oligomers and polymers or heteropolymers of HCN, ethylene and acetylene;
  - non volatile;
  - pyrolyzable at 600-700°C.

## Ocean

In agreement with all the currently available data, the best model of Titan's surface (Lunine et al., 1983; Lunine and Stevenson, 1985) assumes the existence of an ocean of liquid methane and ethane, acting as the dispensing reservoir of atmospheric hydrocarbons. This ocean would also contain a large quantity of dissolved nitrogen and argon. Assuming that equilibrium is reached at the interface between the ocean and the atmosphere, from thermodynamical modelling of these processes, one can derive the main composition of the ocean, as a function of the mole fraction of only one main constituent of the atmosphere or of the ocean (Thompson, 1985; Lellouch et al., 1988). It must be emphasized that a good knowledge of the chemical composition of the near surface atmosphere would indirectly give precious information on the physical state of the surface.

After sedimentation to the surface, the atmospheric aerosols will either float or sink, depending on their density relative to the liquid hydrocarbon ocean, while they will dissolve totally or partially according to their solubility in such a solvent, and their atmospheric flux. Calculation of the volumic mass of the various possible solutes which are solid at the surface temperature (92.5-101 °K), assuming they are not fluffy material, show that only solid ethylene could be lighter than the ocean, and only if the ocean is ethane-rich. However, calculation of the solubility of these solutes (Raulin, 1987) indicates that ethylene is very soluble and should be entirely dissolved. Thus, the surface of this ocean should be free of any organic iceberg. In such a solvent, the solubility of low molecular weight alkanes and alkenes ranges from  $10^{-3}$  to a few  $10^{-1}$  molefraction. More polar compounds, alkynes, benzene and nitriles are less soluble: from  $10^{-7}$  to about  $10^{-3}$  mole fraction (Fig. A.1). In addition, the ocean should also include a fraction of dissolved polymers and several other N-compounds, such as  $\text{NH}_3$ ,  $\text{HN}_3$ ,  $\text{CH}_3\text{N}_3$  and  $\text{C}_2\text{H}_5\text{N}_3$ , formed through the irradiation of the main constituents of the ocean by the high energy cosmic rays. After more than 4 billion years of evolution, this ocean should be a very complex medium, rich in diversified organic compounds.

## References

- Bossard, A., Morey, D., and Raulin, F. (1983). "The escape of molecular hydrogen and the synthesis of organic nitriles in planetary atmospheres". *Adv. Space Res.*, 3 (9), 39-43, and refs. herein.
- Cerreau, F., Raulin, F., Courtin, R., and Gautier, D. (1985). "Infrared spectra of gaseous mononitriles: application to the atmosphere of Titan". *Icarus* 62, 207-220.
- Frère, C., Raulin, F., Israel, G. and Cabane, M. (1988). "Microphysical modelling of Titan's aerosols: application to the in situ analysis". XXVII Cospar Meeting, Identification S-4-3. Submitted to *Adv. Space Res.*
- Lellouch, E., Coustenis, A., Gautier, D., Raulin, F., Dubouloz, N. and Frère, C., (1988). "The composition and thermal structure of Titan's atmosphere : a reanalysis of the Voyager 1 radio-occultation and IRIS 7.7 um data". Submitted to *Icarus*.
- Lunine, J.I., Stevenson, D.J., and Yung, Y.L. (1983). "Ethane ocean on Titan". *Science*, 222, 1229-1230.
- Lunine, J.I. and Stevenson, D.J. (1985). "Evolution of Titan's coupled ocean-atmosphere system and interaction of ocean with bedrock". In *Ices in the Solar System*, J. Klinger et al. Eds., Reidel Pub. Co., Dordrecht, pp. 741-757.

d *appendix 1*

- Raulin, F., (1987). "Organic chemistry in the oceans of Titan", *Adv. Space Res.* 7 (5), 71-81.
- Raulin, F., Accaoui, B., Razaghi, A., Dang-Nhu, M., Coustenis, A. and Gautier, D., (1988). "Infrared spectra of gaseous organics: application to the atmosphere of Titan. II. C<sub>4</sub> alkyne and alkanenitriles and benzene. To be submitted to Icarus.
- Thompson, W.R. (1985). "Phase equilibria in N<sub>2</sub>-hydrocarbon systems: application to Titan". In the *Atmospheres of Saturn and Titan*. ESA SP-241, 109-119.

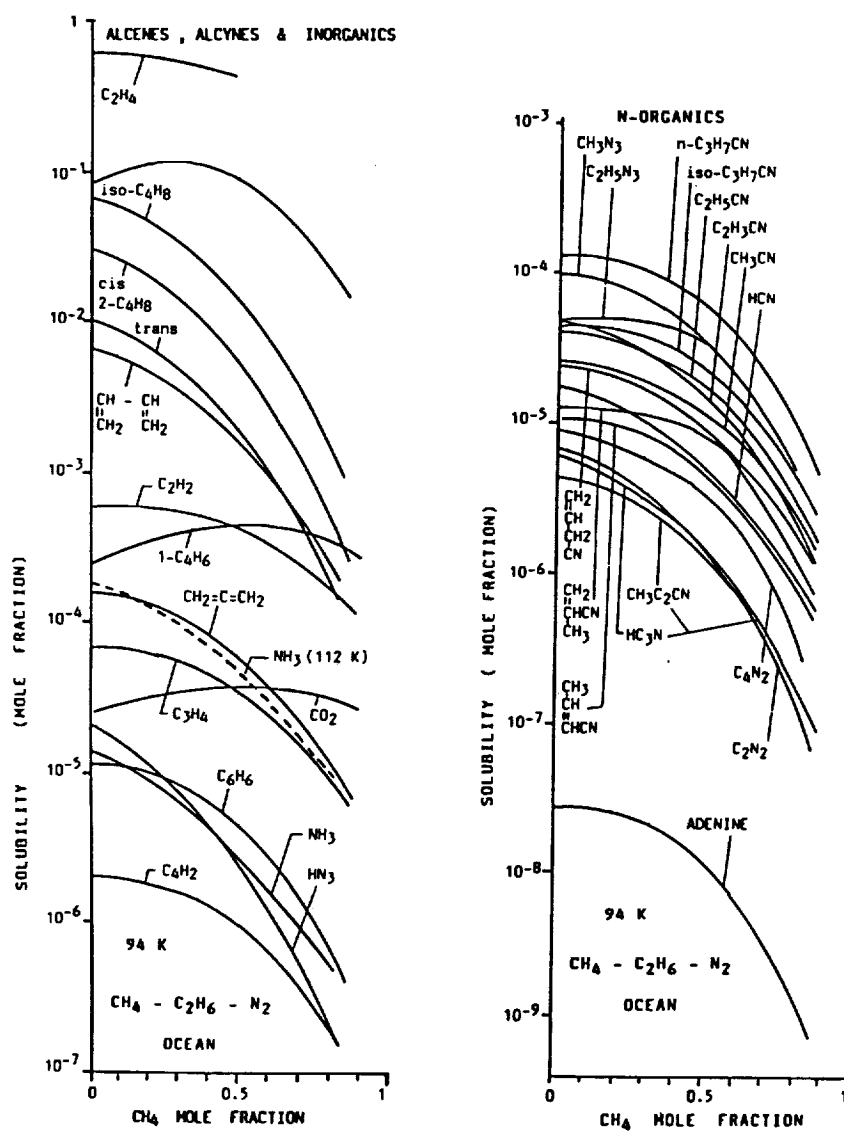


Figure A.1: *Solubility of unsaturated hydrocarbons, inorganics and N-organics in Titan's model atmosphere ocean (94 °K, as a function of its CH<sub>4</sub> model fraction. Solubility of NH<sub>3</sub> at 112 °K is also indicated, for comparison.*

Gaseous and condensed phases				Condensed phases
* Other simple hydrocarbons :				* HCN oligomers :
- additional C <sub>3</sub> and C <sub>4</sub>				- tetramer
- C <sub>5</sub> - C <sub>8-10</sub> aliphatic				
- saturated cyclic				(diaminomaleonitrile)
- unsaturated cyclic :				- adenine
benzene and derivatives				
* Additional simple nitriles :				(formally : HCN pentamer)
- CH <sub>3</sub> - CN				- polymethyneimines (- CH = N -) <sub>n</sub>
- CH <sub>2</sub> = CH - CN				or (- N = CH - C -) <sub>n</sub>    NH
- C <sub>2</sub> H <sub>5</sub> - CN				* Other heterocyclic compounds, cyanopolyynes, cyanamide
- other C <sub>3</sub> nitriles				* Other polymers : polyacetylenes polyethylenes, and heteropolymers
- C <sub>4</sub> nitriles				
* Additional simple dinitriles				
* O-organics at a very low mole fraction				

Table A.1: *Organic molecules likely to be present in Titan's atmosphere (in addition to the already detected compounds)*

Compound	$\nu$	Q or P/R branch cm <sup>-1</sup>	Intensity cm <sup>-2</sup> atm <sup>-1</sup> (base e)	Upper Limit ppmv
Acetonitrile CH <sub>3</sub> CN	$\nu_{2v_6}$ $\nu_{13}$ $\nu_{19}$	363 717 202.5/211.5 784	4.5 8.5 15 9	0.25 0.5
Propionitrile C <sub>2</sub> H <sub>5</sub> CN	$\nu_{15}$ $\nu_{12}$ $\nu_{10}$ $\nu_9$	221.5/261.5 683 955 973	10 33 100 100	0.2
Acrylonitrile CH <sub>2</sub> -CH-CN	$\nu_{16}$ $\nu_{23}$ $\nu_{21}$	148 / 165 278 728	30 10 230	0.04
crotononitrile CH <sub>3</sub> -CH-CH <sub>2</sub> -CN	$\nu_{18}$ $\nu_{22}$ $\nu_{21}$ $\nu_{20}$	160 557 930 942	17 64 110 110	0.04
Allyl cyanide CH <sub>2</sub> -CH-CH <sub>2</sub> -CN	$\nu_{16}$ $\nu_{22}$ $\nu_{21}$ $\nu_{20}$	184 / 199 535 928	11 33 130	0.075
Methacrylonitrile CH <sub>2</sub> -C(CH <sub>3</sub> ) <sub>2</sub> CN	$\nu_{12}$ $\nu_{11}$ $\nu_{10}$ $\nu_9$	140 / 149.6 338 499.7 637 / 648	5 24 15 8	0.05
Cyanopropyne CH <sub>3</sub> -C≡C-CN	$\nu_{27c}$ $\nu_{21s}$ $\nu_{15}$	728 / 742 765 842	3.5 ± 0.5 4 ± 0.2 3.5 ± 0.1	2
Isobutyronitrile 1-C <sub>3</sub> H <sub>7</sub> -CN	$\nu_{13}$ $\nu_{12}$ $\nu_{24}$	538 738 928 / 939	3.3 ± 0.2 3.5 ± 0.3 5.9 ± 0.6	0.5
Cyclopropane- carbonitrile △-CN	$\nu_{13}^{14+14}$ $\nu_{22}$ $\nu_{11}$ $\nu_{10}$	726 818 940 1046	19 ± 3.4 34 ± 6.6 58 ± 11 80 ± 11	0.4
Benzene C <sub>6</sub> H <sub>6</sub>	$\nu_4$ $\nu_{14}$	673.5 1037.5/1039.5	352 ± 23 33.2 ± 1.5	5 × 10 <sup>-3</sup>

Table A.2: *Characteristics of the most intense IR bands of some organics in the 200-1200 cm<sup>-1</sup> region and deduced upper limit of their mole fraction in Titan's atmosphere.*

## Appendix B

# Engineering model of the atmosphere of Titan

### Introduction

For the Phase A study of the Probe, which included studies on the entry behaviour and the descent profile of the Probe, a reference atmospheric model was necessary. The physical quantities that were needed were the mass density and the temperature as functions of altitude. The model gave nominal (most probable) and conservative extreme values of these quantities. Efforts by different research groups in Europe and USA made it possible to converge onto an engineering model. Its purpose was to allow ESA and the Probe Phase A contractor to perform Probe mission analysis and to design an entry and a descent system with sufficient margin.

This report gives a short critical description of most of the previous models and of the final recommended model. (Lellouch and Hunten, 1987).

### Previous models

#### **The Hunten 1981 model (H81)**

This model is an analytic fit of preliminary Voyager radio occultation data for altitudes between 0 and 200 km. Above 200 km, the only available data give the temperature and number density at 1270 km (Smith et al., 1982 ;S82 ) The model consists of an isothermal interpolation obtained by fitting the hydrostatic equation to the data points at 200 and 1270 km. This model was used with a that isothermal behaviour above 200 km is physically unlikely and pointed out the need for more elaborate modelling.

#### **The Lindal model (Lindal et al,1983 ; Li83)**

This model gives the final results of the Voyager radio occultation experiment between 0 and 200 km. The analysis assumes a pure nitrogen atmosphere. Two data sets (ingress and egress) are given, indicating the experimental uncertainty level. Based on high-quality data, this model can safely be used as a nominal profile under 150 km, but it does not include any quantitative analysis of the other sources of uncertainty.

#### **The Hunten model, March 1987 (H871)**

This model in a combination of the last two. Under 200 km, the profile is given by the average of the two Lindal profiles. Above, H81 is used, after multiplying all the densities by a factor 1.18 to get continuity at 200 km.

## The Lellouch model, May 1987 (Le87)

This model is a reanalysis of Li83. Uncertainties due to experimental noise and chemical composition (methane, argon) are considered. In a subsequent version (July 1987), uncertainty due to spatial and temporal variability is included (Flasar, priv. comm.). For altitudes under 200 km, a nominal profile (very close to Li83) and two "extreme" profiles are given.

## The Hunten model, May 1987 (H872)

Additional modelling is introduced to produce a new profile between 200 and 1270 km. This model uses Friedson and Yung's (1984) theoretical prediction above 680 km (with in particular a cold mesopause at 750 km and 104°K). It shows a maximum temperature of 205°K around 370 km. However, testing the model against the 7.7 $\mu$ m emission of methane as observed by Voyager (Coustenis and Gautier, priv. comm.) indicates that it is probably too hot between 200 and 500 km. Moreover, reconsideration of Friedson and Yung model shows a miscalculation that invalidates the resulting profile, although its overall shape is likely (Lellouch and Kockarts, 1987).

## The recommended model

### The 0-200 km range

Under 200 km, Le87 model is used. In addition, it has been agreed that the surface level of Titan is uncertain by  $\pm 2$  km with respect to the reference level defined by L83. (Johnson, priv. comm.). This can be taken into account by cutting the profile at 2 km, or extending it down to the "-2 km" level.

### The 200-1250 km range

The recommended profile has the overall shape of H872, but with some modifications to get better consistency with methane emission at 7.74 $\mu$ m. The shape is in qualitative agreement with present aeronomical models predictions. It must be noted, however, that up to now, these models are in conflict with S82 results (therefore with the present recommended model).

The uncertainty on the density increases rapidly with altitude to reach a factor about 10 at 800 km. The minimal and maximal temperature columns (which are equal respectively to  $\min(T_{\text{rec}}, 175^{\circ}\text{K}) - 30^{\circ}\text{K}$  and  $\max(T_{\text{rec}}, 175^{\circ}\text{K}) + 30^{\circ}\text{K}$ , where  $T_{\text{rec}}$  is the recommended temperature) are not consistent as profiles with the densities measured by S82, but they give for each level the estimated extreme possible temperatures. The recommended model is shown in Fig. A2.1.

## Conclusion

We are confident that the present recommended model of Titan's atmosphere is one of the best that can be built with the present available experimental data and state-of-art of the theory. We believe that the nominal profile adequately represents Titan's atmosphere as it will be at the time of the Cassini Probe release, and that the extreme profiles are conservative. Further theoretical investigations are currently being developed to reconcile aeronomical models with observation data in Titan's upper atmosphere.

## References :

- Friedson A.J. and Yung Y.L.: "The thermosphere of Titan", J. Geo. Res, 89, A1, 85 (1984)
- Hunten D.M.: "Titan atmosphere model, March 1987", (revised version, May 1987)
- Lellouch E.: "Evaluation of the uncertainty on Titan's atmosphere density profile: 0-200 km", May 1987 (revised version, July 1987)
- Lellouch E., and Hunten D.M., "Titan atmosphere engineering model", Space Science Department of ESA,ESLAB 87/199, (1987).

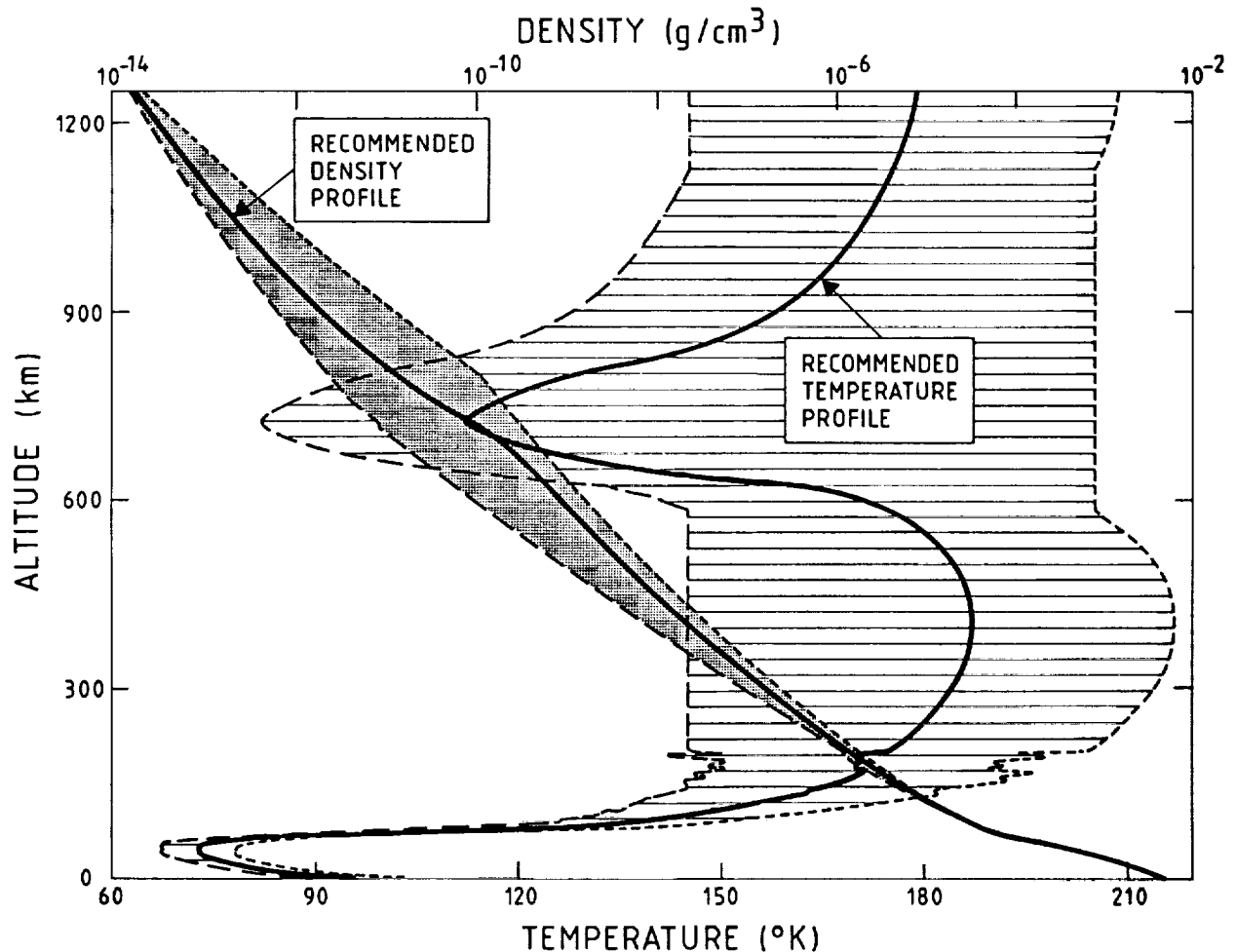


Figure B.1: *Thermal and density profile of the atmosphere of Titan*

- Lindal G.F., Wood G.E., Hotz H.B., Sweetnam D.N., Eshleman V.R., and Tyler G.L.: The atmosphere of Titan: "An analysis of the Voyager 1 Radio occultation measurements", *Icarus*, 53, 348 (1983)
- Smith G.R., Strobel D.F., Broadfoot A.L., Sandel B.R.
- Shemansky D.E., and Holberg J.B.: "Titan's upper atmosphere: composition and temperature from the EUV solar occultation results", *J. Geo. Res.*, 87, A3, 1351 (1982)

## Appendix C

# Bibliography

### General References

#### Books and Proceedings of Workshops

- Saturn, T. Gehrels and M.S. Matthews, eds., University of Arizona Press Tucson, Arizona, 1984.
- Atmospheres and Ionospheres of the Outer Planets and Satellites, Atreya S.K., Springer-Verlag, 1987.
- Satellites, J.A. Burns and M.S. Matthews, eds., University of Arizona Press Tucson, Arizona, 1986.
- The Atmospheres of Saturn and Titan, Proceedings Int. Workshop Alpbach, Austria, 16-19 September 1985 ESA SP-241, 1985.
- The Solid Bodies of the Outer Solar System, Proc. Conf. Vulcano, Italy 9-13 Sept. 1985, ESA SP-242, 1986.
- The Cassini Mission : Infrared and Microwave Spectroscopic Measurements, V. Kunde and R. Courtin eds., NASA Technical Report Oct. (1988).

#### Special Issues on the Voyager Encounter with the Saturn System

- Science, 212, (1981)
- Science, 215, (1982)
- J. Geophys. Res., 88, 1983

### Titan

- de Bergh, C., Lutz, B.L., Owen, T., and Chauville, J. 1988. Monodeuterated methane in the outer solar system III. Its abundance on Titan. *Astrophys. J.* 329, 951-955.
- Hunten, D.M., Tomasko, M.G., Flasar, F.M., Samuelson, R.E., Strobel, D. F., and Stevenson, D.J. 1984 Titan, in *Saturn*, ed. T. Gehrels and M.S. Matthews (Tucson, Univ. of Arizona Press) p. 671.
- Lellouch, E., Coustenis, A., Gautier, D., Raulin, F., Dubouloz, N., and Frère, N. 1988. Titan atmosphere temperature profile: a reanalysis of Voyager 1 radio occultation and IRIS 7.7 m data. *Icarus* (submitted).
- Lindal, G. F., Wood, G.E., Holz, H.B., Sweetnam, D.N., Eshleman, V.Jr., and Tyler, G.L. 1983. The atmosphere of Titan: an analysis of the Voyager 1 radio-occultation measurements. *Icarus* 53, 348-363.
- Lunine, J.I., Stevenson, D.J., and Yung, Y.L. 1983. Ethane ocean on Titan. *Science* 222, 1229-1230.
- Marten, A., Gautier, D., Tanguy, L., Lecacheux, A., Rosolen, C., and Paubert, G. 1988. On the abundance of carbon monoxide in the stratosphere of Titan from millimeter heterodyne observations. *Icarus* (submitted).
- Neubauer, F.M., Garnett, D.A., Scudder, J.D., and Hartle, R.E. 1984. Titan's Magnetospheric Interaction. *ibid*, p. 760.

- Pinto, J.P., Lunine, J.I., Kim, S.J., and Yung, Y.L. 1985. The D to H ratio and the origin and evolution of Titan's atmosphere. *Nature* 319, 388-390.
- Raulin, F., Mourey, D., and Toupane, G. 1982. Organic synthesis from CH<sub>4</sub>-N<sub>2</sub> atmospheres: implications of Titan. *Origins of Life* 12, 267-269.
- Toupane, G., Raulin, F., and Buvet, R. 1975. Formation of prebiochemical compounds in models of the primitive Earth's atmosphere. II. CH<sub>4</sub>-NH<sub>3</sub> and CH<sub>4</sub>-N<sub>2</sub> atmospheres. *Origins of Life* 6, 83-90.
- Yung, Y.L., Allen, M., and Pinto, J.P. 1984. Photochemistry of the atmosphere of Titan: comparison between model and observations. *Astrophys. J. Suppl.* 55, 465-506. References

## Saturn

- Stevenson D.J., 1982, Interiors of giant planets, *Ann. Rev. Earth Planet Sci.*, 10, 257-295.
- Courtin, R., 1985, The composition of the Saturn's atmosphere in the Atmospheres of Saturn and Titan, *ESA SP-241*, pp 13-20.
- Allison, M. and Stone, P.H., 1983, Saturn meteorology: A diagnostic assessment of thin layer configurations for the zonal flow, *Icarus*, 54, 296-308.
- Ingersoll, A., and Pollard, D., 1982. Motions in the interiors and atmospheres of Jupiter and Saturn: Scale analysis, an elastic equations, barotropic stability criterion, *Icarus*, 52, 62-80.
- Lunine, J., 1985, Interior of Saturn in the Atmospheres of Saturn and Titan, *ESA SP-241*, pp 3-11.
- Conrath B.J. and Gierasch P.J., 1984. Global variation of the parahydrogen fraction in Jupiter's atmosphere and implications for dynamics on the outer planets, *Icarus*.
- Godfrey, D.A. and V. Moore, 1986 (Reference to be sent by Mike Allison).
- Gautier, D. 1988. Constraints on the formation of giant planets from their atmospheric chemical composition. *Phil. Trans. R. Soc. London*, A325, 583-595.
- Stevenson, D.J., 1985. Cosmochemistry and structure of the giant planets and their satellites, *Icarus*, 62, 4-15.
- Fegley, B. and Prenn, R., 1985. Equilibrium and non-equilibrium chemistry of Saturn's atmosphere: implications for the observability of PH<sub>3</sub>, N<sub>2</sub>, CO and GeH<sub>4</sub>, *Astrophys. J.*, 299, 1067-1078.

## Rings

- Cuzzi, J. N., J. J. Lissauer, L. W. Esposito, J. B. Holberg, E. A. Marouf, G. L. Tyler, and A. Boisshot (1984) Saturn's rings: properties and processes; in "Planetary Rings", R. Greenberg and A. Brahic, eds. Univ. of Arizona Press
- Durisen, R. H. (1984) Transport effects due to particle erosion mechanisms; in "Planetary Rings", R. Greenberg and A. Brahic, eds. Univ. of Arizona Press
- Esposito, L. W., J. N. Cuzzi, J. B. Holberg, E. A. Marouf, G. L. Tyler, and C. C. Porco (1984) Saturn's rings: structure, dynamics, and particle properties; in "Saturn", T. Gehrels and M. A. Matthews, eds.; Univ. of Arizona Press
- Goertz, C., and G. E. Morfill (1983) A model for the formation of spokes in Saturn's rings; *Icarus*, 53, 219-229
- Goldreich, P., and S. Tremaine (1982) The dynamics of planetary rings; *Ann. Revs. Astron. Astrophys.* 20, 249
- Grün, E., H. A. Zook, H. Fechtig, and R. H. Giese (1985) The collisional balance of the meteoritic complex; *Icarus*, 62, 244-272
- Ip, W.-H. (1984) Ring torque of Saturn from interplanetary meteoroid impact; *Icarus*, 60, 547-552
- Marouf, E. A., G. L. Tyler, H. A. Zebker, and V. R. Eshleman (1983) Particle size distributions in Saturn's rings from Voyager 1 radio occultation; *Icarus*, 54, 189
- Northrop, T. G. and J. E. P. Connerney (1987) A micrometeoroid erosion model and the age of Saturn's rings; *Icarus*, 70, 124-137
- Porco, C. C., and G. E. Danielson (1982) The periodic variation of spokes in Saturn's rings; *Astron. J.* 87, 826

- Showalter, M. R., J. N. Cuzzi, E. A. Marouf, and L. W. Esposito (1986) Satellite "wakes" and the orbit of the Encke gap moonlet; *Icarus*, 66, 297-323
- Shu, F. H., L. Dones, J. J. Lissauer, C. Yuan, and J. N. Cuzzi (1985) Nonlinear spiral density waves: viscous damping; *Astrophys. J.* 299, 542-573
- Smith, B. A., and 26 other authors (1981) Encounter with Saturn: Voyager 1 imaging results; *Science*, 215, 504
- Smith, B. A., and 28 other authors (1982) A new look at the Saturn system; the Voyager 2 images; *Science*, 215, 504
- Weidenschilling, S. J., C. R. Chapman, D. R. Davis, and R. Greenberg (1984) Ring particles: collisional interactions and physical nature; in "Planetary Rings", R. Greenberg and A. Brahic, eds. Univ. of Arizona Press
- Zebker, H. A., E. A. Marouf, and G. L. Tyler (1985) Saturn's rings: particle size distributions for thin layer models. *Icarus*, 64, 531-548

## Satellites

- Satellites (Univ. of Arizona Press)
- Voyager 1, 2 Science issues for Saturn encounters
- Morrison et al., Chapter in *Saturn* (Univ. of Arizona press).

## Magnetosphere

- Neubauer, F.M., D.A. Gurnett, J.D. Scudder and R.E. Harle, Titan's magnetospheric interaction, in "Saturn" (Ed. D.T. Gehrels and M.S. Matthews), Univ. Arizona Press, 671, 1984.
- Ip, W.H., Cassini instruments related to interactions between magnetosphere and surfaces, in "The Solid bodies of the outer solar system", ESA SP-242, p. 179, 1986.
- Van Allen, J.A., Energetic particles in the inner magnetosphere of Saturn, In *Saturn* (Ed. T. Gehrels and M.S. Matthews), p. 281, Univ. of Arizona Press, 1984.
- Scarf, F.L. et al., Measurements of plasma, plasma waves, and suprathermal charged particles in Saturn's inner magnetosphere in *Saturn* (Ed. T. Gehrels, and M.S. Matthews), p. 318, Univ. of Arizona press, 1984.
- Schmidt, A.W. et al., The outer magnetosphere, in *Saturn* (Ed. T. Gehrels and M.S. Matthews), p. 416, Univ. of Arizona press, 1984.
- Sittler, E.C. Jr. et al. The distribution of neutral gas and dust near Saturn, *Nature*, 292, 711, 1981.
- Morfill, G.E. et al., Saturn's E. GT, and F. rings, Modulated by the plasma sheet, *J. Geophys. Res.*, 88, 5573, 1983.

## Asteroid

- ASTEROIDS (T. Gehrels ed.) University of Arizona Press, Tucson, 1978.
- ASTEROIDS, COMETS, METEORS (C.-I. Lagerkvist, H. Rickmann eds.) Uppsala Universitet Reprocentralen HSC, Uppsala 1983.
- ASTEROIDS, COMETS, METEORS II (C.-I. Lagerkvist, B.A. Lindblad, H. Lundstadt, H. Rickmann eds.) Uppsala Universitet Reprocentralen HSC, Uppsala 1986.
- ASTEROID PHOTOMETRIC CATALOGUE, C.-I. Lagerkvist, M.A. Barucci,
- T. Capria, L. Guerriero, M. Fulchignoni, E. Perozzi, V. Zappala, C.N.R. Edizioni, Roma, 1987.

# Appendix D

## List of Acronyms

ACP	Aerosol Collector and Pyrolyzer	NA	Narrow Angle
ASI	Atmospheric Structure Instrument	NGIMS	Neutral Gas and Ion Spectrometer
CIRS	Composite Infrared Spectrometer	PENL	Comet Penetrator Lander
CIDEX	Cometary Ice and Dust experiment	PLS	Plasma Spectrometer
CODEM	Cometary Dust Environment Monitor	PRWS	Plasma and Radio Wave Spectrometer
COMA	Cometary Matter Analyzer	PSS	Probe Support System
CREWE	Coordinated Radio, Electron and waves Experiment	RAD	Radio Science
CRIMS	Cometary Retarding Ion Mass Spectrometer	RAS	Radar Altimeter Science
DWE	Doppler Wind Experiment	RHU	radioisotope Heating Unit
DISR	Descent Imager/Spectral radiometer	RITO	Refraction Index of Titan Ocean
DA	Dust Analyzer	RPA/LP	Retarding Potential Analyzer/Langmuir Probe
ENA	Energetic Neutral Analyzer	RRL	Radio Relay Link
FORS	Fiber Optic Rotation Sensor	RTG	Radioisotope Thermoelectric Generator
GCMS	Gas Chromatograph and Mass Spectrometer	SEMPA	Scanning Electron Microscope and Particle Analyzer
HPD	Hot Plasma Dector	SED	Saturn Electrostatic Discharge
HPSP	High Precision Scan Platform	SKR	Saturn Kilometric Radiation
HSP	High Speed Photometer	SOI	Saturn Orbit Insertion
INMS	Ion/Neutral Mass Spectrometer	SPICE	Suprathermal Plasma Investigation of Cometary Environments
ISS	Imaging Science Subsystem	SSP	Surface Science Package
LRD	Lightning and Radio Emission detector	TIREX	Thermal Infrared Radiometer Experiment
MAG	Magnetometer	TRM	Titan radar Mapper
MIMI	Magnetospheric Imaging Instrument	UVSI	Ultraviolet Spectrometer and Imager
NIRS	Near Infrared Spectrometer	VIMS	Visual and Infrared Mapping Spectrometer
MSAR	Microwave Spectrometer and Radiometer	WA	wide Angle

